



**University of
Reading**

**Developing next generation bioassays and
biotherapeutics: label-free microfluidic phage
measurement by darkfield bacteria imaging**

A Thesis Submitted to the University of Reading in Partial Fulfilment for the Degree of Doctor of Philosophy

School of Chemistry, Food, Pharmacy

by

Sultan İlayda Dönmez

May 2022

AUTHOR'S DECLARATION

Declaration: I confirm that this is my work and the use of all material from other sources has been properly and fully acknowledged.

Sultan İlayda Dönmez

This work is dedicated to my family

Acknowledgements

First of all, I would like to express my gratitude to my honoured supervisor, Dr Al Edwards, who guided my studies with his knowledge and experience, gave a different perspective to my education, and provided the opportunity to improve myself by sharing his experiences throughout my PhD. I would like to offer my special thanks to my supervisor, Dr Helen Osborn, for providing support and feedback throughout this tough period. Her guidance, knowledge and patience have all been instrumental in the completion of this work. I am deeply grateful to my supervisor, Dr Sarah Needs, for her inspiration she gave me and her continuous encouragement during my journey at the University of Reading. I would like to extend my sincere thanks to the following team members, Tai The Diep, Rya Meltem Sariyer, Matt Long and Sophie Jegouic for their help and collaborative effort during weekly meetings. With many thanks to Dr Abdullah Tahir Bayraç and Dr Nuno Reis for supporting me to contribute to my scientific papers.

I would like to thank my friends, lab mates and colleagues for a cherished time spent together in the lab, and in social settings. It is their kind help and support that have made my study and life in the UK a wonderful time.

I would like to offer my biggest thanks to my father Mehmet, my mother Muhterem and my brother Doęuşcan, I could not have done this without you.

Finally, I would like to express my sincere gratitude to the Turkish Ministry of National Education for giving me the scholarship that enabled me to complete my PhD at the University of Reading in the United Kingdom.

Abstract

Currently, antibiotic resistance is one of the biggest risks to global health and food security. Bacteriophages are recognised as a useful alternative to antibiotics and are specific to the host bacterial cell. Phage therapy is gaining popularity as a tool to tackle antibiotic resistance. In each study using bacteriophages, the determination of the bacteriophage and enumeration is critical. However, traditional methods require a long detection time (48 h) to determine applicable phages and their dose. In this thesis, work focused on phage detection and enumeration using microfluidic systems to overcome the shortcomings of traditional method of phage use (double layer agar method) is presented. Label-free, low effort detection of bacteria and bacterial lysis with darkfield imaging using the smartphone camera is also reported. Thus, the companion diagnostic can use the works developed in the thesis, in the next generation tests that can be used in future point of care tests, which are simple to use and give fast results. A Raspberry Pi sensor system has been integrated into the system in order to obtain quantification data and perform cell-based analyses. Thus, for low bacteria and phage concentrations, both colony forming unit/mL and plaque forming unit/mL calculations could be performed in only 4 μ L liquid medium and in 5 hours, while kinetic measurements of cells could be obtained. The last research part of the thesis focused on the detection and aggregation of platelets with similar properties to bacteria, and the aggregation formed by the use of high concentrations of agonists was observed with a working principle similar to aggregometry. It was proved that platelet detection and the effects of 2 agonists on platelets can be determined depending on the light scattering intensity.

Chapter 1 provides a general introduction to bacteriophages. After explaining what bacteriophages are and how they work, their effectiveness for preventing antimicrobial resistance (AMR) is critically appraised. Then, current lytic phage-based detection systems and current studies that are created by adding microfluidic to these systems are explained.

Chapter 2 discusses, how, by combining the extensive analytical capability of these miniature computers in our pockets with new fields, consumer instrumentation can be advanced to realise additional positive implications for healthcare. The chapter focuses on new opportunities in three emerging areas where smartphone capabilities could be combined with biosensors and microfluidics. These are bacteriophages, aptamers and cellular measurements. Especially today, while fighting the covid virus, interest in home-based tele-diagnosis is increasing in order to reduce hospital admissions and achieve faster and more accurate results. In this chapter, the required current state of the field is critiqued. In addition, the review is based on a wide range of references to provide a balanced view of the field, and future directions in the field are summarized based on current developments in the field.

Chapter 3 represents the first time in the literature that label-free microfluidic bacteria detection can be used to determine host specificity for the therapeutic bacteriophage. It has been shown that it is entirely possible to measure light scattering by bacteria with a smartphone in microcapillary film (MCF) test strips placed in the 3D printed dark field imaging system we designed, which includes a simple light source. This demonstrates the potential of microfluidics as companion diagnostic for advanced biological therapeutics in the treatment of bacterial infections. In the designed system, when bacterial target cell suspensions were taken into phage-loaded MCF capillaries, no light scattering signal was observed in the channels after incubation with the effect of lysis. To see if the specificity of the host bacteria could be determined rapidly with this system, light scattering occurred as opposed to the host strain when the loaded phage was tested on MCF test strips of other bacteria that was not the host bacteria. Thus, the potential for measuring bacteria in a number of microbiology methods, including the bacteriophage lysis of the smartphone camera plus MCF, was clearly demonstrated.

Chapter 4 appraises the rapid and simple measurement of CFU/ml and PFU/ml of our automated image capture system, previously unavailable in the literature, which allows for detailed analysis of microbial growth kinetics using dipstick microfluidic strips. Bacteria and bacteriophage counting is a cornerstone for microbiological analysis, and the agar plate method has been used for over 140 years. However, this

process is cumbersome and has innovation potential to make microbiology accessible for field use and point-of-care diagnostics. This section discusses a new method for counting bacteria and bacteriophages in a simple liquid assay using a dipstick microfluidic system without further labelling or coating. In our microfluidic system, it has been shown that individual bacterial colonies can be visualized in as little as 5 hours, even in liquid cultures. Removing the solid media from this process facilitates enumeration and bacteriophage counting, which requires careful control of host bacteria, especially on molten agar. Since this type of growth is not seen in bulk conventional microbiology systems such as microplates or tube cultures, the method also provides a new perspective on microbiology microsystems. In addition, accelerated darkfield imaging using the Raspberry Pi sensor system instead of a smartphone allows for detailed kinetic analysis of colony growth. Thus, while providing a new perspective to single cell-based microbial microfluidic analysis, it made it possible to establish quantitative growth kinetics simultaneously with colony counting.

Chapter 5 interrogates whether platelets can be visualised in the same dark-field system used for bacteria, which would represent a significant advance given their various functions and importance in the body. As a result, we show that we can detect platelets in the dark-field imaging system in microfluidic, based on turbidity-based measurement, thanks to the light scattering feature. In addition, when determining whether we could detect platelet aggregation, significant differences were detected when two different agonists were dried in microchannels and then loaded with platelets reach plasma (PRP). Thus, in the future, a system that could not only detect platelets, but also the effects of the agonist on a particle basis platelet aggregation, is discussed.

In Chapter 6, the important points of the PhD thesis are summarized and critically examined. The usage and importance of bacteriophages are emphasized, and phage-based commercial detection systems are discussed, with the benefits and drawbacks of our system being articulated. The scope for implementing our system and its important contribution to the diagnosis of companion is discussed. The potential for future work, such as new bacteriophage discovery, formulation, and production, is critically addressed.

List of Publications

The present thesis produced the following papers

S.I. Dönmez, A.T. Bayrac, S.H. Needs, J. Hart, H.M.I. Osborn, A.D. Edwards, Future Bioassays and Biosensing Technology for Smartphone Diagnostics: Opportunities for Bacteriophage, Aptamer and Cellular Measurements, Biosensor and Bioelectronics:X, (2022). *Under revision*.

S.I. Dönmez, S.H. Needs, H.M.I. Osborn, A.D. Edwards (2020). "Label-free smartphone quantitation of bacteria by darkfield imaging of light scattering in fluoropolymer micro capillary film allows portable detection of bacteriophage lysis." *Sensors and Actuators B: Chemical* 323: 128645.

S.I. Dönmez, S.H. Needs, H.M.I. Osborn, N.M. Reis, A.D. Edwards. Label-free 1D microfluidic dipstick counting of microbial colonies and bacteriophage plaques, *Lab Chip*, 2022, 2820-2831.

R.M. Sariyer+, S.I. Dönmez+, S.H. Needs, H.M.I. Osborn, C. Jones, A.D. Edwards, Dark-Pi Platelets and Platelets Aggregation Detection, *Microchimica Acta*, (2022). *Manuscript in preparation*.

+ Authors made an equal contribution to this work.

Papers not related to the work of this project

A.T. Bayrac, S.I. Donmez (2018). Selection of DNA aptamers to *Streptococcus pneumonia* and fabrication of graphene oxide based fluorescent assay. *Analytical Biochemistry* 556 (2018) 91–98. (It was generated from MSc)

S.H. Needs, S.I. Donmez, S.P. Bull, C. McQuaid, H.M. I. Osborn, A.D. Edwards. Challenges in Microfluidic and Point-of-Care Phenotypic Antimicrobial Resistance Tests. *Frontiers in Mechanical Engineering*, (2020) 6:73. (It was generated from PhD, but not relative with the thesis)(Major contribution is writing - review & editing)

S.H. Needs, S.I. Donmez, A.D. Edwards. Direct microfluidic antibiotic resistance testing in urine with smartphone capture: significant variation in sample matrix interference between individual human urine samples, *RSC Adv.*, (2021), 11, 38258. (It was generated from PhD, but not relative with the thesis) (Major contribution is elements of experiment)

List of Conferences Attended

S.I. Donmez, S.H. Needs, A.D. Edwards, Label-free bacterial smartphone detection in micro capillary film allows rapid testing of therapeutic bacteriophage specificity, **The 10th APS International PharmSci Conference, Sep 2019, University of Greenwich, UK. Poster.**

S.I. Donmez, H.M.I. Osborn, A.D. Edwards, Label-free Therapeutic Bacterial Detection to Allow Rapid Testing in MCF, **Pharmacy PhD Showcase, Apr 2019, University of Reading, UK. Poster (BEST POSTER WINNER).**

S.I. Donmez, H.M.I. Osborn, A.D. Edwards, Smartphone quantitation of bacteria by darkfield imaging of light scattering in fluoropolymer micro capillary film, **Pharmacy Showcase, University of Reading UK, Apr 2021. Talk.**

S.I. Donmez, H.M.I. Osborn, A.D. Edwards, Label-free smartphone quantitation of bacteria by darkfield imaging of light scattering in fluoropolymer micro capillary film allows portable detection of bacteriophage lysis, **Doctoral Research Conference, University of Reading UK, June 2019. Talk.**

S.I. Donmez, S.H. Needs, M. Rabiey, H.M.I. Osborn, A.D. Edwards, Label-Free Bacterial Smartphone Detection in Micro Capillary Film Allows Rapid Testing of Therapeutic Bacteriophage Specificity, **23rd International Conference on Miniaturized Systems for Chemistry and Life Sciences (μ TAS), Basel Switzerland, Oct 2019. Poster.**

S.H. Needs, S.I. Donmez, A.D. Edwards, Miniaturisation of The Gold Standard Broth Microdilution Method to Make a Multiplex, High Throughput Antibiotic Susceptibility Test for Determination of Susceptibility in Uropathogenic *E. coli* In Urinary Tract Infections, **The 25th International Conference on Miniaturized Systems for Chemistry and Life Sciences (μ TAS 2021), Oct 2021. Poster.**

S.I. Donmez, S.H. Needs, A.D. Edwards, Agar-Free, Fast and Cheap Bacteriophage Counting Assay Using Microfluidic Device in Darkfield Imaging System, **The 25th International Conference on Miniaturized Systems for Chemistry and Life Sciences (μ TAS 2021), Oct 2021. Poster.**

S.I. Donmez, S.H. Needs, H.M.I. Osborn, A.D. Edwards, Novel, Fast and Cheap Individual Bacteria and Bacteriophage Counting Agar-Free Method Using Microfluidic Device in Simple Darkfield Imaging System, **III. International Agricultural, Biological & Life Science Conference AGBIOL, Sept 2021. Talk.**

S.I. Donmez, S.H. Needs, H.M.I. Osborn, A.D. Edwards, Agar-Free, Fast and Cheap Individual Bacteria and Bacteriophage Counting Assay Using Microfluidic Device in Darkfield Imaging System, **4th International Biotechnology and Research Conference, Aug 2021. Talk.**

Table of Contents

Chapter 1: General Introduction	1
Chapter 2: Future Bioassays and Biosensing Technology for Smartphone Diagnostics: Opportunities for Bacteriophage, Aptamer and Cellular Measurements	18
Chapter 3: Label-free smartphone quantitation of bacteria by darkfield imaging of light scattering in fluoropolymer micro capillary film allows portable detection of bacteriophage lysis	19
Chapter 4: Fast Dipstick Microfluidics Plus Open Source Darkfield Biosensor Enable Label-free 1D Counting of Microbial Colonies And Bacteriophage Plaques	20
Chapter 5: Dark-Pi Platelets and Platelets Aggregation Detection	21
Chapter 6: General Discussion	22

Abbreviations

ADP Adenosine Diphosphate

AMR Antimicrobial Resistance

BHI Brain Heart Infusion

CFU Colony Forming Units

CMOS Complementary Metal-Oxide Semiconductor

DAL Double Layer Agar

FDA Food and Drug Administration

LA Lysogeny Agar

LB Lysogeny Broth

LED Light Emitting Diode

LIF Laser Induced Fluorescence

HQ High Quality

MCF Micro Capillary Film

MDR Multi-Drug Resistance

MOI Multiplicity of Infection

N/A Not Applicable

NA Nutrient Agar

NB Nutrient Broth

OD Optical Density

PFU Plaque Forming Units

pH Power of Hydrogen

PPP Platelet-Poor Plasma

PRP Platelet-Rich Plasma

POC Point-Of-Care

PVOH Polyvinyl Alcohol

RGB Red Green Blue

RPM Revolutions Per Minute

UTI Urinary Tract Infections

WHO World Health Organisation

Chapter 1

General Introduction

1. Introduction

The difficulties arising from traditional methods for the detection and quantitation of microorganisms have increased the need for accurate, inexpensive, and rapid diagnostic tools for infectious diseases in practical and clinical fields on a global scale. Point-of-care (POC) tests have been combined with microfluidic equipment to develop a new generation of miniaturized biosensors that do not require advanced equipment, laboratories, and specialists. Without the need for long test steps, these tests, where all the steps can be done in the channels in the microfluidic and can work with miniature computers in our pockets, remove the difficulties of classical methods.

Phages are an alternative to antibiotics, but they are only effective if the infection is susceptible and so to identify the correct phage for a particular infection, quick lysis tests are essential. Herein, after the introduction of AMR and its challenges, bacteriophages and microfluidic integrated phage-based detection systems will be discussed.

1.1. AMR

With the discovery of antibiotics, important advances have been made in the fight against infectious diseases. However, with the widespread use of antimicrobial agents in many areas such as industry, agriculture and the health sector, the incidence rates of AMR of microorganisms are increasing, and hence AMR is a global problem (Muller 2022). AMR is defined as the reduction or complete elimination of the effects of antibiotics by a number of mechanisms. Resistant microorganisms are difficult to treat and require alternative drugs or high dosages of antibiotics during treatment, which can increase treatment costs and cause toxic effects (Prestinaci, Pezzotti et al. 2015). Resistance development is categorized as natural or acquired. The first of these, natural resistance, is defined as the resistance of the bacteria due to its structural properties such as membrane. Acquired resistance development can occur through mutations or resistance development with gene transfer from a resistant bacterial strain to an antibiotic susceptible strain. As previously reported, bacteria can inherit resistance genes from their ancestors transfer them to each other with mobile elements such as plasmids. This last mechanism, which is also defined as horizontal gene transfer, provides the transfer of resistance genes between different types of bacteria. Antibiotics applied to the bacterial group containing strains that developed resistance to antibiotics cause the death of strains that do not carry antibiotic resistance genes but do not affect the survival of resistant strains. As a result of this natural selection, resistant strains multiply and become a greater threat (Read and Woods 2014).

According to Kraker *et al*, by 2050, 10 million people will die every year due to AMR, if the necessary

measures are not taken (de Kraker, Stewardson et al. 2016).

In addition, microorganisms can exchange genes with each other by the same or different kinds of microorganisms forming a biofilm layer, thus producing more resistant strains against antimicrobial agents (Donlan and Costerton 2002).

As bacterial resistance spreads, and fewer antibiotics can be used effectively, the medical world has been looking for new antibiotics and alternative detection methods. This has led to the re-emergence of previously investigated treatments such as phage therapy, which is seen as an alternative treatment method to antibiotics in order to use bacteriophages to destroy bacteria (Jassim and Limoges 2014).

1.2. Alternative treatment: bacteriophages

In today's world where bacteria are increasingly resistant to antibiotics, the medical world has been looking for alternative treatments (Gurney, Brown et al. 2020). Bacteriophages, which are specific to bacterial species and eradicate bacteria, are an important solution to this problem. About 40 years after the start of studies on microorganisms, bacteriophages were identified in the first quarter of the 19th century and were reported in the literature as a bacteria-eating virus (Summers 2001). Bacteriophages play an important role in the global biogeochemical cycle by infecting half of the bacteria that grow daily in the biosphere (Suttle 2005). Compared to antibiotics, phages have several advantages. Most importantly, phages are specific to host cells, so they do not affect the entire microflora, and they show a self-limiting effect because they can only show their presence as long as the target bacteria is present. Single doses can usually be used as they can self-replicate in the host (Opperman, Wojno et al. 2022). Many factors can affect the dose of antibiotic concentrations, phages, on the other hand, achieve efficacy even after a single dose. After the lytic phage kills a bacterium, the phages released into the environment infect the remaining bacteria (Gu Liu, Green et al. 2020). In addition, antibiotic resistance that will occur with the use of antibiotics is not limited to the targeted pathogen and affects the entire microflora, so while exposure to antibiotics can multidrug resistance, on the other hand, phages can self-modify to combat host resistance (Koskella and Brockhurst 2014). The first studies in the field of bacteriophage were made by Felix d'Herelle (1917). Thus the term bacteriophage was first used by Felix d'Herelle, and he also introduced the term plaque to the open zones formed by bacteriophages infecting bacteria by the double layer agar method (Summers 2001). Bacteriophages have received relatively little interest for many years after their discovery because they were discovered at about the same time as antibiotics. The increase in genome research and the increase in non-preventable antibiotic resistance has caused renewed interest in bacteriophages. As a result of genome studies, it was revealed that many bacteria carry lysogenic bacteriophage within

their genomes, termed prophage, and these genetic materials cause changes on the bacterial genome (Brüssow, Canchaya et al. 2004). There are approximately 10^7 bacteriophages per gram of soil and each mL of water. Bacteriophages are considered to be the most common form of life on Earth. According to calculations, there are more than 10^{30} bacteriophages on earth. Bacteriophage is thought to prokaryotic cells on earth by tenfold (Chibani-Chennoufi, Bruttin et al. 2004). A typical lytic phage infects bacteria that generate ~ 200 new phages in the cytoplasm within hours. Produced bacteriophages also infect new-generation bacteria and eradicate them. If each of these lytic phages infects a host cell, at the end of the second cycle 40,000 progeny are produced (200×200). By the end of the fourth cycle, 1.6 billion progeny will have been formed ($200 \times 200 \times 200 \times 200$). This replication cycle of phages ends only when there are no more bacteria to infect.

Bacterial infection begins when bacteriophages are specifically bound to the bacterial cell by adsorption and then transfer their genetic material to the host bacterial cell. During replication of bacteriophages, the phage first binds to specific surface receptors on the target host cell surface. The binding receptors of Gram-negative bacteria are generally lipopolysaccharides, murein, flagella and other surface proteins. In Gram-positive bacteria, they are peptidoglycan, teichoic acid, lipoteichoic acids and other surface proteins. After binding to the surface receptors of the target bacteria, phages transfer the genetic material directly into the cytoplasm of the bacterial cell by penetrating the peptidoglycan and internal membrane structure with the help of a hypodermic syringe motion and enzymes. Once the genetic material has been transferred into the host cell, it must be protected from intracellular exonuclease and restriction enzymes (Molineux 2001, Guttman, Raya et al. 2005, Matthey and Spencer 2008). Lytic bacteriophages rapidly increase their concentration without causing toxicity at the sites of infection (Roos, Ivanovska et al. 2007, Betts, Vasse et al. 2013). The total time spent by bacteriophages in the host cell is called the latent period in lysogenic cycle (Figure 1). Bacteriophages are obligatory intracellular parasites since they cannot produce protein and energy as they do not have a ribosome and necessary cellular mechanisms. Phages are classified according to their morphology and genetic material (Figure 1). Double-stranded DNA (dsDNA) tailed phages constitute the majority of observed phages and are grouped into three groups: myoviridae, siphoviridae, and podoviridae. Classical myoviridae members have a characteristic tail structure. Unlike the tail phages, which show lytic activity, most of the filamentous phages show lysogenic activity like M13. In addition, almost all filamentous phages discovered so far have been noted to infect gram-negative hosts (Betts, Vasse et al. 2013, Hay and Lithgow 2019).

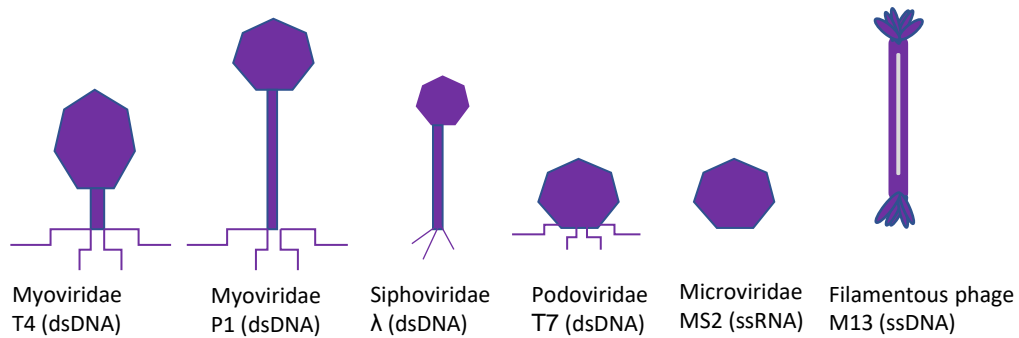


Figure 1. Phages classified based on morphology

Phages must replicate by entering into another cell. When phages infect host cells, they continue through two different life cycles: lytic or virulent and lysogenic or temperate (Figure 1). The growth stages of lytic phages consist of 5 stages: adsorption, penetration, biosynthesis, maturation, and lysis (Figure 2). Adsorption of the tailed phages starts by attaching the target bacteria to the capsule surface by means of tail fibres.

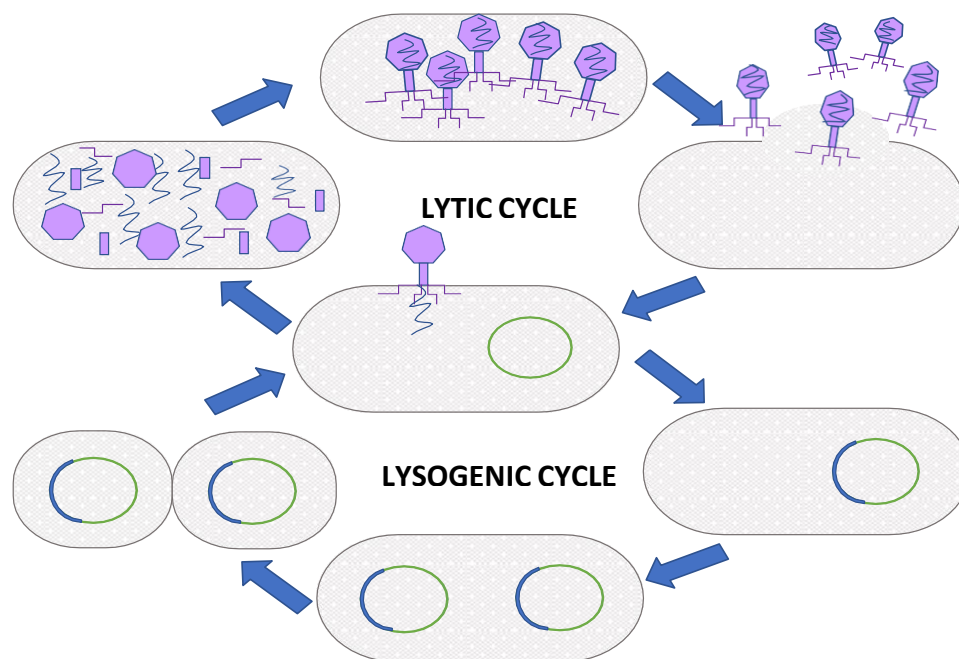


Figure 2: Lytic and lysogenic cycle of phage

Adsorption of tailless phages is achieved by binding of specific receptors to capsomeres. The specificity of phage to host bacteria is determined in the first and most important stage of infection, specifically adsorption. Many phages require divalent ions such as Ca^{2+} or Mg^{2+} for attachment. These ions neutralize the negative charge of bacteria and phage particles, thus facilitating adsorption. The adsorption phase ends approximately 5 minutes after the phage and bacteria come into contact with

each other (Hay and Lithgow 2019). The step by which the bacteriophage transfers the genetic material after adherence to the host cell is the penetration step. This mechanism is specific for all phages. As tailed phages inject genetic information into the host cell, the tail fibres are shortened so that the tail penetrates the bacterial cell wall. The genetic material in the capsule passes through the channel in the tail and into the periplasmic space of gram-negative bacteria and passes easily through the small hole created by the phage in the bacterial cell membrane into the cell cytoplasm. The hole is repaired immediately by the bacterial cell.

The phage sheath that remains on the bacterial cell wall after the release of genetic material is called the phantom phage and the nucleic acid injected into the host is called the non-temperate (Molineux 2001, Guttman, Raya et al. 2005).

The growth and development period of phages in the host cell is the biosynthesis and maturation period. During this period head, tail and other phage structures are synthesized. This period, also called the latent period covers the period from the entry of the genetic information of phages into the cytoplasm of the host cell to the formation of mature phages. After the phage genetic material enters the bacterial cell, the bacterial ribosomes are formed by transcription and begin protein synthesis. The phage disrupts the metabolism of the bacterial cell and allows replication of its genome. Bacteriophage components and enzymes are synthesized, and the separately synthesized phage components begin to combine. Separately synthesized bacteriophage building blocks come together to form mature phage particles (virions) (Roos, Ivanovska et al. 2007).

Phages that reach a certain number and mature in the bacterial cell lyse the bacteria by using their own enzymes and proteins and get out of the bacteria and become free. Two components are used to produce lysis: endolysin and holin proteins. The viral protein, holin, forms pores in the cell membrane. The viral enzyme, endolysin or lysin, which is phage-encoded peptidoglycan hydrolases, breaks down the cell wall (peptidoglycan). Holin opens the pores in the inner membrane, causing the lysin enzyme to reach the peptidoglycan layer, lysing the cell (Figure 3) (Kutter and Sulakvelidze 2004, Hanlon 2007).

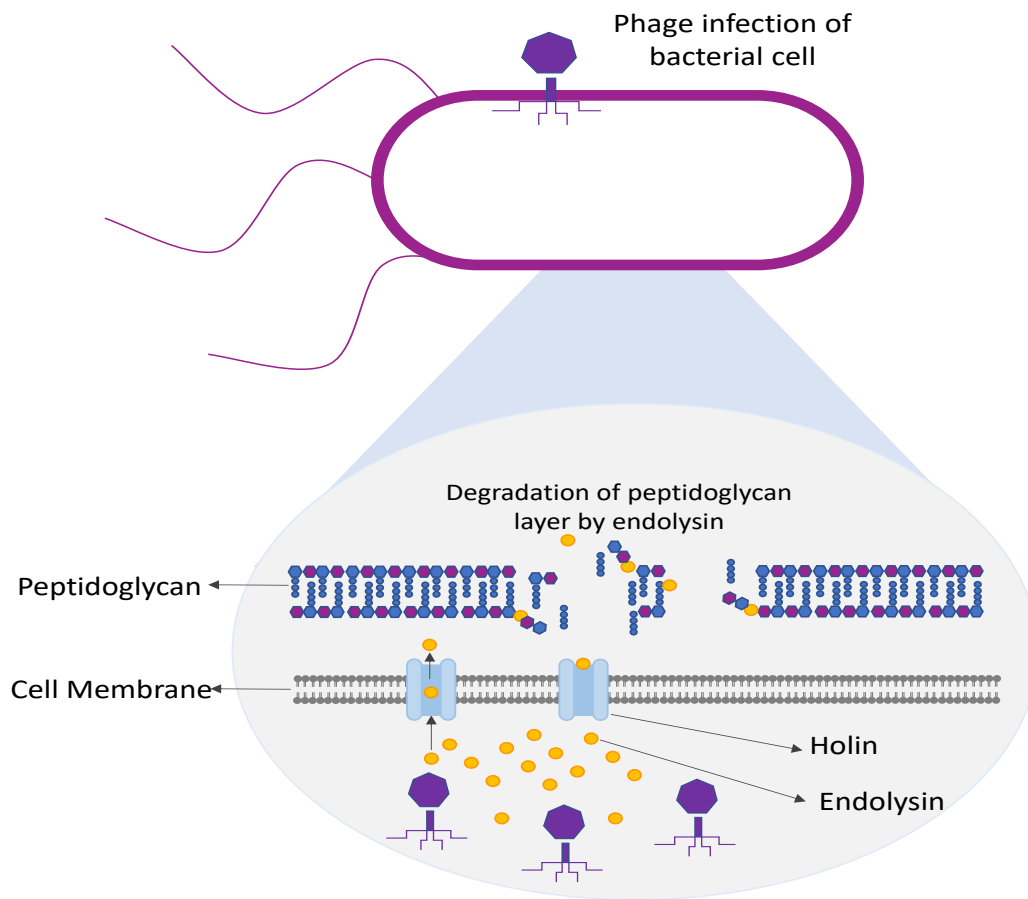


Figure 3: Mechanism of phage endolysins of a Gram-positive bacterial cell (Murray, Draper et al. 2021).

In the lysogenic life cycle, as in the lytic cycle, the phage adsorbs to the host cell and injects its DNA into the bacterial cell. However, after this penetration step, and the formation of newly synthesized phage particles, the latent period does not occur. The introduction of phage DNA into the bacterial chromosome by recombination results in a bacterial cell called a "lysogen" and the phage genetic material that is integrated into the DNA of the host cell is called a "prophage." Bacteria carrying phage in the chromosome in this way are called "lysogenic bacteria". The main difference of the lysogenic cycle from the lytic cycle is that the phage does not cause lysis of the host cell. Phage continues to exist in the host cell as conditions are appropriate. Since it allows the host cell to proliferate, phage remains in the new generation of the cell. However, when the conditions are not suitable for the host cell, the prophage becomes active and the lytic life cycle generating new phage particles, called phage induction. Examples of these conditions include depletion of nutrient sources and changing the incubation temperature, exposure of the host bacterial cell to antibiotics such as mitomycin C, nitrogen gas and UV rays (Lacroix 2010).

In the 1940s, Russia began to use bacteriophages to treat infectious diseases such as dysentery (Murray, Draper et al. 2021). According to a phage treatment center in Poland, phage therapy was calculated to be less costly than antibiotic therapy. The cost of antibiotic treatment for infections caused by methicillin-resistant *S. aureus* is 2-8 times higher than for phage treatment (Stone 2002).

Today, the use of phages in the treatment of mastitis caused by methicillin-resistant *S. aureus* is increasing. The phages used for mastitis are indicated in Table 1. In addition to using only a single phage, phage cocktails are also used to strengthen the lytic effect. In addition to finding alternatives to antibiotics, the need for rapid, sensitive, inexpensive and portable identification systems is developing. Although conventional methods have been used until now, these methods are time-consuming, laborious and consist of lots of steps. There is an urgent need for a rapid, low-cost and reliable setup to allow detection of bacteria and to determine phage specificity of an infectious organism (Miedzybrodzki, Fortuna et al. 2007).

The majority of diagnostic equipment and procedures used nowadays are expensive and require expert knowledge from the operator. This prohibits the effectiveness especially in the less developed regions of the world. Label-free microfluidic platforms have been developed in recent years to overcome these problems and enable more people to use diagnostic systems.

Table 1. Mastitis treatment using therapeutic phage

Host Cell	Phage Type	Ref
<i>S. aureus</i>	Phage K	(Farooq, Yang et al. 2018)
<i>S. aureus</i>	vBSM-A1 and vBSP-A2	(Gill, Pacan et al. 2006)
<i>S. aureus</i>	Phage K	(Geng, Zou et al. 2020)
<i>S. aureus</i> biofilms	Phage K	(Gill, Pacan et al. 2006)
<i>S. aureus</i> biofilms	Phage K + DRA88	(Kelly, McAuliffe et al. 2012)
<i>S. aureus</i>	12 phage cocktail	(Alves, Gaudion et al. 2014)
<i>S. aureus</i>	MSA6	(Breyne, Honaker et al. 2017)
<i>S. aureus</i>	Phage Mixture and a Lactic Acid Bacterium	(Kwiatek, Parasion et al. 2012)
<i>S. aureus</i>	Phage Φ SA012	(Titze and Krömker 2020)
<i>S. aureus</i>	<i>S. aureus</i> phage ISP	(Iwano, Inoue et al. 2018)
<i>S. aureus</i>	Isolate from wastewater	(Vandersteegen, Mattheus et al. 2011)
<i>S. aureus</i> (five methicillin-resistant and five methicillin-sensitive)	4 phages cocktail	(Hamza, Perveen et al. 2016)
<i>E. coli</i>	Phage isolates from wastewater	(Ngassam-Tchamba, Duprez et al. 2020)
<i>E. coli</i>	T4virus vB_EcoM-UFV13	(Porter, Anderson et al. 2016)
<i>K. pneumoniae</i>	Phage CM8–1 isolated from wastewater	(da Silva Duarte, Dias et al. 2018)
<i>Klebsiella oxytoca</i>	4 phage isolates from wastewater	(Zhao, Shi et al. 2021)
<i>Streptococcus dysgalactiae</i> NRRL B-65273, <i>S. agalactiae</i> NRRL B-65272, and <i>S. uberis</i> NRRL B-65274	Streptococcal phage λ SA2 and endolysins B30	(Amiri Fahliyani, Beheshti-Maal et al. 2018)

1.3. Current lytic phage-based detection studies

Bacteriophages have received increasing attention as an antibiotic alternative, but conventional agar method testing is cumbersome, requiring at least 24 hours to produce results, and detection times are critical for therapeutic use, therefore, interest in alternative detection methods has increased. Phages bind to target host cells with a very high specificity and can therefore serve as pathogen recognition agents for phage-based detection systems. In recent years, various phage-based bioassays have been developed using output signals such as colorimetric, fluorescence and luminescence using bacterial lysis signals (Schmelcher, Powell et al. 2015, Ács, Gambino et al. 2020).

Recently, tests have been developed to utilize lytic bacteriophages to lyse the cell and enable colorimetric detection of bacteria as a result of the release of β -galactosidase release (Ács, Gambino et al. 2020).

In a system developed by Chen *et al.* in 2015, bacteriophage T7 attached to magnetic beads have been used in the detection of *E. coli* in drinking water. If *E. coli* is present in the drinking water, the bacteria will bind to the magnetic beads and release intracellular β -galactosidase. Colorimetric detection will be achieved using chlorophenol red- β -D-galactopyranoside and the sample colour will change from yellow to red as a result of the β -galactosidase enzymatic reaction. In this system using phage-conjugated magnetic probes, 10^4 CFU/mL bacteria were detected after 2.5 hours of process, although the whole process took 8 hours with pre-enrichment (Singh, Poshtiban et al. 2013).

In another study targeting lytic progeny phage detection, fluorescent changes occur as a result of β -galactosidase activating a fluorescent probe for the enumeration of phage. The progeny phages were determined by the plaque-droplet assay method. This approach, compared with the agar method, decreases the time for diagnosis from 12 hours to 2.5 hours, thus facilitating rapid identification of phages (Chen, Alcaine et al. 2015). Another approach to bacteriophage-based detection systems is based on the distribution of bacterial cell contents as a result of the lytic reaction, thus changing the characteristic of the environment and the detection and evaluation of this change as a signal. In 2008, using a screen-printed carbon electrode, immobilized T4 bacteriophage was used to detect 10^4 CFU/mL *E. coli* by measuring media impedance (Tjhung, Burnham et al. 2014). After 5 years, the same group reported that they increased the sensitivity of their systems up to 10^3 CFU/mL cells using a microchamber (Shabani, Zourob et al. 2008). In a further example, the lytic bacteriophages have proven that they are useful for biological amplification detection. A device based on lateral flow immunochromatography combined with gamma phage has been developed to detect *Bacillus anthracis*. Thanks to antiphage antibody-coated nanoparticle messengers, the device can detect up to 2.5×10^4 CFU/mL cells in 2 hours (Shabani, Marquette et al. 2013).

1.4. Light scattering and microfluidics

Originally, the Mie scattering (scattering of electromagnetic wave by homogeneous spherical particles) technique was used only for near perfect spherical objects but with time, it became clear that it had the potential to be used on bacteria (Cox, Jensen et al. 2015), for single colony bacteria analysis (Waltham, Boyle et al. 1994), and identification of bacteria directly on skin (Jo, Jung et al. 2015) and tissue (Sweeney and Yoon 2017). It does not require equipment that is especially sensitive to changes in environment, in other words it is very much possible to utilize Mie scattering in non-laboratory settings. Since the bacteria need to be alive to block the light because having cell integrity allows bacteria to light scatter, no label is required.

In recent years, developments that reduce the number of steps in multistep laboratory processes, minimise processing time, and provide more automated assays are increasing, especially through the use of microfluidic systems which can process or manipulate small amounts of fluidics, using microchannels measuring. In 2014, Yu *et al* designed a droplet optofluidic imaging system which is used for bacteriophage detection with its host cell.

In this system, the bacteriophage and bacteria added fluidic system are cultured in the microdroplet and then the bacteriophage effect is determined under condensed light (Yoon, Lee et al. 2016). Although this method is useful for a small number of bacteria (1-100 cells) because dilution method is not appropriate for this system, it is not suitable for the large number of bacteria found in many clinical samples.

One example of a microfluidic device suitable for analytical microbiology is Micro Capillary Film (MCF), a melt-extruded fluoropolymer comprising a flat plastic strip of 10 capillaries (Figure 3). MCF made from the fluoropolymer fluorinated ethylene propylene has a refractive index matching water, minimising optical background and thus allowing sensitive colorimetric and fluorometric bioassays including immunoassays and antibiotic susceptibility testing. Compared to laboratory measurement devices such as microplates and cuvettes, MCF offers the potential to accelerate and simplify bacterial determination methods (Yu, Huang et al. 2014).

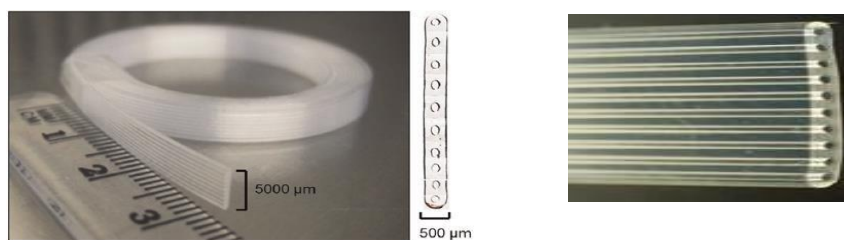


Figure 3: Melt-extruded fluoropolymer Micro Capillary Film (MCF), 200 µm internal diameter of each capillary.

Although label-free phage-based detection systems have been previously reported in the literature,

they have many disadvantages such as the need for genetically modified phages (Reis, Pivetal et al. 2016), expensive equipment (Kim, Kim et al. 2017), surface modifications (Halkare, Punjabi et al. 2021), the inability to be portable (Janik, Brzozowska et al. 2021), and multiple complex steps (Rippa, Castagna et al. 2017). It has previously been investigated whether light scattering by bacteria could be detected with a smartphone camera in the microcapillaries within MCF “lab-on-a-stick” test strips with only LED illumination and label-free bacterial detection has been measured. Once optimized darkfield imaging geometry was created in MCF, it was tested whether the bacteriophage host specificity could be determined with these low cost and simple microfluidic test strips, and it was shown that it was possible to determine label-free phage host specificity in a short time (Yue, He et al. 2017, Dönmez, Needs et al. 2020).

1.5. Open hardware and its role

The development of new laboratory equipment and techniques is both costly and time consuming. Proprietary scientific equipment and techniques require optimization by laboratories around the world to achieve proper use without the high costs. This time spent on the use and optimization of tests slows progress globally (Kim, Kim et al. 2016, Pearce 2017). Open-source hardware allows designers and scientists to share, use and improve their hardware designs. Thus, open-source hardware increases the worldwide availability of laboratory equipment and designs, enabling rapid scientific progress and cost-effective innovations in scientific methods. Open-source hardware gives designers flexibility for specific technical requirements, thus giving them the ability to be developed/modified according to the needs of laboratories and techniques (Pearce 2017). The use of open-source hardware in biological sample imaging is combined with Raspberry Pi computer technology, allowing for greater control over laboratory techniques while tackling alternative costly and inflexible laboratory equipment. The Raspberry Pi camera is likewise versatile and compact, taking real-time images/measurements on samples, reducing turnaround time and increasing real-time detection (Kim, Kim et al. 2016, Sharkey, Foo et al. 2016). With the need for accuracy in tests, a combination of digital computers and portable communication technologies offer an alternative route for biological and microbiological methods (Sharkey, Foo et al. 2016). Since its initial release over a decade ago, the Raspberry Pi, a low-cost computer, has gained more and more attention over the years (Jolles 2021). Thanks to this equipment, private laboratories were able to start the development of high-performance optoelectronic and robotic components and low-cost equipment (Jolles 2021). With its wide applicability in image analysis, Raspberry Pi is employed in many areas of healthcare applications, from temperature monitoring to image analysis (Culmone, Henselmans et al. 2020, Diep, Ray et al. 2022).

1.6. Summary of the research reported in the thesis

Due to the high and widespread AMR reached today, research has focused on these areas again. Phage therapy has rapidly increasing potential use against bacteria and has become a promising topic in the treatment of infectious diseases. More specific antimicrobials are urgently needed to tackle the problem of AMR, which remains one of the greatest threats to global health. Therapeutic bacteriophage can be used to treat bacterial infection as a biological alternative to antibiotics by destroying infectious microorganisms through lytic infection. The phage displays excellent host selectivity by allowing certain bacteria to be killed, leaving the host microbiome intact. Using new diagnostics to determine phage specificity could be an attractive method of infection control. While traditional culture-based assays for phage detection are still the gold standard, there is a growing need for concomitant diagnosis that eliminates the need for cultures, does not require long incubation times, and can directly detect the pathogen without labeling. Differences in susceptibility of target bacteria to different phages aid in the recognition and epidemiological identification of the specific strain. Phage-based diagnostics have the potential to fill this gap as they are capable of rapid and precise target detection in a wide variety of environments. In particular, phages with lytic effect offer potential for rapid diagnostic test kits as they cause changes in many physical and chemical parameters while killing bacteria. **In Chapter 2**, a review of smartphone rapid diagnostic test kits is presented to help detect important microbial targets, including bacteriophage. It has been summarized that smartphone phage detection is now possible, which will allow improved detection and measurement of phages in many areas.

Chapter 3 explores a new way of detecting point-of-care phage lysis and demonstrates for the first time that label-free microfluidic bacteria detection can be used to determine host specificity for therapeutic bacteriophage. **In Chapter 4**, the study was taken one step further and a method to measure bacteriophages using microfluidic dip sticks, that overcomes the difficulties of inexpensive and traditional methods, is presented.

Platelets, like bacteria, are small and scatter light, and hence can be quantified by turbidimetry. **In Chapter 5**, progress towards the development of a platelet detection system that will overcome the difficulties of traditional methods is reported.

The organization of the content of the PhD is summarized in Figure 4.

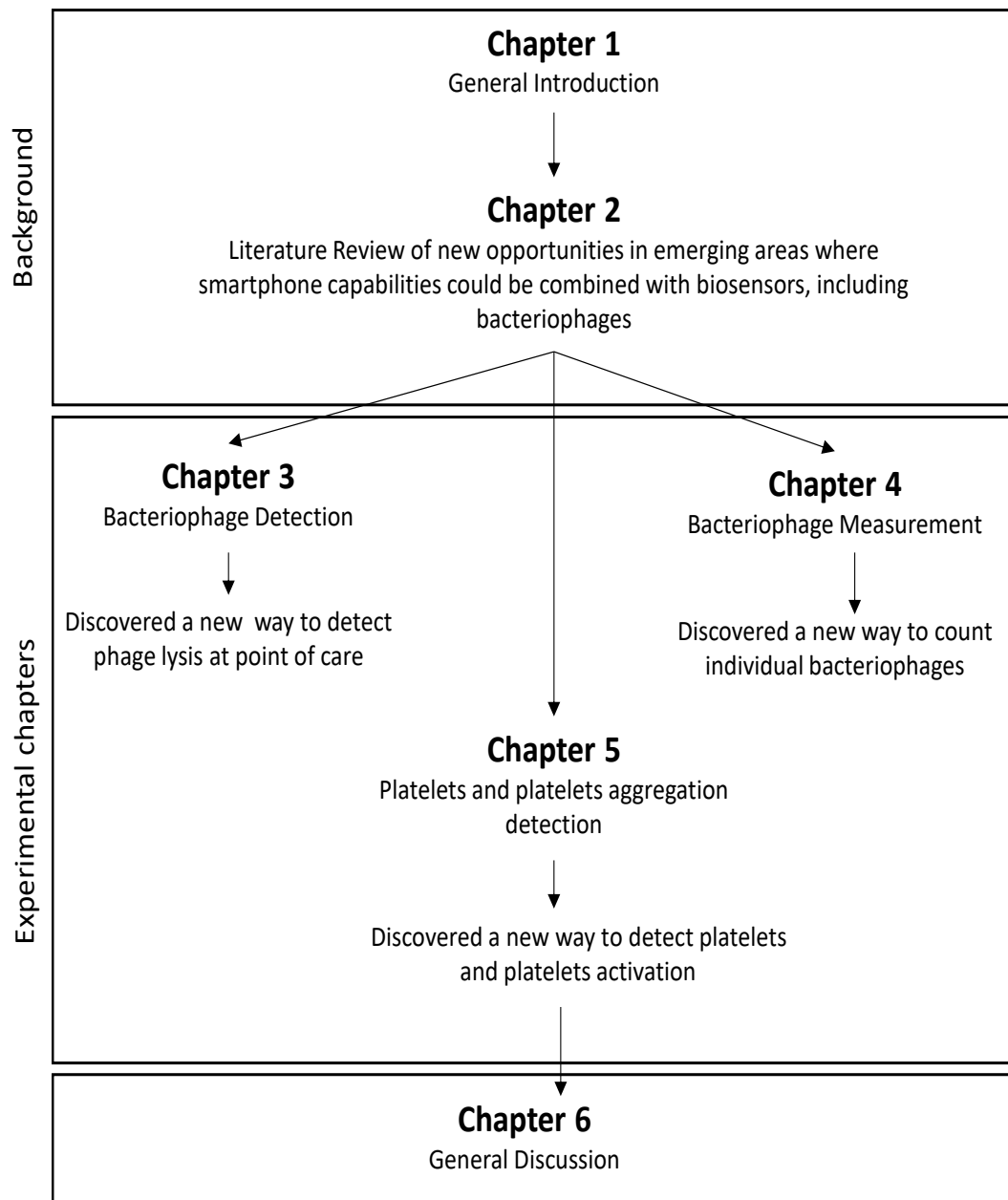


Figure 4: Schematic overview of the thesis

References- General Introduction

- Ács, N., M. Gambino and L. Brøndsted (2020). "Bacteriophage Enumeration and Detection Methods." Front Microbiol **11**: 594868.
- Alves, D. R., A. Gaudion, J. E. Bean, P. P. Esteban, T. C. Arnot, D. R. Harper, W. Kot, L. H. Hansen, M. C. Enright, A. T. A. Jenkins and J. L. Schottel (2014). "Combined Use of Bacteriophage K and a Novel Bacteriophage To Reduce Staphylococcus aureus Biofilm Formation." Applied and Environmental Microbiology **80**(21): 6694-6703.
- Amiri Fahliyani, S., K. Beheshti-Maal and F. Ghandehari (2018). "Novel lytic bacteriophages of Klebsiella oxytoca ABG-IAUF-1 as the potential agents for mastitis phage therapy." FEMS Microbiology Letters **365**(20).
- Betts, A., M. Vasse, O. Kaltz and M. E. Hochberg (2013). "Back to the future: evolving bacteriophages to increase their effectiveness against the pathogen Pseudomonas aeruginosa PAO1." Evol Appl **6**(7): 1054-1063.
- Breyne, K., R. W. Honaker, Z. Hobbs, M. Richter, M. Żaczek, T. Spangler, J. Steenbrugge, R. Lu, A. Kinkhabwala, B. Marchon, E. Meyer and L. Mokres (2017). "Efficacy and Safety of a Bovine-Associated Staphylococcus aureus Phage Cocktail in a Murine Model of Mastitis." Frontiers in Microbiology **8**(2348).
- Brüssow, H., C. Canchaya and W. D. Hardt (2004). "Phages and the evolution of bacterial pathogens: from genomic rearrangements to lysogenic conversion." Microbiol Mol Biol Rev **68**(3): 560-602, table of contents.
- Chen, J., S. D. Alcaine, Z. Jiang, V. M. Rotello and S. R. Nugen (2015). "Detection of Escherichia coli in Drinking Water Using T7 Bacteriophage-Conjugated Magnetic Probe." Analytical Chemistry **87**(17): 8977-8984.
- Chibani-Chennoufi, S., A. Bruttin, M. L. Dillmann and H. Brüssow (2004). "Phage-host interaction: an ecological perspective." J Bacteriol **186**(12): 3677-3686.
- Cox, C. R., K. R. Jensen, R. R. Mondesire and K. J. Voorhees (2015). "Rapid detection of Bacillus anthracis by γ phage amplification and lateral flow immunochromatography." Journal of Microbiological Methods **118**: 51-56.
- Culmone, C., P. W. J. Henselmans, R. I. B. van Starckenburg and P. Breedveld (2020). "Exploring non-assembly 3D printing for novel compliant surgical devices." PLOS ONE **15**(5): e0232952.
- da Silva Duarte, V., R. S. Dias, A. M. Kropinski, S. Campanaro, L. Treu, C. Siqueira, M. S. Vieira, I. da Silva Paes, G. R. Santana, F. Martins, J. S. Crispim, A. da Silva Xavier, C. G. Ferro, P. M. P. Vidigal, C. C. da Silva and S. O. de Paula (2018). "Genomic analysis and immune response in a murine mastitis model of vB_EcoM-UFV13, a potential biocontrol agent for use in dairy cows." Scientific Reports **8**(1): 6845.
- de Kraker, M. E. A., A. J. Stewardson and S. Harbarth (2016). "Will 10 Million People Die a Year due to Antimicrobial Resistance by 2050?" PLOS Medicine **13**(11): e1002184.
- Diep, T. T., P. P. Ray and A. D. Edwards (2022). "Methods for rapid prototyping novel labware: using CAD and desktop 3D printing in the microbiology laboratory." Lett Appl Microbiol **74**(2): 247-257.
- Donlan, R. M. and J. W. Costerton (2002). "Biofilms: survival mechanisms of clinically relevant microorganisms." Clin Microbiol Rev **15**(2): 167-193.
- Dönmez, S. İ., S. H. Needs, H. M. I. Osborn and A. D. Edwards (2020). "Label-free smartphone quantitation of bacteria by darkfield imaging of light scattering in fluoropolymer micro capillary film allows portable detection of bacteriophage lysis." Sensors and Actuators B: Chemical **323**: 128645.
- Farooq, U., Q. Yang, M. W. Ullah and S. Wang (2018). "Bacterial biosensing: Recent advances in phage-based bioassays and biosensors." Biosens Bioelectron **118**: 204-216.
- Geng, H., W. Zou, M. Zhang, L. Xu, F. Liu, X. Li, L. Wang and Y. Xu (2020). "Evaluation of phage therapy in the treatment of Staphylococcus aureus-induced mastitis in mice." Folia Microbiologica **65**(2): 339-351.

Gill, J. J., J. C. Pacan, M. E. Carson, K. E. Leslie, M. W. Griffiths and P. M. Sabour (2006). "Efficacy and Pharmacokinetics of Bacteriophage Therapy in Treatment of Subclinical *Staphylococcus aureus* Mastitis in Lactating Dairy Cattle." Antimicrobial Agents and Chemotherapy **50**(9): 2912-2918.

Gill, J. J., J. C. Pacan, M. E. Carson, K. E. Leslie, M. W. Griffiths and P. M. Sabour (2006). "Efficacy and pharmacokinetics of bacteriophage therapy in treatment of subclinical *Staphylococcus aureus* mastitis in lactating dairy cattle." Antimicrobial agents and chemotherapy **50**(9): 2912-2918.

Gu Liu, C., S. I. Green, L. Min, J. R. Clark, K. C. Salazar, A. L. Terwilliger, H. B. Kaplan, B. W. Trautner, R. F. Ramig and A. W. Maresso (2020). "Phage-Antibiotic Synergy Is Driven by a Unique Combination of Antibacterial Mechanism of Action and Stoichiometry." mBio **11**(4).

Gurney, J., S. P. Brown, O. Kaltz and M. E. Hochberg (2020). "Steering Phages to Combat Bacterial Pathogens." Trends in Microbiology **28**(2): 85-94.

Guttman, B., R. Raya and E. Kutter (2005). "Basic phage biology." Bacteriophages: Biology and applications **4**.

Halkare, P., N. Punjabi, J. Wangchuk, S. Madugula, K. Kondabagil and S. Mukherji (2021). "Label-Free Detection of *Escherichia coli* from Mixed Bacterial Cultures Using Bacteriophage T4 on Plasmonic Fiber-Optic Sensor." ACS Sensors **6**(7): 2720-2727.

Hamza, A., S. Perveen, Z. Abbas and S. U. Rehman (2016). "The Lytic SA Phage Demonstrate Bactericidal Activity against Mastitis Causing *Staphylococcus aureus*." Open Life Sciences **11**(1): 39-45.

Hanlon, G. W. (2007). "Bacteriophages: an appraisal of their role in the treatment of bacterial infections." International Journal of Antimicrobial Agents **30**(2): 118-128.

Hay, I. D. and T. Lithgow (2019). "Filamentous phages: masters of a microbial sharing economy." EMBO Rep **20**(6).

Iwano, H., Y. Inoue, T. Takasago, H. Kobayashi, T. Furusawa, K. Taniguchi, J. Fujiki, H. Yokota, M. Usui, Y. Tanji, K. Hagiwara, H. Higuchi and Y. Tamura (2018). "Bacteriophage Φ SA012 Has a Broad Host Range against *Staphylococcus aureus* and Effective Lytic Capacity in a Mouse Mastitis Model." Biology (Basel) **7**(1).

Janik, M., E. Brzozowska, P. Czyszczon, A. Celebańska, M. Koba, A. Gamian, W. J. Bock and M. Śmietana (2021). "Optical fiber aptasensor for label-free bacteria detection in small volumes." Sensors and Actuators B: Chemical **330**: 129316.

Jassim, S. A. A. and R. G. Limoges (2014). "Natural solution to antibiotic resistance: bacteriophages 'The Living Drugs'." World journal of microbiology & biotechnology **30**(8): 2153-2170.

Jo, Y., J. Jung, M.-h. Kim, H. Park, S.-J. Kang and Y. Park (2015). "Label-free identification of individual bacteria using Fourier transform light scattering." Optics Express **23**(12): 15792-15805.

Jolles, J. W. (2021). "Broad-scale applications of the Raspberry Pi: A review and guide for biologists." Methods in Ecology and Evolution **12**(9): 1562-1579.

Kelly, D., O. McAuliffe, R. P. Ross and A. Coffey (2012). "Prevention of *Staphylococcus aureus* biofilm formation and reduction in established biofilm density using a combination of phage K and modified derivatives." Letters in Applied Microbiology **54**(4): 286-291.

Kim, J., M. Kim, S. Kim and S. Ryu (2017). "Sensitive detection of viable *Escherichia coli* O157:H7 from foods using a luciferase-reporter phage ϕ iV10lux." International Journal of Food Microbiology **254**: 11-17.

Kim, K., H. K. Kim, H. Lim and H. Myung (2016). "A low cost/low power open source sensor system for automated tuberculosis drug susceptibility testing." Sensors **16**(6): 942.

Koskella, B. and M. A. Brockhurst (2014). "Bacteria–phage coevolution as a driver of ecological and evolutionary processes in microbial communities." FEMS Microbiology Reviews **38**(5): 916-931.

Kutter, E. and A. Sulakvelidze (2004). Bacteriophages: biology and applications, Crc press.

Kwiatk, M., S. Parasion, L. Mizak, R. Gryko, M. Bartoszcze and J. Kocik (2012). "Characterization of a bacteriophage, isolated from a cow with mastitis, that is lytic against *Staphylococcus aureus* strains." Archives of Virology **157**(2): 225-234.

Mattey, M. and J. Spencer (2008). "Bacteriophage therapy--cooked goose or phoenix rising?" Curr Opin Biotechnol **19**(6): 608-612.

Miedzybrodzki, R., W. Fortuna, B. Weber-Dabrowska and A. Górski (2007). "Phage therapy of staphylococcal infections (including MRSA) may be less expensive than antibiotic treatment." Postepy Hig Med Dosw (Online) **61**: 461-465.

Molineux, I. J. (2001). "No syringes please, ejection of phage T7 DNA from the virion is enzyme driven." Mol Microbiol **40**(1): 1-8.

Muller, C. (2022). "Antibiotics and Antimicrobials Resistance: Mechanisms and New Strategies to Fight Resistant Bacteria." Antibiotics **11**(3): 400.

Murray, E., L. A. Draper, R. P. Ross and C. Hill (2021). "The Advantages and Challenges of Using Endolysins in a Clinical Setting." Viruses **13**(4).

Ngassam-Tchamba, C., J. N. Duprez, M. Fergestad, A. De Visscher, T. L'Abée-Lund, S. De Vlieghe, Y. Wasteson, F. Touzain, Y. Blanchard, R. Lavigne, N. Chanishvili, D. Cassart, J. Mainil and D. Thiry (2020). "In vitro and in vivo assessment of phage therapy against *Staphylococcus aureus* causing bovine mastitis." Journal of Global Antimicrobial Resistance **22**: 762-770.

Opperman, C. J., J. M. Wojno and A. J. Brink (2022). "Treating bacterial infections with bacteriophages in the 21st century." Southern African Journal of Infectious Diseases **37**(1): 7.

Pearce, J. (2017). "Impacts of open source hardware in science and engineering." The Bridge.

Porter, J., J. Anderson, L. Carter, E. Donjacour and M. Paros (2016). "In vitro evaluation of a novel bacteriophage cocktail as a preventative for bovine coliform mastitis." Journal of Dairy Science **99**(3): 2053-2062.

Prestinaci, F., P. Pezzotti and A. Pantosti (2015). "Antimicrobial resistance: a global multifaceted phenomenon." Pathogens and global health **109**(7): 309-318.

Read, A. F. and R. J. Woods (2014). "Antibiotic resistance management." Evolution, medicine, and public health **2014**(1): 147-147.

Reis, N. M., J. Pivetal, A. L. Loo-Zazueta, J. M. Barros and A. D. Edwards (2016). "Lab on a stick: multi-analyte cellular assays in a microfluidic dipstick." Lab Chip **16**(15): 2891-2899.

Rippa, M., R. Castagna, M. Pannico, P. Musto, G. Borriello, R. Paradiso, G. Galiero, S. Bolletti Censi, J. Zhou, J. Zyss and L. Petti (2017). "Octupolar Metastructures for a Highly Sensitive, Rapid, and Reproducible Phage-Based Detection of Bacterial Pathogens by Surface-Enhanced Raman Scattering." ACS Sensors **2**(7): 947-954.

Roos, W. H., I. L. Ivanovska, A. Evilevitch and G. J. L. Wuite (2007). "Viral capsids: mechanical characteristics, genome packaging and delivery mechanisms." Cellular and molecular life sciences : CMLS **64**(12): 1484-1497.

Schmelcher, M., A. M. Powell, M. J. Camp, C. S. Pohl and D. M. Donovan (2015). "Synergistic streptococcal phage λ SA2 and B30 endolysins kill streptococci in cow milk and in a mouse model of mastitis." Applied Microbiology and Biotechnology **99**(20): 8475-8486.

Shabani, A., C. A. Marquette, R. Mandeville and M. F. Lawrence (2013). "Magnetically-assisted impedimetric detection of bacteria using phage-modified carbon microarrays." Talanta **116**: 1047-1053.

Shabani, A., M. Zourob, B. Allain, C. A. Marquette, M. F. Lawrence and R. Mandeville (2008). "Bacteriophage-Modified Microarrays for the Direct Impedimetric Detection of Bacteria." Analytical Chemistry **80**(24): 9475-9482.

Sharkey, J. P., D. C. Foo, A. Kabla, J. J. Baumberg and R. W. Bowman (2016). "A one-piece 3D printed flexure translation stage for open-source microscopy." Review of Scientific Instruments **87**(2): 025104.

Singh, A., S. Poshtiban and S. Evoy (2013). "Recent Advances in Bacteriophage Based Biosensors for Food-Borne Pathogen Detection." Sensors **13**(2): 1763-1786.

Stone, R. (2002). "Bacteriophage therapy. Stalin's forgotten cure." Science **298**(5594): 728-731.

Summers, W. C. (2001). "Bacteriophage therapy." Annu Rev Microbiol **55**: 437-451.

Suttle, C. A. (2005). "Viruses in the sea." Nature **437**(7057): 356-361.

Sweeney, R. E. and J. Y. Yoon (2017). "Angular photodiode array-based device to detect bacterial pathogens in a wound model." IEEE Sens J **17**(21): 6911-6917.

Titze, I. and V. Krömker (2020). "Antimicrobial Activity of a Phage Mixture and a Lactic Acid Bacterium against Staphylococcus aureus from Bovine Mastitis." Vet Sci **7**(1).

Tjhung, K. F., S. Burnham, H. Anany, M. W. Griffiths and R. Derda (2014). "Rapid Enumeration of Phage in Monodisperse Emulsions." Analytical Chemistry **86**(12): 5642-5648.

Vandersteegen, K., W. Mattheus, P.-J. Ceysens, F. Bilocq, D. De Vos, J.-P. Pirnay, J.-P. Noben, M. Merabishvili, U. Lipinska, K. Hermans and R. Lavigne (2011). "Microbiological and Molecular Assessment of Bacteriophage ISP for the Control of Staphylococcus aureus." PLOS ONE **6**(9): e24418.

Waltham, C., J. Boyle, B. Ramey and J. Smit (1994). "Light scattering and absorption caused by bacterial activity in water." Appl Opt **33**(31): 7536-7540.

Yoon, J., K. Lee and Y. Park (2016). "A simple and rapid method for detecting living microorganisms in food using laser speckle decorrelation." arXiv preprint arXiv:1603.07343.

Yu, J., W. Huang, L. Chin, L. Lei, Z. Lin, W. Ser, H. Chen, T. Ayi, P. Yap and C. Chen (2014). "Droplet optofluidic imaging for λ -bacteriophage detection via co-culture with host cell Escherichia coli." Lab on a Chip **14**(18): 3519-3524.

Yue, H., Y. He, E. Fan, L. Wang, S. Lu and Z. Fu (2017). "Label-free electrochemiluminescent biosensor for rapid and sensitive detection of pseudomonas aeruginosa using phage as highly specific recognition agent." Biosensors and Bioelectronics **94**: 429-432.

Zhao, W., Y. Shi, G. Liu, J. Yang, B. Yi, Y. Liu, J. P. Kastelic, B. Han and J. Gao (2021). "Bacteriophage has beneficial effects in a murine model of *Klebsiella pneumoniae* mastitis." Journal of Dairy Science **104**(3): 3474-3484.

Chapter 2

Future Bioassays and Biosensing Technology for Smartphone Diagnostics: Opportunities for Bacteriophage, Aptamer and Cellular Measurements

Chapter summary: This chapter focuses on new opportunities in three emerging areas where smartphone capabilities can be combined with biosensors and microfluidics.

Bibliographic details: Sultan İlayda Dönmez, Abdullah Tahir Bayraç, Sarah H. Needs, Julie Hart, Helen M.I. Osborn, and Alexander D. Edwards

Author Contributions: S.I.D: Conceptualization, Investigation, Visualization, Formal analysis, Data analysis, Experimental design, Funding acquisition, Writing - original draft, Writing - review & editing. A.T.B: Visualization, Writing - review & editing (Major contribution of A.T.B. is reviewing the aptamer section). S.H.N: Visualization, Writing - review & editing (Major contribution OF S.H.N. is reviewing the spelling mistakes). J.H: Visualization, Writing - review & editing (Major contribution of J.H. is reviewing the cellular measurements section). H.M.I.O: Supervision, Writing - review & editing (Major contribution is supervision and reviewing). A.D.E: Conceptualization, Funding acquisition, Supervision, Writing - review & editing (Major contribution is supervision and reviewing).

Submitted to *Biosensors and Bioelectronics: X*, under revision

Future Bioassays and Biosensing Technology for Smartphone Diagnostics: Opportunities for Bacteriophage, Aptamer and Cellular Measurements

Sultan İlayda Dönmez¹, Abdullah Tahir Bayraç², Sarah H Needs¹, Julie Hart¹, Helen M.I. Osborn¹, and Alexander D Edwards¹

¹*School of Pharmacy, University of Reading, Whiteknights, Reading, RG6 6AD UK*

²*Department of Bioengineering, Karamanoglu Mehmetbey University, Yunus Emre Campus, 70100 Karaman, Turkey*

Author Contributions: Author Contributions: S.I.D: Conceptualization, Investigation, Visualization, Formal analysis, Data analysis, Experimental design, Funding acquisition, Writing - original draft, Writing - review & editing. A.T.B: Visualization, Writing - review & editing (Major contribution of A.T.B. is reviewing the aptamer section). S.H.N: Visualization, Writing - review & editing (Major contribution OF S.H.N. is reviewing the spelling mistakes). J.H: Visualization, Writing - review & editing (Major contribution of J.H. is reviewing the cellular measurements section). H.M.I.O: Supervision, Writing - review & editing (Major contribution is supervision and reviewing). A.D.E: Conceptualization, Funding acquisition, Supervision, Writing - review & editing (Major contribution is supervision and reviewing).

ABSTRACT

The potential for portable sensing, computing, and imaging capabilities of consumer smartphones to be exploited in healthcare has been explored in many areas, from reading lateral flow immunoassays, to supporting clinical decision-making and symptom tracking. This review looks forward beyond recent demonstrations that smartphones can record immunoassay and nucleic acid test results, towards novel bioanalytical methods. We focus on three emerging areas where smartphone capabilities can be coupled with biosensors and microfluidics. Firstly, bacteriophages are valuable for microbial detection, and detection of bacteriophage is increasingly important to realise their potential as novel antimicrobial therapeutics. Secondly, aptamers can be used to detect targets in a manner similar to antibodies, but with distinct benefits. Finally, cellular measurements are vital in laboratory bioscience, but for cellular measurements to become mainstream for clinical diagnostics, increased portability is important. For all three areas, smartphone analysis could transport these bioassays out of the lab and towards the patient. After briefly introducing the main concepts of smartphone bioassay detection, we outline recent innovations in these three detection areas that are already – or could soon be – combined with a smartphone readout. By combining the extensive analytical capacity for these miniature computers in our pockets, with novel bacteriophage, aptamer, and cellular analysis, this sophisticated consumer instrumentation may bring new diagnostic healthcare products into our homes.

KEYWORDS: smartphone, bacteriophage, cellular measurement, aptamers, clinical diagnostic, point-of-care testing

Contents

1. INTRODUCTION: BIOSENSING WITH SMARTPHONES, AND NOVEL BIOLOGICAL BIOSENSING METHODS.....	2
1.1 Opportunities for Smartphone Diagnostics: Why Might Smartphones Be Useful?	2
1.2 Opportunities for Smartphone Diagnostics: What Can They Measure?	2
1.3 Challenges for Smartphone Diagnostics	3
1.4 Emerging Biosensing Approaches: What Kind of Assays Could Fit with Smartphones?.....	4
2. PHAGE-BASED BIOSENSING AND SENSING PHAGES	5

2.1 Bacteria Detection Using Phage.....	6
2.2 Need For Detecting Phages and Emerging Tools and Methods.....	8
2.3 Bacteriophage Biosensing Conclusions	11
3. APTAMERS	11
3.1 Introduction to Aptamers- Advantages and Opportunities.....	11
3.2 Binding Assays	12
3.2.1 Diagnosis of Pathogens.....	12
3.3 Diagnosis for Blood	13
3.4 Detection of Pharmaceuticals.....	14
3.5 Monitoring of Environmental Contaminants	15
3.6 Summary of Aptamer Section.....	16
4. CELLULAR MEASUREMENT	16
4.1 Simplified Cellular Measurements.....	16
4.2 Phone Based Flow cytometry	17
4.2.1 Blood Cell Counting	17
4.3 Smartphone Microscopy	18
4.4 Cellular Measurements Conclusions.....	19
5. CONCLUSION.....	19

1. INTRODUCTION: BIOSENSING WITH SMARTPHONES, AND NOVEL BIOLOGICAL BIOSENSING METHODS

1.1 Opportunities For Smartphone Diagnostics: Why Might Smartphones Be Useful?

The potential for bringing medical services such as point-of-care diagnosis directly to the site of patient treatment have been increasing in recent years, built on miniaturised healthcare technology. While we may still need to go to a healthcare facility even for simple tests or to consult a clinician, a move towards diagnosis of illness without the need to go to a hospital or wait for samples to travel to a diagnostic lab for testing, is a major trend both for healthcare professionals and patients. The long-term drivers for point-of-care and point-of-need testing have been amplified by the COVID-19 pandemic, where infection control and workforce pressures have made access to hospital care and lab testing harder (May, Tran et al. 2021). Beyond public health, portable testing is playing an increasingly important role in other areas of great need for bioanalytical measurements, including environmental monitoring and food safety testing. Together, these expanding opportunities for portable, rapid, point-of-need bioassays may in part be met by combining smartphones and in particular smartphone-based imaging devices alone or in combination with additional devices or accessory instruments, in a wide variety of biomedical and public health applications (Valera, Jankelow et al. 2021). In medicine, biochemical and biological measurements are almost always combined with clinical measurements such as symptoms reported by patients and with clinical observations. Smartphones can also help by combining diagnostic measurements with these additional clinical parameters plus other external factors (Brintz, Haaland et al. 2021, Reimer, Ahmed et al. 2021). They can combine measurements and data in algorithms, as well as record and document data, as healthcare moves into a digital age.

1.2 Opportunities for Smartphone Diagnostics: What Can They Measure?

With the rapid growth of mobile technologies, phones have been adorned with high-performance computing, networking, instruments, lenses, and sensors, making smartphones cost-effective yet powerful, portable, and widely available devices. As well as facilitating telehealth consultations, compliance aids through prompting medicines use, and related diverse mobile health applications, they can be used to record or read the result of a point-of-care test. Smartphones can be most easily adapted for point-of-care testing through two broad approaches. Firstly, inbuilt sensors can be

exploited directly. The simplest example is taking a digital photograph of a totally independent assay device (e.g., lateral flow test), often one that would previously be read by the eye (Mak, Beni et al. 2016). Likewise, smartphone cameras can be readily adapted to record typical quantitative laboratory measurements such as 96-well plate absorbance measurements (Bergua, Álvarez-Diduk et al. 2022). Another example of sensors that can be exploited medically is accelerometers and phone features that track movement. Secondly, the powerful computing power of smartphones can be combined with external equipment or instrumentation to make measurements, for example electrochemical bioassays; in this case the inbuilt electronics record and analyse external sensors of any (portable) nature. The extensive wireless communication options including Bluetooth and WiFi plus broadband mobile networking permit a wide range of connections to be made locally between the test or sensor and phone handset, and globally via the internet for example to cloud storage, data integration, or remote analysis. Thus, arguably, any portable instrumentation may benefit from the smartphone as a human interface, as a networking connection, and as an analysis tool.

There is a distinction between a single test to detect target or measure analyte concentration using a bioassay, vs continuous measurement by a biosensor. Smartphones are technologically capable of recording both bioassays and biosensors and in this review, we will discuss opportunities for both. One notable advantage of smartphone-connected diagnostic testing is in facilitating longer term time-resolved measurements. Frequent measurements are particularly onerous to the patient and health service if tests require laboratory processing. In contrast, smartphone-enabled bioassays or biosensors provide a ready means of monitoring patients over time.

1.3 Challenges for Smartphone Diagnostics

Given these technical opportunities, why are smartphones not used more? In spite of extensive publications demonstrating that smartphones can read diagnostic bioassays of a range of complexity, they are far from mainstream in clinical diagnostics. Significant barriers remain to adoption of such technology into health systems. The consumer nature of smartphones must be considered – the clinical diagnostic developers and manufacturers currently have no control over the technical capability of smartphones, raising regulatory challenges alongside the difficulty of standardising. Furthermore, instrumentation and handset specification is dictated by consumer choice, not bioassay or medical requirements. For example, most smartphone cameras use complementary metal oxide semiconductor (CMOS) sensors. As more advanced CMOS sensors become cheaper, they should have improved performance with greater potential for useful bioassay results recording (Frederick, 2013). However, assay dynamic range can be significantly limited not only by sensor capability but also by proprietary post-processing in image capture and smartphone software, designed to make personal photos desirable, not to standardise optical measurements. The technical capabilities can vary between products, and even the same handset can change performance when software is updated. The technical capability of cameras can limit performance of bioassays and sensing; for example, filters in the photo detectors used can affect assay readout. Thus, the commonly used filter model for colour photography is the Bayer model, where green filter is used excessively, imitating the human eye. The spectral sensitivity (e.g., bias to green) must therefore be taken into account (Madden and Giorgianni, 2007) making it harder to directly substitute some laboratory instruments (e.g., spectrophotometers) with a smartphone camera. Likewise, smartphones are not specifically designed to record data input from external instruments or devices, so significant effort is required to exploit the input-output capability. Security, privacy and data management considerations are further critical barriers. Regulatory barriers are considerable – products are likely to need to meet not only medical device regulations, but also data privacy laws. Finally, clinical uptake of new near-patient test products such as smartphone diagnostics will inevitably require innovation in healthcare processes, which can delay uptake. Nevertheless, if the tension between consumer design drivers (cost, purpose, data security)

versus technical requirements needed for instrumentation can be overcome, then the range of bioassay measurements that can be made is potentially extensive. Many innovative companies are driving smartphone diagnostics forward and working hard to overcome these barriers, including 1drop, Biomeme, Cellscope, Cellmic, Healthyio, MinuteUTL, ical-Q, iXensor, Interpath, inui Health, Lifelens, Novarum, Reliance Immune Diagnostics, and Scanwell. However, this review is focussed on technological possibilities for smartphone readout of bioassays and biosensors, rather than surveying products that have reached the market and/or been adopted; it must be remembered that the above barriers must still be overcome before such concepts can become mainstream clinical reality.

1.4. Emerging Biosensing Approaches: What Kind of Assays Could Fit with Smartphones?

A wide range of bioassay approaches and biosensing modes have been applied to healthcare especially in clinical diagnostics. These include enzymatic, chemical and electrochemical assays, alongside immunoassays and nucleic acid detection (NAT) and sequencing methods (Nasser, Soleimani et al. 2018). Perhaps the assay classes that have been most widely demonstrated using smartphone readout are immunoassays and nucleic acid detection (Chuang, Deng et al. 2019), reflecting the broad range of clinical applications that these two detection methods can address. The use of smartphones for immunoassays has been reviewed by (Vashist and Luong 2018). The application of smartphones to nucleic acid testing was recently reviewed by (Rajendran, Bakthavathsalam et al. 2021). Together, these assay classes have provided technological demonstration of the great potential of smartphones for the capture and analysis of biomedical measurements. Although this illustrates the technical feasibility for recording immunoassays or nucleic acid tests by recording colour change by imaging (and other readouts), to be performed using smartphones, many other emerging biosensing and detection approaches could also benefit portable formats combined with smartphone measurement. These include novel bacteriophage assays, the use of aptamers, and measurement of cells (Figure 1).

The diverse applications of immunoassays and NAT to clinical diagnostics are established, and the potential for these two assay classes to be combined with smartphones are clear, yet they cannot address all clinical needs. This review looks to the future, identifying emerging opportunities for smartphone diagnostics that explore three novel biosensing methods. These offer alternatives to antibody-based binding of analytical targets, and to NAT that detects target sequences. Novel microbial detection tools based on bacteriophages – viruses that infect bacteria – may offer improved analytical sensitivity and speed of identification (Figure 1A); and in parallel better assays and biosensors for detecting and measuring phages are essential to make best use of bacteriophage, for example as novel antimicrobial agents to replace conventional antibiotic drugs (Figure 1A). We also summarise recent biosensing methods that exploit aptamers (Figure 1B) – an alternative binding agent distinct from antibodies. Finally, several studies have explored portable, miniaturised measurement of cells, for example in blood testing (Figure 1C), and we outline examples that illustrate the potential of this approach. All three methods can offer additional benefits if integrated with smartphones, and have the potential to allow smartphones to become portable biosensors in future. Many of these examples are suited to optical detection, and therefore can be compatible with digitally recording results via the smartphone camera.

Where already published, we highlight proof-of-concept using smartphones; with other examples, we identify technology that is compatible with, or could be adapted for, smartphone detection. We note that each of these three topics has a small yet rapidly growing rate of publications, based on simple Scopus literature searches (Figures 1D-G) including examples of each including the term “smartphone”, confirming these represent emerging topics of increased research attention. Finally, we also mention where there is overlap for example where immunoassays and NAT can be used to measure phage or cells.

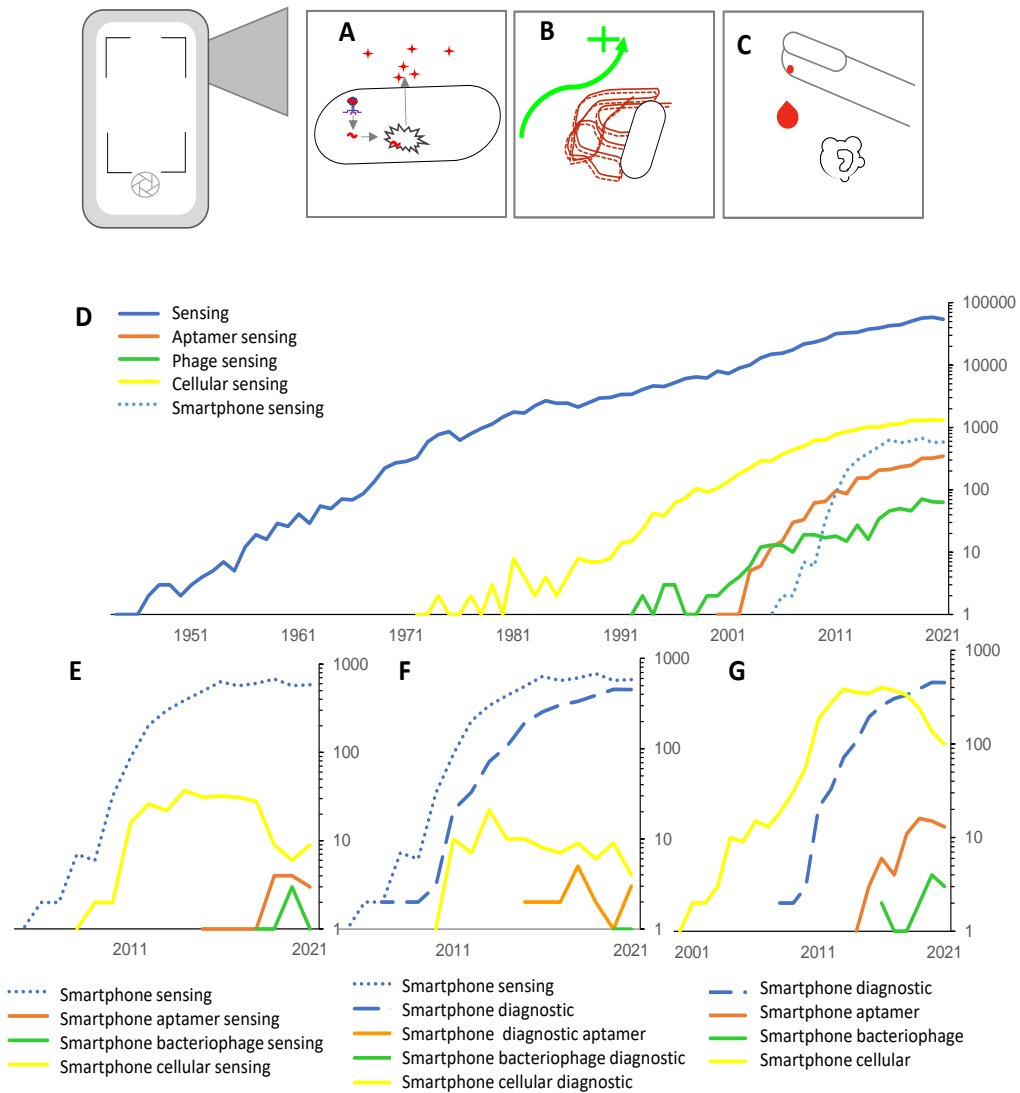


Figure 1. Emerging trends and opportunities for smartphone sensing and diagnostics. Diagram illustrating (A) bacteriophage biosensing, (B) aptamers and (C) cellular measurements including blood testing. (D-G) Scopus searches indicating number of articles with indicated search parameters. (Indicate date that the analysis was performed is 02/2022)

2. PHAGE-BASED BIOSENSING AND SENSING PHAGES

Phage-based detection systems have started to attract attention having high specificity and sensitivity for microbial targets, with low cost, and increasingly easy replication. Phages typically confer a very high natural affinity to the host cells they target, and can therefore serve as recognition agents for sensors. Phage amplification could become a very powerful tool for analytical microbiology, and has great potential to be combined with smartphones to permit out-of-lab operation. Firstly, we will describe recent advances in phage-based detection of microbes in a variety of configurations (Figure 2) that are already – or may soon be compatible with – smartphone detection. In parallel, better methods and assays to detect and measure phages are urgently needed, because bacteriophages also have great potential as novel antimicrobial therapies. To produce effective biologic drugs and subsequently use these for patients, phages must be discovered and quantified. We will therefore secondly outline advances in the detection of bacteriophages, and how these assays and methods can deliver smartphone measurement of phages.

2.1. Bacteria Detection Using Phage

The WHO has predicted that 2 billion people use a drinking water source contaminated with faeces, and around a million people are estimated to die from unhealthy drinking water and sanitation every year (Edition 2011). *Escherichia coli* in drinking water is a major cause of water pollution and mostly comes from untreated waste from households and factories, or from other sources like animal manure. Exploiting bacteriophages that specifically infect bacterial hosts that are common contaminants is an alternative method to develop biosensor methods and devices that can detect human and animal pathogens for water safety testing.

In recent years, phage-based bioassays have been developed using various output signals suited to recording by smartphone imaging, such as colorimetric, fluorescence and luminescence using either modified bacteriophage (Figure 2A) or signals of bacteria lysis (Figure 2B). Fluorescence based detection assays include modified phage for bacterial detection. Once the phage has transferred its genetic material into the host, it can be detected using fluorescent emissions of the fluorophore encoded within nucleic acid in the phage genome (Goodridge, Chen et al. 1999, Mosier-Boss, Lieberman et al. 2003, Willford, Bisha et al. 2011) (Figure 2A). A portable system has been developed that detects *E. coli* and *Salmonella* via a fluorescent reporter. A bacteriophage is genetically modified to include GFP reporter which is synthesised by the bacteria following infection. The fast and sensitive system can reproducibly detect viable bacteria in sea water with the sensitivity of 10 CFU / mL in 1 hour without an enrichment step (Vinay, Franche et al. 2015) (Figure 2A). *E. coli* was detected in water samples by monitoring galactosidase release after cell lysis in a paper-based culture device using T4 bacteriophage with a digital camera. It has been shown that <10 CFU/ml cells can be detected with bioluminescence signal after 5.5 hours incubation and colourimetrically after 8 hours incubation (Burnham, Hu et al. 2014) (Figure 2B).

Bacterial detection method using phages integrated into magnetic beads (Figure 2C) or for electrochemical detection method is an older method. The use of phages for targeted binding might avoid centrifugation or filtration steps. While it is necessary for this technique to use flow cytometry for bacteria detection, successful high binding efficiencies were observed for bacteria at high cell concentrations. However, when the bacterial concentration drops to 10^3 , 10^2 CFU/mL, the binding affinity critically drops respectively to 50% and 8% respectively, this brings back the need for centrifuge (Shabani, Marquette et al. 2013). With the addition of a smartphone to this method, which detects bacteria with bacteriophage-conjugated magnetic beads, the need for flow cytometry is eliminated. *E. coli* capturing with T7 bacteriophage conjugated magnetic beads was conducted for rapid detection of *E. coli* from drinking water. After phage infection, galactosidase is released from the lysed bacteria, which changes an enzyme substrate color from yellow to red, allowing for smartphone-based detection. After 2.5 hours of incubation, the detection limit of *E. coli* was found to be 10^4 CFU/mL. The samples were pre-enriched for 6 hours in order to lower this limit and make more precise measurements. At the end of this period, the detection limit was found to be 10 CFU/mL. Thus, it has been shown that *E. coli* can be detected from drinking water without the need for large laboratory equipment (Chen, Alcaine et al. 2015). By using genetically modified and magnetized phages, it was desired to detect *E. coli* with higher sensitivity from drinking water. After magnetic enrichment, the detection limit was increased to <10 CFU/100 mL of *E. coli*, exploiting the luminescence emitted by phages encoding luminescent reporter enzymes using a smartphone (Zurier, Duong et al. 2020). In a study to detect *Staphylococcus aureus* from milk, bacteria are captured with a magnetic nanoparticle and enzyme-linked phage fusion protein and with the help of a magnet, this complex bound to target pathogen is separated from the milk. By adding chromogenic substrate, oxidation based color change was observed proportional to the number of bacteria (Liu, Wang et al. 2020) (Figure 2C).

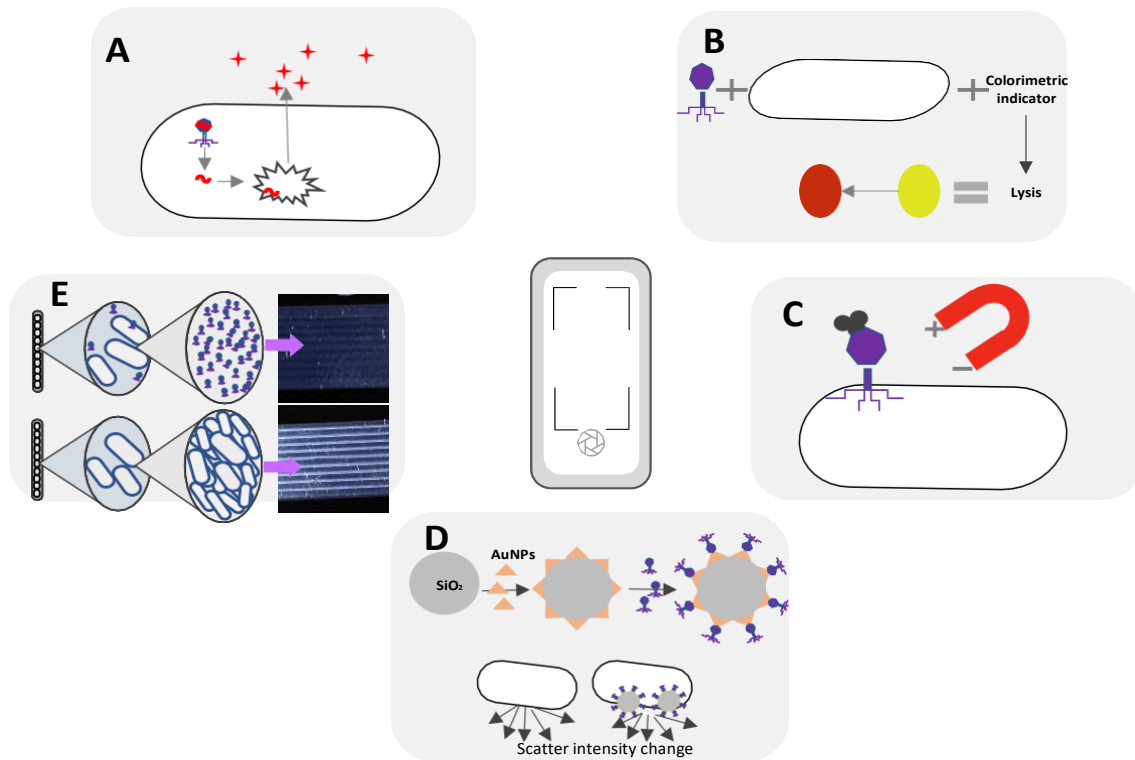


Figure 2. Examples of the range of phage detection methods for pathogens and microbes A) After the fluorescent reporter gene is added to the phage, bacteria can be detected by detecting the fluorescent products formed as a result of the expression of this gene in the host cell (Dow, Kotz et al. 2018). B) After cell lysis as caused by phages, bacteria can be detected in a short time with a colorimetric indicator (Burnham, Hu et al. 2014). C) Bacteria can be captured and rapidly detected with bacteriophage-conjugated magnetic beads (Chen, Alcaine et al. 2015). D) Darkfield detection of bacteria using bacteriophage-immobilized SiO₂@Aunp core-shell nanoparticles (Imai, Mine et al. 2019). E) In the darkfield imaging system, by measuring the light scattering by bacterial cells, bacteria and phage can be detected quickly and cheaply using a single LED plus smartphone (Dönmez, Needs et al. 2020).

Detection systems that make use of darkfield imaging of light scattering can be adapted to microbial detection by combining with phages if those phages can lyse bacterial particles, either increasing or decreasing scatter. To detect *S. aureus*, suitable phages were conjugated to silica nanospheres plus gold nanoparticles (AuNPs). When added to a bacterial suspension, the conjugates bound the target with high specificity, increasing the light scattering intensity of the target bacteria. Using this aggregation-induced light scattering signal, 10⁴ CFU/mL target bacteria could be detected (Imai, Mine et al. 2019) (Figure 2D). In a simple darkfield microfluidic device imaging system, unlabelled bacteria can be detected directly using a very simple and inexpensive method capable of measuring the lytic effect of phages. With a single LED and portable 3D-printed box, the high light scattering signal produced in the presence of bacterial cells was eliminated by adding a lytic bacteriophage. Strain-specific phage activity was detected in just 1.5 hours of incubation, with complete lysis and elimination of the light scatter signal complete at 4 hours (Dönmez, Needs et al. 2020) (Figure 2E).

Rapid diagnostic platforms are essential for more effective treatment of bacteremia to lower mortality. In 2018, Dow et al., who detected bacteria in the blood with luminescence-dependent phages, with

the potential for far faster results, over conventional assays that could take days with standard laboratory techniques. They used microfluidic chips to separate the bacteria from the blood, taking advantage of the size difference between blood cells and bacteria. By making this separation, they eliminated the lost time that would occur with the bacterial enrichment by blood culture. These purified bacteria were subsequently detected with luminescence-bound phages in 60 minutes, 33 times better than the standard method (Dow, Kotz et al. 2018).

Typhoid, an infectious disease caused by *Salmonella enterica* serovar Typhi and related bacterial enteric pathogens, affects 21 million people/year and is responsible for about half a million people deaths each year (WHO 2008). Because traditional serological tests for typhoid diagnosis require days, faster and cheaper alternatives are essential. It is underdeveloped and resource-limited areas where typhoid epidemics are common, thus portable, robust and rugged as well as inexpensive methods are vital. A study conducted in 2020 developed a simple and inexpensive phage-based biosensor for detection of typhoidal *Salmonella*. High-titre *Salmonella* phages were mixed in separate wells of a microtiter plate, without pre-enrichment, with *Salmonella* and resazurin. After 2 hours of incubation, 5×10^4 CFU/well could be detected with colour change from blue to pink (Vaidya, Ravindranath et al. 2020). To extend this phage-based detection to different bacterial pathogens, in 2019, Peng et al designed chimeric phages to detect the desired bacteria more quickly and sensitively. After the phages bind to the target, they also allow the gold nanoparticles to bind, causing a color change. This study showed that two strains of *E. coli*, *Pseudomonas aeruginosa*, *Vibrio cholerae*, and two strains of *Xanthomonas campestris* could be detected in less than 1 hour (Peng and Chen 2019). This phage pathogen detection method was subsequently applied to complex biological samples such as milk, urine, and samples from infected pigs, proving the potential for rapid and sensitive detection of pathogenic bacteria in drinks, food and clinical samples. Furthermore, the phage-AUNP system may be adapted to phenotypically detect antibiotic susceptibility of pathogens (If the result shows a color change in the presence of antibiotics, the pathogen is resistant to the selected antibiotic/antibiotics and able to grow in the presence of the antibiotic. If there is not color change, the pathogen is not able to grow in the system, it is susceptible to the selected antibiotic), essential to help determine antibiotic selection and dosage in the future (Peng, Borg et al. 2020).

2.2. Need For Detecting Bacteriophages and Emerging Tools and Methods

Bacteriophages have great potential for therapy, as powerful alternatives to antibiotics in the face of creeping drug resistance in bacterial infections. Therapeutic use of phage is discussed extensively elsewhere (Brives and Pourraz 2020), with significant developments and biopharmaceuticals becoming ever more widespread meaning we can expect phage therapy to reach the clinic in the near future. But in order to best make use of therapeutic phage, it is vital to be able to detect and count them, from screening and identification through medicines manufacture all the way to near-patient testing. In this section we discuss novel detection and biosensing methods and technologies that have been developed to measure bacteriophage. As diagnostic testing may be necessary to check if an infection is susceptible to a therapeutic phage preparation prior to treatment; we will describe methods for testing bacterial susceptibility to particular phages. Phage bioassays can output or be combined with various signals that can make them compatible with detection by smartphones; we highlight where this has been already demonstrated, and where there is future potential.

The conventional method – often known as double agar layer (DAL) method – for functional phage detection and enumeration has remained unchanged for 60 years in spite of the many technical difficulties of this protocol (Rajnovic, Muñoz-Berbel et al. 2019). The method requires recently cultured host bacteria, to be combined carefully with LB soft agar at the correct temperature to produce an even lawn of host cells. The phage plaques then form overnight as holes in the lawn, allowing determination of the number of functional particles, outputting the critical measurement of Plaque Forming Units. This remains the most important bioassay because measuring viable phage is more important than counting viral particles, many of which may not be capable of infecting target cells. As medicines based on viable virus preparations (including therapeutic bacteriophage) become more valuable, better methods for quantifying phage concentration are urgently needed, driving innovation in phage detection, measurement, and sensing. Some examples of this innovation are sketched in Figure 3.

Smartphones have been used to capture unusual bioassay readouts. For example, one new technique has been developed that detects viruses by measuring gas bubble formation with a nanoparticle-enabled smartphone and does not require a dye. Briefly, nanoprobe-labelled virus which labelling with platinum-nanoprobes is captured on a microchip (20 min). When 5% hydrogen peroxide is added to the medium, gas bubble formation starts from the catalytic property of the nanoprobe (10 min) (Figure 3 A). The bubbles formed are detected with the help of a smartphone in a fast and simple way (30 min) (Draz, Vasan et al. 2020). This illustrates that although many smartphone bioassays simply exploit the digital camera to quantify an existing colour or fluorescent readout, a wide diversity of measurements is possible.

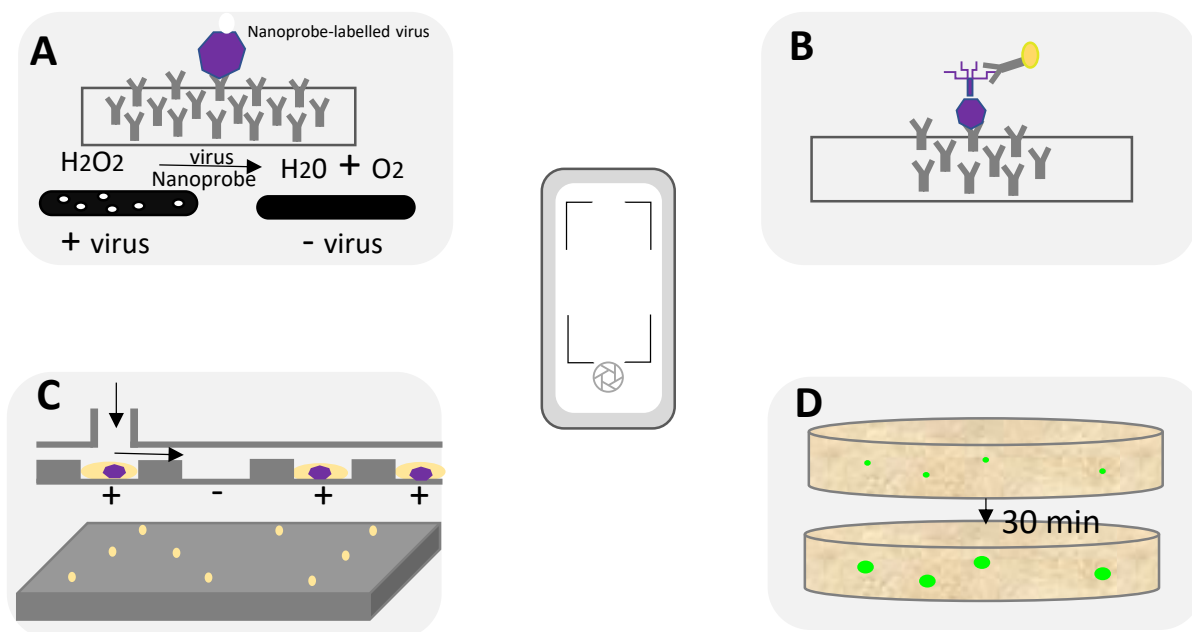


Figure 3. Emerging phage measurement methods that might allow smartphone detection. A) The nanoprobe-labelled virus is captured on a microchip, and when hydrogen peroxide is added, oxygen forms from the nanoprobe by the catalysis reaction (Draz, Vasan et al. 2020). B) Sandwich ELISA technique was demonstrated to detect and quantify phages (Khan, Pande et al. 2015, Alcaine, Law et al. 2016). C) The digital virus counting method can detect with encapsulation of a single virion in a reactor, if there is virus in the well, by converting the fluorogenic substrate and giving a fluorescent signal (Tabata, Minagawa et al. 2019). D) Viral particles immobilized with LAMP (Loop-mediated isothermal amplification) reagents in the hydrogel can be detected by isothermal amplification technique based on generating amplicon dots (Huang, Lin et al. 2018).

Conventional methods have likewise been adapted for smartphone readout. Alongside plaque assays in petri dishes (e.g., DAL), virus can be detected, or viral concentration can be quantified using immunoassays. Whilst smartphone immunoassays are outside the scope of this review, it's worth noting they have been used to quantify virus concentrations including bacteriophages. Paper-based adaptations of enzyme-linked immunosorbent assays (ELISA) methodology have been widely explored for the detection of a wide variety of targets, exploiting the binding properties and signal amplification of enzyme-linked antibodies. Target concentrations are determined through colorimetric or fluorimetric changes by conjugating different enzymes combined with a range of substrates. In one study performed for virus detection by the paper-fluidics sandwich ELISA method, filter paper was coated with a phage-specific primary antibody. The antibody coated paper was immersed in different phage solutions, allowing the specific phages to bind to the primary antibodies and the antibody target complex was formed. Antibodies conjugated with a colorimetric enzyme are added to the system, and then secondary antibodies that bind to the other end of the target molecule form a sandwich complex. The enzyme conjugated to the secondary antibody reacts with the enzyme substrate solution, with a coloured product signalling the presence of the target virus (Figure 3 B) (Khan, Pande et al. 2015). The combination of paper simplification of assays with a smartphone camera to record results permits portable immunoassay-based phage enumeration.

Many bacteriophages are of course biochemically and structurally similar to other viruses which have a type of genome and surrounded by a capsid (Ng, Jafari et al. 2012, Moineau 2013). Thus, the extensive research into detection of common and important viral infections can also be applied to bacteriophages, thus we will note briefly how other viral immunoassays have been adapted for smartphones. Viral proteins are readily detected by immunoassay- for example with influenza, antibodies binding the nucleoproteins of the virus were used as bioreceptors. Nucleoproteins are captured by a detection antibody, subsequently labelled a second time by an enzyme conjugated antibody. Complexes can then be captured with antibody functionalized superparamagnetic beads, adopting a typical sandwich ELISA. These complexes are added individually to microwells placed on a magnet. After incubation with a fluorogenic substrate, fluorescent products are formed in complexes that capture nucleoproteins in each well, and influenza A nucleoproteins are detected with great sensitivity by counting these fluorescent positive wells. Because influenza viruses retain their nucleoproteins even if they mutate other surface proteins, the study focused on these target proteins (Leirs, Tewari Kumar et al. 2016). However, manual steps (washing steps for bound and unbound antibodies) still make detection unwieldy. These assays can readily adapted from influenza to bacteriophages by using antibodies against relevant phage protein targets.

In another study published in 2019 for the detection of influenza, a method was developed for counting positive dots (signals) without the need for antibodies. The fluorogenic substrate and virus are injected together into the flow cell of the system. If virus is present in the well, the fluorogenic substrate is cleaved to generate a fluorescent signal based on neuraminidase activity and is counted as positive. After being photographed with a camera, it is analysed with Image J software. This system, which eliminates the extra steps and does not require the use of antibodies, has also been shown to be 1000 times more sensitive than commercial antibody based rapid kits (Figure 3 C) (Tabata, Minagawa et al. 2019).

Just as *E. coli* indicates pollution in water, an increasing number of coliphages also indicates pollution, and can be used to track water quality for public health. Again, improved bacteriophage detection methods can contribute to public safety. In a study to detect coliphage in water, modified *E. coli* was used. This concept reverses the use of modified phage to detect bacterial targets outlined above in 2.1. When the bacteriophage lyses the reporter cell, the β -glucuronidase enzyme originating from the bacterial cell is detected sensitively by the X-glucuronide substrate in the medium, producing a blue colour. The culture-based method allows detection of the presence / absence of 1 coliphage at 3.5 hours, while as the number of phages increases, the detection time decreases to 2.5 hours (Muniesa, Ballesté et al. 2018). Just as viral detection n by immunoassay can be applied to bacteriophage, NAT methods can be applied to detect phage, which contain characteristic viral genomes amenable to detection. Another study explored coliphage detection without culture-based plaque counting and showed coliphage could be detected in natural water samples in 30 minutes using an isothermal amplification technique with simple laboratory instruments and results recorded by smartphone. The viral particles immobilized with LAMP (Loop-mediated isothermal amplification) reagents in the hydrogel were amplified. With the effect of immobilization, each viral particle produces only one amplicon dot, so counting the fluorescent amplicon dots is sufficient to determine the concentration. Considering the sensitivity of the method, it was found that it gave similar results with RT-qPCR (Figure 3 D) (Huang, Lin et al. 2018). Many efforts to develop inexpensive, portable, smartphone-compatible NAT may therefore be adapted for phage detection.

2.3 Bacteriophage Biosensing Conclusions

Many of these methods deliver optical readouts, yet only a few of them have so far made use of smartphone detection. We see application of phage to microbial detection in a range of fields, and of many different target organisms; many of these applications would benefit from portable, out-of-lab measurement. At the same time, a broad range of analytical techniques can be readily applied to detection and measurement of bacteriophage, helping deliver next-generation biopharmaceuticals. We therefore expect to see in the future more demonstrations of smartphone phage detection and measurement. Whilst only a few examples combine phage detection with smartphone readouts, many recently developed methods include an optical readout likely to be smartphone readable, so we predict this is an exciting future direction.

3. APTAMERS

3.1 Introduction to Aptamers- Advantages and Opportunities

Aptamers are a novel molecular recognition element with a short single-strand oligonucleotide which self-folds into a structure that can bind targets with high avidity. They offer an alternative binding agent to antibodies and are suitable for detection and measurement of biomarkers in complex biological samples, but adding some desirable properties of nucleic acid chemistry (e.g., stability, synthesis) to the binding properties characteristic of antibodies. Aptamers that bind to targets with high affinity, are selected through methods such as SELEX (systematic evolution of ligands through exponential enrichment) (Ellington and Szostak 1990, Robertson and Joyce 1990, Tuerk and Gold 1990). Besides the dissociation constant (K_d) values of aptamers selected from large libraries of oligonucleotides, which can reach nanomolar levels against many target molecules, they also offer unique features such as simple synthesis, easy modification, and very high chemical stability (Jenison, Gill et al. 1994). Moreover, while the researcher determines the target region in aptamers, the immune system determines the target region in antibodies, that is, the target scale of antibodies may be narrower than aptamers (Jayasena 1999). Because of these distinct properties, aptamers have great potential as molecular receptors and sensing elements to create novel detection platforms.

Aptamer interactions can be effortlessly converted to an optical signal. They therefore not only offer great potential for clinical diagnostics, but many assays are likely to be compatible with portable smartphone measurement, bringing their particular benefits (e.g. chemical stability of nucleic acid probes) to point-of-care tests. Aptasensors coupled to gold nanoparticles are used in colorimetric detection of the target in multiple fields. The colorimetric approach is attractive for aptamer readout because of its simplicity, short detection time and low cost. As these tests can be read with the naked eye, we can be confident that such colorimetric detection must be suitable for on-site detection and capture by smartphone cameras (McConnell, Nguyen et al. 2020). As an alternative to capture of colored tags to a detection site (e.g., in lateral flow immunochromatography), the color change following aggregation of nanoparticles with diameters around the wavelength of visible light has been exploited for biosensing. In the presence of the target, nanoparticle-conjugated aptamers bind and form a structured complex. When this complex is washed with salt solution, AuNPs aggregation occurs, resulting in a characteristic red to blue (520 to 620 nm) color change. Without target the AuNPs complex is surrounded by aptamers and remains red (Chang, Chen et al. 2019).

Many detection systems have been developed using this aggregation-based color change principle. Since the color change can be detected with the naked eye and many such assays are in a format suitable for on-site detection, such assays can be exploited in many fields from the diagnosis of infection through detection of pharmaceuticals, to monitoring of environmental contaminants (McConnell, Nguyen et al. 2020).

3.2 Binding Assays

3.2.1 Diagnosis of Pathogens

Aptamer-based detection systems do not need a long incubation period, so they can meet the requirements for rapid tests that may facilitate early diagnosis, which is important in for some infections (Wan, Liu et al. 2021). Moreover, aptamers can be selected from an endless library and are easily modified to suit the desired sensing function, therefore, they can be quickly selected for a wide variety of targets including whole living cells with Cell-SELEX. Aptamers selected this way bind the 3D structure of the target molecule on the cell surface and thus detect targets without lysis or purification of cellular proteins. Aptamers can be selected using Cell-SELEX, without knowledge of cell surface target molecules. Thus, viable cell sensors can be used directly without prior preparation (Ohuchi 2012). An aptamer-based smartphone diagnostic device has been developed that diagnoses malaria without any further equipment. The biochemical sensor targeting malaria provides successful recognition by changing color in the presence of the malaria biomarker. The system, which requires a low sample volume (20 μ L), has been demonstrated with purified or spiked whole blood samples (Dirkzwager, Liang et al. 2016). If this is shown to be effective in clinical samples, such tests could support malaria control programs. In a study conducted on *Salmonella* Enteritidis, after 13 rounds of Cell-SELEX selection, two high-affinity aptamers were identified for *S. Enteritidis* with K_d values of 43.8 and 56.2nM and showed low binding activity to other foodborne bacterial isolates, suggesting binding specificity alongside high affinity. These aptamers were added to a gold-based colorimetric aptasensor and used to specifically identify *S. Enteritidis* from clinical, environmental and food samples in 20 minutes (Zhang, Liu et al. 2019). Another study designed for *S. aureus* detection used aptamers combined with tyramine signal amplification for pathogen detection in milk. The detection sensitivity of this gold nanoparticle-based colorimetric aptasensor system has reached 9 CFU/mL (Yuan, Wu et al. 2014). *Mycobacterium tuberculosis* aptamers were used in a study that could detect multiple samples simultaneously for screening tuberculosis infection. The system was able to detect tuberculosis with higher accuracy (R^2 value = 0.983) compared to traditional staining methods (R^2 value = 0.773). After the HRP-labeled aptamers were attached to the target, H_2O_2 was added and a color change from white to blue was achieved depending on the number of bacteria present. In addition, a smartphone application that can analyze this colorimetric change has been developed and it has been proven that it can allow online editing of diagnostic reports especially for developing countries (Li, Liu et al. 2018).

Many of such colorimetric assays have potential to be recorded by smartphone. But again, novel and non-optical readouts can likewise be combined with smartphones. A smartphone / sensor design was able to detect the Zika virus using the electron tunnel at room temperature, depending on current and voltage measurements. Tunnelling can detect aptamers that bind to capsid proteins on Zika viruses and the difference in free unbound aptamer so that the Zika virus could be detected without the need for genetic sequencing or additional molecular labels (Dolai and Tabib-Azar 2020). The same research team has started to design an aptamer-based smartphone prototype that can detect the COVID virus, inspired by Zika virus detection. After the saliva sample is dropped on the sensor, the sensor will be plugged into the phone and operated, and if SARS-CoV-2 binds to specific aptamers in the sensor, detection will be possible due to the electrical changes in the sensor (Dutton May 11, 2020).

Rapid and sensitive aptamer-based systems are being studied for rapid detection of *S. aureus*, which is one of the most important human infections, from hospital-acquired infections to food poisoning

(Shahdordizadeh, Taghdisi et al. 2017). In a Cell-SELEX study for the detection of *S. aureus*, a culture-free, smartphone-based system was developed from liquid samples using fluorescent magnetic nanoparticles with aptamer function. Labelled *S. aureus* fluorescence was detected using a smartphone camera with a light-emitting diode. 10 CFU/ml was determined from the peanut milk sample by efficiently capturing *S. aureus* cells within 10 minutes (Shrivastava, Lee et al. 2018). Direct detection of pathogens is possible with Cell-SELEX, but also pathogen entities can be detected indirectly by detection of pathogen-derived toxins. Alpha toxin is one of the most important toxins secreted by *S. aureus*. In one study, when choosing a high-affinity aptamer with SELEX for alpha toxin, molecules that are structurally similar to alpha toxin or likely to be in the same environment with the target, were also used as negative targets, thereby increasing specificity of the aptamer assay. The selected high-affinity aptamer was used as the capture element of a sandwich ELISA - suggesting it could be compatible with any smartphone-compatible immunoassay format. In the developed system, clinical human serum samples were used, and alpha toxin could be detected with a sensitive detection ($K_d = 93.7 \pm 7.0$ nM) (Hong, Battistella et al. 2015).

3.3 Testing Blood for Clinical Diagnostics

Thrombin level in the blood increases rapidly with conditions such as septic shock and covid infection. By measuring thrombin, patients at risk of coagulopathy can be detected early and can reduce SARS-CoV-2-related adverse outcomes with drug therapy. Therefore, measurement of thrombin levels can be very useful in the treatment of COVID-19 and for monitoring treatment. A lateral flow method similar to immunochromatography has been developed for thrombin quantification, but with antibody-aptamer combinations. It is portable, cheap and smartphone-compatible design that has so far been shown to perform well with complex samples containing 10% serum to simulate real clinical samples (Mahmoud, Ruppert et al. 2021). An electrode-integrated aptasensor has been developed for the one-step detection of norovirus, a common gastroenteritis pathogen. The sample injected into the microfluidic chip is first passed through the silica microbead region to filter and enrich it. The sample is then placed on unique aptamer-coated graphene-gold nanoparticles, the sensing zone for the detection of norovirus. Interacting with the ferrocene labelled aptamer, norovirus reduces the electrochemical signal and provides norovirus detection. One-step norovirus detection on a disposable microfluidic platform has been proposed for monitoring and detection from clinical samples following initial proof-of-concept demonstrated with spiked blood (Chand and Neethirajan 2017). Although this indicates aptamer-based detection should be possible of biomarkers in blood, it remains important to determine if this method can be adapted for samples that are more clinically relevant to norovirus (such as faeces), because current clinically approved diagnostic tests for norovirus do not test blood (Chhabra, Gregoricus et al. 2017).

According to the WHO report, 241 million cases of malaria were seen in 2020 (WHO 2021). There is still a critical need for portable equipment-free biosensors for the detection and diagnosis of malaria-not least to make best use of antimalarial drugs and avoid antimicrobial overuse that can drive resistance. In a study to meet this need, an aptamer-mediated, magnet-guided calorimetric malaria biosensor was developed. In a biosensor containing 3 separate microfluidic chambers, micromagnetic beads are incubated in human blood, respectively, then the beads are magnetically driven through the wash solution and separated from non-specific blood components. The beads magnetically turn purple in the presence of the target in the presence of *Plasmodium falciparum* lactate dehydrogenase (PfLDH). In the study, which also evaluated real clinical samples, a point-of-care aptamer-mediated biosensor was integrated into a mobile tele-medical setup with 90% sensitivity in all patient samples. Such innovations could have a significant impact on malaria diagnosis in regions with limited access to laboratory testing around the world (Fraser, Kinghorn et al. 2018).

3.4 Detection of Other Pharmaceuticals

Antibiotics are widely used in animal products and agriculture to treat bacterial infections. The WHO declared that the use of antibiotics in agriculture and animal product is increasing globally (Hu and Cowling 2020). This growing use of antibiotics threatens humans in two ways. Firstly, overuse drives antibiotic resistance that can pass to human pathogens, and secondly antibiotic residues in food products leads to needless human consumption of antimicrobials. Part of the WHO strategy to combat antimicrobial resistance is innovation in surveillance (and diagnostics). It is therefore very important to develop fast, simple, and portable detection systems of antibiotics to track their use and spread after use, to protect human health by ensuring food safety. Many examples of innovative antibiotic detection and sensing technology exploit aptamers, and many are compatible with smartphones.

Wu et al. designed a multifunctional colorimetric aptasensor platform that recognizes real-time multiplex antibiotics from real samples using antibiotic-specific DNA aptamers and gold nanoparticles. As with conventional aptamer technology, aptamers are absorbed onto the surface of gold nanoparticles and are then treated with the sample. If the target antibiotic is encountered, the aptamers release AuNPs and attach to the target because its interest in the target is much more than AuNPs, causing a color change from red to blue. The concentration of the antibiotic is determined by performing RGB (red, green, blue) analysis on this color change (Wu, Huang et al. 2020). To detect the kanamycin antibiotic, a flexible aptasensor, which was developed for wireless potentiometric measurement with the smartphone, was able to perform ultra-low detection of kanamycin from real milk samples (Yao, Jiang et al. 2019). For streptomycin detection, a point of care test system was created with a smartphone, which monitors the fluorescence change depending on the streptomycin concentration. Although this selective and simple system can measure only one analyte at a time, it was able to detect streptomycin concentrations in real milk and chicken samples with a mean detection limit of 94 nM, even lower than the WHO-defined maximum residue limit. Experts' operators are not required to operate this simplified system, and it can be used for the detection of other antibiotics by changing the aptamer sensors. (Lin, Yu et al. 2018). Another study adapted the enrofloxacin target to capture by sandwich technique using two different aptamers selected against this target. The first aptamer was thiolated and labeled with AuNPs, while biotin modified, and second aptamer was loaded into the test site via streptavidin coupling. In the presence of the target, these two aptamer complexes capture the target and develop color through expanding polymeric arms binding many AuNPs complexes with the catalysis of the terminal deoxynucleotidyl transferase enzyme. This color change was transformed into a quantitative reading in the developed image processing mobile application using the smartphone camera. With this application developed into a compact paper-based system, a digital platform might be created for on-site monitoring of metabolites and residue levels (Tian, Ji et al. 2020).

The detection of other pharmaceuticals also grows in importance from increased consumption- not only antibiotics are harmful to the environment. With distinct metabolisms, pharmaceuticals safe for humans may exhibit significant toxicity to wild animals. To address this, a sensitive android smartphone application was developed for the colorimetric detection of ibuprofen residues in water samples. Gold nanoparticles were coated with aptamers selected for the two chiral enantiomers of ibuprofen. If even one of the ibuprofen enantiomers is present in the water sample, the solution color changes from red to blue. A simple and fast Android-based color analysis application was developed to quantify enantiomer analysis. This concept was demonstrated in practical applications by testing river samples and tap water samples (Ping, He et al. 2018). Such assays are compatible with a wide range of samples, including detecting antibiotic residues in foodstuffs, to respond to the overuse of fluoroquinolones (FQs), often used in veterinary medicine as broad spectrum therapeutics (Chen, Li et al. 2015). An aptamer-based colorimetric assay method has been established for the rapid detection of fluoroquinolones. Gold nanoparticles modified with FQ-binding aptamers have a yellow

color in the absence of ciprofloxacin, whereas in the presence of ciprofloxacin, the flower-shaped aptamer complex opens, and the aptamers bind to the target, resulting in a color change from yellow to colorless. Thus, a simple contaminant detection method based on the catalytic activity of the gold surface is introduced (Lavaee, Danesh et al. 2017).

3.5 Monitoring of Other Environmental Contaminants

Detecting and quantifying the presence of toxic heavy metals and particles in the environment is both costly and time consuming; aptamer bioassays are suitable for sensitive and specific sensing of such analytes. A simple, rapid, high-throughput method for detecting Cd^{2+} using Aptamer and AuNPs has been reported. Thus in 2014, Wu et al selected a high-affinity aptamer that identifies cadmium ions. This aptamer was accepted as a recognition element for the colorimetric detection of cadmium based on the aggregation of AuNPs by the cationic polymer and could detect cadmium in aqueous solution as low as 4.6 nM. Thus, it will not only enable the detection of cadmium with great sensitivity, but it can also be used in studies aimed at separating cadmium from polluted samples (Wu, Zhan et al. 2014). In 2020, another lab team working for cadmium detection has similarly proposed a colorimetric method based on aptamer-functionalized gold nanoparticles to perform Cd^{2+} detection. The specific interaction between aptamers and Cd^{2+} leads to reduction of free aptamers, which weakens the stability of AuNPs and causes color change of the solution. Gang et al have developed the detection of cadmium one step further with the smartphone-based colourimetric system they designed. This color change, which can be captured within 10 minutes, is analyzed by the developed smartphone system (Gan, Liang et al. 2020).

An aptamer-based smartphone sensor platform has also been developed for the digital measurement of mercury. The prototype consists of a battery-operated reader connected to the existing camera module of the smartphone to monitor a plasmonic AuNPs and aptamer-based colorimetric test. In the case of mercury in the sample, the color change is captured on the phone using LEDs and digital image processing is achieved onboard by an android application. The sensitivity of the system (3.5 ppb) matches the maximum allowable level of mercury defined by WHO (6 ppb) in drinking water. Using this smartphone-based lightweight platform, water samples from 50 different California regions were tested with on-site detection without the need for a laboratory, and California's mercury pollution map was created (Wei, Nagi et al. 2014).

Estradiol is an endocrine disruptor chemical that affects organic systems and ecological equilibrium. Therefore, estradiol levels should be monitored for public health. A fluorescent-based, mobile biosensor that can detect estradiol has been designed. Smartphone-integrated fluorescent biosensors are often limited in their bioassay accuracy due to high background and low signal-to-noise ratios. In the study, with metal enhanced fluorescence, the substrate fluorescence was strengthened to increase the accuracy of the assay. In this way, samples with increased fluorescence intensity were added to a 3D printed prototype, together with an excitation light source and a mobile fluorescent reader. Samples for which fluorescence imaging was performed by the dual wavelength mobile reader proved to be of similar accuracy to the ELISA results. This new method could provide a novel way to introduce mobile fluorescent biosensors for environmental monitoring with increased accuracy (Lee, Shrivastava et al. 2017).

A smartphone-based system has been developed to combine aptamers, nanoparticles and microfluidics to create a portable and inexpensive method that not only tests a single set of samples, but also collects multiple parameters in a single test. A lateral flow nanoparticle integrated aptasensor that is precise and highly sensitive has been developed, allowing for simultaneous detection of multiple targets. Nanoparticles with red, green and blue emission peaks were synthesized in the system and used as detection probes that generate fluorescent signal for each target (green-

ochratoxin A, red-mercury, blue-Salmonella). Determination of the concentration of each target could be determined from the color intensity of the corresponding-colored band. The successful portable system integrated into the smartphone and analyzing the color change proves that small molecules, ions and bacteria can be detected from real water samples in just 30 minutes with specially developed nanoparticles. Thus, in monitoring the quality and safety of food and drinking water, it can collect all critical parameters in the same test and can be used in a short time, for example, to determine whether the water is potable / clean (Jin, Yang et al. 2018).

3.6 Summary of Aptamer Section

Aptamer detection systems have benefits that may allow them to meet the analytical performance needed in many applications. As well as small molecule targets (drug residues or metal contaminants), with Cell-SELEX, a detection method can be developed for large biological targets by selecting aptamers for the whole organism. Indeed, small and large targets can be detected simultaneously through multiplex analytical methods. Aptamer-based smartphone detection systems can be designed to deliver portable, cheap, fast and sensitive systems, requiring simple steps to process, which should meet many challenges both now and in the future.

4. CELLULAR MEASUREMENT

The foundations of modern biomedical science and clinical progress are built upon cell biology. Measurements of cells during disease can also provide valuable insight into pathology. But cell separation and manipulation techniques, and analysis of cells by cytometry and microscopy, are often laborious, costly and require extensive user training plus sophisticated instrumentation, which directly limits accessibility and usability. We believe that smartphone-connected cellular measurements have the capability to bring cell-based assays out of the lab and eventually permit portable diagnostic testing. The scope of cellular measurements and miniaturised cytometry is too broad to cover comprehensively here, instead we select diverse examples where integration of cellular measurements with smartphones has been explored, to illustrate the huge potential of this rapidly growing field.

4.1 Simplified Cellular Measurements

Cellular measurement – including the identification, phenotyping, and counting of cells – is essential for biomedical and biotechnology studies as well as for clinical diagnostics. Technology advances provide a greater appetite for at home or point-of-care cell-based testing. Smartphones can easily be adapted to telemedicine and diagnostic point-of-care tests for mobile health applications and so if they can perform cellular measurement, new avenues are opened. With the continuous enhancement of smartphones, advanced camera and CMOS (complementary metal oxide semiconductor) imaging units with high enough performance (e.g. increasing image resolution and lens quality), it has become practical to consider performing single cell analysis, or capture of cell populations, in terms of (Zhang, Li et al. 2020, Banik, Melanthota et al. 2021). Combining miniature-sized microfluidic devices with smartphones should bridge the gap between established portable tests (e.g., lateral flow rapid tests) and ever-shrinking yet still large and expensive of laboratory flow cytometers. Microfluidic equipment can perform multiple bioassays and automate manipulations, and may reduce the sample volume needed to fit fingerprick capillary blood samples thereby avoiding the need for venous blood draw (Xu, Huang et al. 2018). The potential for on-site disease diagnosis and rapid personal health monitoring is increasing through recently developed smartphone-based single-cell analysis using novel assay format and microfluidics (Xu, Huang et al. 2018).

4.2 Phone Based Flow cytometry

Flow cytometers are routinely used in the laboratory for research and clinical diagnostics, ranging from simple bench-top instruments up to sophisticated, multi-parameter cell sorting installations. Whilst the oldest cytometers were based on impedance measurement (Bull, Schneiderman et al. 1965) the most common current cytometers measure laser scatter and fluorescence from antibody-labelled and dyed cells within a flow cell. Leading-edge cytometers image every cell, sort for single-cell sequencing/transcriptomics, or incorporate mass spectrometry to measure relentlessly increasing numbers of cellular parameters. However, in the opposite direction from these highest complexity analysers, microfluidics and miniaturised optoelectronics offer the potential for portable, point-of-care cytometry (Vembadi, Menachery et al. 2019).

4.2.1 Blood Cell Counting

Counting blood cells is the most basic step in blood sample analysis. In blood cell counts, many acute or chronic diseases or clinical conditions can be diagnosed based on above- or below-normal levels. Thus, abnormal white blood cell counts may indicate infection or leukaemia, or high erythrocyte counts may indicate cardiovascular problems. While blood cells were previously counted manually with the aid of an optical microscope, this has been replaced by digital microscopy and most commonly flow cytometers and blood cell counters of a wide variety of formats.

While simpler measurements may be performed outside of a lab – such as hematocrit measurements for volume of red blood cells – these are not designed for home use. Microfluidic devices may be able to make these, or even more complex blood measurements with the aid of a smartphone. One example used fluorescently labelled white blood cells, pumped into a microfluidic chamber with a syringe. Fluorescently labelled white blood cells are stimulated by the light from the blue LEDs attached to the sides of the microfluidic circle placed on the camera of the smartphone. Videos of cell movement in the device were recorded and the concentration of labelled white blood cells was determined and showed high similarity when compared with a hematology analyser (<5% error) (Zhu, Mavandadi et al. 2011).

In impedance-based cytometers, different cells are detected by measuring the dielectric properties of the cells during the passage of single cells through a flow cell. A microflow cytometer based on direct sensing the impedance change of red blood cells has been developed, especially in a system designed to quickly detect situations where sickle cell anaemia individuals encounter oxygen deficiency in the future. This single-cell-based analysis system consists of an impedance analyser to interpret the electrical impedance change of RBCs (red blood cells), a microfluidic that allows red blood cells to pass through as single cells, and an Arduino interfacing with a special Android application that allows impedimetric scans. Although the membrane tension of RBCs in a healthy person did not change significantly with oxygen exchange, it was observed that the cytoplasmic resistance and membrane capacitance of RBCs affected by sickle cell disease decreased significantly and a correlation was found between these two (Dieujuste, Qiang et al. 2020, Dieujuste, Qiang et al. 2021). In another study using impedance-based indirect measurement, a portable wristband was designed for biomarker counting and analysis by combining a wearable flexible microfluidic cytometer with a smartphone. White blood cells were counted by taking electrochemical readings with cyclic voltammetry on this wristband under the control of a smartphone. This online reading device converts analog readings to digital signals that can be shared with a specialist and can provide vital information about the patient with all-day examination (Furniturewalla, Chan et al. 2018).

Cell measurements can be made without fully analysing individual cells. For example, a lateral flow format smartphone compatible immunoassay has been developed that can measure CD4 T cell levels in whole blood to monitor the health of HIV infected individuals (Glynn, Kinahan et al. 2013). This

system is notable because it performs simplified manipulations to separate elements from whole blood that would interfere with the core analysis (e.g., red blood cells) and then detects cellular components as a surrogate for whole cell detection, using an established lateral flow format that is both well-studied but crucially mass-manufactured. ABO blood typing can also be performed using paper (Li, Then et al. 2014) or with microcapillaries (Reis, Pivetal et al. 2016) which can facilitate smartphone based optical detection of red cell aggregation, exploiting differences in flow properties between whole blood and blood with aggregated cells, again detecting an important property indirectly to simplify assay format. As these examples illustrate, it can be possible to measure clinically important cellular responses with smartphone-compatible simplified devices, without even detecting whole cells directly, but instead by converting them to fluorescent, impedimetric, or optical signals.

Together, either by miniaturising cytometers or by simplifying bioassays to avoid needing to measure cells themselves, these permit near patient or at home testing, avoiding the need to send samples to a laboratory.

4.3 Smartphone Microscopy

Smartphone cameras have become so small yet high performance that they are nearly competitive with conventional microscopes – used traditionally to diagnose many diseases – in terms of resolution, magnification and image quality. The continuous updating of these advanced cameras and CMOS imaging sensors plus powerful graphics processing that enable rapid data capture and onboard image analysis. Microscopic imaging and fluorescent microscopy imaging and detection are clearly possible with a mobile phone, and imaging sensitivity can be increased with optofluidic tips integrated into the smartphone's camera module (Zhu, Gong et al. 2020). Many smartphone-based bright field microscopes and fluorescence microscopes have been built and demonstrated using standard microscopy slide preparation. The sample is dropped as a cell suspension, or tissue finely sliced and placed on the slide, then the illumination light on the sample is focused on the light attenuation, scattering and color changes for image capture (Zhu, Gong et al. 2020). For many of these demonstrations, simplified sample preparation must now be combined with these optical methods for eventual use outside the laboratory.

A smartphone-based microscopic detection method has been developed to prevent contamination of food and water from *Cryptosporidium* and *Giardia* from causing significant health problems. This study, tested samples from vegetables, stained with iodine, images were captured with sufficient magnification and contrast to distinguish *Cryptosporidium* and *Giardia* (oo)cysts with the light from a white LED light source, using a smartphone camera (Shrestha, Duwal et al. 2020). A portable microscopic platform was built from a smartphone and a microfluidic chip, to automate somatic cells counts in milk. A single ball lens adapted 3D-printed piece allows the smartphone to perform as a microscope, while a microfluidic chip enables the sample to be run. The results of this inexpensive, portable imaging device matched those made by classic microscopy (Zeng, Jin et al. 2018).

Other lab systems have been transformed into mobile smartphone-compatible platforms. As an alternative to the standard ELISA method, a 3D-printed battery-operated system with a reader suitable for a mobile phone-based 96-well plate has been developed. After the LED light used in the system based on colorimetric detection is collected by optical fiber connected to each of the 96 wells separately, the results are interpreted with the algorithm created, thus, this method might replace costly plate readers but also include the analysis in a single device. Mumps, measles, and herpes simplex virus antibodies were tested, and results were 99% accurate compared to the traditional ELISA test result. This wireless and inexpensive system can be helpful in achieving rapid results or in support of vaccination campaigns where there are insufficient resources, equipment and personnel (Berg, Cortazar et al. 2015). Given microscopes and plate reader instruments can be miniaturised, it's likely

that many cell measurement tools and instruments – not just flow cytometers – will likewise soon be transported out of the lab using smartphones and similar technology.

4.4 Cellular Measurements Conclusions

Smartphone-based bio-imaging systems have been developed to detect cells and pathogens by imitating classical flow cytometry and microscopy, and/or using the smartphone's high-pixel density camera and usability with the power for image capture, storage, transfer, and analysis. Furthermore, some cellular measurements can be made without actually analysing intact cells themselves, for example by simplifying the assay to measure a parameter that follows cell properties; this allows smartphone-compatible portable measurements of cellular parameters even without remote cell detection. Together, there is now great potential for cellular parameters to be tested at the point of need, using portable bioassay and sensing platforms, especially when smartphones are combined with microfluidic devices.

5. CONCLUSION

Smartphones offer great potential for improved access to current healthcare tools, and to new bioanalytical and biosensing applications; the combination of cameras and other sensors, with powerful computing onboard, and multiple network connections allows integration of multiple diverse diagnostic measurements with tele-healthcare systems. There remain several significant barriers – it is not easy to replace medical instrumentation with consumer products. However, the portability achieved by smartphone integration permits point-of-care use of many vital bioassays, and the integration into larger data systems supports real-time monitoring and tracking over time, which should provide the incentive for innovation and drive us to overcome those barriers. Recording results of invasive tests (e.g., blood, urine, swabs) but also combining these with non-invasive biomarkers and sensor measurements, together with other more conventional clinical measurements in the form of clinician or patient observations, can together be integrated with rapid access to health-related information to users and patients.

The emerging bioassays and biosensor systems identified here, including novel methods and devices alongside adaptations of conventional methods such as immunoassay or nucleic acid testing, can together allow a broad range of targets to be detected or measured. Bacteriophage will help detect other important microbial targets, and new tools will permit improved detection and measurement of viruses including phage in many areas; smartphone phage detection is now possible. Aptamers offer an alternative binding agent with some advantages over antibodies, and – like immunoassays – many aptamer bioassays are smartphone compatible. Finally, cellular measurements – until recently confined to labs and requiring specialist instrumentation – are beginning to be miniaturised into formats that could lead to smartphone cellular clinical diagnostic tests. These include miniature cytometers, smartphone microscopy, and simplified assays that measure cellular parameters but avoid the need to measure cells themselves. Even the many and diverse range of novel bioassays and biosensors that have yet to be proven to be smartphone compatible are likely to be adapted in the near future to integrate with these ubiquitous “instrument in our pockets”.

REFERENCES

Alcaine, S. D., K. Law, S. Ho, A. J. Kinchla, D. A. Sela and S. R. Nugen (2016). "Bioengineering bacteriophages to enhance the sensitivity of phage amplification-based paper fluidic detection of bacteria." *Biosensors and Bioelectronics* **82**: 14-19.

Banik, S., S. K. Melanthota, Arbaaz, J. M. Vaz, V. M. Kadambalithaya, I. Hussain, S. Dutta and N. Mazumder (2021). "Recent trends in smartphone-based detection for biomedical applications: a review." Analytical and Bioanalytical Chemistry **413**(9): 2389-2406.

Berg, B., B. Cortazar, D. Tseng, H. Ozkan, S. Feng, Q. Wei, R. Y.-L. Chan, J. Burbano, Q. Farooqui, M. Lewinski, D. Di Carlo, O. B. Garner and A. Ozcan (2015). "Cellphone-Based Hand-Held Microplate Reader for Point-of-Care Testing of Enzyme-Linked Immunosorbent Assays." ACS Nano **9**(8): 7857- 7866.

Bergua, J. F., R. Álvarez-Diduk, A. Idili, C. Parolo, M. Maymó, L. Hu and A. Merkoçi (2022). "Low-Cost, User-Friendly, All-Integrated Smartphone-Based Microplate Reader for Optical-Based Biological and Chemical Analyses." Analytical Chemistry **94**(2): 1271-1285.

Brintz, B. J., B. Haaland, J. Howard, D. L. Chao, J. L. Proctor, A. I. Khan, S. M. Ahmed, L. T. Keegan, T. Greene, A. M. Keita, K. L. Kotloff, J. A. Platts-Mills, E. J. Nelson, A. C. Levine, A. T. Pavia and D. T. Leung (2021). "A modular approach to integrating multiple data sources into real-time clinical prediction for pediatric diarrhea." eLife **10**: e63009.

Brives, C. and J. Pourraz (2020). "Phage therapy as a potential solution in the fight against AMR: obstacles and possible futures." Palgrave Communications **6**(1): 100.

Bull, B., M. Schneiderman and G. Brecher (1965). "Platelet counts with the Coulter counter." American journal of clinical pathology **44**(6): 678-688.

Burnham, S., J. Hu, H. Anany, L. Brovko, F. Deiss, R. Derda and M. W. Griffiths (2014). "Towards rapid on-site phage-mediated detection of generic Escherichia coli in water using luminescent and visual readout." Analytical and Bioanalytical Chemistry **406**(23): 5685-5693.

Chand, R. and S. Neethirajan (2017). "Microfluidic platform integrated with graphene-gold nano- composite aptasensor for one-step detection of norovirus." Biosensors and Bioelectronics **98**: 47-53. Chang, C.-C., C.-P. Chen, T.-H. Wu, C.-H. Yang, C.-W. Lin and C.-Y. Chen (2019). "Gold Nanoparticle- Based Colorimetric Strategies for Chemical and Biological Sensing Applications." Nanomaterials **9**(6): 861.

Chen, G., M. Li and X. Liu (2015). "Fluoroquinolone Antibacterial Agent Contaminants in Soil/Groundwater: A Literature Review of Sources, Fate, and Occurrence." Water, Air, & Soil Pollution **226**(12): 418.

Chen, J., S. D. Alcaine, Z. Jiang, V. M. Rotello and S. R. Nugen (2015). "Detection of Escherichia coli in Drinking Water Using T7 Bacteriophage-Conjugated Magnetic Probe." Analytical Chemistry **87**(17): 8977-8984.

Chhabra, P., N. Gregoricus, G. A. Weinberg, N. Halasa, J. Chappell, F. Hassan, R. Selvarangan, S. Mijatovic-Rustempasic, M. L. Ward, M. Bowen, D. C. Payne and J. Vinjé (2017). "Comparison of three multiplex gastrointestinal platforms for the detection of gastroenteritis viruses." J Clin Virol **95**: 66-71. Dieujuste, D., Y. Qiang and E. Du (2020). "A Portable Impedance Microflow Cytometer for Measuring Cellular Response to Hypoxia." bioRxiv: 2020.2007.2028.224006.

Dieujuste, D., Y. Qiang and E. Du (2021). "A portable impedance microflow cytometer for measuring cellular response to hypoxia." Biotechnology and Bioengineering **118**(10): 4041-4051.

Dirkzwager, R. M., S. Liang and J. A. Tanner (2016). "Development of Aptamer-Based Point-of-Care Diagnostic Devices for Malaria Using Three-Dimensional Printing Rapid Prototyping." ACS Sensors **1**(4):420-426.

Dolai, S. and M. Tabib-Azar (2020). "Microfabricated Nano-Gap Tunneling Current Zika Virus Sensors With Single Virus Detection Capabilities." IEEE Sensors Journal **20**(15): 8597-8603.

Dönmez, S. İ., S. H. Needs, H. M. I. Osborn and A. D. Edwards (2020). "Label-free smartphone quantitation of bacteria by darkfield imaging of light scattering in fluoropolymer micro capillary film allows portable detection of bacteriophage lysis." Sensors and Actuators B: Chemical **323**: 128645.

Dow, P., K. Kotz, S. Gruszka, J. Holder and J. Fiering (2018). "Acoustic separation in plastic microfluidics for rapid detection of bacteria in blood using engineered bacteriophage." Lab on a Chip **18**(6): 923- 932.

Draz, M. S., A. Vasan, A. Muthupandian, M. K. Kanakasabapathy, P. Thirumalaraju, A. Sreeram, S. Krishnakumar, V. Yogesh, W. Lin, X. G. Yu, R. T. Chung and H. Shafiee (2020). "Virus detection using nanoparticles and deep neural network-enabled smartphone system." Science advances **6**(51): eabd5354.

Dutton, G. (May 11, 2020). "NSF-funded Smartphone COVID-19 Diagnostic Test Could Put Testing in the Hands of the Public." from <https://www.biospace.com/article/nsf-funded-smartphone-covid-19-dx-puts-testing-in-the-hands-of-the-public/>.

Edition, F. (2011). "Guidelines for drinking-water quality." WHO chronicle **38**(4): 104-108.

Ellington, A. D. and J. W. Szostak (1990). "In vitro selection of RNA molecules that bind specific ligands." Nature **346**(6287): 818-822.

Fraser, L. A., A. B. Kinghorn, R. M. Dirkzwager, S. Liang, Y.-W. Cheung, B. Lim, S. C.-C. Shiu, M. S. L. Tang, D. Andrew, J. Manitta, J. S. Richards and J. A. Tanner (2018). "A portable microfluidic Aptamer- Tethered Enzyme Capture (APTEC) biosensor for malaria diagnosis." Biosensors and Bioelectronics **100**: 591-596.

Furniturewalla, A., M. Chan, J. Sui, K. Ahuja and M. Javanmard (2018). "Fully integrated wearable impedance cytometry platform on flexible circuit board with online smartphone readout." Microsystems & Nanoengineering **4**(1): 20.

Gan, Y., T. Liang, Q. Hu, L. Zhong, X. Wang, H. Wan and P. Wang (2020). "In-situ detection of cadmium with aptamer functionalized gold nanoparticles based on smartphone-based colorimetric system." Talanta **208**: 120231.

Glynn, M. T., D. J. Kinahan and J. Ducreé (2013). "CD4 counting technologies for HIV therapy monitoring in resource-poor settings – state-of-the-art and emerging microtechnologies." Lab on a Chip **13**(14): 2731-2748.

Goodridge, L., J. Chen and M. Griffiths (1999). "The use of a fluorescent bacteriophage assay for detection of Escherichia coli O157:H7 in inoculated ground beef and raw milk." International Journal of Food Microbiology **47**(1): 43-50.

Hong, K. L., L. Battistella, A. D. Salva, R. M. Williams and L. J. Sooter (2015). "In vitro selection of single-stranded DNA molecular recognition elements against S. aureus alpha toxin and sensitive detection in human serum." Int J Mol Sci **16**(2): 2794-2809.

Hu, Y. J. and B. J. Cowling (2020). "Reducing antibiotic use in livestock, China." Bulletin of the World Health Organization **98**(5): 360-361.

Huang, X., X. Lin, K. Urmann, L. Li, X. Xie, S. Jiang and M. R. Hoffmann (2018). "Smartphone-Based in- Gel Loop-Mediated Isothermal Amplification (gLAMP) System Enables Rapid Coliphage MS2 Quantification in Environmental Waters." Environmental Science & Technology **52**(11): 6399-6407.

Imai, M., K. Mine, H. Tomonari, J. Uchiyama, S. Matuzaki, Y. Niko, S. Hadano and S. Watanabe (2019). "Dark-Field Microscopic Detection of Bacteria using Bacteriophage-Immobilized SiO₂@AuNP Core– Shell Nanoparticles." Analytical Chemistry **91**(19): 12352-12357.

Jayasena, S. D. (1999). "Aptamers: An Emerging Class of Molecules That Rival Antibodies in Diagnostics." Clinical Chemistry **45**(9): 1628-1650.

Jenison, R. D., S. C. Gill, A. Pardi and B. Polisky (1994). "High-Resolution Molecular Discrimination by RNA." Science **263**(5152): 1425-1429.

Jin, B., Y. Yang, R. He, Y. I. Park, A. Lee, D. Bai, F. Li, T. J. Lu, F. Xu and M. Lin (2018). "Lateral flow aptamer assay integrated smartphone-based portable device for simultaneous detection of multiple targets using upconversion nanoparticles." Sensors and Actuators B: Chemical **276**: 48-56.

Khan, M. S., T. Pande and T. G. M. van de Ven (2015). "Qualitative and quantitative detection of T7 bacteriophages using paper based sandwich ELISA." Colloids and Surfaces B: Biointerfaces **132**: 264- 270.

Lavaee, P., N. M. Danesh, M. Ramezani, K. Abnous and S. M. Taghdisi (2017). "Colorimetric aptamer based assay for the determination of fluoroquinolones by triggering the reduction-catalyzing activity of gold nanoparticles." Microchimica Acta **184**(7): 2039-2045.

Lee, W. I., S. Shrivastava, L. T. Duy, B. Yeong Kim, Y. M. Son and N. E. Lee (2017). "A smartphone imaging-based label-free and dual-wavelength fluorescent biosensor with high sensitivity and accuracy." *Biosens Bioelectron* **94**: 643-650.

Leirs, K., P. Tewari Kumar, D. Decrop, E. Pérez-Ruiz, P. Leblebici, B. Van Kelst, G. Compennolle, H. Meeuws, L. Van Wesenbeeck, O. Lagatie, L. Stuyver, A. Gils, J. Lammertyn and D. Spasic (2016). "Bioassay Development for Ultrasensitive Detection of Influenza A Nucleoprotein Using Digital ELISA." *Analytical Chemistry* **88**(17): 8450-8458.

Li, L., Z. Liu, H. Zhang, W. Yue, C.-W. Li and C. Yi (2018). "A point-of-need enzyme linked aptamer assay for Mycobacterium tuberculosis detection using a smartphone." *Sensors and Actuators B: Chemical* **254**: 337-346.

Li, M., W. L. Then, L. Li and W. Shen (2014). "Paper-based device for rapid typing of secondary human blood groups." *Analytical and Bioanalytical Chemistry* **406**(3): 669-677.

Lin, B., Y. Yu, Y. Cao, M. Guo, D. Zhu, J. Dai and M. Zheng (2018). "Point-of-care testing for streptomycin based on aptamer recognizing and digital image colorimetry by smartphone." *Biosensors and Bioelectronics* **100**: 482-489.

Liu, P., Y. Wang, L. Han, Y. Cai, H. Ren, T. Ma, X. Li, V. A. Petrenko and A. Liu (2020). "Colorimetric Assay of Bacterial Pathogens Based on Co₃O₄ Magnetic Nanozymes Conjugated with Specific Fusion Phage Proteins and Magnetophoretic Chromatography." *ACS Applied Materials & Interfaces* **12**(8): 9090-9097.

Mahmoud, M., C. Ruppert, S. Rentschler, S. Laufer and H.-P. Deigner (2021). "Combining aptamers and antibodies: Lateral flow quantification for thrombin and interleukin-6 with smartphone readout." *Sensors and Actuators B: Chemical* **333**: 129246.

Mak, W. C., V. Beni and A. P. F. Turner (2016). "Lateral-flow technology: From visual to instrumental." *TrAC Trends in Analytical Chemistry* **79**: 297-305.

McConnell, E. M., J. Nguyen and Y. Li (2020). "Aptamer-Based Biosensors for Environmental Monitoring." *Frontiers in Chemistry* **8**(434).

Mosier-Boss, P. A., S. H. Lieberman, J. M. Andrews, F. L. Rohwer, L. E. Wegley and M. Breitbart (2003). "Use of fluorescently labeled phage in the detection and identification of bacterial species." *Appl Spectrosc* **57**(9): 1138-1144.

Muniesa, M., E. Ballesté, L. Imamovic, M. Pascual-Benito, D. Toribio-Avedillo, F. Lucena, A. R. Blanch and J. Jofre (2018). "Bluephage: A rapid method for the detection of somatic coliphages used as indicators of fecal pollution in water." *Water Research* **128**: 10-19.

Nasser, B., N. Soleimani, N. Rabiee, A. Kalbasi, M. Karimi and M. R. Hamblin (2018). "Point-of-care microfluidic devices for pathogen detection." *Biosensors & bioelectronics* **117**: 112-128.

Ohuchi, S. (2012). "Cell-SELEX Technology." *BioResearch open access* **1**(6): 265-272.

Peng, H., R. E. Borg, A. B. N. Nguyen and I. A. Chen (2020). "Chimeric Phage Nanoparticles for Rapid Characterization of Bacterial Pathogens: Detection in Complex Biological Samples and Determination of Antibiotic Sensitivity." *ACS Sensors* **5**(5): 1491-1499.

Peng, H. and I. A. Chen (2019). "Rapid Colorimetric Detection of Bacterial Species through the Capture of Gold Nanoparticles by Chimeric Phages." *ACS Nano* **13**(2): 1244-1252.

Ping, J., Z. He, J. Liu and X. Xie (2018). "Smartphone-based colorimetric chiral recognition of ibuprofen using aptamers-capped gold nanoparticles." *ELECTROPHORESIS* **39**(3): 486-495.

Rajendran, V. K., P. Bakthavathsalam, P. L. Bergquist and A. Sunna (2021). "Smartphone technology facilitates point-of-care nucleic acid diagnosis: a beginner's guide." *Crit Rev Clin Lab Sci* **58**(2): 77-100. Rajnovic, D., X. Muñoz-Berbel and J. Mas (2019). "Fast phage detection and quantification: An optical density-based approach." *PloS one* **14**(5): e0216292-e0216292.

Reimer, J. R., S. M. Ahmed, B. J. Brintz, R. U. Shah, L. T. Keegan, M. J. Ferrari and D. T. Leung (2021). "The Effects of Using a Clinical Prediction Rule to Prioritize Diagnostic Testing on Transmission and Hospital Burden: A Modeling Example of Early Severe Acute Respiratory Syndrome Coronavirus 2." *Clin Infect Dis* **73**(10): 1822-1830.

Reis, N. M., J. Pivetal, A. L. Loo-Zazueta, J. M. S. Barros and A. D. Edwards (2016). "Lab on a stick: multi-analyte cellular assays in a microfluidic dipstick." *Lab on a Chip* **16**(15): 2891-2899.

Robertson, D. L. and G. F. Joyce (1990). "Selection in vitro of an RNA enzyme that specifically

cleaves single-stranded DNA." Nature **344**(6265): 467-468.

Shabani, A., C. A. Marquette, R. Mandeville and M. F. Lawrence (2013). "Magnetically-assisted impedimetric detection of bacteria using phage-modified carbon microarrays." Talanta **116**: 1047- 1053.

Shahdordizadeh, M., S. M. Taghdisi, N. Ansari, F. Alebooye Langroodi, K. Abnous and M. Ramezani (2017). "Aptamer based biosensors for detection of Staphylococcus aureus." Sensors and Actuators B:Chemical **241**: 619-635.

Shrestha, R., R. Duwal, S. Wagle, S. Pokhrel, B. Giri and B. B. Neupane (2020). "A smartphone microscopic method for simultaneous detection of (oo)cysts of Cryptosporidium and Giardia." PLOS Neglected Tropical Diseases **14**(9): e0008560.

Shrivastava, S., W.-I. Lee and N.-E. Lee (2018). "Culture-free, highly sensitive, quantitative detection of bacteria from minimally processed samples using fluorescence imaging by smartphone." Biosensors and Bioelectronics **109**: 90-97.

Tabata, K. V., Y. Minagawa, Y. Kawaguchi, M. Ono, Y. Moriizumi, S. Yamayoshi, Y. Fujioka, Y. Ohba, Y. Kawaoka and H. Noji (2019). "Antibody-free digital influenza virus counting based on neuraminidase activity." Scientific Reports **9**(1): 1067.

Tian, R., J. Ji, Y. Zhou, Y. Du, X. Bian, F. Zhu, G. Liu, S. Deng, Y. Wan and J. Yan (2020). "Terminal- conjugated non-aggregated constraints of gold nanoparticles on lateral flow strips for mobile phone readouts of enrofloxacin." Biosensors and Bioelectronics **160**: 112218.

Tuerk, C. and L. Gold (1990). "Systematic Evolution of Ligands by Exponential Enrichment: RNA Ligandsto Bacteriophage T4 DNA Polymerase." Science **249**(4968): 505-510.

Vaidya, A., S. Ravindranath and U. S. Annapure (2020). "Detection and differential identification of typhoidal Salmonella using bacteriophages and resazurin." 3 Biotech **10**(5): 196-196.

Vashist, S. K. and J. H. T. Luong (2018). Chapter 16 - Smartphone-Based Immunoassays. Handbook of Immunoassay Technologies. S. K. Vashist and J. H. T. Luong, Academic Press: 433-453.

Vembadi, A., A. Menachery and M. A. Qasaimeh (2019). "Cell Cytometry: Review and Perspective on Biotechnological Advances." Frontiers in bioengineering and biotechnology **7**: 147-147.

Vinay, M., N. Franche, G. Grégory, J.-R. Fantino, F. Pouillot and M. Ansaldi (2015). "Phage-Based Fluorescent Biosensor Prototypes to Specifically Detect Enteric Bacteria Such as E. coli and Salmonella enterica Typhimurium." PLOS ONE **10**(7): e0131466.

Wan, Q., X. Liu and Y. Zu (2021). "Oligonucleotide aptamers for pathogen detection and infectious disease control." Theranostics **11**(18): 9133-9161.

Wei, Q., R. Nagi, K. Sadeghi, S. Feng, E. Yan, S. J. Ki, R. Caire, D. Tseng and A. Ozcan (2014). "Detection and Spatial Mapping of Mercury Contamination in Water Samples Using a Smart-Phone." ACS Nano **8**(2): 1121-1129.

WHO (2008). **Typhoid vaccines : WHO position paper** Weekly Epidemiological Record **83**: 49-60. WHO (2021). World Malaria Report.

Willford, J. D., B. Bisha, K. E. Bolenbaugh and L. D. Goodridge (2011). "Luminescence based enzyme- labeled phage (Phazyme) assays for rapid detection of Shiga toxin producing Escherichia coli serogroups." Bacteriophage **1**(2): 101-110.

Wu, Y.-Y., P. Huang and F.-Y. Wu (2020). "A label-free colorimetric aptasensor based on controllable aggregation of AuNPs for the detection of multiplex antibiotics." Food Chemistry **304**: 125377.

Wu, Y. G., S. S. Zhan, L. M. Wang and P. Zhou (2014). "Selection of a DNA aptamer for cadmium detection based on cationic polymer mediated aggregation of gold nanoparticles." Analyst **139**(6): 1550-1561.

Xu, D., X. Huang, J. Guo and X. Ma (2018). "Automatic smartphone-based microfluidic biosensor system at the point of care." Biosensors and Bioelectronics **110**: 78-88.

Yao, Y., C. Jiang and J. Ping (2019). "Flexible freestanding graphene paper-based potentiometric enzymatic aptasensor for ultrasensitive wireless detection of kanamycin." Biosensors and Bioelectronics **123**: 178-184.

Yuan, J., S. Wu, N. Duan, X. Ma, Y. Xia, J. Chen, Z. Ding and Z. Wang (2014). "A sensitive gold

nanoparticle-based colorimetric aptasensor for Staphylococcus aureus." Talanta **127**: 163-168.

Zeng, Y., K. Jin, J. Li, J. Liu, J. Li, T. Li and S. Li (2018). "A low cost and portable smartphone microscopic device for cell counting." Sensors and Actuators A: Physical **274**: 57-63.

Zhang, S., Z. Li and Q. Wei (2020). "Smartphone-based cytometric biosensors for point-of-care cellular diagnostics." Nanotechnology and Precision Engineering **3**(1): 32-42.

Zhang, Z., D. Liu, Y. Bai, Y. Cui, D. Wang and X. Shi (2019). "Identification and characterization of two high affinity aptamers specific for Salmonella Enteritidis." Food Control **106**: 106719.

Zhu, H., S. Mavandadi, A. F. Coskun, O. Yaglidere and A. Ozcan (2011). "Optofluidic Fluorescent Imaging Cytometry on a Cell Phone." Analytical Chemistry **83**(17): 6641-6647.

Zhu, W., C. Gong, N. Kulkarni, C. D. Nguyen and D. Kang (2020). Chapter 9 - Smartphone-based microscopes. Smartphone Based Medical Diagnostics. J.-Y. Yoon, Academic Press: 159-175.

Zurier, H. S., M. M. Duong, J. M. Goddard and S. R. Nugen (2020). "Engineering Biorthogonal Phage- Based Nanobots for Ultrasensitive, In Situ Bacteria Detection." ACS Applied Bio Materials **3**(9): 5824- 5831.

Highlights

- An increasing range of biosensor and bioassay types are becoming portable and rapid, improving access to testing for public health
- We review three emerging fields where novel portable rapid measurement tools and technology are now compatible with smartphones
- Smartphones can exploit bacteriophages to detect microbes, and smartphones can now measure bacteriophages
- Aptamer-based biosensors and bioassays are likewise highly suited to smartphone format, expanding our range of binding assays
- Smartphones can also make measurements of cells, so clinically important cellular blood testing may soon leave labs and enter our homes
- Smartphones are becoming “instrument in our pockets” that will improve access to tests that are essential for healthcare

Chuang, C. S., C. Z. Deng, Y. F. Fang, H. R. Jiang, P. W. Tseng, H. J. Sheen and Y. J. Fan (2019). "A Smartphone-based Diffusometric Immunoassay for Detecting C-Reactive Protein." *Sci Rep* **9**(1): 17131.

May, L., N. Tran and N. A. Ledebor (2021). "Point-of-care COVID-19 testing in the emergency department: current status and future prospects." *Expert Rev Mol Diagn* **21**(12): 1333-1340.

Moineau, S. (2013). Bacteriophage. *Brenner's Encyclopedia of Genetics (Second Edition)*. S. Maloy and K. Hughes. San Diego, Academic Press: 280-283.

Ng, S., M. R. Jafari and R. Derda (2012). "Bacteriophages and Viruses as a Support for Organic Synthesis and Combinatorial Chemistry." *ACS Chemical Biology* **7**(1): 123-138.

Valera, E., A. Jankelow, J. Lim, V. Kindratenko, A. Ganguli, K. White, J. Kumar and R. Bashir (2021). "COVID-19 Point-of-Care Diagnostics: Present and Future." *ACS Nano* **15**(5): 7899-7906.

Chapter 3

Label-free smartphone quantitation of bacteria by darkfield imaging of light scattering in fluoropolymer micro capillary film allows portable detection of bacteriophage lysis

Chapter summary: In this section, the detection of unlabelled bacteria and bacteriophage lysis by darkfield imaging of light scattering in a microfluidic device using a smartphone is demonstrated. This can be considered as an alternative to classical microbiology methods.

Bibliographic details: Sultan İlayda Dönmez, Sarah H. Needs, Helen M.I. Osborn, and Alexander D. Edwards

Author Contributions: S.I.D: Conceptualization, Investigation, Visualization, Formal analysis, Funding acquisition, Writing - original draft, Writing - review & editing. S.H.N: Investigation, Visualization, Writing - review & editing. H.M.I.O: Supervision, Writing - review & editing. A.D.E.: Conceptualization, Funding acquisition, Supervision, Writing - review & editing.

It is published at Sensors and Actuators: B. Chemical.



Label-free smartphone quantitation of bacteria by darkfield imaging of light scattering in fluoropolymer micro capillary film allows portable detection of bacteriophage lysis

Sultan İlayda Dönmez, Sarah H. Needs, Helen M.I. Osborn, Alexander D. Edwards *

School of Pharmacy, University of Reading, Whiteknights, Reading, RG6 6AD, UK

ARTICLE INFO

Keywords:

Label-free detection
Light scattering
Bacteria
Microfluidic
Bacteriophage
Smartphone diagnostics

ABSTRACT

Conventional methods for the detection and quantitation of bacteria are slow, laborious and require a laboratory. Microfluidic systems offer faster and portable testing, and smartphone cameras can record colorimetric or fluorometric bioassays, but this requires dye addition. Here, we demonstrate for the first time label-free smartphone detection of bacterial light scattering by darkfield microfluidic imaging to measure bacteria and bacteriophage lysis. A single LED and portable 3D printed imaging box allowed bacterial concentration and growth to be measured by direct imaging of bacterial light scattering. Bacteriophage lysis was detected within a 10-channel microfluidic device made from melt-extruded fluoropolymer micro capillary film, allowing rapid detection of host specificity. Elimination of unwanted reflections and optimising illumination angle are critical for successful darkfield bacterial imaging, with 15° giving maximal intensity. Bacterial sedimentation was directly observed within microfluidic devices, and detection sensitivity significantly increased by allowing bacteria to sediment for 30 min. With this simple, low-cost, 3D printed system bacterial concentrations down to an optical density of 0.1 could be measured corresponding to 8×10^4 colony forming units (CFU) per micro-device, approaching the sensitivity of conventional spectrophotometers. Bacteriophage lysis could be detected at a range of starting cell concentrations. With a low starting cell concentration, the increase in light scatter signal with incubation was prevented in the presence of bacteriophage. Conversely, with high starting cell concentration, the light scatter signal detected at the start was clearly eliminated when phage were added, indicating this simple system allows direct visualisation of bacteriophage eliminating light scattering by lysis.

1. Introduction

Antimicrobial resistance (AMR) is a major global challenge as antibiotic resistance becomes more prevalent, for example due to microorganisms exchanging resistance genes, and more complex resistance mechanisms, such as biofilm formation, are identified. This makes it harder to treat bacterial infections (WHO, 2014) and it is estimated that by 2050, 10 million people could die annually as a consequence of AMR (Kraker et al., 2016). To tackle this challenge, alternative antimicrobials are essential, and improved tools for rapid microbial detection and antibiotic susceptibility testing are needed to inform antibiotic selection using surveillance and diagnostics (van Belkum et al., 2019). Lytic bacteriophages, which are diverse viruses that replicate whilst killing specific bacteria, are not affected by common antibiotic resistance mechanisms and hence are valuable alternatives to antibiotics (El

Haddad et al., 2018, Debarbieux et al., 2010, Altamirano and Barr, 2019). However, therapeutic phages can only be effective if the infectious agent is a susceptible host, so new methods for rapid determination of bacterial lysis by phage are needed. The traditional double agar layer bacteriophage detection method takes around 24–48 h to complete. Suspensions of phage and host bacteria are combined in agar, with the solid medium limiting the spread of bacteria and phage such that clear plaques can be detected after overnight incubation representing areas where phage have lysed a layer of bacteria.

Bacteriophage have been exploited in the search for rapid and sensitive bacterial detection (Farooq et al., 2018). Lytic T7 bacteriophage attached to magnetic beads were used to detect *E. coli* in drinking water, providing colorimetric detection via a β -galactosidase substrate within 2.5 h (10^4 cfu/mL), but in order to detect fewer bacteria (10 cfu/mL), 6 h of pre-enrichment is required. (Chen et al., 2015). Lytic phage

* Corresponding author.

E-mail address: a.d.edwards@reading.ac.uk (A.D. Edwards).

<https://doi.org/10.1016/j.snb.2020.128645>

Received 31 March 2020; Received in revised form 4 July 2020; Accepted 23 July 2020

Available online 1 August 2020

0925-4005/© 2020 Published by Elsevier B.V.

progeny were also detected via β -galactosidase activated fluorescent probes, allowing phage enumeration with a plaque-droplet assay, cutting detection time to 90 min (Tjhung et al., 2014). Bacteriophage lysis can also be measured by changes in media impedance following lysis, allowing *E. coli* detection via a screen-printed carbon electrode and immobilized T4 bacteriophage (Shabani et al., 2013). Lytic bacteriophages were used as a signal amplification method for detection of *Bacillus anthracis* using lateral flow immunochromatography (Cox et al., 2015). Enzyme-tagged phage allow rapid *E. coli* enumeration in drinking water either colorimetrically on filters (Hinkley et al., 2018), or electrochemically (Wang et al., 2019), and droplet microfluidics allow direct observation of bacteriophage lysis (Yu et al., 2014).

Smartphone cameras have been exploited to digitally record and quantify colorimetric and fluorometric bioassays outside the lab (Huang et al., 2018) and smartphone bacteriophage detection would allow near-patient testing. However, bacteriophage have a different mechanism of action on bacteria compared with antibiotics, so conventional antibiotic susceptibility testing methods (disc diffusion/broth microdilution) cannot be used. Phage lysis is typically detected by turbidity measurement and enumerated with plaque assays on solid media, in the double agar layer (DAL) method. Both these methods require significant user time to complete and the DAL method requires overnight incubation.

Neither is ideally suited to colorimetric or fluorometric smartphone detection, so label-free smartphone bacteria measurement is preferable. Bacterial cell suspensions are most commonly quantified in routine microbiology methods without using dyes, instead relying on visible light attenuation by light scattering in a spectrophotometer. 'Turbidity' is typically measured at 600 nm and expressed as Optical Density (OD). Bacterial cells tend to be largely colourless but contain multiple structures with transitions in refractive index (e.g. cell wall), and therefore suspensions of bacteria tend to scatter light rather than absorb it. In contrast to absorbance measurements of solutions of compounds at specific wavelengths, light scattering by bacteria is largely independent of wavelength across the visible light range, resulting in a milky white appearance and a similar OD at differing wavelengths (Myers et al., 2013, McBirney et al., 2016). This laboratory technique is not especially sensitive and a standard measurement range for spectrophotometers with a 1 cm pathlength cuvette is an OD of 0.1–1 cm⁻¹ where there is a linear relationship between cell concentration and OD. However, in spite of the narrow dynamic range of bacterial cell measurement by turbidity, and high cell concentration required – with an OD of 0.1 corresponding to around 10⁸ CFU/mL (Myers et al., 2013) – it remains ubiquitous because so many analytical microbiology methods use cell concentrations in this range.

Instead of measuring the attenuation of collimated light as OD in a spectrometer, bacterial light scattering can also be measured as an increased positive signal. Light scatter by bacteria has been measured multiple ways. The angle and intensity of light scatter from colloids is affected by particle size, but the complex composition of bacteria makes light scattering by these heterogenous particles – containing multiple structures with mixed refractive index – more difficult to model than with more uniform colloids. For example, flow cytometry routinely measures light scatter on an individual cell level at two angles, allowing some different species to be distinguished by differences in these two values even without dyes or staining. Forward scatter is generally associated with overall cell size and side scatter indicates granularity of cell contents (Felip et al., 2007, Shvalov et al., 1999). Particle sizes larger than the wavelength of the incidence light result in Mie scattering with greater amount of forward scatter (low angle scatter) and for uniform particles information about particle size can be gained from the intensity variation with scatter angle. This has been used for bacterial detection (Waltham et al., 1994, Jo et al., 2015, Hussain et al., 2019), and identification of bacteria directly on skin (Sweeney et al., 2017). In contrast, for particles smaller than the incident wavelength Rayleigh scatter is more prominent with more intense scattering at larger angles.

Laser nephelometry measures light scatter by a wide range of biological colloids with an intense coherent beam of incident light, including very small biological particles such as antibody-antigen complexes. Laser nephelometry has also been used for the detection of microorganisms. While forward scatter would provide the most sensitivity, this can be difficult to measure as the detector cannot distinguish the intense incidence light from the scattered light; therefore a detector is usually placed at 90° to the incident laser (Hoppensteadt and Molnar, 2020)..

Because light scattering can be recorded by digital imaging it is therefore ideal for analysis outside the laboratory by making use of the latest generation of low-cost optoelectronics, such as a smartphone camera combined with LED illumination. Such portable digital imaging has been combined with microfluidic devices to offer further benefits, as miniaturisation into microdevices not only provides a portable format but can also decrease assay times compared to conventional laboratory-based bioassays.

Melt-extruded microcapillary film (MCF) with 10 parallel capillaries can be easily and cost-effectively turned into multiplex bioassay strips suitable for microbial detection (Reis et al., 2016a, Alves and Reis, 2019b, Needs et al., 2019). Microfluidic devices are commonly made of polymers with a different refractive index to water, which can complicate use of imaging techniques such as quantitation of light scattering as light can be refracted or reflected at the device-sample interface (Polanco et al., 2018). In contrast, MCF made from fluoropolymer fluorinated ethylene propylene (FEP) has a refractive index matching water, minimising optical background by diffraction or reflection at the sample-device interface, allowing sensitive colorimetric and fluorometric bioassays (Edwards et al., 2011, Barbosa et al., 2015, Alves and Reis, 2019b, Needs et al., 2019, Reis et al., 2016a). Here we show for the first time that this exceptional transparency also makes label-free bacterial detection by darkfield imaging of light scattering in a microfluidic device feasible. Light scattering by bacteria was recorded within MCF test strips by digital imaging including smartphone camera imaging illuminated with a single LED. Bacterial cell concentration could be quantified over the ranges typically measured in microbiology labs by absorbance in a spectrometer. To illustrate use of this tool we demonstrate that important analytical microbiology methods can be performed in this portable and miniaturised system by showing that bacterial growth kinetics and bacteriophage lysis can be directly monitored without specialised equipment, using microfluidic devices, a bespoke 3D printed box, illuminated by a single LED, and captured with a smartphone camera.

2. Experimental

2.1. Materials

MCF was produced from FEP by Lamina Dielectrics Ltd (Billingshurst, West Sussex, UK) with external dimensions of 4.3 mm wide and 0.4 mm thick, and contained 10 capillaries each with an internal diameter of 200 μ m. To produce hydrophilic test strips, 1 m batches were internally coated by incubation with 5 mg/mL polyvinyl alcohol (PVOH) solution in ultrapure water, as previously described (Reis et al., 2016a). Cameras included smartphone cameras iPhone 6S and Xperia model L1 (Sony), compact camera S120 (model DS126621, Canon) and digital SLR EOS 1300 with 18 megapixel sensor and an EF-S f/2.8 Macro Lens (Canon). 3 mm and 5 mm through-hole white LEDs with forward voltage of 3.4 V and forward current of 20 mA were from RS Components Ltd (Northants, UK) and CPC Farnell (Leeds, UK) powered with a 5 V USB power bank (Amazon UK) and 68 Ω resistor in series; several different LED components were compared including single colour and white LEDs, but the LED type was found to make no significant difference to the light scatter intensity. LB broth and LB agar media were from Sigma (Dorset UK). *E. coli* reference strain ATCC 25922 was obtained from LGC Standards (Middlesex UK). *E. coli* B strain was obtained from the National Centre for Biotechnology Education, University of Reading

(Reading, UK) and bacteriophage T2 was obtained from Mojgan Rabiey, School of Biological Sciences, University of Reading (Reading UK).

2.2. Darkfield imaging system design and optimization

To achieve darkfield imaging and allow dye-free detection of bacteria inside MCF through light scattering from bacterial cells, an initial optimisation process utilised a simple box enclosing key components comprising: light source (LED), sample (MCF test strip), blockers (for blocking unscattered light directly from the LED) and a camera or smartphone (Fig. 1).

The simple LED light-source was chosen as a low-cost and accessible component. A collimated light-source may help to increase sample illumination intensity or reduce glare caused by incoherent light reflecting on the surfaces of the 3D printed prototype, increasing the signal:noise ratio. By reducing the unwanted light, it may also be possible to image the device at a lower angle increasing the scattering intensity. Similar readers to detect light scatter have used an opaque rod at the focal plane to block direct laser light from the detector in a low angle detection scheme (Sun et al., 2019).

MCF test strips loaded with either water alone or differing concentrations of non-viable *E. coli* cells (inactivated by 70 % ethanol, 15 min). The relative positions of the light source and sample were altered to determine optimal parameters for bacterial detection, ranging from: LED illumination angles 5° up to 25°; LED to sample distance 100–200 mm; LED colours of white, blue, green and red; camera distances 100–200 mm. We also examined the microfluidic device orientation: firstly, the capillary orientation was varied (vertical vs horizontal) to study the effect of gravity on the bacterial sample; and secondly the device orientation with respect to illumination angle was varied by comparing images with the LED offset by 15° in a plane with the test strip and capillaries, vs the LED offset by a 15° angle about the capillary axis. Finally, the camera type was examined with images taken in parallel using digital SLR, compact digital camera, iPhone 6S and low-cost Android smartphone (Sony Xperia L1). Tested parameters are shown in Table 1.

With all cameras it was possible to image clear lines showing light scattering by bacterial cells (e.g. Fig. 1B) although with some it was easier to control imaging conditions (exposure, focus). The colour of the line depended on the LED colour used for illumination, but no significant difference was found in scatter intensity between different illumination colours. Unwanted light either directly from LED to camera, or from reflections, was blocked by adding black 3D printed frames, or black fabric which had low light reflection. In conventional laboratory microbiology, attenuation by bacterial light scatter decreases the signal intensity from a collimated light-source to a detector placed in direct line from the source through the sample to the detector. Whilst absorbance by dyes can be readily measured within microcapillary film by imaging on a white light background (in spite of the decreased path-length, 0.2 mm compared to 10 mm in a spectrophotometer) (Reis et al., 2016b, Pivetal et al., 2017, Needs et al., 2019), in contrast bacterial light scatter cannot be detected when placed on a white background. Therefore, to detect light scattering the detector is not placed in line with the light source and darkfield imaging is used instead (Hussain et al., 2019).

Bacterial cells are roughly 1–3 µm long, larger than the wavelength of visible light, therefore, Mie scattering might be expected, with forward scatter giving the highest intensity. Therefore, the greatest signal intensity should be with the camera in-line with the incidence beam. However, at lower illumination angles it became more difficult for the camera to distinguish light scattered by the sample from light directly from the illumination LED. The camera was kept in line with the microdevice (i.e. orthogonal to the face of the devices) to capture the microdevice architecture fully and ensure the capillaries were all in the same focal plane. The scatter angle was altered by moving the LED to vary the angle of the incident light, and was optimised to increase scatter intensity and reduce capture of unscattered light and unwanted

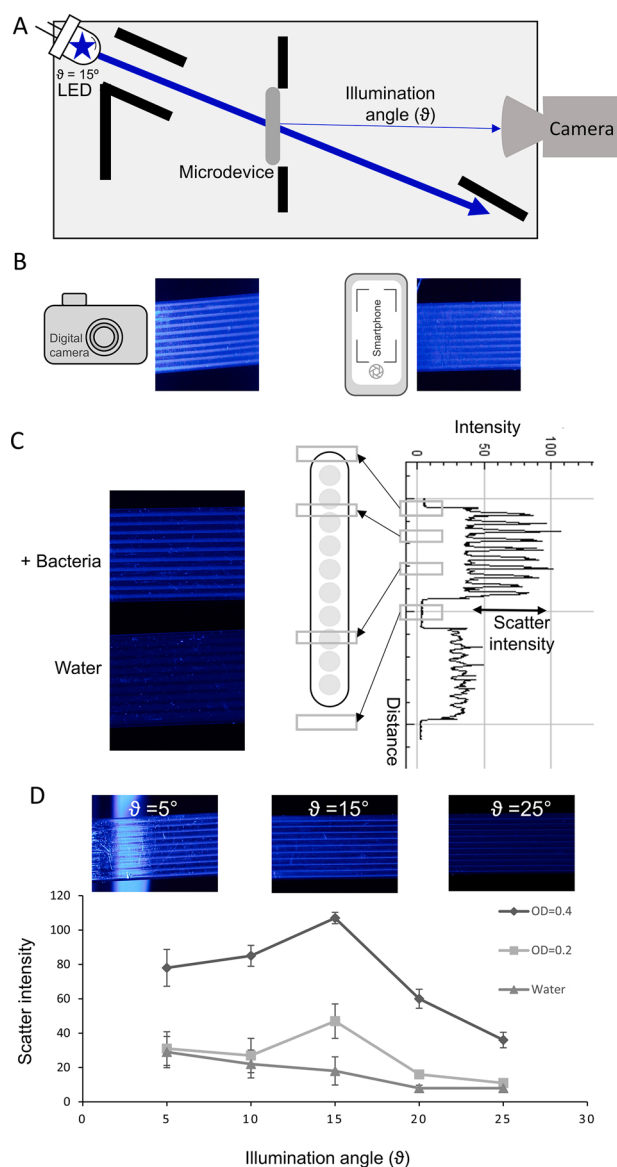


Fig. 1. Darkfield imaging allows label-free smartphone detection of bacteria within a microfluidic device.

A) Geometry of darkfield imaging setup using simple blue LED light source, microfluidic bacterial signal and digital camera. B) Example of bacterial light scattering images taken using camera vs smartphone camera. C) Illustration of image analysis allowing measurement of scatter intensity with an intensity plot across microcapillary device, showing background scatter from microdevice between capillaries. Boxes indicate the following features from top to bottom: reflection from air-water interface at edge of microdevice; light scatter by fluoropolymer device between capillaries; scatter; light scattering by bacteria within capillary; darkfield background. Scatter intensity was defined as the intensity between capillaries to the maximum capillary intensity as indicated. D) Illumination angle was varied and scatter intensity plotted with the indicated 0.2 and 0.4 OD suspensions of killed *E. coli* and compared to no cells. Although bacterial scatter intensity increased with decreasing illumination angle, at very low angles LED was visible directly and background scatter increased. Scatter intensities plotted indicate means and error bars indicate standard deviation of 10 replicate capillaries. Images presented are representative of at least 5 similar images from independent experiments.

reflections. The smaller the angle of the incidence light the greater the light scattering effect (Fig. 1D). However, at $\zeta < 10^\circ$ while the signal increased, the detection of unwanted light also increased, and we selected an optimal illumination angle of $\zeta = 15^\circ$ as having the optimal signal:noise ratio.

Table 1
Imaging parameters tested. Underlined parameters indicate optimised system.

Parameter	Range tested	Optimal condition	Comment
LED distance to sample	70 mm, 80 mm, 90 mm, 100 mm, 110mm	90 mm	As LED is moved closer to sample, glare and background light increases
Illumination angle	5°, 10°, 15°, 20°, 25°	15°	Lower angles give higher signal but higher noise
Relative angle of device to light source	In plane of capillary axis vs offset from capillary axis	Illumination offset in plane with MCF test strip axis	Reduces reflections from curved edge of MCF test strip
Camera to sample distance	150 mm, 160 mm, 170 mm, 180 mm, 190 mm	170 mm	Must
LED colour	Red, green, or blue single colour LED and white LED	N/A	No change in scatter intensity with wavelength; but imaging was simpler with white LED
Camera type	Canon, S120 (compact digital camera) Canon, SLR EOS 1300D with 60 mm macro lens (DSLR) Sony Xperia L1 (Android smartphone) iPhone 6S (iOS smartphone)	N/A	All digital cameras tested were capable of capturing images of scatter; but manual control of exposure and focus is desirable

2.3. Bacteria and bacteriophage preparation and testing

E. coli B strain and T2 bacteriophage and the non-permissive strain, *E. coli* 25922 were selected as a convenient and safe model system to study bacteria and phage detection. *E. coli* B strain was grown in LB broth and agar media at 37 °C overnight, a single colony was re-suspended into LB media at OD600 and adjusted to between 0.1–1 OD600. For T2 bacteriophage amplification, 2 mL of an overnight *E. coli* B strain culture from a single colony isolate was added to 23 mL fresh LB medium and shaken for 3–4 h at 37 °C; 1 mL of the phage stock was added and incubated overnight, centrifuged at 4500 rpm for 45 min, the supernatant phage suspension was filtered through a 0.22 µm syringe filter and stored at 4 °C.

MCF ribbon was cut to 33 mm long test strips corresponding to 1 µL test volume per capillary. Capillaries were filled with bacteria either by capillary action or injection. To measure detection sensitivity and monitor bacterial sedimentation, ethanol-inactivated bacterial cell suspensions were used at 0.1–1.0 OD600. For growth kinetics, an *E. coli* colony inoculated in LB medium was incubated at 37 °C and growth monitored every hour in parallel in a spectrophotometer vs light intensity with darkfield imaging in MCF and bacteria grown in MCF. To determine host cell specificity, *E. coli* B strain and *E. coli* 25922 cultures were grown in LB from single colonies. The two bacterial strains were filled at the indicated concentrations into MCF test strips either loaded with or without T2 phage, and incubated at 37 °C. The MCF capillaries were loaded with phage by filling with a 10⁸ pfu/mL T2 phage suspension, followed by aspiration of the loading material by syringe, leaving a thin film of bacteriophage suspension on the hydrophilic PVOH surface of the microcapillary, as described previously for antibiotic loading (Reis et al., 2016a). Overnight plating was used to determine colony forming units (CFU) for each experiment.

2.4. Data analysis

Digital images were analysed to quantify the light scattering signal using ImageJ (Abràmoff et al., 2004), and the scatter intensity was defined as the difference in light intensity between the space between capillaries and the brightest intensity maximum within each capillary (Fig. 1C). Images presented are representative of multiple images and replicate experiments with the number of repeat experiments indicated in the figure legends.

3. Results and discussion

3.1. Optimising imaging geometry and maximising signal for bacterial quantitation using darkfield imaging of light scatter

Although turbid bacterial suspensions are clearly visible to the eye, within microcapillaries in MCF, they appear as a grey/white line that was difficult to record with a digital camera. Careful optimisation of the darkfield imaging geometry was needed to maximize the bacterial scattering signal and minimize noise from the illumination LED or unwanted reflections, before bacterial light scattering could be robustly quantified in this way (Fig. 1A and B).

Using optimised geometry, it was possible to clearly distinguish bacterial suspensions from controls without bacteria (Fig. 1C). Two major barriers to detecting light scattering by bacteria were identified: firstly when detecting low concentrations of bacteria, the low intensity of signal from bacteria made it hard for the digital camera to focus; secondly bright reflections and unwanted light (termed glare) surrounding the microfluidic device needed to be avoided. The signal was weak with side (side scatter) or epi-illumination (back scatter), and signal:noise varied with illumination angle (Fig. 1D). The clearest light scattering images were obtained when samples were illuminated with a light source almost directly behind the MCF at a 15° angle to the camera, suggesting that forward scatter measurement is most effective (Table 1).

Using the optimal darkfield imaging geometry (illumination angle = 15; camera to sample distance = 170 mm; LED to sample distance = 90 mm) bacterial light scattering was robustly detected. With MCF strips containing water alone, a negative scatter intensity was observed because water-filled capillaries had a lower scattering coefficient than the solid FEP material between capillaries. Reflected and refracted light was seen from the edges of 3D printed blockers, the microfluidic device holder, the surrounding box, and from the microfluidic devices themselves – specifically from its rounded edge and from surface flaws. Reflections from the rounded edge could be minimised by ensuring the LED was offset in line with the MCF test strips rather than rotated around the capillary axis. As expected, LED colour had no significant impact, as light scattering by bacterial cell suspensions appears white and is therefore largely wavelength-independent over the visible light range. However, LED colour did affect some automatic cameras as colour balance features on smartphones attempted to optimise images for even colour intensity potentially distorting image intensity; with such cameras white LED illumination may be preferable.

Label-free smartphone bacterial detection is clearly feasible using direct darkfield imaging of light scattering by bacterial cell suspensions in MCF, allowing quantitation without addition of dyes or probes. We defined key parameters (Table 1) to maximise signal (light scattered by bacteria) and minimise noise (from glare) and found that label-free bacterial measurement in microfluidic devices is only possible with carefully designed illumination geometry. The parameter that had the biggest impact on signal and noise was illumination angle, with lowest angles, $\theta = 5^\circ$, showing high noise, preventing clear bacterial quantitation and the signal:noise intensity of scattered light peaking at an illumination angle of 15° (Fig. 1D). Light scattering and reflection occur not only from bacteria, but also from the device, especially at interfaces between materials of differing refractive index (device-air and device-water), and from light scattering by the device material itself. Using a

microfluidic device fabricated from a fluoropolymer material that has a refractive index matched to the aqueous sample simplifies this by eliminating the device-water reflection and diffraction.

3.2. Sensitivity of bacterial measurement is improved following bacterial sedimentation within capillaries

One remarkable observation was that when MCF test strips were imaged horizontally, it was possible to directly observe bacterial sedimentation within the device (Fig. 2) and improve the detection of bacterial suspensions. *E. coli* suspensions of 0.1–1.0 OD600 were filled into parallel microcapillaries within the same MCF test strip. The scatter intensity was proportional to cell density. Initially, the lowest cell density showing clear scattering at 0.34 OD600 was 2.8×10^5 CFU/capillary with volume of 1 μ L. Sequential images showed sedimentation within the capillaries, with intensity increasing whilst line width

reduced (Fig. 2A). After sedimentation, bacterial concentrations as low as 0.1 OD600 were clearly detected corresponding to a cell density of 8×10^4 CFU/capillary. The intensity reached after sedimentation was even higher for larger capillary diameter, although this took longer to settle, plateauing after 40 min (Fig. 2B).

Using only the smartphone camera plus single LED light source, with 1 μ L sample volumes and a pathlength of only 0.2 mm (compared to 10 mm for conventional spectrophotometer), cell densities as low as 0.1 OD600 could be detected. Whilst this label-free technique still requires relatively high cell densities with the minimum detectable concentration being 8×10^7 CFU/mL, by using the microfluidic design to allow sedimentation to increase signal we achieved similar measurement range to the ubiquitous microbiology laboratory method using a conventional spectrometer to make turbidity measurements that quantify attenuation of collimated light by the bacterial cell suspension. While spectrophotometer measurements typically use a sample volume of 0.1–1 mL, the

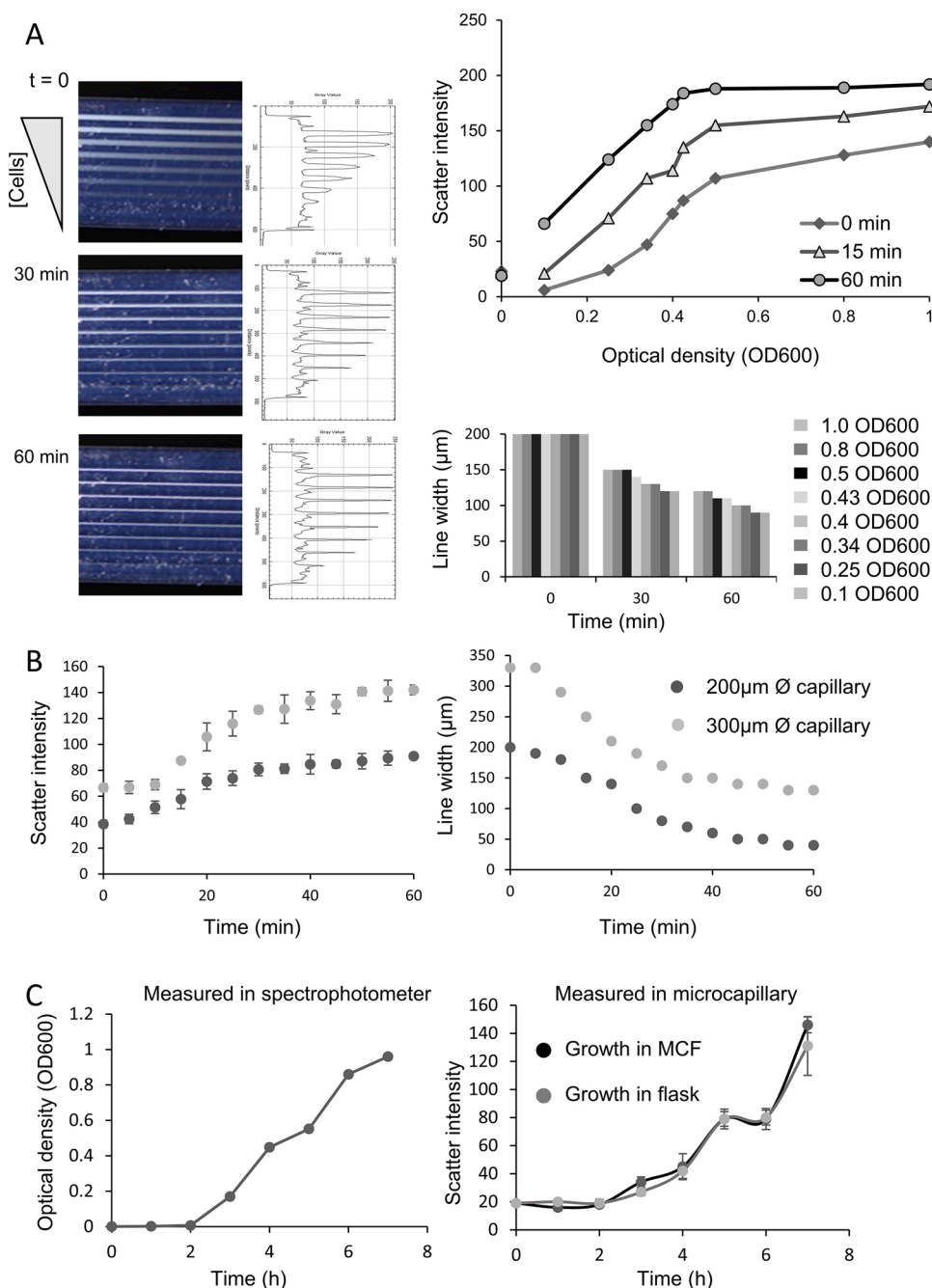


Fig. 2. Direct observation of bacterial sedimentation and growth in MCF by light scattering.

A) Sedimentation of eight concentrations of *E. coli* were imaged in 200 μ m internal diameter MCF strips, with the top and bottom capillary being filled with water alone, and highest bacterial density in the topmost capillary were imaged using a white LED. Scattering intensity increased, and width of scattering signal decreased with time as bacteria sedimented to the bottom of the microcapillaries. Light scatter intensity was plotted against cell density (measured as OD600) without sedimentation and after 30 or 60 min, showing increased sensitivity with sedimentation. B) Bacterial sedimentation was observed over time within two different microcapillary diameters (200 μ m and 300 μ m) using *E. coli* at 0.3 OD. Data indicates the mean of 20 replicate microcapillaries C) Growth curves were measured in parallel using cuvette in spectrophotometer vs within MCF and comparing cell growth kinetics in flask vs within 20 replicate microcapillaries. All error bars are plotted and indicate the standard deviation, in some cases this is smaller than the symbol size.

microcapillary device uses only 1 μL per capillary. Although the overall concentration of bacteria did not change, as bacteria settled to the bottom of the capillaries the local concentration increased significantly and therefore increased the intensity of light scattering that could be imaged. Sedimentation of bacteria by gravity has been observed in MCF strips, using immunocapture of *E. Coli* in MCF, and demonstrates that higher number of *E. Coli* are captured in the lower 35 μm section of 200 μm diameter capillaries after sedimentation (Alves and Reis, 2019a). The line thickness of the bacterial sample in the same microcapillary film reduced from 200 μm to below 50 μm after 30 min (Fig. 2B). Without sedimentation, the lowest bacterial concentration that can be measured was 0.34 OD600, but within 30 min a further increase in detection sensitivity allowed clear detection down to 0.1 OD600. Even with this increased sensitivity, label-free detection is less sensitive than dye-labelled detection (e.g. chlorophenol red- β -D-galactopyranoside) or other amplified systems where detection of 10^3 or 10^4 CFU/mL (1×10^{-4} or 1×10^{-5} OD) can be achieved (Chen et al., 2015, Shabani et al., 2013). However, many microbiological techniques rely on turbidity measurements of cell concentrations in this 0.1–1.0 OD600 range which is the range measured by the spectrophotometer (Fig. 2C), and we propose our system is a viable alternative to spectrometer measurements.

3.3. Portable smartphone detection of growth kinetics and bacteriophage lysis

Bacterial growth was monitored in MCF vs cuvettes, comparing darkfield scattering intensity with OD measurements in a spectrophotometer. Similar growth kinetics were observed when grown in a shaker flask – either measured in cuvette or transferred to MCF for measurement – or grown directly and measured in MCF (Fig. 2C), indicating both that measurement between cuvette and MCF is comparable, and *E. coli* growth is similar in MCF to shaken flask, demonstrating that label-free growth kinetics can be measured in microfluidics. A major advantage of label-free bacterial cell detection is for the detection of bacterial lysis,

for example, by phage. This cannot easily be monitored using metabolic growth dyes, because the dye can be converted by viable bacteria prior to lysis.

One critical purpose of this device was to detect lytic fragmentation of target bacteria in microfluidic devices to determine bacteriophage host specificity. We designed and 3D printed a prototype portable smartphone bacteriophage lysis reader (Fig. 3A), using the optimised parameters for darkfield bacterial scatter imaging. When bacterial target cell suspensions were taken up into MCF capillaries loaded with phage and incubated, no light scattering signal was seen (Fig. 3B and C). This demonstrates that smartphone imaging with darkfield illumination can detect bacterial lysis in microdevices. To determine if host specificity could be rapidly determined with this system, two strains of *E. coli* were tested. As expected, when permissive *E. coli* B strain were tested in T2 phage loaded MCF test strips, light scattering was lost in contrast to the T2 resistant *E. coli* 25922 strain that showed high scattering signal in the presence of T2 phage (Fig. 3B and C). During incubation, strips were kept in the same conformation to allow bacterial sedimentation throughout the experiment, increasing signal intensity of the bacteria. This also minimised any changes in light scattering due to time to image.

In many important microbiology assays (e.g. antibiotic susceptibility testing), bacterial inoculum has a significant impact on results (Smith and Kirby, 2018). We therefore evaluated phage lysis assays with high or low bacterial starting concentrations, with the high concentration being clearly visible by light scattering at the start. Varying the starting concentration did not change the outcome and an absence of light scattering was always clear when phage matched host. This observation may be useful when testing environmental or clinical samples directly as normalisation of bacterial concentration prior to testing is time consuming and laborious. Lysis can still be detected at high starting cell density as bacteriophages replicate much faster than bacteria (Carlton, 1999) and the lytic cycle leads to degradation of target cells eliminating the light-scattering particles. This observation is extremely important for the rapid detection of phage lysis. Many devices depend on differentiation between a bacterial growth curve with and without phage,

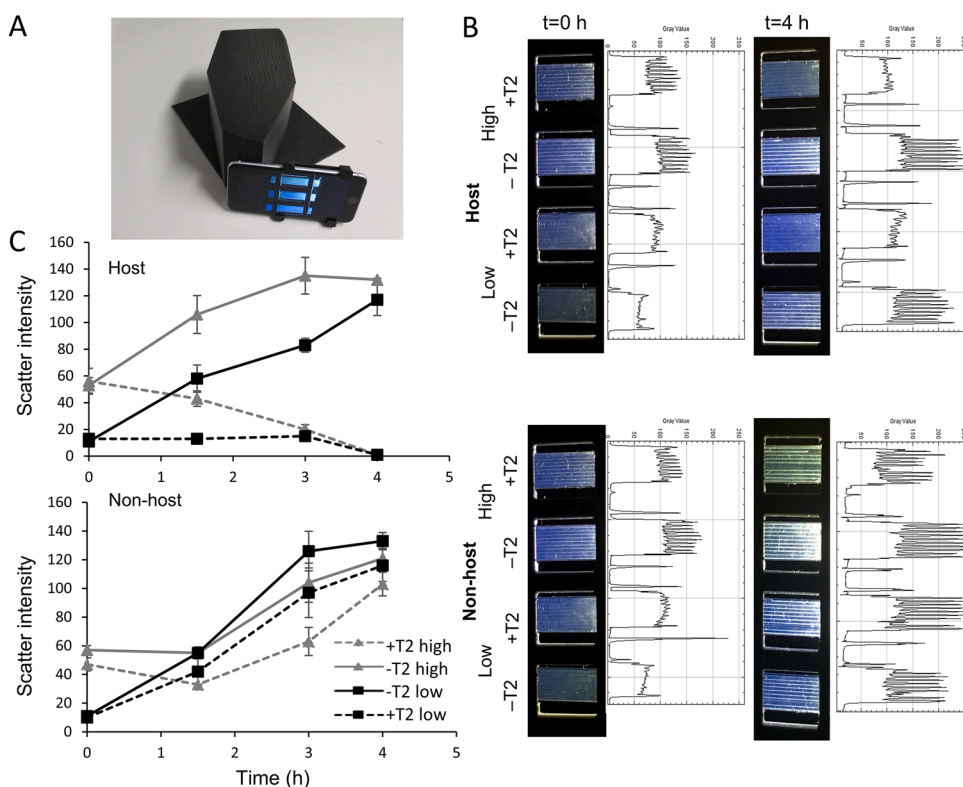


Fig. 3. Detection of growth inhibition and lysis by T2 bacteriophage in MCF allows host specificity to be determined by smartphone.

A) Illustration of 3D printed prototype “Phageoscope”, a smartphone-compatible darkfield bacterial light scattering measurement device. This offers optimal illumination with a single white LED and combination of light barriers to eliminate unwanted reflections, a holder for microfluidic devices in the centre, and a smartphone clip to position the camera for imaging into the box. B) Images of sets of 4 test strips in the Phageoscope with an iPhone 6S, of tests strips with the indicated combination of bacterial strain (host = *E. coli* B strain, non-host = *E. coli* 25922) and T2 bacteriophage. High starting concentration was 0.3 OD600 (2.4×10^8 CFU /mL), low was 0.1 OD600 (8×10^7 CFU /mL). C) Plot of scatter intensity for strips in B indicating mean of 10 replicate capillaries. All error bars are shown and represent one standard deviation. Data are representative of at least 3 independent repeats.

therefore the detection speed is constrained by bacterial growth rate. However, by starting with a high concentration of bacteria, the detection rate becomes dependent only on the phage lysis kinetics which can be far faster. This has been reported when using optical density measurements of phage lysis, which identified that a higher bacterial starting density reduced the time to phage lysis detection (Rajnovic et al., 2019). In our label-free microfluidic system, differential light scatter intensity showed evidence of phage activity as early as after 1.5 h incubation, but full lysis and elimination of light scattering signal was complete at 4 h (Fig. 3C). Further work to incorporate a fully automated time-lapse imaging setup is now justified to further decrease time-to-result of lysis detection. Increasing the resolution of the growth curves will allow differentiation between bacterial growth and lysis earlier.

It is important to be able to rapidly determine if a target pathogen is a lytic host for a therapeutic phage prior to treatment. This proof-of-concept shows that phage can be loaded within MCF devices and lysis detected with a range of target cell densities, suggesting this method could be used as a companion diagnostic for bacteriophage therapy. Further work to characterise and optimise the loading process to quantify and stabilise bacteriophage within the MCF, and to load panels of different bacteriophage with distinct host specificity, is justified. Ultimately, validation will be required for specific therapeutic applications of therapeutic phage to treat specific infections such as hospital-acquired *S. aureus* infection.

4. Conclusions

We demonstrate for the first time that label-free microfluidic bacterial detection can be used to determine host specificity for lytic bacteriophage in a portable device using smartphone imaging of light scattering from bacteria illuminated with a single LED.

Digital imaging of MCF in darkfield illumination allowed measurement of bacteria for analytical microbiology such as bacterial growth kinetics, sedimentation and phage lysis of both low and high bacterial cell densities. The major parameters affecting measurement of bacteria in a microfluidic device by light scattering and darkfield imaging were defined, and the optimum illumination angle identified as 15°, with elimination of unwanted light reflected or diffracted by the device, holder or container being critical to sensitivity. We propose that microcapillaries should be incubated horizontally for as imaging to allow bacterial sedimentation that increases scattering intensity and thus significantly increases analytical sensitivity. Likewise, illumination should be offset in a horizontal plane to reduce reflections by the curved sides of the device.

Comparison with other microfluidic devices is now justified to identify how important refractive index matching and device geometry is for cell measurement by light scattering. While microfluidic devices have been developed that measure both absorbance and light scattering in bacterial and other biological samples, many of these remain low throughput or require specialised equipment (Strzelak et al., 2016, Strzelak et al., 2020, Keays et al., 2016, Sun et al., 2019). Many of these devices test a single sample can be tested, whereas our digital camera setup can image multiple at once (5 strips each with 10 capillaries i.e. 50 conditions per image). Furthermore, no pumps or fluidic controllers are required, with the sample simply drawn up into 10 microcapillaries by capillary action.

Having demonstrated proof-of-concept and the potential of label-free darkfield imaging for miniaturising analytical microbiology, such as companion diagnostics for advanced biological therapeutics in the treatment of bacterial infections, further miniaturisation is now possible retaining the core requirements of the 3D printed prototype, and evaluation with a larger range of hosts and phage is justified.

CRedit authorship contribution statement

Sultan İlayda Dönmez: Conceptualization, Investigation, Visualization, Formal analysis, Funding acquisition, Writing - original draft, Writing - review & editing. **Sarah H. Needs:** Investigation, Visualization, Writing - original draft, Writing - review & editing. **Helen M.I. Osborn:** Conceptualization, Supervision, Writing - original draft, Writing - review & editing. **Alexander D. Edwards:** Conceptualization, Funding acquisition, Supervision.

Declaration of Competing Interest

ADE is one of the inventors of patent application protecting aspects of the novel microfluidic devices tested in this study, and are directors and shareholders in Capillary Film Technology Ltd, a company holding a commercial license to this patent application.

References

- M.D. Abràmoff, P.J. Magalhães, S.J. Ram, Image processing with ImageJ, *Biophotonics Int.* 11 (2004) 36–42.
- F.L.G. Altamirano, J.J. Barr, Phage therapy in the postantibiotic era, *Clin. Microbiol. Rev.* 32 (2019) e00066–18.
- I.P. Alves, N.M. Reis, Immunocapture of *Escherichia coli* in a fluoropolymer microcapillary array, *J. Chromatogr. A* 1585 (2019a) 46–55.
- I.P. Alves, N.M. Reis, Microfluidic smartphone quantitation of *Escherichia coli* in synthetic urine, *Biosens. Bioelectron.* 145 (2019b), 111624.
- A.I. Barbosa, P. Gehlot, K. Sidapra, A.D. Edwards, N.M. Reis, Portable smartphone quantitation of prostate specific antigen (PSA) in a fluoropolymer microfluidic device, *Biosens. Bioelectron.* 70 (2015) 5–14.
- J. Chen, S.D. Alcaine, Z. Jiang, V.M. Rotello, S.R. Nugen, Detection of *Escherichia coli* in drinking water using T7 bacteriophage-conjugated magnetic probe, *Anal. Chem.* 87 (2015) 8977–8984.
- C.R. Cox, K.R. Jensen, R.R. Mondesire, K.J. Voorhees, Rapid detection of *Bacillus anthracis* by gamma phage amplification and lateral flow immunochromatography, *J. Microbiol. Methods* 118 (2015) 51–56.
- L. Debarbieux, D. Leduc, D. Maura, E. Morello, A. Criscuolo, O. Grossi, V. Balloy, L. Touqui, Bacteriophages can treat and prevent *Pseudomonas aeruginosa* lung infections, *J. Infect. Dis.* 201 (2010) 1096–1104.
- A.D. Edwards, N.M. Reis, N.K. Slater, M.R. Mackley, A simple device for multiplex ELISA made from melt-extruded plastic microcapillary film, *Lab Chip* 11 (2011) 4267–4273.
- L. El Haddad, C.P. Harb, M.A. Gebara, M.A. Stibich, R.F. Chemaly, A systematic and critical review of bacteriophage therapy against multidrug-resistant ESKAPE organisms in humans, *Clin. Infect. Dis.* 69 (2018) 167–178.
- U. Farooq, Q. Yang, M.W. Ullah, S. Wang, Bacterial biosensing: recent advances in phage-based bioassays and biosensors, *Biosens. Bioelectron.* 118 (2018) 204–216.
- M. Felip, S. Andreatta, R. Sommaruga, V. Straskrbová, J. Catalan, Suitability of flow cytometry for estimating bacterial biovolume in natural plankton samples: comparison with microscopy data, *Appl. Environ. Microbiol.* 73 (2007) 4508–4514.
- T.C. Hinkley, S. Singh, S. Garing, A.-L.M. Le Ny, K.P. Nichols, J.E. Peters, J.N. Talbert, S.R. Nugen, A phage-based assay for the rapid, quantitative, and single CFU visualization of *E. coli* (ECOR# 13) in drinking water, *Sci. Rep.* 8 (2018) 1–8.
- D.A. Hoppensteadt, J.A. Molnar, 42 - hemostasis and coagulation instrumentation, in: E. M. Keohane, C.N. Otto, J.M. Walenga (Eds.), *Rodak's Hematology*, 6th ed., Content Repository Only, St. Louis (MO), 2020.
- X. Huang, D. Xu, J. Chen, J. Liu, Y. Li, J. Song, X. Ma, J. Guo, Smartphone-based analytical biosensors, *Analyst* 143 (2018) 5339–5351.
- M. Hussain, M. Lv, J. Xu, X. Dong, T. Wang, Z. Wang, W. Wang, N. He, Z. Li, B. Liu, Rapid identification of pathogens based on MIE light scattering and machine learning approach, 2019 IEEE International Symposium on Medical Measurements and Applications (MeMeA), 26–28 June 2019 (2019) 1–5.
- Y. Jo, J. Jung, M.H. Kim, H. Park, S.J. Kang, Y. Park, Label-free identification of individual bacteria using Fourier transform light scattering, *Opt. Express* 23 (2015) 15792–15805.
- M.C. Keays, M. O'Brien, A. Hussain, P.A. Kiely, T. Dalton, Rapid identification of antibiotic resistance using droplet microfluidics, *Bioengineered* 7 (2016) 79–87.
- M.E.A. Kraker, A.J. Stewardson, S. Harbarth, Will 10 million people die a year due to antimicrobial resistance by 2050? *PLoS Med.* 13 (11) (2016).
- S.E. McBirney, K. Trinh, A. Wong-Berlinger, A.M. Armani, Wavelength-normalized spectroscopic analysis of *Staphylococcus aureus* and *Pseudomonas aeruginosa* growth rates, *Biomed. Opt. Express* 7 (2016) 4034–4042.
- J.A. Myers, B.S. Curtis, W.R. Curtis, Improving accuracy of cell and chromophore concentration measurements using optical density, *BMC Biophys.* 6 (2013), 4–4.
- S.H. Needs, T.T. Diep, S.P. Bull, A. Lindley-Decaire, P. Ray, A.D. Edwards, Exploiting open source 3D printer architecture for laboratory robotics to automate high-throughput time-lapse imaging for analytical microbiology, *PLoS One* 14 (2019), e0224878.
- J. Pivetal, F.M. Pereira, A.I. Barbosa, A.P. Castanheira, N.M. Reis, A.D. Edwards, Covalent immobilisation of antibodies in Teflon-FEP microfluidic devices for the

- sensitive quantification of clinically relevant protein biomarkers, *Analyst* 142 (2017) 959–968.
- E.R. Polanco, N. Western, T.A. Zangle, Fabrication of refractive-index-matched devices for biomedical microfluidics, *J. Vis. Exp.* (2018) 58296.
- D. Rajnovic, X. Muñoz-Berbel, J. Mas, Fast phage detection and quantification: an optical density-based approach, *PLoS One* 14 (2019), e0216292.
- N.M. Reis, J. Pivetal, A.L. Loo-Zazueta, J.M. Barros, A.D. Edwards, Lab on a stick: multi-analyte cellular assays in a microfluidic dipstick, *Lab Chip* 16 (2016a) 2891–2899.
- N.M. Reis, J. Pivetal, A.L. Loo-Zazueta, J.M.S. Barros, A.D. Edwards, Lab on a stick: multi-analyte cellular assays in a microfluidic dipstick, *Lab Chip* 16 (2016b) 2891–2899.
- A. Shabani, C.A. Marquette, R. Mandeville, M.F. Lawrence, Magnetically-assisted impedimetric detection of bacteria using phage-modified carbon microarrays, *Talanta* 116 (2013) 1047–1053.
- A.N. Shvalov, I.V. Surovtsev, A.V. Chernyshev, J.T. Soini, V.P. Maltsev, Particle classification from light scattering with the scanning flow cytometer, *Cytometry* 37 (1999) 215–220.
- K.P. Smith, J.E. Kirby, The inoculum effect in the era of multidrug resistance: minor differences in inoculum have dramatic effect on MIC determination, *Antimicrob. Agents Chemother.* 62 (2018) e00433–18.
- K. Strzelak, C. Malasuk, Y. Oki, K. Morita, R. Ishimatsu, 3D printed silicone platforms with laser-scattering protein detection under flow analysis conditions as a development of Silicone Optical Technology (SOT), *Microchem. J.* 157 (2020), 104936.
- K. Strzelak, J. Misztal, Ł. Tymecki, R. Koncki, Bialyalyte multicommutated flow analysis system for microproteinuria diagnostics, *Talanta* 148 (2016) 707–711.
- Q. Sun, W. Zheng, C. Lin, D. Shen, A low-cost micro-volume nephelometric system for quantitative immunoagglutination assays, *Sensors (Basel, Switzerland)* 19 (2019) 4359.
- R.E. Sweeney, E. Budiman, J.Y. Yoon, Mie scatter spectra-based device for instant, contact-free, and specific diagnosis of bacterial skin infection, *Sci. Rep.* 7 (2017) 4801.
- K.F. Tjhung, S. Burnham, H. Anany, M.W. Griffiths, R. Derda, Rapid enumeration of phage in monodisperse emulsions, *Anal. Chem.* 86 (2014) 5642–5648.
- A. Van Belkum, T.T. Bachmann, G. Lüdke, J.G. Lisby, G. Kahlmeter, A. Mohess, K. Becker, J.P. Hays, N. Woodford, K. Mitsakakis, Developmental roadmap for antimicrobial susceptibility testing systems, *Nat. Rev. Microbiol.* 17 (2019) 51–62.
- C. Waltham, J. Boyle, B. Ramey, J. Smit, Light scattering and absorption caused by bacterial activity in water, *Appl. Opt.* 33 (1994) 7536–7540.
- D. Wang, T. Hinkley, J. Chen, J.N. Talbert, S.R. Nugen, Phage based electrochemical detection of *Escherichia coli* in drinking water using affinity reporter probes, *Analyst* 144 (2019) 1345–1352.
- WHO, Antimicrobial Resistance: Global Report on Surveillance, World Health Organization, 2014.
- J.Q. Yu, W. Huang, L.K. Chin, L. Lei, Z.P. Lin, W. Ser, H. Chen, T.C. Ayi, P.H. Yap, C. H. Chen, A.Q. Liu, Droplet optofluidic imaging for lambda-bacteriophage detection via co-culture with host cell *Escherichia coli*, *Lab Chip* 14 (2014) 3519–3524.



Sultan Ilayda Donmez I completed my master's education at Karamanoglu Mehmetbey University, Engineering Faculty, Department of Bioengineering. I also worked as a Project Assistant at TUBITAK (Scientific and Technological Research Council of Turkey) Project entitled as 'Development and Characterisation of DNA Aptamers for *Streptococcus pneumoniae*'. My interest in biotechnology studies led me to study for my PhD with Dr Edwards. My current topic is label-free therapeutic bacterial detection and bacteriophage therapy in microfluidic systems.



Alexander D Edwards With a background in fundamental immunology combined with expertise in biochemical engineering, I am an interdisciplinary researcher focused on solving current and future healthcare challenges using an engineering science approach that combines a range of fields from biology, biochemistry, chemistry and physics. I work at the interface between academic technology discovery and industrial development and have experience of both fundamental research and the commercialisation of new technology.

Chapter 4

Label-free 1D Microfluidic Dipstick Counting of Microbial Colonies and Bacteriophage Plaques

Chapter summary: In this section, it is demonstrated that the biosensing platform, where microfluidics are combined with digital imaging, can be performed accurately, quickly and highly efficiently for viable bacterial cell and simplified bacteriophage plaque counting. The Raspberry Pi provides more control over the system, which gives it an edge over the smartphone. With a smartphone, most settings are selected automatically, on the contrary, with Raspberry, the ISO, aperture, and exposure settings of the system can be adjusted manually. Thus, not only automatic photo shooting at the desired range is provided, but also it provides better quality photos by avoiding background glare.

Bibliographic details: Sultan İlayda Dönmez, Sarah H. Needs, Helen M.I. Osborn, Nuno M. Reis and Alexander D. Edwards

Author Contributions: S.I.D: Conceptualization, Investigation, Visualization, Formal analysis, Funding acquisition, Writing - original draft, Writing - review & editing. S.H.N: Investigation, Visualization, Writing - review & editing. H.M.I.O: Supervision, Writing - review & editing. N.M.R: Conceptualization, Visualization, Writing - review & editing. A.D.E: Conceptualization, Funding acquisition, Supervision, Writing - review & editing.

Submitted to: *Lab on a chip, published.*



Cite this: DOI: 10.1039/d2lc00280a

Label-free 1D microfluidic dipstick counting of microbial colonies and bacteriophage plaques†

 Sultan İlayda Dönmez, ^{*,a} Sarah H. Needs, ^a Helen M. I. Osborn,^a
 Nuno M. Reis ^{bc} and Alexander D. Edwards ^{*,ac}

Counting viable bacterial cells and functional bacteriophage is fundamental to microbiology underpinning research, surveillance, biopharmaceuticals and diagnostics. Colony forming unit (CFU) and plaque forming unit (PFU) counting still requires slow and laborious solid culture on agar in Petri dishes or plates. Here, we show that dip-stick microfluidic strips can be used without growth indicator dye for rapid and simple CFU mL^{-1} and PFU mL^{-1} measurement. We demonstrate for the first time that fluoropolymer microcapillaries combined with digital imaging allow bacteriophage plaques to be counted rapidly in a dip-and-test format. The microfluidic length scales offer a linear 1-dimensional alternative to a 2D solid agar medium surface, with colonies or plaques clearly visible as “dashes” or “gaps”. An inexpensive open source darkfield biosensor system using Raspberry Pi imaging permits label-free detection and counting of colonies or plaques within 4–8 hours in a linear, liquid matrix within $\sim 200 \mu\text{m}$ inner diameter microcapillaries. We obtained full quantitative agreement between 1D microfluidic colony counting in dipsticks *versus* conventional 2D solid agar Petri dish plates for *S. aureus* and *E. coli*, and for T2 phage and phage K, but up to 6 times faster. Time-lapse darkfield imaging permitted detailed kinetic analysis of colony growth in the microcapillaries, providing new insight into microfluidic microbiology and colony growth, not possible with Petri dishes. Surprisingly, whilst *E. coli* colonies appeared earlier, subsequent colony expansion was faster along the microcapillaries for *S. aureus*. This may be explained by the microenvironment offered for 1D colony growth within microcapillaries, linked to a mass balance between nutrient (glucose) diffusion and bacterial growth kinetics. Counting individual colonies in liquid medium was not possible for motile strains that spread rapidly along the capillary, however inclusion of soft agar inhibited spreading, making this new simple dip-and-test counting method applicable to both motile and non-motile bacteria. Label-free dipstick colony and plaque counting has potential for many analytical microbial tasks, and the innovation of 1D colony counting has relevance to other microfluidic microbiology.

 Received 25th March 2022,
 Accepted 1st July 2022

DOI: 10.1039/d2lc00280a

rsc.li/loc

1. Introduction

Viable cell or virus counting is a central method in microbiology and remains vital from fundamental research to clinical and public health. Measuring microbial cell concentrations may aid diagnosis of infection or treatment decisions, and can allow detection and prevent contamination, controlling the safety of food products and water sources.^{1–3} This method involves the spreading of serial sample dilutions onto solid agar medium in Petri dishes and

counting colony-forming units (CFU). Bacteriophage enumeration requires the addition of host bacteria cells to the solid media alongside sample of phage to allow lytic growth leading to a clear patch that allows counting of plaque-forming units (PFU).^{4,5} Colony counting on solid media measures viable cells that can form colonies specifically, which is why it remains a standard reference method for quantifying viable bacteria. Although minimal equipment is needed, and plates can be scanned or counted with the naked eye, it requires some skill plus sufficient incubation space for large numbers of Petri dishes, and is limited to microorganisms able to form colonies on agar. Counts are only made after overnight incubation, yet viable cell numbers can change very quickly, severely delaying knowledge of true viable cell count until after other experiments are completed.

Turbidimetry, microscopy or flow cytometry can be used to rapidly estimate cell concentration. Although quick and

^a Reading School of Pharmacy, University of Reading, Whiteknights, RG6 6AD, UK
 s.ilyadadnmez@gmail.com, a.d.edwards@reading.ac.uk

^b Department of Chemical Engineering and Centre for Biosensors, Biodevices and Bioelectronics (C3Bio), University of Bath, Claverton Down, Bath BA2 7AY, UK

^c Capillary Film Technology Ltd, Daux Road, Billingshurst, West Sussex RH14 9SJ, UK

† Electronic supplementary information (ESI) available. See DOI: <https://doi.org/10.1039/d2lc00280a>



convenient, turbidimetry measurements (typically with a spectrophotometer) are only suitable for non-cloudy samples⁶ and have a limited range ($\sim 10^8$ to 10^{10} CFU mL⁻¹); estimating cell number simply by light scattering means it cannot distinguish between live and dead cells, and requires calibrating for particular species, instrument, and growth conditions. Flow cytometers are quantitative and sensitive for counting individual cells, where instrumentation is available. Microscopy can be conducted by trained staff or using digital microscopy plus image analysis, but care is needed in sample preparation. For both microscopy and cytometry, fluorescent dyes can be used to distinguish live from dead cells.⁷

Accurate counting of viable viral particles is significantly harder than cell counting. Viral particles are smaller than bacterial cells, making standard cytometry and microscopy techniques challenging. Molecular methods such as real-time quantitative PCR for sequence-specific measurement or using dyes for bulk viral nucleic acid concentration can be used.⁸ However, non-viable particles can also contain nucleic acid, so such molecular measures do not fully correlate with viable infectious particle counts. Culture based methods add further methodological complications. For bacteriophage enumeration, host bacteria must not only be available to permit viral replication but must be retained in place to permit individual replicating viral particles to be identified through plaque formation. Typically, a solid media matrix is used to retain host cells plus viral particles in a 2D plane, allowing visualisation of lysed host cells as an empty space. The double agar layer (DAL) method for bacteriophage enumeration developed by Felix d'Herelle in 1917 allows formation of visible lysis plaques in a uniform lawn of host bacteria, to detect and enumerate phages.⁹ But although DAL remains the standard tool for viable phage detection and measurement, plaque counting methods are restricted to skilled staff in the laboratory and remain challenging to automate or standardise to increase efficiency. To respond to antibiotic resistance using biological therapeutics such as therapeutic phage,^{10,11} and to simplify pathogen detection using phage,¹² improved methods for phage enumeration are therefore vital. Viruses of eukaryotic hosts are likewise counted as plaque forming units on a solid culture surface coated with a monolayer of host cells. Among alternatives to the classical DAL method, one promising method for phage enumeration uses compartmentalisation into monodisperse droplets, as an alternative to a 2D solid medium surface. Droplet enzymatic testing is used to detect phage amplified in a simple droplet. Thus, phage in the emulsion culture can be visualized and counted. For example, reporter phages were detected using a reporter enzyme. However, in addition to requiring a fluorescent dye substrate, the requirement for reporter enzyme limits this example method to only certain samples.¹³

Microfluidic devices are increasingly used by many disciplines to overcome the limitations of traditional "millifluidic" laboratory methods. By simplifying and/or automating fluidic processing steps, speeding up diffusion-

limited processes, and cutting sample volume, microfluidics provide opportunities to make faster, easier and more cost-effective biological analyses. Biosensors add monitoring and time-resolved measurements, with the potential to study microbial growth alongside enumeration.¹⁴ The speed of detection of microbes by growth may not be limited by diffusion to the same degree as other bioassays that depend on the analyte needing to diffuse to the site of a binding agent; instead miniaturisation may offer a different benefit: by confining growing cells within a smaller space, earlier detection may be possible for example by retaining converted dye in a smaller volume, increasing local concentration and thus signal intensity.¹⁵ However, timescales for bacteria counting methods that rely on growth will not necessarily yield a reduction in detection times through miniaturisation alone.¹⁶

Microfluidic devices can be used to detect and characterize cell number/density with a digital growth readout within microdroplets or compartments which can be converted into viable cell counts using simple statistical distribution models.^{17,18} The compartment size and number affects analytical dynamic range so can be adjusted depending on the analytical need.¹⁶ Microdroplets have been used extensively for single cell characterisation studies but can also be used for accurate density calculations. A laser-induced fluorescence (LIF) based method has been developed to count the dispersion of bacterial and eukaryotic cells encapsulated in droplets. By tracking the peaks within the droplets, cell counts were accurately calculated.¹⁹ Another study used 4 pL microdroplets to determine cell counts for urinary tract infections, in which cell count is a diagnostic marker. Similarly, detection of bacteria was determined by fluorescence readout from a molecular probe for bacterial 16S.²⁰ In another study, the concentration of live bacteria was determined by fluorescent imaging of bacteria under magnetic fields using magnetically assisted microfluidic method. Capture to antibody modified magnetic-microbeads detected $\sim 5 \times 10^3$ CFU ml⁻¹ *E. coli* within 1 hour.²¹ Fewer methods have been demonstrated for enumerating phage.

To exploit microfluidics for analytical microbiology, a more detailed understanding of similarities and differences in bacterial growth between conventional systems and microsystems is needed. Digital imaging has become a major tool for biosensing, with inexpensive digital microscopy and miniaturised cameras becoming particularly relevant for microbial biosensing. Smartphone cameras or the CMOS image sensors mass-produced for consumer smartphones can be adapted, for example using Raspberry Pi camera platform. Biosensing and digital imaging has the potential to provide essential insight into the engineering science of microfluidic microbiology.²² In a phage lysis monitoring by smartphone emulsion-based application, a single phage in a droplet is highly replicated in a short time by amplifying the bacteriophage in monodisperse droplets. An increase in the number of phages *via* β -galactosidase-activated fluorescent probes results in a fluorescent signal, and the droplet



receiving the signal is considered phage positive.¹³ Increasing interest in open-source hardware has increased the development of inexpensive, customizable personal or analysis equipment. A fluorescence microscope device consisting of blue LEDs, a Raspberry Pi camera, and a filter allows imaging of bacteria.²³ For scaled-up analytical microbiology screening, a low-cost and high-performance imaging system was developed adding the Raspberry Pi camera to a 3D printed robotic motion system allowing time-resolved automated imaging of hundreds of colorimetric and fluorescence microbiology tests.²⁴ We believe that such biosensing platforms that combine microfluidics with digital imaging will allow us to better understand microbial growth in microfluidic culture volumes. We therefore developed a darkfield biosensing platform that detects bacteria and bacteriophage by light scattering,²⁵ built from inexpensive, open-source hardware, for sensing bacterial growth within multiplex dip-stick microfluidic devices made from microcapillary film.²⁶

We assessed whether the confinement of sub-mm channels was sufficient to retain bacteria and bacteriophage hosts in place to detect colonies and phage without any further labelling or plating. We demonstrate for the first time that microfluidic dip-sticks can be used as an easy-to-use “dip-and-test 1D liquid microbial media” for rapid counting of viable bacterial colony-forming units and bacteriophage plaque-forming units. Darkfield imaging allows label-free detection with simple LED plus inexpensive CMOS digital camera, and the simple microcapillary dipsticks avoid the challenge of agar plating. We explored how quickly plaques and colonies could be detected using an automated image capture system permitting detailed analysis of microfluidic microbial growth kinetics. We show these microbial dipsticks represent a compact, accurate, rapid, simple, and inexpensive way to count colonies and plaques in liquid media, thereby replacing 140 year old agar Petri dishes with microfluidics.

2. Materials and methods

2.1 Materials and bacterial strains

Microcapillary film (MCF) produced from Teflon® fluorinated ethylene propylene (FEP) was sourced from Lamina Dielectrics Ltd (Billingshurst, West Sussex, UK) with external dimensions of 4.3 mm wide and 0.4 mm thick, containing 10 microcapillaries each with an internal diameter of approximately 200 μm .²⁶ Non-motile *E. coli* B strain (a host for T2 phage) was obtained from the National Centre for Biotechnology Education, University of Reading (Reading, UK) and bacteriophage T2 was obtained from Mojgan Rabiey, School of Biological Sciences, University of Reading (Reading UK). *S. aureus* ATCC 19685 and *S. aureus* phage K ATCC 1985-B1 (family *Myoviridae*) were obtained from Danish Malik, Biotechnology and Biomedical Engineering, Loughborough University. Motile *E. coli* strain ATCC 25922 was purchased from LGC Standards (Middlesex, UK).

2.2 Darkfield imaging sensor system design

A Raspberry Pi model 4 with HQ Camera (Farnell, UK) was mounted with an 8MP 50 mm 14.5 \times 10.9° angle of view C-Mount lens (Cool Components, UK) focussed closely to capture macro images with an approximate field of view of 50 mm. White LED strip (RS Components, UK, product code: 153-3639) powered with a 12 V power supply (Amazon UK) were used as light source. To achieve darkfield imaging and allow dye- or label-free direct detection of bacteria inside MCF through light scattering from bacterial cells, a simple box enclosing key components comprising: light source (LED), samples of up to 8 MCF test strips spaced 9 mm apart in a 3D printed holder, 3D printed blockers to create the darkfield behind the samples (carefully aligned to eliminate

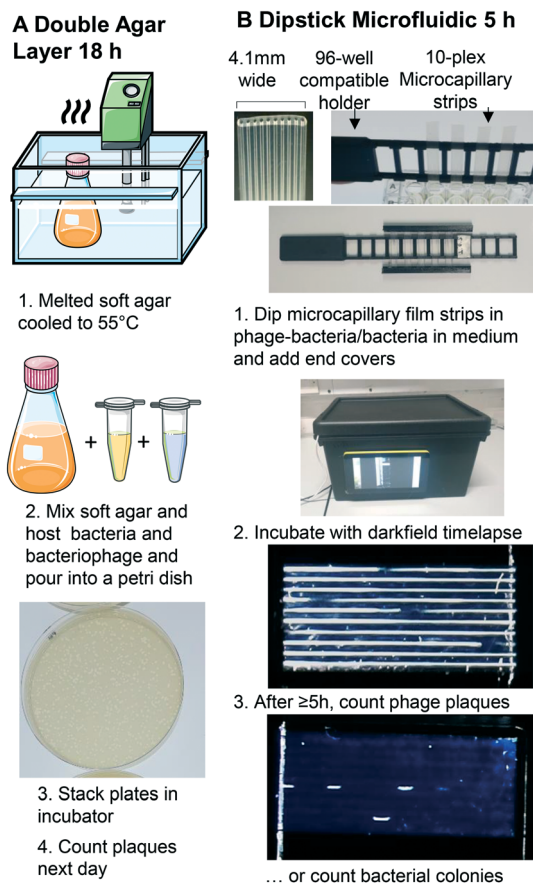


Fig. 1 Double layer agar method vs. miniaturised 1D liquid colony and plaque counting method. A. Double layer agar method. B. 1: Sample preparation and uptake into $10\times \sim 1 \mu\text{L}$ microcapillary array per strip. Steps 1–5 illustrate key steps for analysis of bacterial growth kinetics within microcapillaries. A 3D printed holder permits simple uptake of up to 8 samples from a 96-well plate, and 3D printed end covers containing silicone grease seal ends to avoid air bubbles from entering or sample drying out. 2: A darkfield illuminated imaging box monitors growth by timelapse imaging with Raspberry Pi and HQ camera, operated via touchscreen. 3: The small portable imaging box fits into incubator for culture at 37 °C to capture colony or plaque growth kinetics. After incubation, bacteriophage plaques or bacterial colonies are clearly visible, from as early as 5 h.



direct and reflected light from the LED around the sample) and Raspberry Pi HQ camera. A 3D printed base plate to mount all components, with the camera mounted on aluminium extrusion, and added the Raspberry Pi computer and blockers to this base (Fig. 1 and S1B†). A touchscreen mounted on the side of the box helped run python scripts to take photos every 10 minutes. The photographs were subsequently analysed on an external PC using ImageJ (NIH, USA) software.²⁷

2.3 1D microcapillary dip-strip assay to measure bacterial CFU

Hydrophilic test strips were produced in 1 m long batches of MCF. MCF lengths were filled with 5 g L⁻¹ polyvinyl alcohol (PVOH) solution in ultrapure water, as previously described.²⁶ *E. coli* B strain was routinely cultured on LB agar media at 37 °C overnight, a single colony was re-suspended into lysogeny broth (LB) to 0.2 OD₆₀₀. *S. aureus* was routinely cultured on BHI agar at 37 °C overnight, a single colony was re-suspended into brain heart infusion (BHI) broth to 0.2 OD₆₀₀. Bacterial suspensions were diluted a further 1:1000 to obtain approximately 10⁵ CFU mL⁻¹. *E. coli* and *S. aureus* strains were prepared in 96-well plates in LB or nutrient broth (NB) respectively and serially diluted to the range of 1–3 × 10³ CFU mL⁻¹. Bacteria counts were confirmed by overnight colony counting on LB agar using the spread plate method (ESI† Methodology).

Individual hydrophilic 33 mm MCF strips were clipped into the 3D printed rack compatible with a 96 well plate (Fig. 1B and ref. 16). One end of the microcapillary test strips were dipped into each well allowing the sample to fill the 10 microcapillaries by capillary action. Endcaps filled with silicone grease cover the end of the strips to eliminate evaporation. The test rack was put into the darkfield imaging system such that each capillary ran horizontal and incubated at 37 °C (Fig. 1B).

2.4 1D microcapillary dip-strip assay to measure bacteriophage PFU

Detailed methods of bacteriophage amplifications, storage and standard DAL can be found in the ESI† (S1 Methodology); the basic methodology is outlined in Fig. 1A. To measure PFU in Petri tubes, serial dilutions of phage K (10³, 2 × 10³, 4 × 10³ PFU mL⁻¹) were prepared and mixed with 4 × 10⁸ CFU mL⁻¹ host bacteria. A volume of 100 μL of the mix was added to wells in a microplate and MCF test strips were used as before. Bacteriophage number was confirmed using DAL method and incubated at 37 °C overnight (S1† Methodology).

2.5 Image analysis

Time-lapse images from the full incubation period were stacked in the ImageJ software for analysis, including counting the number of colonies and plaques, estimating the length of the colony along the individual capillaries over

time, and estimating microbial growth through analysis of “Normalised Intensity” for individual colonies. To determine the normalised intensity, identical rectangular area was selected around each bacterial colony identified at a late timepoint, and a set of 6 timepoints at regular intervals defined from before the colony first became visible – considered the baseline – to the late timepoint. The mean grey scale pixel intensity in this rectangular area was taken for each single colony at the selected time points using ImageJ (NIH, USA).²⁷ The mean intensity for each timepoint was then normalised by firstly subtracting the mean intensity at baseline before the colony appeared, and secondly dividing by the end mean intensity at the latest time measured. Thus 100% was defined at the last time the colony measured, and 0% the starting point before the colony was visible. This analysis was conducted with the full 8-bit RGB colour image, as no significant difference in scatter intensity was seen between red, green and blue channels.

3. Results and discussion

3.1 Microfluidic 1D liquid matrix counting of individual bacterial colonies using microcapillary dip-sticks

We show here for the first time that ~200-micron diameter capillaries can be used as a 1-dimensional (1D) liquid matrix in which it is simple to detect and count bacterial colonies and phage plaques, when imaged with darkfield illumination. We termed this method 1D culture to reflect the replacement of classical 2D surface of solid agar medium in Petri dishes with liquid media in microcapillaries that constrain the growing capillaries through microfluidic dimensions.

We first assessed if accurate measurement of bacterial colony forming units was possible. When growing bacteria *in situ* within microcapillaries, we observed bacterial colonies becoming visible after a short incubation allowing us to make absolute counts of bacterial CFU down to very low concentrations (around 250 CFU mL⁻¹), with (Fig. 2). Instead of spreading on the surface of a 2D solid hydrogel medium, the long narrow microcapillaries allowed enumeration of colonies in a 1D liquid matrix. Each individual viable bacterial cell that could grow into a colony appeared after incubation as a clear white area of bright light scatter, enabling clear label-free counting of individual bacterial colonies (Fig. 1). 1D colony counts were compared with gold-standard, solid agar plate counts, with *E. coli* and *S. aureus* diluted to multiple cell densities. A starting target inoculum of 5 × 10³ CFU mL⁻¹ was used, a concentration at which only a few bacteria are present in each capillary (10⁻³ mL per ~33 mm length). After sample loading into microcapillary dip-strips simply through capillary action and incubation, colonies became clearly visible after ~5.5 h and ~8.5 h for *E. coli* and *S. aureus* respectively (Fig. 2A and B) *versus* overnight incubation for Petri dishes. Individual colonies were easily distinguishable within microcapillaries at these cell densities and timepoints. When multiple colonies grew in a single



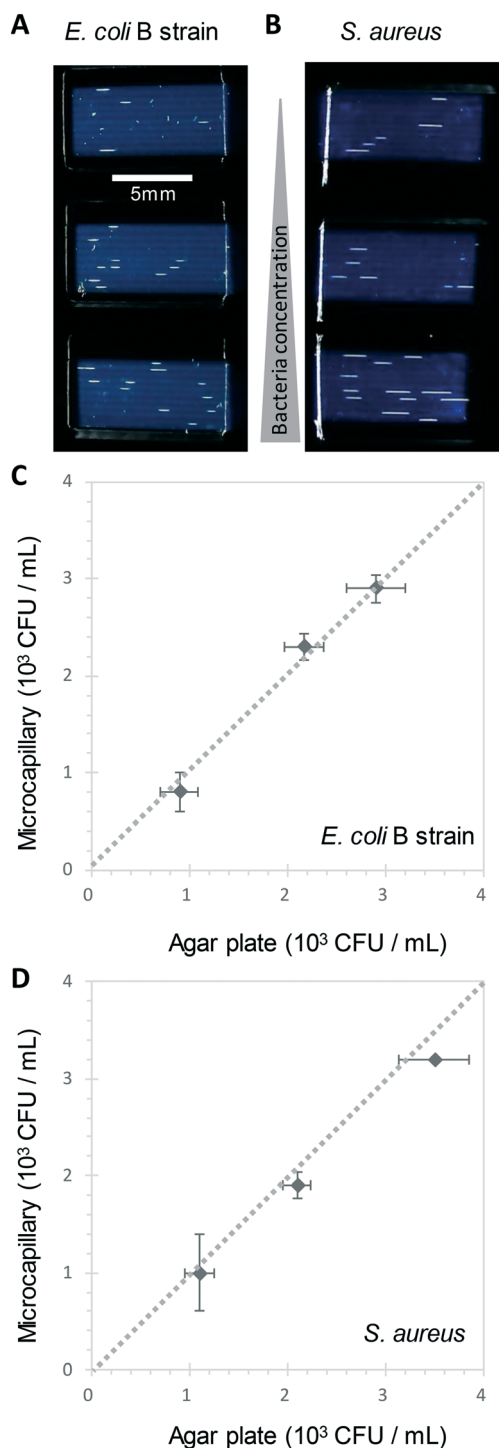


Fig. 2 1D counting of single bacterial CFU within microcapillaries in liquid broth. A and B Image at 6 h of 3 different *E. coli* B strain (A) and *S. aureus* (B) concentrations grown in 4 μ L broth per strip distributed within 10 individual microcapillaries, with individual colonies visible as short white horizontal lines along the horizontal microcapillaries. The test strips appear dark blue through light scatter by the plastic surrounding microcapillaries. C) and D) Comparison of colony forming unit (CFU) counts for *E. coli* (C) and *S. aureus* (D) measured in liquid in microcapillaries vs. solid agar plate counts. Error bars represent \pm standard deviation from 3 independent replicate experiments. Dashed line indicates 1:1 relationship between the two counting methods.

microcapillary, as long as they were far enough apart to not overlap they could be clearly distinguished, meaning the technique is fully quantitative and not binary/digital (yes vs. no) in terms of initial number of cells per capillary, and could tolerate operation over a broader range of concentrations than simple limiting dilution counting.¹⁶ When CFU mL⁻¹ values were calculated by 1D colony enumeration in microcapillaries, near-identical counts were obtained to gold standard 2D agar plate count ($r^2 = 0.99$ for both *E. coli* and *S. aureus*, Fig. 2C and D). Although *E. coli* and *S. aureus* both showed close agreement between microcapillary and agar plate counts, a later timepoint was imaged for *S. aureus* because these colonies appeared later. Surprisingly we found the 1D microcapillary method counts had smaller standard deviations than agar plate counts (compare size of the error bars Fig. 2C and D) when each was measured in triplicate experiments, suggesting the 1D colony microcapillary counting may be more reproducible.

The imaging area of each test strip was approximately 10 mm long corresponding to a test volume of $\sim 4 \mu$ L in the area visible in the darkfield imaging setup for 10 capillaries, resulting in a lower limit of detection (LOD) of 2.5×10^2 CFU mL⁻¹, assuming detection of a minimum of 1 colony forming unit. At that point the technique becomes digital and only able to differentiate between growth versus no growth. For higher concentrations there is an increasing probability of two or more CFU on the same microcapillary, potentially overlapping, similar to when plating higher cell concentrations onto agar. As the size of the colonies grows with time it becomes more probable that nearby colonies will overlap, and thus the exact upper limit of detection will vary depending on species, growth condition, and timepoint imaged. This is discussed in greater depth in section 3.2. Here, we found counts of $\sim 3 \times 10^3$ CFU mL⁻¹ remained accurate (Fig. 2C and D).

A disadvantage of the current capillary system is that within the relatively small imaging area inherent in microfluidic systems, in contrast to a traditional 100 mm diameter Petri dish, only a few colonies or plaques are counted in each experiment. It's well known when measuring viable cell numbers that as the numbers of colonies counted falls towards low absolute numbers (e.g. 5–15 colony range), the uncertainty around the absolute CFU mL⁻¹ increases. Some guidelines advise counting at least 25 colonies on agar plates to gain sufficient resolution for accurate counts. We conducted counts with larger numbers of replica samples ($n = 6$) and observed counts to be very repeatable even with low absolute numbers of colonies (Fig. S4†). Viable cell counts are typically measured over multiple orders of magnitude expressed on logarithmic scales, and note that care is required in diluting samples prior to colony counting. However, it should be remembered that higher uncertainty might be encountered in methods such as this 1D microcapillary system where a low absolute number of counts are recorded, and advise that where precise measurement of absolute viable cell numbers are important, only appropriate



statistical expression of uncertainty in counts are used. For example, with low absolute colony counts, parametric statistical tests should be avoided since variation in counts would not be expected to be normally distributed. To overcome this limitation, longer strips or larger numbers of strips could be assessed, providing a larger growth volume and imaging area, thus higher absolute numbers of colonies or plaques to be counted. We also note that in common with many other viable cell or viral counting methods there are other sources of variation in measuring viable cell numbers; for example if sampling a growing population with a doubling time approaching 20 minutes, cell counts can change considerably depending on the exact timing of sample application to the strip.

3.2 Kinetics of bacterial colony growth in microcapillaries

The Raspberry Pi HQ camera darkfield imaging biosensor system used offered full control over imaging and gathering of time-resolved growth data, enabling detailed analysis 1D

colony growth kinetics within microcapillaries. This setup was optimised for simultaneous capture of up to 8 microcapillary dip-strips, with total volume sampled of $8 \times 4 \mu\text{L}$ tests, corresponding to 80 individual microcapillaries. From images recorded every 10 minutes, it was possible to generate time-lapse videos illustrating colony growth (Video S1 and Fig. S2†). The time-lapse image sets allowed us to clearly visualise colony growth using distance *versus* time plots that showed very distinct growth dynamics between the two bacterial species tested (Fig. 3). Thus, *E. coli* colonies appeared at earlier timepoints and yet the speed of colony expansion quickly slows (Fig. 3A). In contrast, although *S. aureus* colonies appeared later, they showed faster and more sustained colony expansion along the capillaries (Fig. 3B).

Initially, we asked how fast colony counts could be made, by comparing growth of multiple individual capillaries in one set of strips. As expected, given the clonal nature of the suspensions tested, all individual colonies appeared at almost the same time for each sample tested. The earliest *E. coli* colonies to appear were visible 4.5 hours after incubation, and all colonies were visible within 50 minutes of these earliest colonies (Fig. 4A). For *S. aureus*, the fastest colonies to appear became visible after 8 h of incubation (Fig. 4B), again with all colonies growing at a similar rate and all becoming detectable within 1 h of the first colony detected. We conclude that confident final counts could be determined at 6 h and 9 h for *E. coli* and *S. aureus* respectively, without the risk of missing slower-growing colonies.

Notably, 1D colonies were far clearer with non-motile bacterial strains. The initial samples of *E. coli* B strain and *S. aureus* are non-motile; but when low cell concentrations of a motile strain of *E. coli* 25922 were incubated in microcapillaries, although at earlier time points initial bright foci appeared indicating colony growth were transiently observed, shortly after appearing became impossible to distinguish individual colonies of bacteria, presumably with their motility allowing rapid seeding and further growth along the length of the capillary (Video S2 and bottom pane in Fig. S3†). However, colonies of motile strains could be more clearly distinguished upon inclusion of a low concentration of agar in the culture medium, replicating the semi-solid agar used in traditional Petri dish methods that significantly limits the spread of the motile bacteria (top pane in Fig. S3 and Video S2†). The inclusion of low agar concentrations does add an extra step to the testing method, and semi-solid agar needs to be prepared by melting and maintained at an adequate temperature, otherwise flow of sample into capillaries by capillary action was not possible due to viscosity of solution. Thus, whilst 1D colony counting is far easier with non-motile strains, use of conventional semi-solid media additives makes this technique compatible with motile bacteria.

The time-resolved darkfield imaging of 1D colony growth allowed us to explore the rate of growth using different measurements. First, we analysed colony length as a

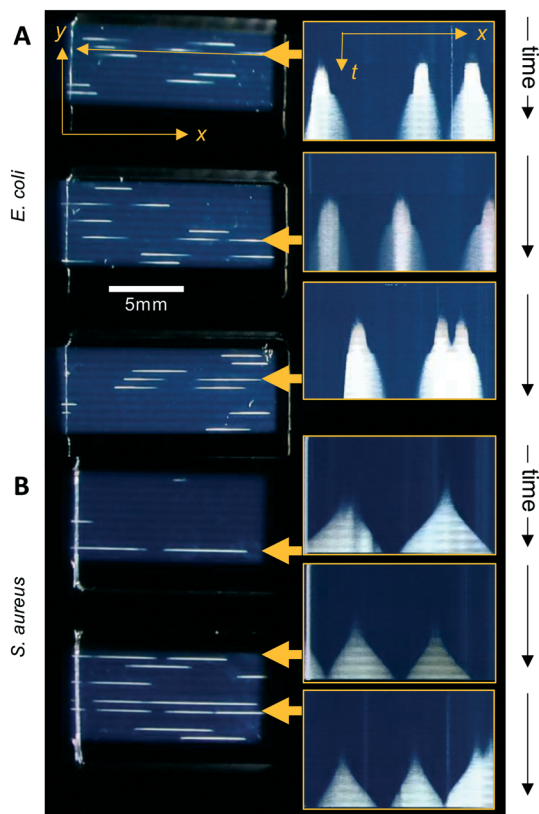


Fig. 3 Visualising capillary growth dynamics in 1D liquid culture. On the right-hand side: intensity along the length of individual capillaries was plotted *vs.* time from analysis of timelapse image stacks, to illustrate the different colony growth dynamics for (A) *E. coli* *vs.* (B) *S. aureus*. The 6 capillaries indicated by yellow arrows were plotted on the left hand side, with the vertical axis representing time increasing downwards, with 1 pixel representing one individual image; images were captured at 10 minute intervals and are ~ 80 pixels high, representing ~ 13 hours total incubation. Scale measurement bar is the same for images to left as for *x-t* plots to right.



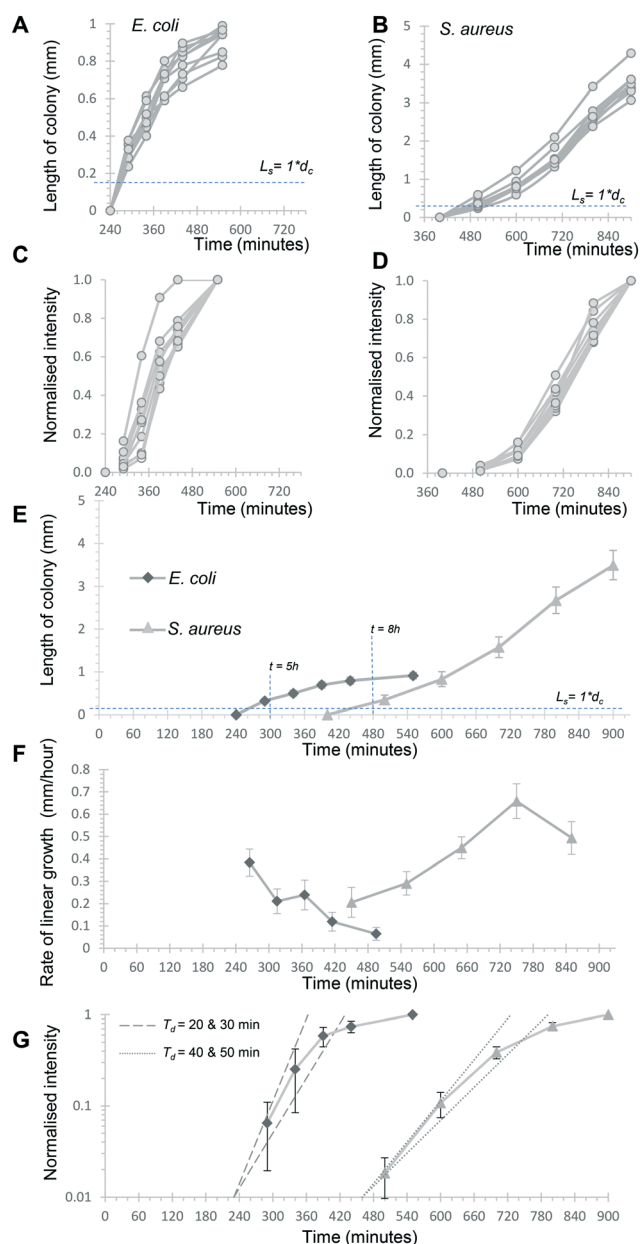


Fig. 4 Kinetics of capillary colony growth in 1D liquid culture. Linear growth of 9 individual *E. coli* and *S. aureus* colonies was measured at the 6 timepoints indicated and all colonies plotted individually (A) and (B) to see variation in growth between colonies. Note different time and length axes are used given the different rates and sizes between these species. Bacterial growth kinetics within colonies was also estimated by calculating a normalised light scattering intensity measurement for both species (C and D) for the same 9 colonies. The mean length was plotted for both species (E) for the full experiment to show the distinct growth dynamics, with earliest time for counting at the marked timepoints. F) The rate of linear colony growth was calculated for each pair of length measurements for individual colonies and plotted at the middle timepoint. Mean rates for the 9 colonies are plotted, with error bars indicating ± 1 standard deviation. G) By plotting mean normalised intensities on a log_y scale, it's possible to estimate initial colony intensity rise during exponential growth. Dotted and dashed lines illustrate theoretical exponential growth for 20- and 30 minute doubling times (T_d), starting from a normalised intensity of 0.01 at 240 minutes (pair of dashed lines) vs. 430 minutes (dotted pair).

simplified 1D measure of colony growth in liquid media, schematically represented in Fig. S6A and B.† It was clear this increased over a similar profile for multiple individual colonies over the 6 time points selected, from just before the first colony became visible (Fig. 4A and B), again confirming uniform growth of individual CFU. Secondly, we explored if quantitative measurement of growth of the bacterial suspension could be estimated from light scatter intensity. Other recent studies measuring bacterial cell density using innovative digital imaging techniques that detect light scatter have shown good correlation with colony counts.^{28,29} The dynamic range of darkfield scatter intensity was limited as images were optimised for early colony detection (*i.e.* brightest possible images at early timepoints) and for 8 test strips (*i.e.* lower resolution, larger number of samples); thus intensities rapidly became saturated and intensity non-linear to microbial cell density as the colony expanded. With this exact setup, the outline of each colony was hard to define automatically using methods such as particle analysis. We therefore calculated a normalised intensity to estimate growth, by defining a single fixed rectangular area of interest that fully contained the colony at a late stage of growth, to avoid artefacts from defining the colony area, and then calculating a normalised scatter intensity for this area of interest, such that the mean intensity of the final image varied from 0% (before colony appeared) to 100% (at last timepoint analysed) for the same rectangular area of interest (Fig. 4C and D). The normalised intensity and 1D length increased together but were clearly independent measurements, with length initially increasing faster than intensity (Fig. S5†). The close overlay of normalised intensity kinetics for 9 separate colonies each of *E. coli* and *S. aureus* suggests this measurement is repeatable (Fig. 4C and D). Without the normalisation step, the mean greyscale pixel intensity varied more between individual colonies (Fig. S6†) likely due to different areas of interest being selected for each colony. Small drift in microcapillary position during incubation prevented analysis of smaller areas of interest to more precisely define each colony. We therefore believe that, in spite of some limitations, this normalised intensity measurement provides a useful estimate of colony growth through increasing intensity as cell density increases (expected to correspond to turbidity measurements in conventional liquid culture), as opposed to linear expansion along the microcapillary.

3.3 Understanding bacterial colony growth dynamics in microfluidic culture

Having established that these two measurements – linear 1D colony growth and normalised intensity – were repeatable for sets of 9 individual colonies for each species, we then examined the microfluidic bacterial colony growth dynamics both in space and in cell density. This confirmed the very distinct patterns of colony growth between *E. coli* and *S. aureus* that were visible from distance-time plots (Fig. 3). We



observed faster linear expansion of the latter despite a slower time to colony appearance and slower initial logarithmic growth in intensity. Whilst *E. coli* colonies appeared earlier, once colonies were visible the rate of linear colony growth was significantly faster for *S. aureus* and these colonies achieved a longer length (Fig. 4E). This could be explained by changes in colony growth speed – an initial rapid linear growth rate for *E. coli* of 0.4 mm h^{-1} declined as the colony grew, such that $\sim 5 \text{ h}$ after first appearing the rate was $4\times$ slower than *S. aureus* and the colony length remained under 1 mm (Fig. 4F). In contrast, although *S. aureus* colonies appeared $\sim 3 \text{ h}$ later with a slower initial growth rate of 0.2 mm h^{-1} , this speed steadily increased to around $0.4\text{--}0.5 \text{ mm h}^{-1}$ (Fig. 4F), with colonies exceeding 3 mm in length by the end of the experiment.

The plots of normalised intensity followed a typical microbial growth *s*-curve, suggesting an initial exponential growth period as the colony first appears, after which image intensity becomes saturated so we could no longer distinguish between image intensity saturation *versus* a growth plateau from nutrient depletion. We were able to estimate the rate of initial exponential growth and compare with expected liquid culture log phase growth rates for the two organisms studied. For *E. coli* initial exponential growth rates appear to approach a 20 minute doubling time (Fig. 4G – dashed lines indicate theoretical 20 and 30 minute doubling times). Previous studies of growth in fluoropolymer MCF using colorimetric resazurin dye agree that *E. coli* can grow with doubling time between 20–30 minutes.¹⁶ *S. aureus* typically grows rapidly with similar doubling time to *E. coli*, yet we observed later appearance and slower initial growth for this species, suggesting the environment within the microcapillaries may become anaerobic slowing the growth rate for this facultative anaerobe. The initial exponential rate appeared closer to 40 minutes doubling time for *S. aureus* (Fig. 4G – dotted lines indicate theoretical 40 and 50 minute doubling times).

Previously, we reported that darkfield imaging could detect *E. coli* suspensions with turbidity at or above 0.34 OD_{600} ,²⁵ corresponding to cell concentrations of $2.8 \times 10^8 \text{ CFU mL}^{-1}$. For a colony with a length with L_s equal to one microcapillary diameter d_c and thus a volume of 6 nanolitres, this corresponds to ~ 1700 cells. Starting from 1 CFU in this volume, this represents 1700-fold growth, requiring 11 successive doublings ($2^{11} = 2048$ -fold expansion). For a constant 20 minute doubling time this would take 220 minutes, not far from the 260 minutes before *E. coli* colonies reached this length. Similarly, at a constant 40 minute doubling time it would take 440 minutes to grow 1 CFU up to ~ 2000 cells, consistent with the 480 minutes before *S. aureus* colonies reached this size. These estimates do not account for any initial lag prior to exponential growth, or in differences in the minimum cell density that can be detected through darkfield imaging given that we are using a slightly different configuration of camera; furthermore, light scattering intensity may differ between these species.

It was informative to contrast colony appearance times and increase in normalised intensity with linear colony growth kinetics. Surprisingly, linear colony expansion was not only faster but more sustained for *S. aureus* than *E. coli*, contrasting to the slower rate of initial intensity rise and later appearance. This discrepancy of appearing later plus slower initial intensity growth from an individual CFU, followed by faster linear colony expansion at later timepoints, could be due to differences in growth properties of the Gram-negative *E. coli*, *vs.* Gram-positive *S. aureus*. The later appearance of *S. aureus* might also be attributed to lower light scattering from these smaller cocci,³⁰ but this would not affect the gradient of initial exponential increase in scatter intensity, that indicate that *S. aureus* does indeed growing slower than *E. coli* in this microsystem – possibly due to limited oxygen levels. However, when we evaluated growth of an obligate aerobic bacterial strain in rich broth in microcapillaries, no difference was found between growth in a shaker incubator *vs.* in fluoropolymer microcapillaries imaged by darkfield illumination, with similar growth curves observed in both conditions (Fig. S8†). This clearly indicates that even if oxygen may be depleted at some point by microbial metabolism within microcapillaries, there is sufficient oxygen in the system to clearly detect strong light scattering signal at microbial cell densities high enough for detecting colonies by darkfield imaging (Fig. S8†).

To understand this further, we calculated the expected rate of nutrient diffusion along a microcapillary. Assuming growth of bacteria is limited by carbon source (glucose), the diffusion time of glucose also becomes relevant to the dynamics of colony growth (Fig. S7†). We have estimated a rate of diffusion for glucose around 0.8 mm h^{-1} based on data from the literature.³¹ As the size of the colony reaches the diameter of the microcapillary, the 1D growth of the colony becomes limited by the diffusion of glucose. Also, in light of Monod's equation, the rate of growth of a microorganism is dependent on the concentration of the limiting nutrient on the interface. As the colony grows further, the carbon source fully depletes within the colony, therefore stimulating the growth of the colony along the length of the microcapillary. The rate of growth of the microorganism may also have a strong influence on the 1D rate of expansion of the colony. In our case *S. aureus*, with the linear rate of colony growth being smaller than rate of glucose diffusion, it is likely the glucose concentration at the interface will remain high, therefore the microorganism is able to grow near the maximum rate (Fig. S7C, bottom†). In contrast, with a faster-growing microorganism like *E. coli*, the glucose concentration in the interface can be entirely depleted as diffusion is not rapid enough to replenish at the interface, which forces the colony to grow at a lower growth rate (Fig. S7C, top†). This means the rate of growth of the colony becomes dependent on the rate of mass transfer of the limiting nutrient (glucose) from the bulk of the microcapillary to the interface, demonstrating 1D microcapillary counting can be manipulated by playing with



the microenvironment, in particular growth conditions of the microorganism (such as temperature, different carbon and energy sources, or pH), the mass transport, or both, which is far harder to control on a standard solid medium such as agar Petri dish.

3.4 Simple, accurate, 1D microfluidic agar-free bacteriophage plaque counting

Bacteriophage enumeration is far more challenging than agar plate counting of bacterial colonies. The reference method, DAL, requires the live host organism to be seeded and movement restricted by plating soft agar on top of another agar layer. Careful addition of the correct concentration of bacteria to agar while it is still liquid requires careful temperature control to ensure the bacteria remain viable. We tested bacteriophage with *E. coli* and *S. aureus* host strains to determine whether phage count could be rapidly determined using a 1D capillary liquid medium method, a major improvement over the current method (Fig. S1†). The permissive *S. aureus* host bacteria were mixed with dilutions of bacteriophages and the hydrophilic MCF test strips added to the samples. As with the bacteria colony counts, an excellent agreement between phage plaque numbers and PFU concentrations for phage K were observed with 1D capillary counting compared to conventional DAL (Fig. 5). Likewise accurate phage counting of T2 phage concentration was achieved with the *E. coli* B strain host ($r^2 = 0.99$ both T2 and phage K) (Fig. 6). This was also confirmed using soft agar in the capillary strips with no difference in results irrespective of whether liquid or agar was used in microcapillary dip-strips, indicating agar is not necessary for bacteriophage enumeration with these non-motile hosts (Fig. 6).

Plaques could be clearly counted after just 5 h and detected at concentrations down to 250 PFU mL^{-1} (Fig. 5 and 6) corresponding to the theoretical viral concentration where 1 plaque is present per $4 \mu\text{L}$ sample volume in 10 capillaries along the visible section of test strip. As with the reference method, changes in parameters like host inoculum and media viscosity can affect the assay measurements including plaque size.³² We found plaque size within 1D capillaries varied depending on host/phage system studied. Phage K had larger plaque sizes compared to T2 (Fig. 5 and 6). The smaller plaque size of T2 made it possible to count much higher numbers of bacteriophage with an upper limit approaching $3 \times 10^4 \text{ PFU mL}^{-1}$, before plaques began overlapping (Fig. 6).

Of particular note, the current gold standard DAL method for phage counting involves suspending host bacteria in warm agar, requiring care to ensure even seeding while avoiding killing host bacteria if the temperature of the melted agar is not optimal. Secondly, through miniaturisation, the storage and incubator space required for large stacks of Petri dishes is avoided alongside the refrigerated storage for prepared agar plates. Due to the small size, the test can be combined with a small portable incubating reader for timelapse imaging. This allows the

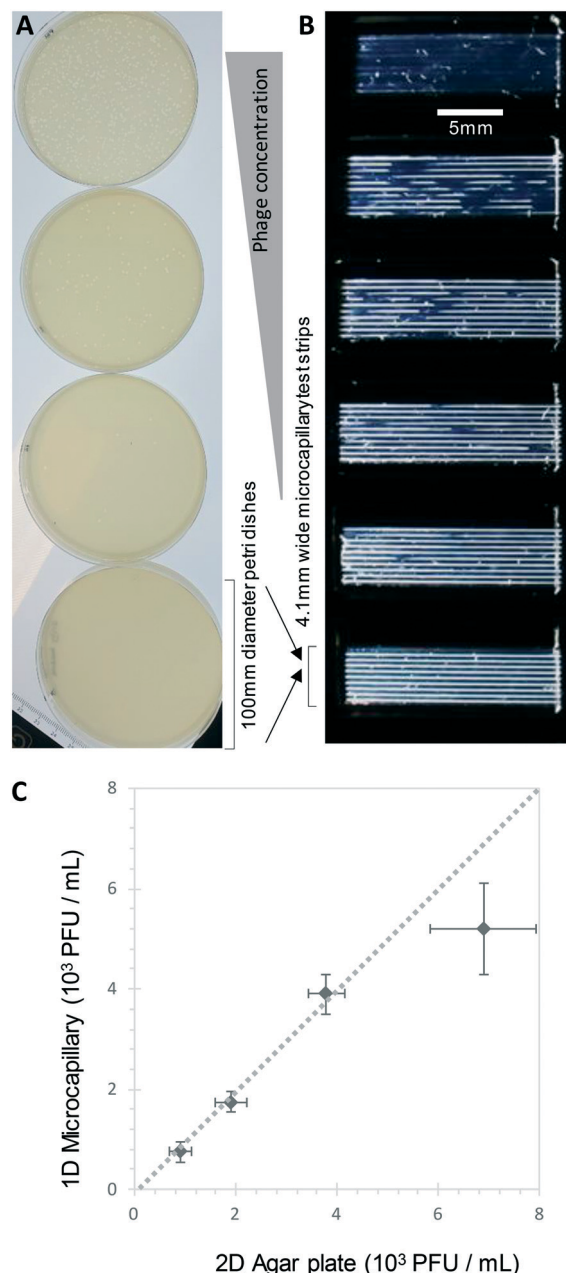


Fig. 5 1D counting *S. aureus* phage K plaques in liquid broth within microcapillaries. A) Example endpoint images of five increasing phage K concentrations plated with conventional double agar layer method in Petri dishes, plus no phage control. B) The same phage K concentrations were measured within microcapillary dip-strips. C) Comparison of plaque forming units counted in microcapillaries vs. double agar layer method; it was not possible to calculate plaques for the highest concentration sample as most of the capillary was cleared hence only 4 concentrations were plotted. Mean counts of 10 replicate capillaries are plotted with error bars indicating ± 1 standard deviation. Dashed line indicates 1:1 relationship between the two counting methods.

development of automated image capture and analysis of more samples than traditional methods. Counting within 1D microcapillaries also significantly reduced the time needed to count CFU or PFU to between 5–9 h depending on culture



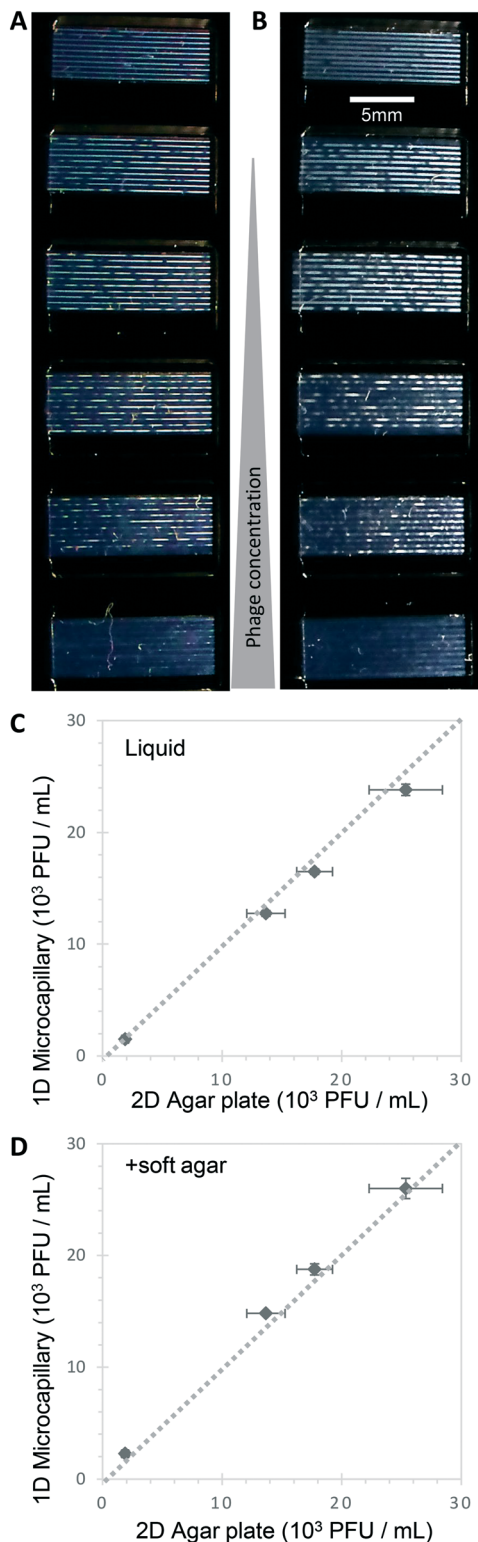


Fig. 6 Agar is not required to detect T2 bacteriophage plaques within microcapillaries. A) and B): *E. coli* capillary phage counting in liquid broth was similar with or without soft agar. Endpoint images showed the same number and size of bacteriophage plaques in liquid media without agar (A), as seen with addition of 0.5% agar to broth prior to dipping and testing (B) within microcapillaries. C) Counting T2 phage concentration via DAL (double agar layer) on plate vs. microcapillaries in liquid broth. D) Counting T2 phage concentration via DAL (double agar layer) vs. microcapillaries with inclusion of soft agar. Dashed line indicates 1:1 relationship between the two counting methods.

characteristics of different bacteria – faster than typical overnight timepoints needed for agar plate colony or plaque counts. By permitting simple counting of individual colonies or plaques, grown from single cells or viral particles, we achieved a lower limit of detection approaching 250 CFU mL⁻¹ or PFU mL⁻¹, similar to agar colony or DAL plaque counting in Petri dishes. Lower concentrations can be measured simply by increasing the sample volume using more test strips or imaging longer microcapillary sections.

3.5 Benefits of open source darkfield microfluidic imaging system

Previously we combined microfluidic capillary measurements with light scatter detection to detect bacterial cell suspensions. A minimum of $\sim 0.5\text{--}0.1$ OD₆₀₀ turbidity, corresponding to $\sim 10^7\text{--}10^8$ CFU mL⁻¹, was needed to produce a solid line that was immediately visible with darkfield illumination geometry optimised for smartphones (Dönmez *et al.*, 2020 (ref. 25)). Whilst this provides a microfluidic smartphone alternative to conventional cuvette plus spectrometer, our new observations move beyond estimating only high cell concentrations, to precisely measuring absolute CFU and PFU at many orders of magnitude lower concentrations. At the same time, we replaced smartphone imaging with an open source sensor system, exploiting the computing and imaging power of the Raspberry Pi HQ camera equipped with a macro lens.

While bacterial colonies for rapidly dividing *E. coli* strains on solid agar media can be visible in as little as 7 h,²⁴ these systems tend to be low-throughput and rarely is kinetic data collected due to the size/shape of Petri dishes which are not optically well designed for digitally recording results. However, some studies have examined the kinetics of solid agar colony growth of organisms such as *S. aureus*,³³ *Vibrio* spp.,³⁴ *E. coli*, *Klebsiella aerogenes*, and *Klebsiella pneumoniae*³⁵ by time-lapse imaging of Petri dishes. The imaging systems used are designed to examine Petri dishes, with different approaches used, including light scattering but can often only examine one Petri dish at a time, and it can be hard to define colony appearance as agar and colony appear similar. Fluorescence and dyes can be added but can further complicate the analytical system. For example, label-free bacterial detection is especially valuable for detecting bacterial lysis by phage. This cannot be easily monitored using metabolic growth dyes because the dye is likely to be irreversibly converted by bacteria before lysis occurs. The darkfield imaging system therefore adds the benefits of time-resolved darkfield imaging to microsystems; label-free detection being especially beneficial.

Counting bacterial colonies grown within capillaries has been exploited in the past, having been described as early as 1956 (ref. 36 and 37) using individual glass capillaries with colonies detected visually by eye. This confirms that the initial measurements here with a few defined strains are likely to be representative of a wider range of organisms.



However, the flat, multiplex format possible using microcapillary film significantly increases throughput over individual glass capillaries. The refractive index match between aqueous culture medium and fluoropolymer device results in high optical transparency, allowing small colonies to be detected earlier. The benefits of digital camera for time resolved imaging further increases the utility of this method, especially with the inexpensive optoelectronic components now available (e.g. Raspberry Pi camera and LED illumination used here). We believe that microcapillary bacteriophage plaque counting has not previously been reported, and given the complexity of performing DAL method, we suggest this may be the most significant step forward with this method.

One limitation of the capillary method is that in contrast to the surface of solid medium on a plate, there is no straightforward way to sample bacterial colonies or phage plaques for subsequent analysis. This makes it more suitable to counting and quantitation than to identification or phenotypical characterisation. The inability to further sample colonies or plaques is shared with several other closed microfluidic systems. The melt-extrusion manufacturing method makes MCF especially suited to disposable quantitation devices, whereas other microsystems (e.g. droplet microfluidics) that are more complex and expensive may be more suitable for applications requiring downstream manipulations. Another limitation of the current method is that it was far less effective with motile organisms that could spread rapidly along the capillary, preventing clear colony or plaque detection (Fig. S3†). This again was clearly visible through time-resolved imaging, and with further optimisation it may be possible to count colonies as very transient points of bright scatter prior to spread. The inclusion of low concentration of agar in the sample medium did inhibit this spread but also reduced the simplicity of performing the test. It remains important therefore to further develop these methods of delaying or inhibiting the spread of motile organisms within the microcapillaries, for example substituting alternative hydrogel-forming polymers, or incorporating such polymers inside the hydrophilic coated capillaries. The transient detection further illustrates another advantage of time-resolved reader *versus* endpoint image. Time-lapse imaging also improves counting with higher concentrations of bacteria. Over time, the colony length increased making identification of several colonies per capillary more challenging.

4. Conclusion

This microfluidic method can accurately count bacterial CFU and bacteriophage PFU in liquid media, label-free. 1D counting of bacteria and plaques in Petri Tubes allows low concentrations of bacteria and phage, down to ~ 250 CFU mL⁻¹ or 250 PFU mL⁻¹ to be counted in a simple liquid media, reducing the number of steps compared to reference methods. The 1D method was also found to reduce variability compared to the reference methods. The microfluidic

geometry permits a miniaturised 1D liquid alternative to 2D distribution of bacterial cells over a solid media surface. The miniaturised test permits the application of timelapse imaging for multiple samples in parallel (80 distinct microcapillaries in 8 dip-strips; total sample volume 32 microlitres) for detailed kinetic growth analysis providing a wealth of quantitative information not easily obtained for standard Petri dish culture. The use of simple liquid microcapillary cultures may be beneficial for specific applications including environmental sampling in the field or where resources are limited. Overall, this concept of 1D liquid culture for colony and plaque counting demonstrates a novel and effective way to make use of miniaturisation to speed up and simplify analytical microbiology over conventional agar-based culture methods; this approach has the potential to deliver significant impact from research to clinical microbiology and beyond.

Conflicts of interest

ADE and NMR are the inventors of patent application protecting aspects of the novel microfluidic devices tested in this study and is a director and shareholder in Capillary Film Technology Ltd, a company holding a commercial license to this patent application: WO2016012778 “Capillary assay device with internal hydrophilic coating” AD Edwards, NM Reis.

Acknowledgements

We thank Danish Malik from Loughborough University for Phage K and host. We thank the Turkish Ministry of National Education, Republic of Turkey for Postgraduate Study Abroad Program to support Sultan İlayda Dönmez. This project was partially funded by Engineering and Physical Science Research Council (EPSRC) grants EP/R022410/1 and EP/S010807/1. Images from Servier Medical Art (<https://smart.servier.com>) were adapted and used for Fig. 1 and S1,† under a Creative Commons Attribution license.

References

- 1 A. Kumar, *et al.*, Duration of hypotension before initiation of effective antimicrobial therapy is the critical determinant of survival in human septic shock*, *Crit. Care Med.*, 2006, **34**(6), 1589–1596.
- 2 F. Edition, Guidelines for drinking-water quality, *WHO Chron.*, 2011, **38**(4), 104–108.
- 3 A. H. Havelaar, *et al.*, World Health Organization Global Estimates and Regional Comparisons of the Burden of Foodborne Disease in 2010, *PLoS Med.*, 2015, **12**(12), e1001923.
- 4 J. T. P. Larry Maturin, *Aerobic Plate Count*, 2001 January, 27, 2022, Available from: <https://www.fda.gov/food/laboratory-methods-food/bam-chapter-3-aerobic-plate-count>.
- 5 J. Alford and E. E. Steinle, A double layered plate method for the detection of microbial lipolysis, *J. Appl. Bacteriol.*, 1967, **30**(3), 488–494.



- 6 A. Zapata and S. Ramirez-Arcos, A Comparative Study of McFarland Turbidity Standards and the Densimat Photometer to Determine Bacterial Cell Density, *Curr. Microbiol.*, 2015, **70**(6), 907–909.
- 7 J. Robertson, C. McGoverin, F. Vanholsbeeck and S. Swift, Optimisation of the Protocol for the LIVE/DEAD® BacLight™ Bacterial Viability Kit for Rapid Determination of Bacterial Load, *Front. Microbiol.*, 2019, **10**, 801.
- 8 S. Heider and C. Metzner, Quantitative real-time single particle analysis of virions, *Virology*, 2014, **462–463**, 199–206.
- 9 M. d'Herelle, Sur un microbe invisible antagoniste des bacilles dysentériques, *Acta Kravsi*, 1961, **165**, 373–375.
- 10 C. Brives and J. Pourraz, Phage therapy as a potential solution in the fight against AMR: obstacles and possible futures, *Palgrave Commun.*, 2020, **6**(1), 100.
- 11 D. J. Malik, *et al.*, Formulation, stabilisation and encapsulation of bacteriophage for phage therapy, *Adv. Colloid Interface Sci.*, 2017, **249**, 100–133.
- 12 J. Paczesny, Ł. Richter and R. Hołyst, Recent Progress in the Detection of Bacteria Using Bacteriophages: A Review, *Viruses*, 2020, **12**(8), 845.
- 13 K. F. Tjhung, *et al.*, Rapid Enumeration of Phage in Monodisperse Emulsions, *Anal. Chem.*, 2014, **86**(12), 5642–5648.
- 14 S. F. Berlanda, *et al.*, Recent Advances in Microfluidic Technology for Bioanalysis and Diagnostics, *Anal. Chem.*, 2021, **93**(1), 311–331.
- 15 S. A. Byrnes, *et al.*, Polydisperse emulsion digital assay to enhance time to detection and extend dynamic range in bacterial cultures enabled by a statistical framework, *Analyst*, 2018, **143**(12), 2828–2836.
- 16 S. H. Needs, H. M. I. Osborn and A. D. Edwards, Counting bacteria in microfluidic devices: Smartphone compatible 'dip-and-test' viable cell quantitation using resazurin amplified detection in microliter capillary arrays, *J. Microbiol. Methods*, 2021, **187**, 106199.
- 17 O. Scheler, W. Postek and P. Garstecki, Recent developments of microfluidics as a tool for biotechnology and microbiology, *Curr. Opin. Biotechnol.*, 2019, **55**, 60–67.
- 18 T. S. Kaminski, O. Scheler and P. Garstecki, Droplet microfluidics for microbiology: techniques, applications and challenges, *Lab Chip*, 2016, **16**(12), 2168–2187.
- 19 H. Lu, *et al.*, High throughput single cell counting in droplet-based microfluidics, *Sci. Rep.*, 2017, **7**(1), 1366.
- 20 P. Zhang, *et al.*, Facile syringe filter-enabled bacteria separation, enrichment, and buffer exchange for clinical isolation-free digital detection and characterization of bacterial pathogens in urine, *Analyst*, 2021, **146**(8), 2475–2483.
- 21 D. Rodoplu, *et al.*, A simple magnetic-assisted microfluidic method for rapid detection and phenotypic characterization of ultralow concentrations of bacteria, *Talanta*, 2021, **230**, 122291.
- 22 L. Castillo-Henríquez, *et al.*, Biosensors for the Detection of Bacterial and Viral Clinical Pathogens, *Sensors*, 2020, **20**(23), 6926.
- 23 I. Nuñez, *et al.*, Low cost and open source multi-fluorescence imaging system for teaching and research in biology and bioengineering, *PLoS One*, 2017, **12**(11), e0187163.
- 24 S. H. Needs, *et al.*, Exploiting open source 3D printer architecture for laboratory robotics to automate high-throughput time-lapse imaging for analytical microbiology, *PLoS One*, 2019, **14**(11), e0224878.
- 25 S. İ. Dönmez, *et al.*, Label-free smartphone quantitation of bacteria by darkfield imaging of light scattering in fluoropolymer micro capillary film allows portable detection of bacteriophage lysis, *Sens. Actuators, B*, 2020, **323**, 128645.
- 26 N. M. Reis, *et al.*, Lab on a stick: multi-analyte cellular assays in a microfluidic dipstick, *Lab Chip*, 2016, **16**(15), 2891–2899.
- 27 C. A. Schneider, W. S. Rasband and K. W. Eliceiri, NIH Image to ImageJ: 25 years of image analysis, *Nat. Methods*, 2012, **9**(7), 671–675.
- 28 F. Zhang, *et al.*, Rapid Antimicrobial Susceptibility Testing on Clinical Urine Samples by Video-Based Object Scattering Intensity Detection, *Anal. Chem.*, 2021, **93**(18), 7011–7021.
- 29 S. Vargas, *et al.*, Dynamic light scattering: A fast and reliable method to analyze bacterial growth during the lag phase, *J. Microbiol. Methods*, 2017, **137**, 34–39.
- 30 B. K. Wilson and G. D. Vigil, Automated bacterial identification by angle resolved dark-field imaging, *Biomed. Opt. Express*, 2013, **4**(9), 1692–1701.
- 31 S. Miyamoto, *et al.*, Estimating the Diffusion Coefficients of Sugars Using Diffusion Experiments in Agar-Gel and Computer Simulations, *Chem. Pharm. Bull.*, 2018, **66**(6), 632–636.
- 32 D. Rajnovic, X. Muñoz-Berbel and J. Mas, Fast phage detection and quantification: An optical density-based approach, *PLoS One*, 2019, **14**(5), e0216292.
- 33 J. Bär, *et al.*, Efficient microbial colony growth dynamics quantification with ColTapp, an automated image analysis application, *Sci. Rep.*, 2020, **10**(1), 16084.
- 34 K. Huff, *et al.*, Light-scattering sensor for real-time identification of *Vibrio parahaemolyticus*, *Vibrio vulnificus* and *Vibrio cholerae* colonies on solid agar plate, *Microb. Biotechnol.*, 2012, **5**(5), 607–620.
- 35 H. Wang, *et al.*, Early detection and classification of live bacteria using time-lapse coherent imaging and deep learning, *Light: Sci. Appl.*, 2020, **9**(1), 118.
- 36 T. Yanagita, Capillary tube method for counting viable bacteria, *J. Bacteriol.*, 1956, **71**(3), 381–382.
- 37 R. L. Bowman, P. Blume and G. G. Vurek, Capillary-Tube Scanner for Mechanized Microbiology: A photoelectric scanner measures growth in agar-filled capillaries and gives a new approach to microbiology, *Science*, 1967, **158**(3797), 78–83.



Lab on a Chip

Supplementary Information

Title: Label-free 1D Microfluidic Dipstick Counting Of Microbial Colonies And Bacteriophage Plaques

Authors: Sultan İlayda Dönmez, Sarah H. Needs, Helen M. I. Osborn, Nuno M. Reis, and Alexander D Edwards

Contents

Supplementary Methods.....	2
Phage Stock Preparation	2
Double Agar Layer Method (DAL).....	2
Figure S1.	3
Plate Spread Method.....	3
Supplementary Results.....	4
1D individual non-motile bacterial colony formation.....	4
Figure S2.	4
1D individual motile bacterial colony formation	4
Figure S3.	4
Figure S4.	5
Properties of capillary colonies	6
Figure S5.	7
Figure S6.	8
Figure S7.	9
Figure S8.	10

Supplementary Methods

Phage Stock Preparation

For phage K bacteriophage amplification, inoculate with a single colony of *S. aureus* into a sterile BHI broth and place in incubator at 37 °C, 150 RPM. This overnight culture was used to inoculate a new sterile BHI broth flask with an initial 0.05 OD₆₀₀. Typically, this was achieved with 1 ml added overnight to 99 ml of BHI broth and placed this in the Incubator at 37 °C, 150 RPM. When the OD₆₀₀ reached 0.2 (approximately 90-120 minutes), the bacteria were inoculated with phage K at a multiplicity of infection (MOI) of 0.1. After 4 hours and the OD₆₀₀ started to decrease, it was centrifuged at 4500 x g for 10 minutes. The supernatant was filtered using a 0.45 µm filter and stored at 4°C until use.

For T2 bacteriophage amplification, inoculate with a single colony of *E. coli* into a sterile LB broth and place in incubator at 37 °C, 150 RPM. This overnight culture was used to inoculate a new sterile LB broth flask with an initial 0.05 OD₆₀₀. Typically, this was achieved with 1 ml added overnight to 99 ml of LB broth and placed this in the Incubator at 37 °C, 150 RPM. When the OD₆₀₀ reached 0.2 (approximately 120-150 minutes), the bacteria were inoculated with T2 phage at an MOI of 0.1. After 4-5 hours and the OD₆₀₀ started to decrease, it was centrifuged at 4500 x g for 10 minutes. The supernatant was filtered using a 0.45 µm filter and stored at 4°C until use.

Double Agar Layer Method (DAL)

For bacteriophage enumeration, 10 mL of BHI top agar (BHI broth with 0.5% agar) was mixed with 5 mL of salt solution (400mM MgCl₂ and 100mM CaCl₂) for *S. aureus* and LB top agar (LB with 0.5% agar) for *E. coli* were prepared. This was kept in a water bath at 60°C for 1 hour. 10 µl of host bacteria at 4x10⁸ CFU/mL and 10µl of bacteriophage were added to this tube, which was left to cool but still molten. The mix was poured into a Petri dish and left to dry. These procedures were repeated for serial dilutions of bacteriophage samples and incubated for 24 h at 37 °C and plaques counted (Figure S1).

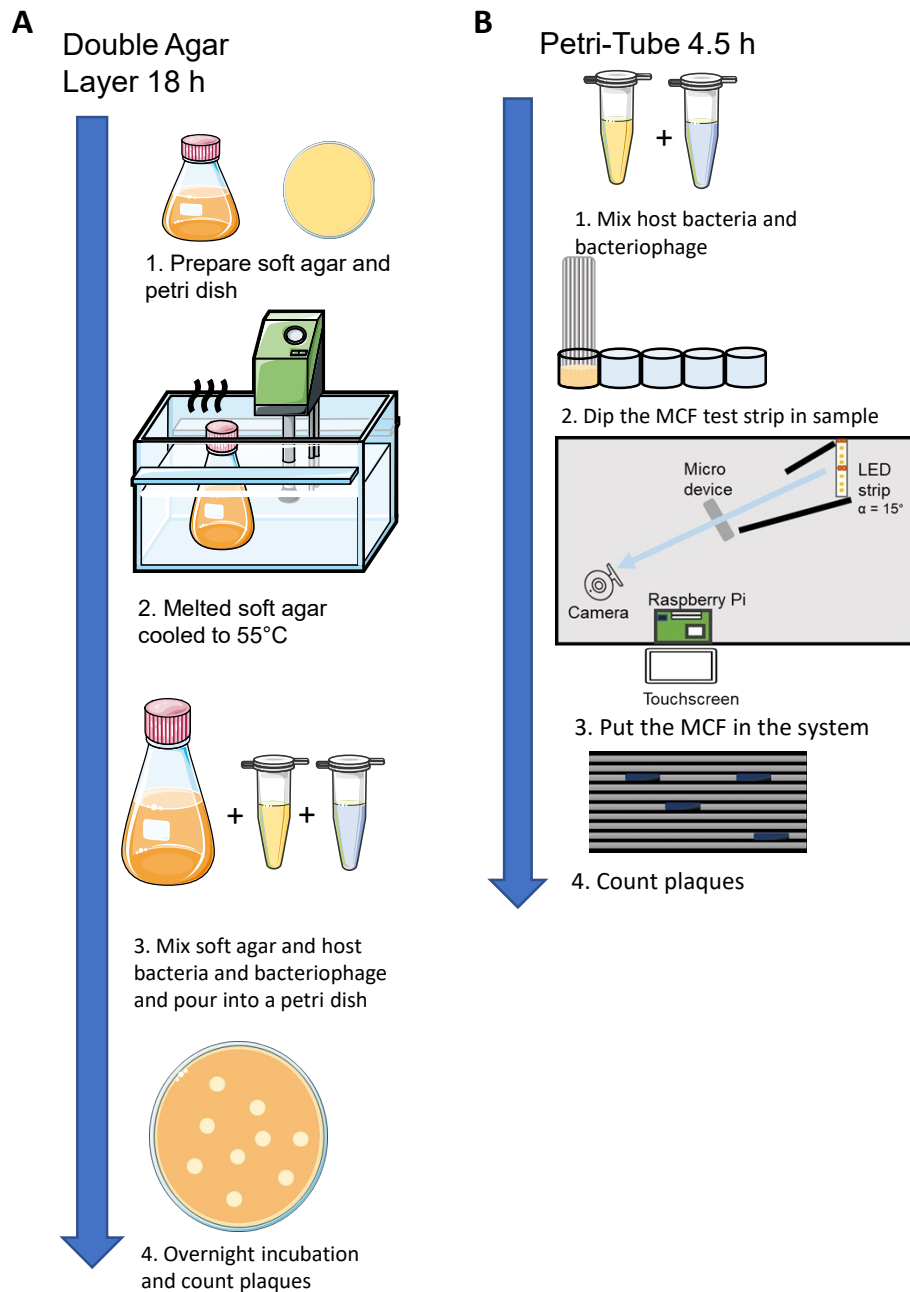


Figure S1. Conventional petri dish double agar layer (DAL) method comparison with liquid microcapillary film (MCF) method.

Plate Spread Method

An aliquot of a $\sim 8.0 \times 10^8$ CFU/mL *E. coli* stock (ATCC 25922 and B strain) is divided into 3 titrations (250, 500, and 1000 CFU/mL), and 100 μ L of each titration is plated in LB agar plates, resulting in expected CFU counts of 25, 50, and 100, respectively. After a night, 37 °C incubation, the number of colonies from each titration was counted and recorded directly on the plate. After repeating the same experiment for 3 titrations in triplicate, the counted number of colonies is plotted against the expected number of colonies, with error bars showing ± 1 standard deviation in both axes- all error bars are plotted but in some cases are too small to distinguish.

Supplementary Results

1D individual non-motile bacterial colony formation

MCFs were dipped in *E. coli B* samples of different concentrations and photographed with time-lapse imaging every 10 min in the darkfield system. Colony formation was observed after 4 hours, and colony formations could be counted after 5.5 hours. Since the formed colonies did not have the ability to move, they remained in a limited area and allowed to be counted. During growth, using the point where it started to grow as the origin, its growth is not distributed over the entire capillary (Figure S2). The full video is shown in S1 Video.fileformat.

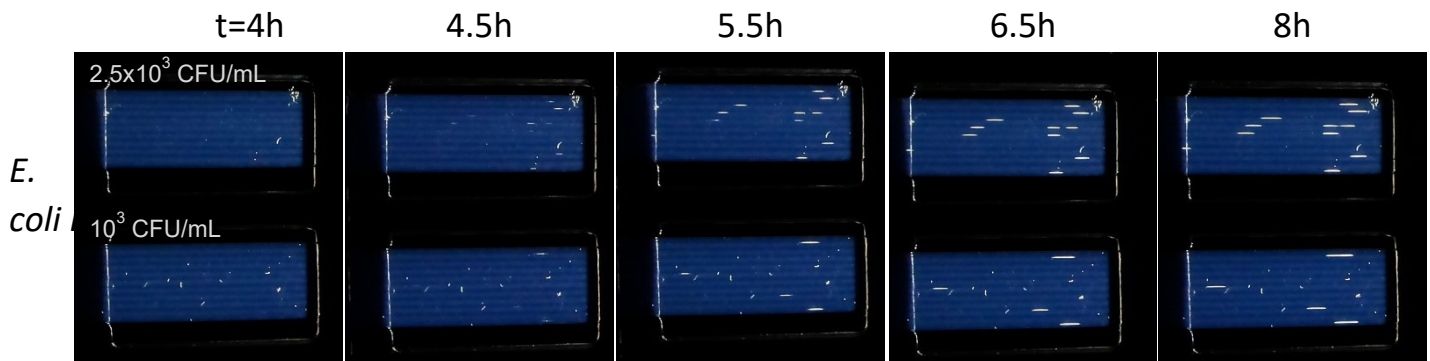


Figure S2. Diagram illustrating various timepoints and endpoint to accompany video of individual bacteria counting in 1 dimensional microcapillaries by time-lapse imaging. First MCF test strip was dipped into suspension of 2.5×10^3 CFU/mL *E. coli B* strain, second MCF test strip with 10^3 CFU/mL.

1D individual motile bacterial colony formation

To understand how motile *E. coli 25922* grew as a single colony in MCF, different concentrations of both broth and soft agar were prepared and MCFs were dipped into these samples. Prepared MCFs were photographed with time-lapse imaging every 10 minutes in the darkfield system. Colonies started to grow after 4 hours in this motile bacterium like *E. coli 25922*. However, the bacteria growing at one point spread throughout the whole capillary thanks to their motility. Soft agar was also not sufficient to restrict the movement of this bacteria (Figure S3). The full video is shown in S2 Video.fileformat.

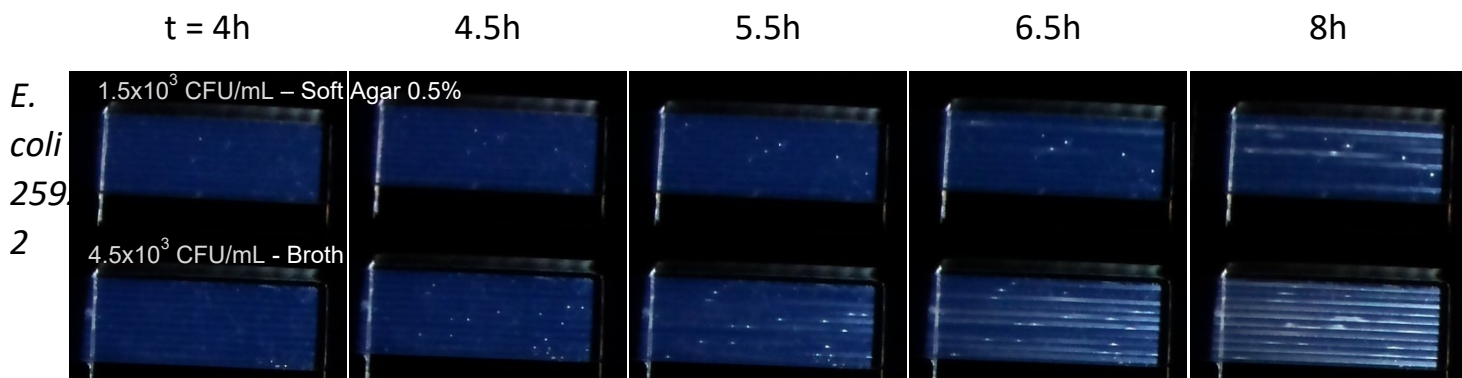


Figure S3. Motile *E. coli 25922* growth in soft agar vs liquid broth in MCF. Starting inoculum at 1.5×10^3 CFU/mL in soft agar and 4.5×10^3 CFU/mL in liquid media.

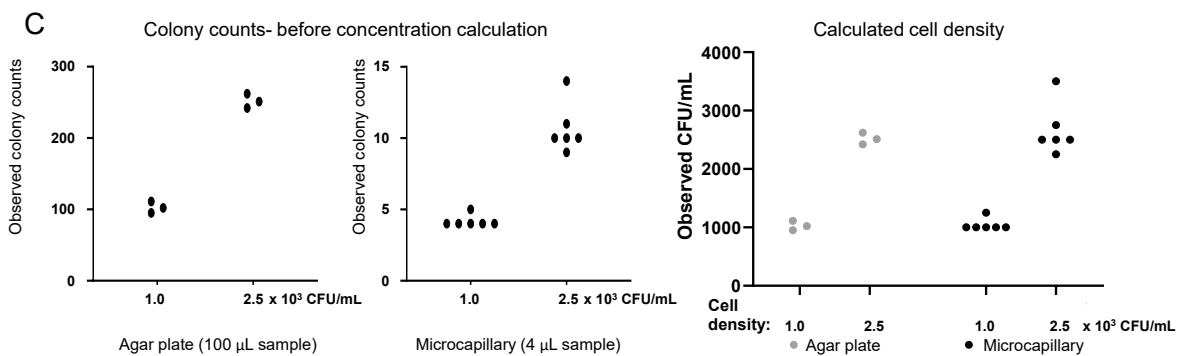
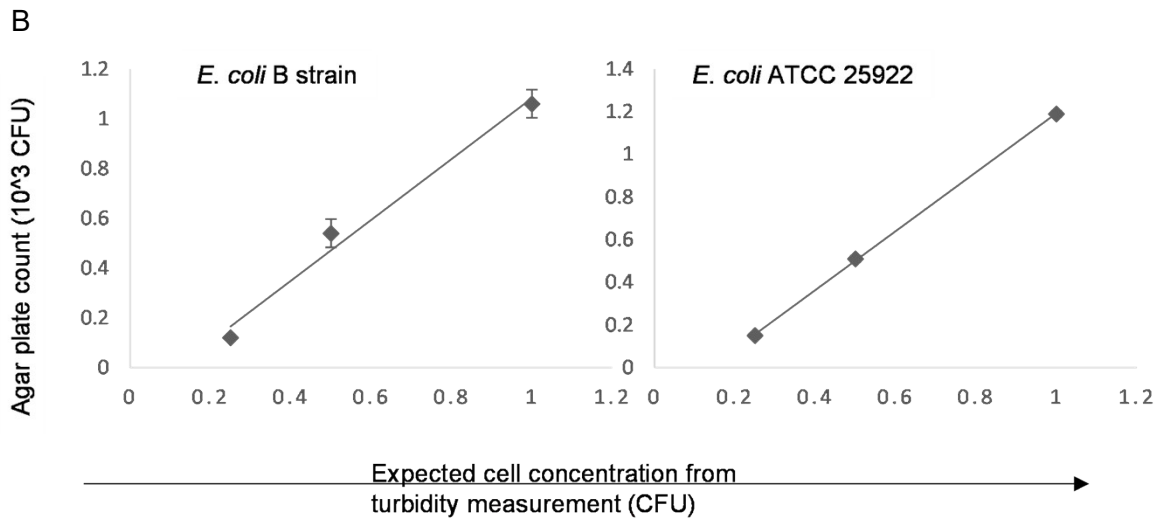
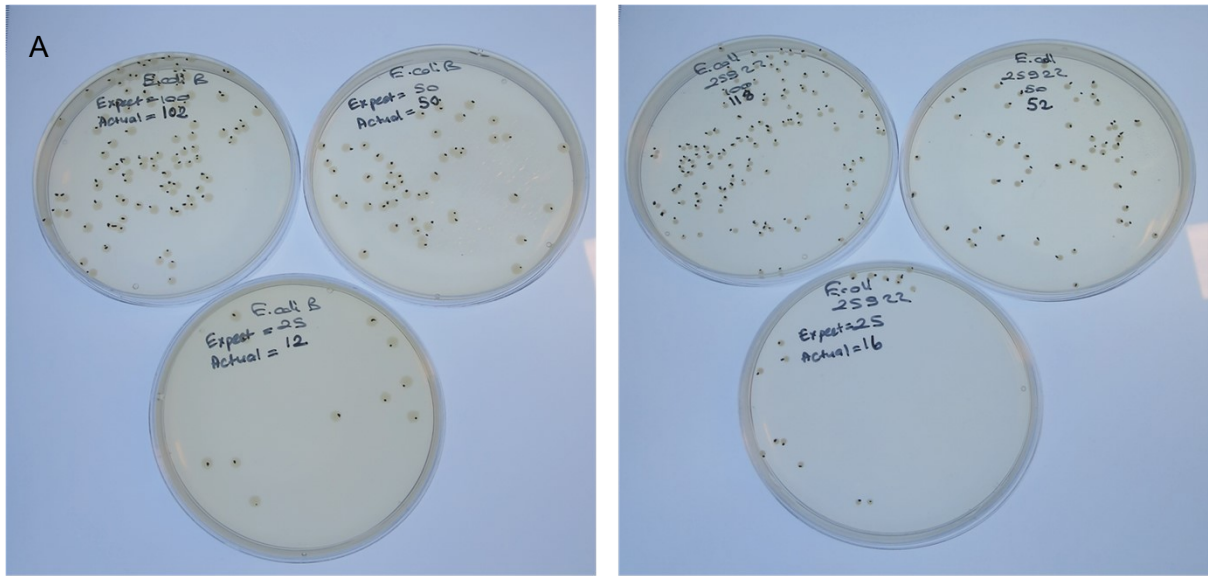


Figure S4. Measurement of *E. coli* Cell Concentration by Plating and Microcapillary Counts. **A)** The turbidity of an aliquot of a $\sim 8.0 \times 10^8$ CFU/mL *E. coli* culture (ATCC 25922 and B strain) was used to calculate expected cell concentrations and diluted into 3 suspensions (250, 500, and 1000 CFU/mL), and 100 μ L of each plated onto LB agar plates, expected to give expected CFU counts of 25, 50, and 100, respectively for these 3 plates. Images illustrate manual colony counting for replicate plates. **B)** the number of colonies from each was manually counted and recorded directly on the plate. After repeating the same

experiment in triplicate, the counted number of colonies was plotted against the expected number of colonies based on turbidity, with error bars showing ± 1 standard deviation in both axes of the triplicate experiments- all error bars are plotted but in some cases are too small to distinguish. **C)** To explore the repeatability of colony counting in microcapillaries a set of 6 repeat measurements were taken (each comprising 4 μL total volume per MCF strip within 10 capillaries) and compared with triplicate agar plate counts (plating 100 μL). Raw colony counts for the two methods were plotted (left) and calculated cell densities (right) and in all cases all individual points are shown to illustrate the distribution of counts.

Properties of capillary colonies

We examined colony length for *E. coli* B and *S. aureus* as a 1-dimensional measure of colony growth in liquid media. Photographs were selected at 6 regular time points from the full time-lapse image stack, including the first time that the colony became clearly visible. Graphs of the mean colony lengths of 6 time points of different colonies were plotted against on the mean light scattering intensity (Figures S5-6A). Then, the light scatter intensity of 9 different bacteria was examined for 6 different time points for both organisms. Graphs prepared without normalization showed much variation for each colony (Figure S6).

Growth kinetics were normalized to define a single fixed rectangular area of interest that completely contained the colony at the final stage of growth, and then calculate the grayscale intensity with that area. At this stage, it was observed that the two organisms drew very different growth patterns from each other. While *E. coli* started to rapidly multiply, it lost its growth rate at some point and continued to expand more slowly in the capillary. On the contrary, *S. aureus* started at a slower growth rate but maintained this rate throughout the entire period (Figure S7). Here, taking advantage of Monod's kinetics, which correlates microbial growth rates in an aqueous medium with a limiting nutrient concentration, we can say that while *E. coli* showed a rapid growth regime, it quickly consumed the nutrient concentrations in the environment and thus the growth rate of the bacteria was limited.

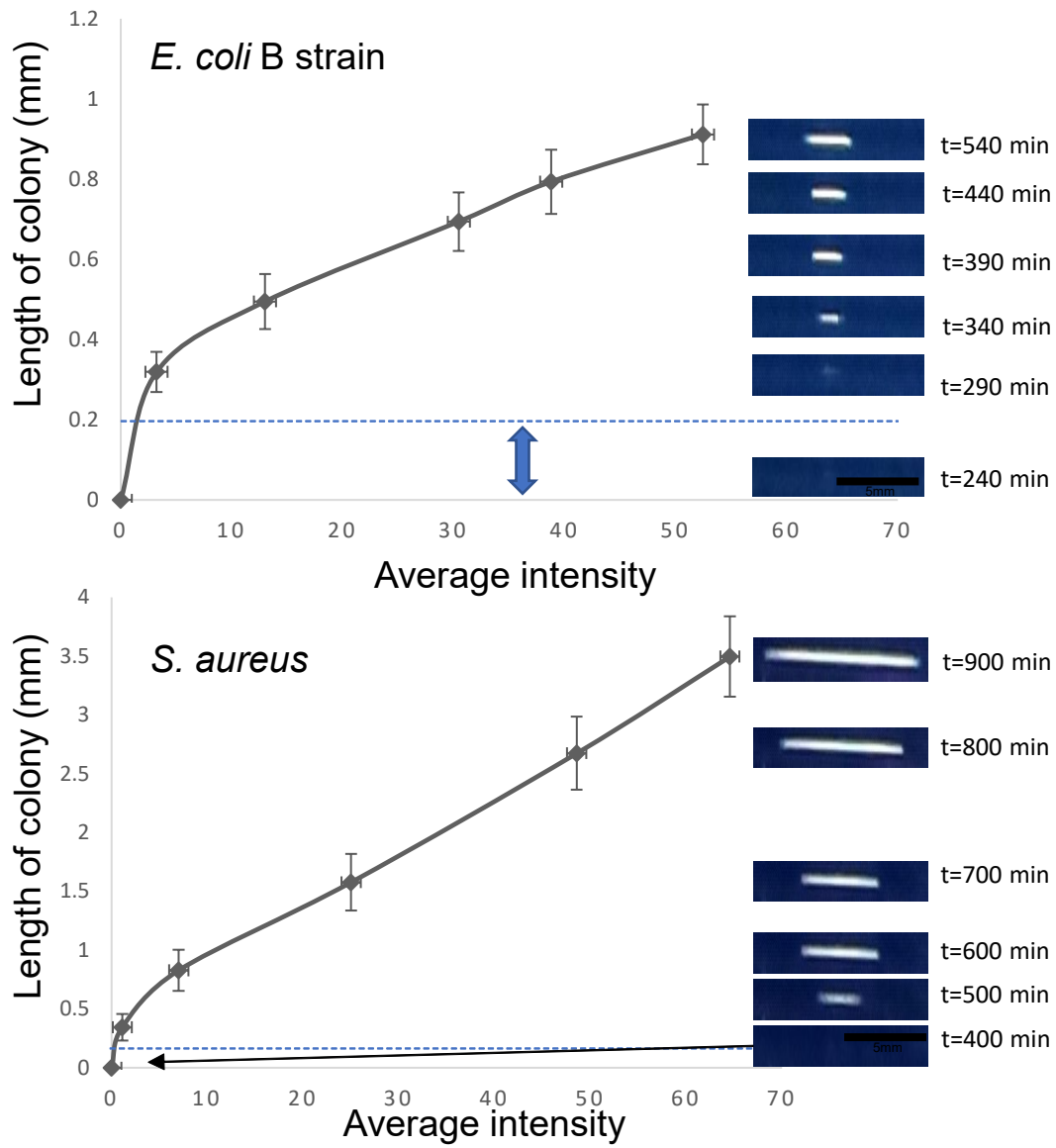


Figure S5. Properties of capillary colonies. Colony length and light scattering intensity were measured for 9 *E. coli* (top) and *S. aureus* (lower) colonies at the 6 timepoints indicated in figure 3, and images of one example colony displayed at each time. Mean length versus integrated intensity of the 9 colonies are plotted, with error bars indicating ± 1 standard deviation.

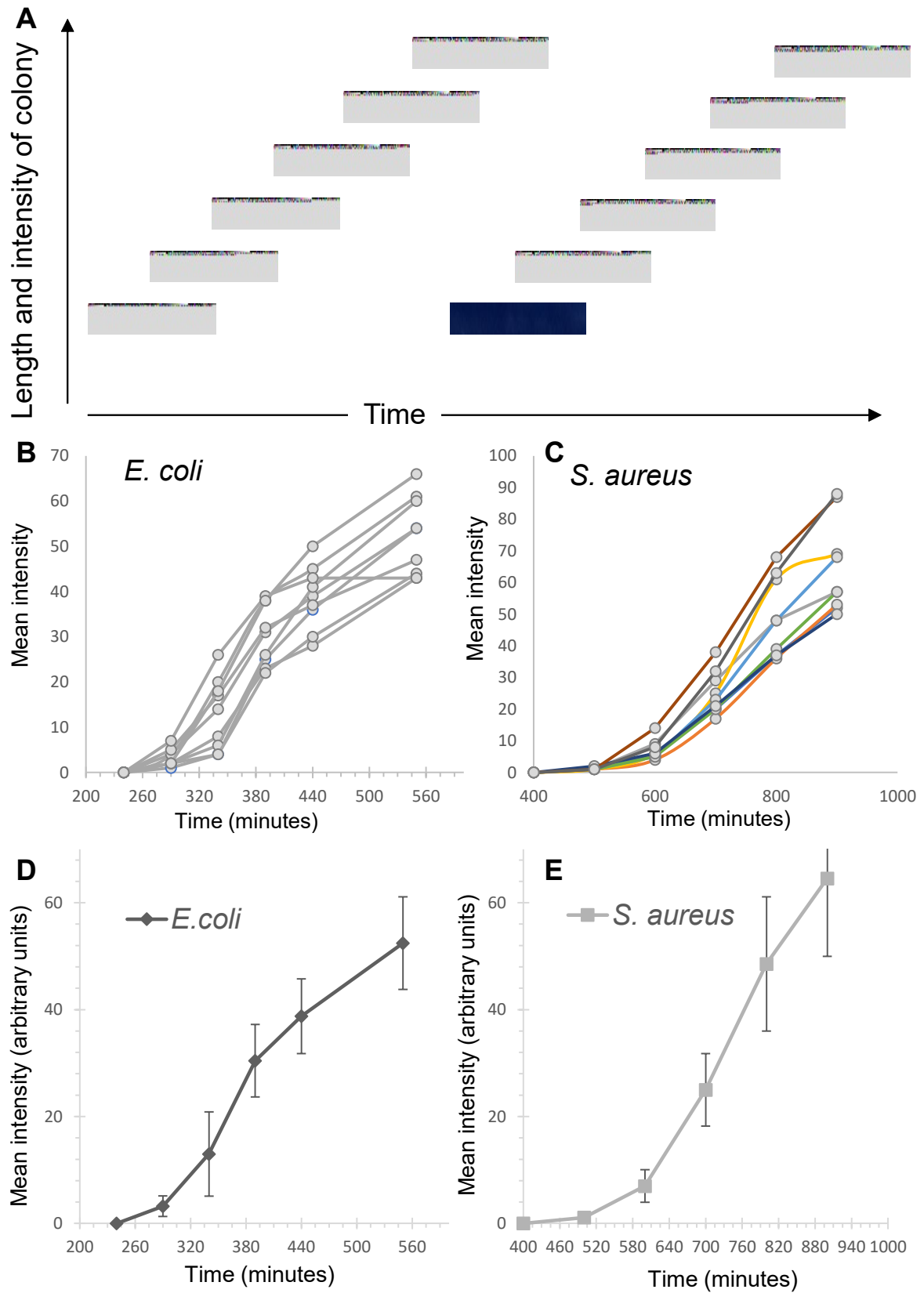


Figure S6. Colony intensity estimating initial growth. Each colony was identified, and a box used to select that contained the whole colony at a late time-point, and the same box

highlighted for all measured timepoints; images in A show example for colonies for each organism, increasing in length and intensity as the colony grows. B-D Mean light scattering intensity were measured for 9 individual *E. coli* (B, D) and *S. aureus* (C, E) colonies at the 6 timepoints indicated in figure 3. B, C individual mean intensities for all colonies plotted to illustrate spread in intensity. D, E Means for the 9 colonies plotted with error bars indicating ± 1 standard deviation.

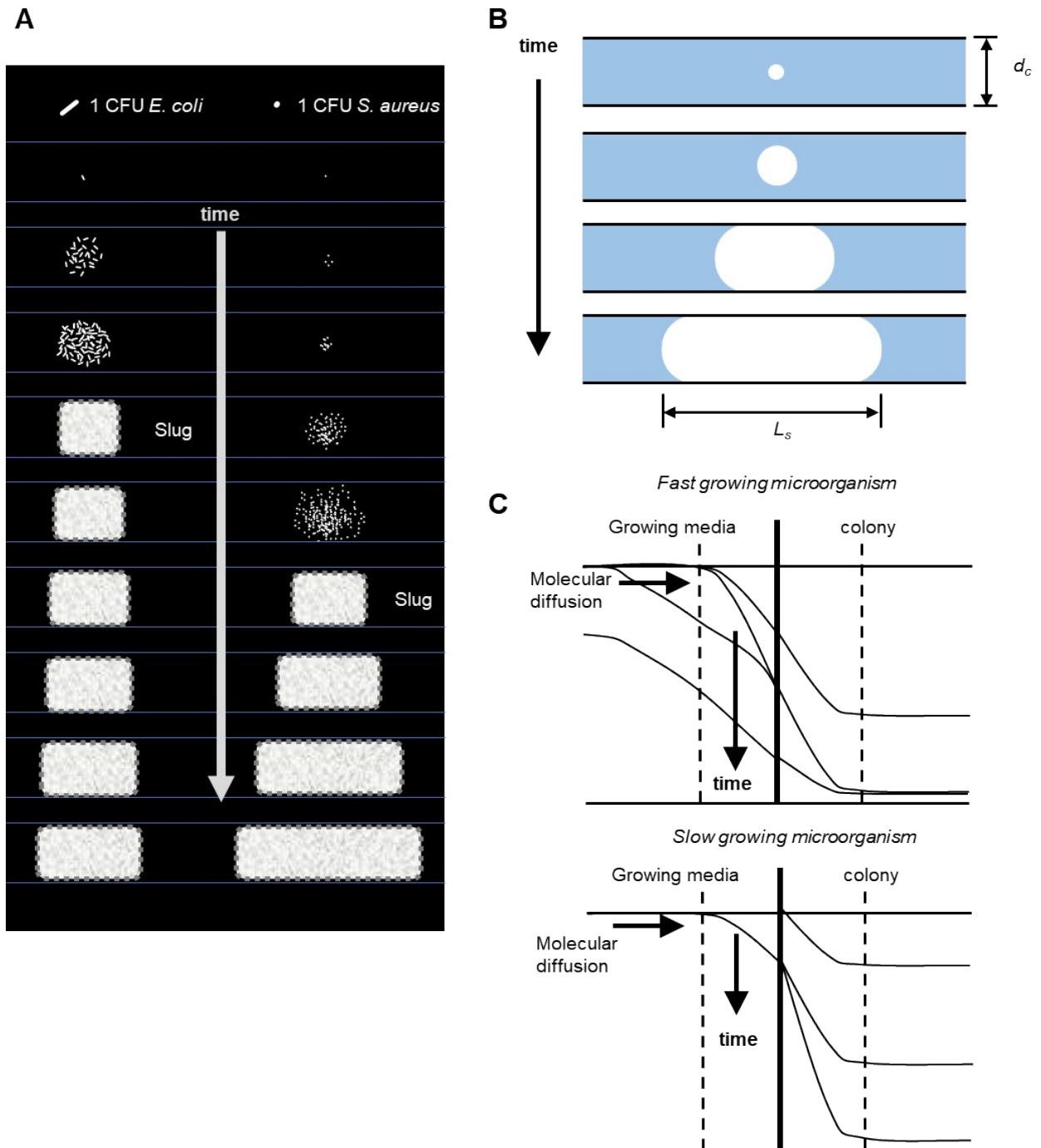


Figure S7. Representative growth chart of fast and slow growing colonies. A) Capillary growth chart for *E. coli* and *S. aureus*. When the size of the colony reaches the microcapillary diameter, the 1-dimensional growth of the colony becomes limited by the diffusion of carbon source, glucose. B) 1-dimensional expansion of length of colony 'slug', L_s in a microcapillary with inner diameter d_c . C) Predicted diffusion plot for a fast-growing

organism. With a fast-growing microorganism such as *E. coli*, the glucose concentration at the interface is depleted, forcing the colony to grow at lower concentration of glucose, therefore showing reduced growth rate and linear expansion rate of the colony. With a slow growing microorganism such as *S. aureus*, there is sufficient time for glucose to diffuse to from the bulk of the microcapillary to the liquid-colony interface, therefore enabling growth of the colony closer to maximum growth rate, sustaining longer linear expansion along the microcapillary.

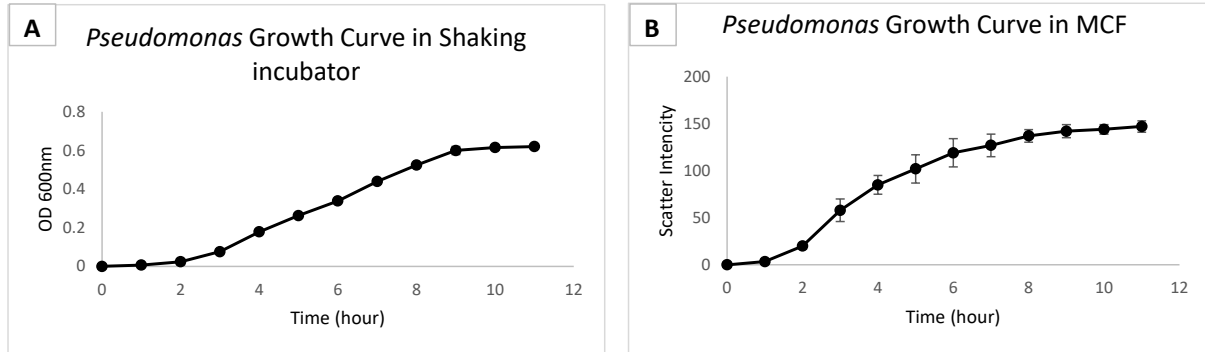


Figure S8. *Pseudomonas* growth curves were measured in parallel using cuvette (A) in spectrophotometer vs within MCF (B) and comparing cell growth kinetics in flask vs within 20 replicate microcapillaries. All error bars are plotted and indicate the standard deviation, in some cases this is smaller than the symbol size.

Amendments and Notes

1. Amendment: LB and Nutrient broth do not include glucose. We mention glucose consumption, but growth curves in the system as being caused by nutrient consumption such as amino acids.
 2. Amendment: In addition to nutrient consumption, harmful pH changes, oxygen consumption and toxic waste production, which occur with the effect of bacterial metabolism, are also effective in MCF growth at the end of the growth periods.
 3. Amendment: The growth differences between *E. coli* and *S. aureus* can be both species dependent and environment dependent. Growing two different types of bacteria in two different media can be misleading, but in our previous studies (not included in this publication) with *E. coli* B, nutrient broth was used, and the growth of the bacteria was observed to be no different to than achieved with LB broth. However, for better accuracy, more precise information can be obtained by growing these two types of microorganisms in an environment with the same content.
 4. Amendment. Although fluoropolymers are relatively oxygen permeable, we are unable to determine achievable oxygen levels in MCF test strips, as with many other clinically and industrially important bacteria. In this case, as an oxygen obligate bacterium can grow in the MCF, it would be misleading to consider that the growth conditions are fully oxygen restricted.
-
1. Note: Motility can vary significantly due to differences between strains within a single species. *E. coli* 25922 and *E. coli* B are different morphologically and physiologically. Deletion of the *recA* gene (Phue, Lee et al. 2008) and sigma factor *flhDC* (Soutourina and Bertin 2003) *E. coli* B results in lack of motility.
 2. The Gitlab link of the system includes the details of the technical details;
<https://gitlab.com/AIEdwards/bacterioscope>

Phue, J. N., S. J. Lee, L. Trinh and J. Shiloach (2008). "Modified Escherichia coli B (BL21), a superior producer of plasmid DNA compared with Escherichia coli K (DH5alpha)." Biotechnol Bioeng **101**(4): 831-836.

Soutourina, O. A. and P. N. Bertin (2003). "Regulation cascade of flagellar expression in Gram-negative bacteria." FEMS Microbiology Reviews **27**(4): 505-523.

Chapter 5

Dark-Pi Open-Source Imaging Systems Permits Direct Analysis of Platelet Aggregation in Dip-and-Test Microcapillary Film Strips

Chapter summary: Platelets, like bacteria, are small in size and thus have a size similar to that of bacteria. They also scatter light like bacteria and are measured typically by turbidimetry. For all these reasons, we aimed to utilise the technology developed in this thesis for a new, easy and inexpensive method for platelet measurement. In this section, it is demonstrated that platelets and their aggregation can be detected and measured by the light diffraction method, thus avoiding the disadvantages of classical methods and providing an alternative method for clinical testing.

Bibliographic details: Rüyâ Meltem Saryer, Sultan İlayda Dönmez, Chris Jones, Helen M.I. Osborn, and Alexander D. Edwards

Author Contributions: R.M.S: Conceptualization, Formal analysis, Elements of experiments, (Major contribution is elements of experiments. R.M.S. provided isolation of platelets from blood, and prepared agonists and dried them in the microfluidic) S.I.D: Conceptualization, Investigation, Visualization, Formal analysis, Data analysis, Experimental design, Funding acquisition, Writing - original draft, Writing - review & editing. C.J: Investigation, Visualization, Writing - review & editing (Major contribution is elements of experiments. C.J. provided platelets agonists). H.M.I.O: Supervision, Writing - review & editing (Major contribution is supervision. H.M.I.O is reviewed the manuscript). A.D.E: Conceptualization, Funding acquisition, Supervision, Writing - review & editing (Major contribution is supervision and elements of experiment. A.D.E. provided the microfluidics).

This manuscript is prepared for submission to *Microchimica Acta*

Dark-Pi Open-Source Imaging Systems Permit Direct Analysis of Platelet Aggregation in Dip-and-Test Microcapillary Film Strips

Rüya Meltem Sarıyer¹, Sultan İlayda Dönmez¹, Chris Jones², Helen M.I. Osborn¹, and Alexander D. Edwards¹

¹Reading School of Pharmacy, University of Reading, Whiteknights, Reading, RG6 6AD, United Kingdom

²Reading School of Biological Sciences, University of Reading, Whiteknights, Reading, RG6 6AS, United Kingdom

Author Contributions: R.M.S: Conceptualization, Formal analysis, Elements of experiments, (Major contribution is elements of experiments. R.M.S. provided isolation of platelets from blood, and prepared agonists and dried them in the microfluidic) S.I.D: Conceptualization, Investigation, Visualization, Formal analysis, Data analysis, Experimental design, Funding acquisition, Writing - original draft, Writing - review & editing. C.J: Investigation, Visualization, Writing - review & editing (Major contribution is elements of experiments. C.J. provided platelets agonists). H.M.I.O: Supervision, Writing - review & editing (Major contribution is supervision. H.M.I.O is reviewed the manuscript). A.D.E: Conceptualization, Funding acquisition, Supervision, Writing - review & editing (Major contribution is supervision and elements of experiment. A.D.E. provided the microfluidics).

Keywords: platelets, platelet aggregation, Dark-Pi, Open-source, ADP, thrombin

ABSTRACT

Measuring the functions of platelets, which have an essential role in haemostasis, is of great importance for the early diagnosis of many serious diseases and for antiplatelet drug research. Platelet variations that change from individual to individual are still not fully understood. It is thought that large-scale studies will illuminate these incomprehensible processes. The necessity of large-scale studies leads to the requirement for inexpensive and high-performance biological tests. The bacterial analysis has been previously reported. Here we develop this technology further for platelet analysis with a low-cost, open-source, high-throughput and customizable darkfield imaging system (Dark-Pi) using microfluidic technology. The hardware developed here consists of a camera and a light source controlled by the Raspberry Pi, and 3D printed parts. Using the Dark-Pi the results show that platelet

aggregation was increased in adenosine diphosphate (ADP) and thrombin loaded capillaries in a concentration dependant manner. The system previously reported for bacteria had to be further developed and optimised for the application described herein. Thus, capturing high quality and time-lapse images of activated platelets in capillaries allowed us to measure time-dependent changes based on light scattering in platelet-rich plasma (PRP). The classical aggregometry, which is based on light transmission, is still not standardized and a high sample volume is needed. However, the novel system that we have built will make it suitable for use in large-scale platelet studies due to its simplicity and low cost.

1. INTRODUCTION

Platelets are small blood cells mostly produced by the bone marrow (Gianazza, Brioschi et al. 2020). Since platelets play central roles in different processes such as hemostasis, inflammation, metastasis, wound closure and defence, platelets allow us to have an idea about many diseases (Jurk and Kehrel 2005), therefore, platelet investigation is very important. Platelet function tests (PFTs) are diagnostic tests that check whether platelets are physically deconstructed and functionally active (Favaloro 2019). PFT should be performed without delay after blood collection. Processes such as freezing, storing, and transporting of platelet containing samples over long distances must be avoided. Therefore, the laboratory where the test will be performed should be in the same or proximity to the blood collection location, and assays should be performed by experienced and skilled personnel (Favaloro 2019, Alessi, Sié et al. 2020).

Light transmission platelet aggregation (LTA), which is fundamental in the investigation of various platelet functions, has been used since the 1960s. LTA is simply light transmission aggregometry that measures the transmission of light transmitted from a platelet-rich plasma (PRP) sample and is based on the principle of increasing light transmission by platelet aggregation (O'brien 1961, Born 1962). LTA, which is still the gold standard, is still used in many studies and in the investigation of different platelet pathways. There are extensive studies on the working principles of platelet activation by adding different agonists to platelet-rich plasma (PRP) (Zhou and Schmaier 2005).

Although it works on a simple principle, the high cost of the device and the ability to read only a few samples (generally 4 channels) can limit the ability to conduct multiple analyses in parallel. LTA is also time consuming, requiring at least 5 minutes for each test, and multiple testing is often not possible within the recommended timeframe for platelet function (Vinholt,

Nybo et al. 2017). Another challenge of LTA is that it is affected by many preanalytical and analytical variables such as anticoagulant type, lipid plasma, haemolysis or low platelet count, as well as different procedural conditions such as PRP preparation, and the use of different agonist concentrations (Cattaneo, Cerletti et al. 2013). Therefore, the standardization of the LTA with the developed guidelines should be checked continuously (Harrison, Mackie et al. 2011, Chan, Armstrong et al. 2018). Also, 250 μ L of platelet-rich plasma (PRP) is required for only 1 sample measurement, which requires a large sample volume for one trial. The biggest problem with traditional aggregometry is that it is a crude way to measure platelet activation. Essentially, light is shone on a platelet cuvette and the reduction in the light intensity is measured. While this method measures a specific cuvette size, it is very old compared to tracking analysis of nanoparticles looking at individual particles (Paniccia, Priora et al. 2015). Platelet aggregation is detected by increased light transmission as platelets begin to aggregate in the presence of an agonist in the aggregometer cuvette and this leads to the development of an aggregation curve (Tsoupras, Zabetakis et al. 2019).

Although LTA is the first diagnostic step in platelet evaluation, platelet dysfunction can be caused by many factors (Podda, Femia et al. 2012), so further specific testing needs to be confirmed before a conclusion can be drawn (Paniccia, Priora et al. 2015). While this method measures a particular size, it is very outdated compared to nanoparticle tracking analysis that looks at individual particles. Another alternative for looking at platelet aggregation is confocal microscopy, but it is impractical because confocal microscopy is not used for clinical testing, it only tells the bulk measurement.

Considering all these disadvantages of LTA, there is a need for point-of-care (POC) tests that can evaluate platelets in a fast and simple method, can allow high throughput analysis with even small sample volumes, and can be used by non-experts including within non-laboratory settings. Many companies produce different kinds of POC tests to overcome the challenges of traditional methods for platelets measurements including PFA-100, PFA-200 (Siemens), VerifyNow (Werfen), Plateletworks (Helena Laboratories), Impact R (DANED SA), Multiplate (Roche Diagnostics), TEG/ROTEM (TEG; Haemonetics Corporation/ ROTEM), Global thrombosis test (Thromboquest Ltd) (Paniccia, Priora et al. 2015, Gorog and Becker 2021). Although these studies have been well thought through and have been in development for a long time, they have not found use in clinical practice and therefore these techniques are still not recommended for routine clinical use (Gorog and Jeong 2015, Gorog and Becker 2021).

Platelets are small and light scattering and can be measured by turbidimetry. Bacteria are small cells and can also be measured by turbidity. We previously developed a darkfield imaging system for visualising bacteria in microfluidic devices (Dönmez, Needs et al. 2020). In this study, it was first aimed to see the platelets in the dark field system in the microfluidic. We hypothesized that platelets could be measured similarly to bacteria based on turbidity-based measurement, thanks to the light scattering property. We hypothesized that platelets can be measured in a similar way to bacteria, which rely on turbidity-based measurement thanks to its light scatter feature. Beyond that, being able to see platelet aggregation was also very important. We were able to see the effect of high concentrations of ADP and thrombin on platelets in MCFs. While ADP clearly causes aggregation between platelets, thrombin fairly adheres all platelets to a corner in the channels. In the Dark-Pi, it was easily possible to see platelets. The effect of 2 different agonists on platelets is obvious enough to be seen. Although it is not clear whether the analysis method used is the best method for platelet studies, we demonstrated the time-dependent variation of time-dependent monitoring of platelet aggregation on a particle basis with a very simple system.

2. MATERIAL AND METHOD

2.1 Preparation of MCF test strip: Hydrophilic coating protocol

The inner surface of MCF was coated with poly (vinyl alcohol) (PVOH) (Sigma-Aldrich, UK) to gain hydrophilicity. This involved cutting a 1 m long MCF with the scraper blade and connecting it to a KNF Laboport mini vacuum pump (Sigma-Aldrich, UK), and filling it with 10 gL⁻¹ PVOH in distilled water. To prevent evaporation and leakage, 2 ends of the MCF coated with paraffin were sealed. Afterwards, this was incubated for 2 hours at room temperature (RT). After incubation, the PVOH solution was removed using the vacuum pump, following that, the inner capillary strips were washed with 0.05% v/v Tween 20 (Sigma-Aldrich, UK) solution in distilled water. The MCF was left attached to the vacuum pump for 20 minutes to dry.

2.2 Reagent loading protocol

1m PVOH coated MCF were cut into 3.3 cm segments. Reagent solutions (0.01 M and 0.003 M ADP) (Sigma-Aldrich, UK) at different concentrations were injected into the PVOH coated MCFs via a 5mL syringes and 30 Gauge needles. 5 out of the 10 capillaries were

loaded with high concentration and the rest with low concentration ADP. Control strips were loaded with distilled water. The strips then were cut into desired lengths and put in the -80°C freezer for 1 hour. Following that the strips were placed in the Virtis adVantage Plus Freeze Dryer (SP Industries Inc., Warminster, PA, USA) overnight.

2.3 Blood samples preparation

The amount of blood required for the test (approximately $10\ \mu\text{L}$ per 3 m MCF strip) was collected from healthy donors into the sodium citrate tube which prevents coagulation. After taking the blood, it was incubated at 37°C for 5 min. The citrated blood was centrifuged at $102\times g$ for 20 min at 20°C to separate platelet-rich plasma (PRP) from the whole blood (WB). PRP was centrifuged at $17.0\times g$ for 2 min to obtain platelet-poor plasma (PPP) from the PRP.

2.4 Darkfield Imaging Protocol

The strips were gently cleaned with a microscope lens cleaning wipe to remove any dust that could affect the imaging. ADP-loaded strips were dipped into the PRP. Control strips (10 capillaries) were divided into two (5 – 5 capillaries) with a razor blade. 5 capillaries were dipped into PRP and the remaining 5 into PPP. After that the strips placed in the system. Time-lapse images were taken every 10 seconds for 3 minutes.

2.5 Light Transmission Aggregometry (LTA)

The cuvettes were calibrated through $250\ \mu\text{L}$ PPP. For this, PPP was added to an aggregometer cuvette without a stirrer and this cuvette was placed in the wells row by row in the aggregometer. Platelet aggregometry was performed at 37°C , 2 mins. at 1200 rpm. $225\ \mu\text{L}$ PRP was added to the aggregometry cuvette, and the stirrer was added to the cuvette. The cuvette was placed on the aggregometer. After 20 - 25 seconds, a $25\ \mu\text{l}$ agonist was added and the response was recorded.

2.6 Data Analysis

Images were analysed by using ImageJ – histogram. Demonstration of image analysis allows evaluation of light scatter intensity by plotting the distribution of grey values across a selected area of the microcapillary film by a histogram plot and showing the background scattering stems from microdevice between the two capillaries. The marked points show, in order from top to bottom: background light scattering by the microcapillary film between two

capillaries, light scattering by platelet-rich plasma within the capillary, background light scattering, and light scattering by platelet-poor plasma within the capillary. With platelet aggregation in classical LTA, light transmission through the cuvette increases depending on the agonist concentration. In the system we designed, while the PRP in the microfluidic has a high scatter density, the scatter density decreases as a result of aggregation in the presence of agonist.

3. RESULTS AND DISCUSSION

3.1 Detection of Platelets in Microcapillaries Using Raspberry Pi Darkfield Imaging System

The classical aggregometer works by measuring light transmittance. Since the PRP solution is dense with platelets, its light permeability is low. However, with the interactions that occur in the presence of the agonist, the platelets begin to aggregate. With the effect of aggregation, the light transmission starts to increase in some places and this transmittance increases the signal intensity detected by the detector. Thus, a relationship is established between PRP and agonist concentration (Figure 1A). While light transmission increases with aggregation in aggregometry, the designed darkfield imaging system works in the opposite way with aggregometry, and light transmission decreases with aggregation. As with bacteria (Dönmez, Needs et al. 2020), platelets give a high scatter intensity with the light coming from the LED in the dark area and this light intensity is displayed by the camera. Clumps formed by the addition of agonist to the medium still produce scatter intensity, while the spaces left in place of particles reduce scatter intensity. Thus, the average light intensity is reduced (Figure 1A). In general, we found platelets were clearly visible by darkfield imaging in microcapillaries.

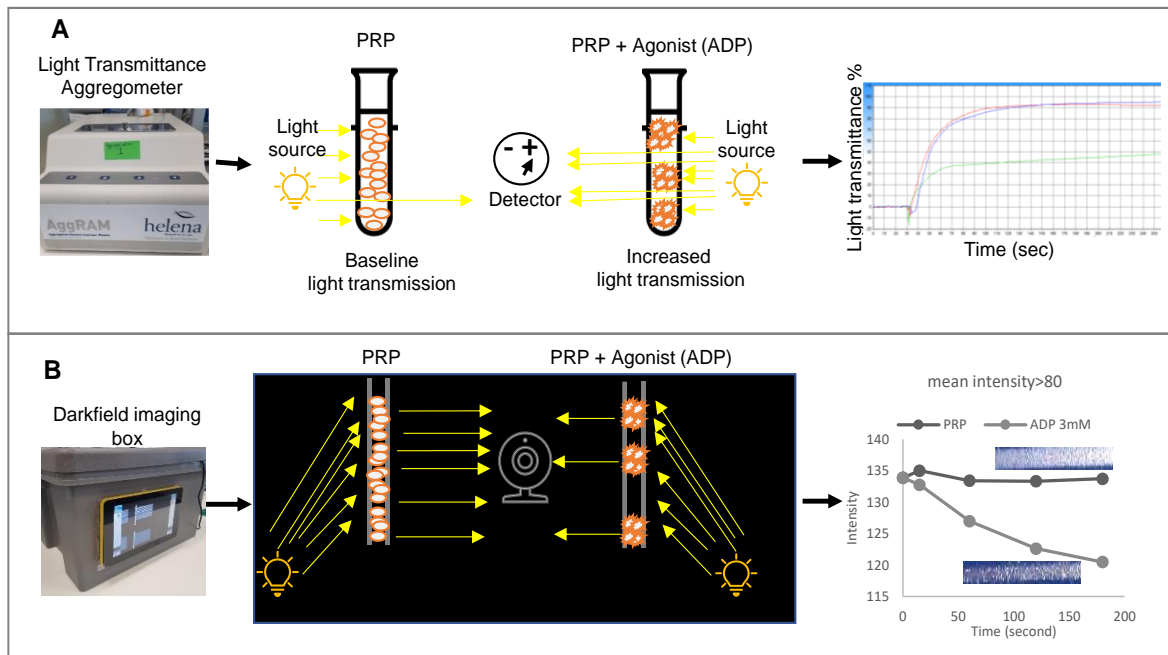


Figure 1. Concept of microfluidic darkfield assessment of platelet aggregation. A) How it is achieved in aggregometry in the cuvette (Tsoupras, Zabetakis et al. 2019) B) Microfluidic version shows how signal is “inverse” to cuvette.

3.1 How platelets seem difference then bacteria in the MCF?

From Figure 2, it is evident that water did not give a scatter signal in the MCF. However, platelets and bacteria showed scatter intensity and visibly reflected the light signal. However, there was a noticeable difference in distribution between platelets and bacteria. While the PRP sample had the appearance of more particle distribution (more heterogenic distribution) (Figure 3 B), a more uniform distribution was observed in bacteria (Figure 3). While one of the reasons for this may be the particle size of bacteria and platelets, the most likely reason may be the separation and centrifugation processes during the separation of platelets from the blood. During these processes, platelets may have interacted with each other (Sang, Roest et al. 2021). On the contrary, the bacterial sample was allowed to grow directly in broth and showed a much more uniform distribution in the MCF. The difference in the distribution image of two different samples led us to use a different analysis method. The methods used are explained in detail in 3.3.1. We found platelets were clearly visible by darkfield imaging in microcapillaries. We observed that the images were not identical to bacterial cell suspensions, there is a heterogeneous distribution then bacterial suspension.



Figure 2. How the different samples seem in MCF. Images after zooming (300%) different samples into a single capillary in MCF A) Water B) Platelets C) Bacteria.

3.2. Imaging Conditions (Table) Darkfield imaging system design and optimization

The first camera set up for the bacteria was not effective for the platelet's detection, because the camera was too far away to focus well on the platelets, hence, here, the system was further developed and optimised versus our previous report (Dönmez, Needs et al. 2020). The basic idea was the same, but the camera and its exact positions were different. A high-resolution lens was used to see the platelets, which are smaller particles ($2 \mu\text{m}$), in more detail and to have an idea about aggregation. Having fewer samples reduced the number of MCFs used but reduced the distance of the samples from the camera to see each sample closer. Since the number of MCFs decreased, the samples were loaded into the 5 out of the 10 capillaries were loaded with high concentration, so the number of repetitions decreased, but the number of concentrations used was increased.

Table 1. Tested parameters and optimal conditions.

Parameter	Range tested	Optimal condition	Comment
Distance between LED and sample	100 mm, 130 mm, 170 mm	100 mm (for 6 mm lens), 170 mm (for 16 mm lens)	Using 170 mm as a distance needs two blockers to prevent shadows appearing on the samples.
Distance between camera and sample	35 mm, 50 mm, 100mm, 130 mm	35 mm (for 16 mm lens), 130 mm (for 6 mm lens)	Distance between camera and sample depend on number of the MCF placed into the box and lens type.
Camera lens type	35 mm 10 MP Telephoto Lens, 16 mm 10 MP Telephoto Lens	Both	The wide lens is suitable for seeing 5 MCFs, the telephoto lens is reduced the number of MCFs to 2 but, gives closer and detailed examination.
3D parts and box colour	Black, gray	Black	Gray background and parts caused unwanted shadows in photos.
MCF length	8 mm, 14 mm	8 mm	It has been determined that the light coming into the sample is more homogeneous.

3.3 Analyses of Platelets Activation

3.3.1 How ADP affects PRP?

Initially the first method in the initial paper (Dönmez, Needs et al. 2020) used to analyse digital images to quantify the light scattering signal used ImageJ (Abràmoff, Magalhães et al. 2004). This method was sufficient to define the scatter intensity, because the scatter has a different light intensity range from low and high bacteria concentration.. However, here, after platelet aggregation, the clumps increased the scatter intensity too. This made it impossible to measure platelet aggregation with our initial image analysis method even though the stimulated platelets are clearly visible (Figure 3).

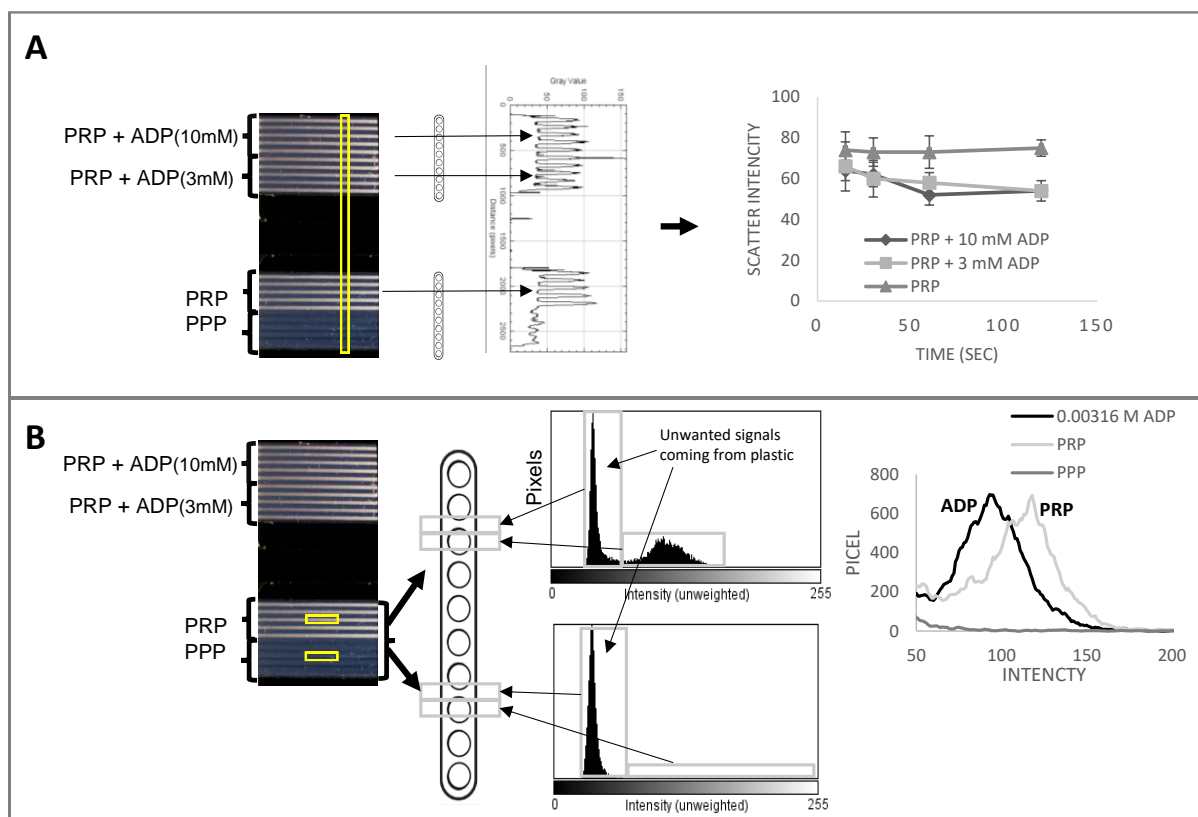


Figure 3. Demonstration of image analysis of ADP aggregation A) Illustration of initial image analysis allows limited measurement of scatter intensity with an intensity plot across microcapillary device B) Histogram plotting allows evaluation of light scatter intensity by plotting the distribution of grey values across a selected area of the microcapillary film.

Histogram analysis was used to measure platelets in MCF. Instead of plotting the profiling density and looking at the peaks, a box from the tool tab of ImageJ was used to precisely surround the capillary to plot a histogram of all pixels. This was done so all that are not in the capillary could be eliminated since the signals received from the plastic are much less

dense. We were thus able to observe greater differences between capillaries with platelets and capillaries with platelets+ADP. This may be evidence that stimuli may affect the image, but further study is still required. Density versus time graphs seem to be effective however, a closer look usually reveals the intensity value for platelets with ADP to be different than for platelets without ADP. We believe this analysis says there is something we can detect, but this analysis method needs to be developed for general testing by adding different variables.

3.3.2 How Thrombin affects PRP?

It was investigated whether the effect of thrombin, the strongest physiological activator of platelets, could be seen in MCF. As expected, thrombin showed a high activity and activated all platelets in the capillary, causing full aggregation.

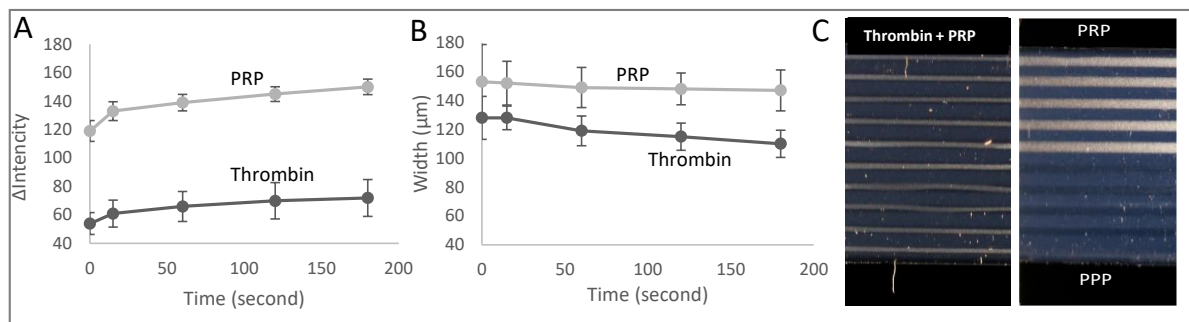


Figure 4. Demonstration of thrombin aggregation. A) Initial image analyse allow to see scatter intensity differences between trombin and PRP. B) Width changanges with time for thrombin and PRP. C) The image of the effect of thrombin on PRP, PRP and PPP in MCF.

A very large scatter intensity difference was evident from the onset and this difference was maintained for 3 min (Figure 4A). In addition, the compression of all platelets in one side with full aggregation also caused a clear width thickness difference in the canal compared to PRP (Figure 4B).

The time-dependent scatter intensity change rate remained unchanged for 3 min, which we think is an effect of the high concentration of thrombin used, because a higher concentration was used than the thrombin concentration used in the aggregometer to observe the rapid reaction in the microfluidic. However, the big difference from the beginning shows us the thrombin effect clearly. If we look at the thickness of the aggregation formed within the capillary, the complex formed by the effect of thrombin occupied 85% ($\sim 170\mu$ M) of the volume of the capillary, while it shrank to 75% ($\sim 150\mu$ M) at the end of 3 minutes. This

showed us that the activity of thrombin continues during the first 3 minutes. We found ADP and thrombin loaded in capillaries dramatically changed the appearance of the platelets.

CONCLUSION

Although platelets are critical importance as they are the first element involved in primary haemostasis, methods for aggregation detection are limited. In addition to the high cost of the classical aggregometer and the high volume of sample needed, its information for clinical testing is also very limited. The biggest problem with traditional aggregometry is that it is a rough way to measure platelet activation. Essentially, what is done is to shine a light on a platelet cuvette and only see how much the platelets reduce the light intensity. In fact, the information to be obtained about aggregation is also limited. To overcome these disadvantages, we have developed a simpler, more applicable darkfield imaging system (Dark-Pi) that combined with a microfluidic device which can get more information about platelets aggregation. After different concentrations of agonists were dried in the microfluidic capillary and immersed in the platelet sample, they were photographed using an inexpensive open-source darkfield imaging system. Samples can be analysed based on their light scattering properties and aggregation and accurate aggregation concentration can be determined, in this way, it was proved that, platelet detection in a suspension and the effects of agonists on platelets can be determined depending on the light scattering intensity. Thus, we not only report a simple method to evaluate platelets, but also have the opportunity to examine the effects of the agonist on a particle basis. We hypothesise that this system will have a profound impact and advance on research on platelet aggregation and functions in the future. Apart from clear differences in appearance indicating platelet activation had taken place, it was not straightforward to extract quantitative measures of platelet activation. While capturing high-quality and time-lapse images of platelets with the darkfield imaging system, it also enabled us to measure time-dependent changes in PRP based on light scattering at the particulate level and in real time unlike standard aggregometry, which is based on light transmission and gives a bulky measurement. In contrast to bacteria where changes in intensity corresponded to bacterial cell density, alterations in light scatter following stimulation required a different image analysis. While the transmission method is the gold standard for platelets measurement, the fact that the method we developed is based on light scattering requires its optimization and standardization for each test in accordance with the

purpose to be used for end users. Further work should focus on optimisation and better extraction of changes in appearance.

ACKNOWLEDGEMENTS

We thank the Turkish Ministry of National Education, Republic of Turkey for Postgraduate Study Abroad Program to support Sultan İlayda Dönmez and Ruya Meltem Sariyer. This project was partially funded by Engineering and Physical Science Research Council (EPSRC) grants EP/R022410/1 and EP/S010807/1.

REFERENCES

- Abràmoff, M. D., P. J. Magalhães and S. J. Ram (2004). "Image processing with ImageJ." Biophotonics international **11**(7): 36-42.
- Alessi, M.-C., P. Sié and B. Payrastre (2020). "Strengths and Weaknesses of Light Transmission Aggregometry in Diagnosing Hereditary Platelet Function Disorders." Journal of clinical medicine **9**(3): 763.
- Born, G. V. R. (1962). "Aggregation of Blood Platelets by Adenosine Diphosphate and its Reversal." Nature **194**(4832): 927-929.
- Cattaneo, M., C. Cerletti, P. Harrison, C. P. M. Hayward, D. Kenny, D. Nugent, P. Nurden, A. K. Rao, A. H. Schmaier, S. P. Watson, F. Lussana, M. T. Pugliano and A. D. Michelson (2013). "Recommendations for the standardization of light transmission aggregometry: a consensus of the working party from the platelet physiology subcommittee of SSC/ISTH." Journal of Thrombosis and Haemostasis **11**(6): 1183-1189.
- Chan, M. V., P. C. Armstrong and T. D. Warner (2018). "96-well plate-based aggregometry." Platelets **29**(7): 650-655.
- Dönmez, S. İ., S. H. Needs, H. M. I. Osborn and A. D. Edwards (2020). "Label-free smartphone quantitation of bacteria by darkfield imaging of light scattering in fluoropolymer micro capillary film allows portable detection of bacteriophage lysis." Sensors and Actuators B: Chemical **323**: 128645.
- Favaloro, E. J. (2019). "Novel approaches to quality control and external quality assessment for platelet function testing with a focus on the platelet function analyser (PFA-100 and PFA-200)." Annals of Blood **4**.
- Gianazza, E., M. Brioschi, R. Baetta, A. Mallia, C. Banfi and E. Tremoli (2020). "Platelets in Healthy and Disease States: From Biomarkers Discovery to Drug Targets Identification by Proteomics." International journal of molecular sciences **21**(12): 4541.
- Gorog, D. A. and R. C. Becker (2021). "Point-of-care platelet function tests: relevance to arterial thrombosis and opportunities for improvement." Journal of thrombosis and thrombolysis **51**(1): 1-11.
- Gorog, D. A. and Y. H. Jeong (2015). "Platelet function tests: why they fail to guide personalized antithrombotic medication." Journal of the American Heart Association **4**(5): e002094.
- Harrison, P., I. Mackie, A. Mumford, C. Briggs, R. Liesner, M. Winter, S. Machin and B. C. f. S. i. Haematology (2011). "Guidelines for the laboratory investigation of heritable disorders of platelet function." British journal of haematology **155**(1): 30-44.
- Jurk, K. and B. E. Kehrel (2005). "Platelets: physiology and biochemistry." Semin Thromb Hemost **31**(4): 381-392.
- O'brien, J. (1961). "The adhesiveness of native platelets and its prevention." Journal of clinical pathology **14**(2): 140-149.

Paniccia, R., R. Priora, A. A. Liotta and R. Abbate (2015). "Platelet function tests: a comparative review." Vasc Health Risk Manag **11**: 133-148.

Paniccia, R., R. Priora, A. A. Liotta and R. Abbate (2015). "Platelet function tests: a comparative review." Vascular health and risk management **11**: 133-148.

Podda, G., E. A. Femia, M. Pugliano and M. Cattaneo (2012). "Congenital defects of platelet function." Platelets **23**(7): 552-563.

Sang, Y., M. Roest, B. de Laat, P. G. de Groot and D. Huskens (2021). "Interplay between platelets and coagulation." Blood Rev **46**: 100733.

Tsoupras, A., I. Zabetakis and R. Lordan (2019). "Platelet aggregometry assay for evaluating the effects of platelet agonists and antiplatelet compounds on platelet function in vitro." MethodsX **6**: 63-70.

Vinholt, P. J., M. Nybo, C. B. Nielsen and A. M. Hvas (2017). "Light transmission aggregometry using pre-coated microtiter plates and a Victor X5 plate reader." PLoS One **12**(10): e0185675.

Zhou, L. and A. H. Schmaier (2005). "Platelet aggregation testing in platelet-rich plasma: description of procedures with the aim to develop standards in the field." American journal of clinical pathology **123**(2): 172-183.

Chapter 6

General Discussion

6. Summary of the research

In this thesis, studies focusing on phage lysis and enumeration using microfluidic systems are presented to overcome the shortcomings of traditional phage handling methods. A compact, accurate, fast, simple, inexpensive and label-free way of counting colonies and plaques in liquid media, has been introduced for the first time in the literature. The system we have designed can replace 140-year-old agar petri dishes for the detection, formulation and production of phage required in POC testing and bacteriophage therapy. In this section, the important points of the doctoral thesis are summarized and critically examined. After emphasizing the use and importance of bacteriophages; biocontrol of phages on food products, therapeutic use of phages and phage-based commercial detection systems are discussed, and the advantages and disadvantages of our system are summarized.

6.1. Critical evaluation of the present studies

About 50 million people are diagnosed with sepsis every year, and 11 million die because of the difficulty of early diagnosis and treatment (Reinhart, Daniels et al. 2017). In addition, undiagnosed patients can cause the spread of the disease. At this point, early diagnosis can both increase the effectiveness of treatments and eliminate long-term risks for infected patients. A core outcome from this study was the ability to detect lytic fragmentation of the target bacteria in MCF using lytic bacteriophages. This method could be used as a companion diagnostic for bacteriophage therapy to detect host specificity for treatment of bacterial infections. To achieve this, it was shown that phage lysis could be measured using smartphone label-free detection. As in other systems based on lytic degradation (Vaidya, Ravindranath et al. 2020), the underpinning principle is that the growth rate of bacteriophages is much faster than that of bacteria and is based on the lytic degradation of target cells of phages. When the initial bacterial concentration is low, pre-amplification is usually required because phages can remove small numbers of bacteria before they are detected and without allowing them to multiply. so wrong results can be obtained. Hence, after MCF was coated with bacteriophage, the high or low concentration of the bacterial sample did not change the effect of the bacteriophage, because bacteria with low concentration can be detected at the starting point and more detailed results are obtained in the system that allows for a large number of samples and concentrations. Experiments were performed to determine whether the phage can affect the growth of bacteria at a low cell density, and secondly, to show that the bacteriophage can still illuminate the host

cell when high cell density is present. In both cases the bacteriophage showed a lytic effect on the sample during the same period (4.5 h), thus, unlike other methods (Yang, Wisuthiphaet et al. 2020), there is no need for a pre-enrichment process such as 5 hours. In another experiment with bacteriophages, the phage T2 was able to affect only the host *E. coli* B strain but did not have a lytic effect on *E. coli* 25922, thus, host specificity of phages was shown in MCF. The reason for the therapeutic use of the phages is that they are highly specific to the hosts compared to antibiotics and usually affect a single species or even bacterial subspecies. For this reason, it is important to determine the host specificity of the hosts targeting the desired bacterial group. Thus, we show that we can detect host specificity sensitively in our system and that the system can contribute to early pathogen detection in the future. Notably, in this experiment a starting cell density of 0.3 OD was used which is clearly visible using darkfield illumination; after a 4.5-hour incubation period, complete lysis was clearly detected showing for the first-time bacteriophage lysis within MCF microdevices. At this point, the phage concentration can be increased to reduce the incubation time, further reducing the shortened test time. High phage concentration can detect host cell in less than 4.5 hours and can further the results we obtained in the study. Thus, classical test methods that take days can result in a few hours and at the same time offer use in many areas.

6.1.1. Benefits of darkfield microfluidic imaging system design and maximising signal

In Chapter 3, a method to detect bacteria by “label-free” light scattering imaging in MCF, that allows smartphone detection of bacterial cells without addition of dye or reagent, is described for the first time. Light scattering from bacterial cells for dye-free detection was measured by darkfield imaging. Whilst darkfield illumination at its simplest comprises a dark background shielded from light source, plus illumination of the microfluidic device anywhere except behind the imaging plane, initial tests identified that label-free bacterial measurement is only possible with careful design of illumination geometry. The two biggest barriers in detecting bacterial scatter were increasing signal whilst avoiding bright reflections, -termed glare-, from the surroundings. The signal was very weak from side or back scatter with epi-illumination. Glare from barriers, the microfluidic device holder, the MCF test strip itself or direct camera illumination by the LED were minimalized by blockers. Recent experiments suggest this is likely to be due to weak light scattering at high angles used in this experimental setup, with clear evidence of light scattering visible when samples were illuminated with a light source

behind the MCF. Only the smartphone camera and LED light source are needed to measure bacterial concentration without fluorescence or colorimetric dye, and with tiny sample volumes. Thus, widespread use of the test can be achieved without using the label, which is not widely available and sometimes requires extra steps. Also, as it requires very little sample volume of a few microliters, there is no need for sample augmentation and pathogen detection with high specificity can be achieved even when large volumes of sample cannot be obtained from the patient.

Having identified a darkfield imaging geometry where bacterial light scattering could be robustly detected, it was necessary to establish the optimal conditions for measuring bacterial concentration and establish a suitable image analysis method for consistent quantitation of scatter. The most important parameter was found to be the illumination angle, with bacterial scatter within microfluidic devices a major source of background glare. In this system, digital camera and phone camera were compared to examine the importance of camera quality. When looking at the image taken by phone, it was remarkable that the background was too bright. With digital camera, background glare was avoided because aperture, ISO and exposure can be set, but with a phone and automatic imaging the background density was high because all these were automatically selected in the phone camera. Although the background had high glare, the scatter intensity which differs between bacteria and capillaries was distinguishing. Thus, it has been proven that bacterial detection can be performed using a mobile phone in this system. Thus, with smartphones available to a very large majority, our system provides a great advantage to work in the field for POCTs and biosensors, increasing the usability and accessibility of the systems and can be adapted to different systems for various applications such as home care services, unmanned systems.

In Chapter 4, we replaced smartphone imaging of darkfield bacteria measurement in microfluidics with an open-source sensor system, exploiting the computing and imaging power of the Raspberry Pi HQ camera equipped with a macro lens to gather quantitative data. Addition of a switched LED power supply permitted programmable illumination- for example allowing future customisation to combine darkfield, brightfield and fluorescence illumination. As each strip draws up 10 samples each of around 0.4 microlitres in the visible section of microcapillaries, the system senses bacterial growth within up to 80 microdevices in parallel. this paves the way for detecting and analyzing large numbers of samples simultaneously, as well as for more precise measurements. In Chapter 5, a modified version of the system with the similar system setup and high-resolution lens to analyse platelet detection and aggregation.

In Chapter 5, a modified version of the system with similar system setup and high-resolution lens was used to analyze platelet detection and aggregation. At this point there are factors that affect the camera distance, these are the balance between the quality of the readout, the image resolution and the sample number. It was possible to obtain a more detailed image of sample of platelets by zooming in the MCF. A distinctly different appearance was obtained from platelets than from bacteria. Bacterial concentrations appeared more uniform, while platelets were observed as more particles. In order to obtain platelets from the blood, some separation and centrifugation processes are required, so it is possible for the platelets, to adhere to each other, interact, and show a more heterogeneous distribution in the MCF (Chapter 5, Figure 2 B). However, it is normal for bacteria grown directly in liquid media to appear more homogeneously dispersed compared to platelets (Dönmez, Needs et al. 2020). Thus, we have shown that we can see different cell types in our system, but their appearance/light distribution may be different.

6.1.2. Individual colony counting in liquid media in MCF

Counting bacteriophage plaques or bacterial colonies on the surface of solid media agar is still a mainstay in most microbiology labs. However, especially for the DAL method used for phage enumeration, it is important to adjust the temperature of the molten agar in which the bacteria will be suspended. If the temperature is not optimal, it can kill the host bacteria, and uniform distribution in the petri dish will not occur (Cormier and Janes 2014). We have introduced and demonstrated the concept of 1D microfluidic colony and plaque counting. Growing bacteria or phage plus host in static capillaries allows optical visualisation of colonies and plaques in liquid media, permitting faster readout and increased usability. Thus, studies that used to take days with traditional methods have been reduced to a few hours with this approach. The liquid culture for colony and plaque counting system, which demonstrates a novel and effective way to make use of miniaturisation to speed up and simplify analytical microbiology, has the potential to provide significant impact from research to various detection and diagnostic studies and clinical microbiology.

In recent years, portable bacterial detection systems have been developed using various output signals like fluorescence and luminescence (Shin, Gutierrez-Wing et al. 2020, Gopal, Yan et al. 2022). Label-free bacterial detection is especially valuable for the detection of bacterial lysis by phage. This cannot be easily monitored using metabolic growth dyes because the dye is

likely to be converted by bacteria before lysis. Previously at high phage concentrations, we were able to use lytic degradation of target bacteria as a microfluidic method to determine host specificity, but it was challenging to enumerate phage (Levin and Angert 2015). In Chapter 4 we expand the method to detect single bacteriophage plaque-forming units. Importantly, we found the 1D microcapillary counts to be equal to conventional plate counts, for two important microbial species and for bacteriophage that lyse each of these species. In order to detect bacteria, at least one colony must be visible, with an absolute lower limit of detection of one colony/ 4 μ L which is 250 CFU/mL. Likewise, a single plaque corresponds to 250 PFU/mL. For accurate concentration determination, counting more than one colony or phage plaque is important. Surprisingly, we found smaller sample-to-sample error with replicates with the 1D microcapillary counts than with agar plating (The relationship between the two counting methods is 1:1). Thus, we show that our system is comparable to traditional methods and is as reliable as conventional methods.

The ability to use liquid medium and “dip-to-test strips” for colony counting and especially for bacteriophage counting offers benefits over conventional agar/soft agar plating firstly by using simpler methodology reducing the skill in preparation. Of particular note, the double layer agar (DAL) for phage counting involves suspending host bacteria in warm agar, requiring care to ensure even seeding at the same time as avoiding killing host bacteria if the temperature of the melted agar is not optimal. Secondly, through miniaturisation, it is possible to avoid the need for an incubator, storage space for large stacks of petri dishes, and refrigerated storage of prepared agar plates. Furthermore, addition of timelapse capability allows the development of automated image capture and analysis of more samples than traditional methods. Counting within 1D microcapillaries also significantly reduced the time needed to count CFU or PFU to between 5-9 h, from typical overnight timepoints used for agar plate colony counts. By permitting simple and fast counting of individual colonies or plaques, grown from single cells or viral particles, we achieved a lower limit of detection approaching 250 CFU or PFU. This could be reduced further by using more test strips or imaging longer capillary sections.

6.1.2.1. Kinetics of bacterial colony growth in microcapillaries

A limitation of the current method is that it was far less effective with motile organisms that could spread rapidly along the capillary, preventing clear colony or plaque detection. The inclusion of low concentration of agar in the sample medium did inhibit this spread but also reduced the simplicity of the test. It remains important therefore to develop better methods of delaying or inhibiting the spread of motile organisms within the microcapillaries, for example by substituting alternative hydrogel-forming polymers, or incorporating such polymers inside the hydrophilic coated capillaries. Even with motile *E. coli* 25922, the use of time-lapse imaging did permit initial foci of growth to be transiently detected, illustrating the advantage of sensing reader over a single endpoint image. Using timelapse analysis with the darkfield sensor system, we were able to estimate initial growth in cell density at the start of colony formation. This was then followed with monitoring expansion in a second phase of linear colony growth along the capillary. In particular, this provided insight that modelling nutrient diffusion kinetics might explain an apparent discrepancy with initially slower-growing *S. aureus* colonies expanding faster than rapidly growing *E. coli* (1.5 μm) (Levin and Angert 2015). *S. aureus* (1 μm) are smaller and the same cell concentrations scatter less (Wilson and Vigil 2013) which may be responsible for some of the differences in colony appearance. It is also possible that growth rates within capillary microdevices could be different for bacteria strains, in addition media difference could be effect growth rate of strains. Further studies allowing more detailed comparison of varying capillary dimensions, media composition, and oxygen permeation rates are needed to understand this effect. Cell growth will be followed with different capillary sizes (270, 200, 160 μm) but with the same cell concentrations, and then the growth rates of different bacterial strains will be examined with media using different media components. Since both ends of the capillaries are blocked with silicone caps to prevent dehydration of the medium during the experiment, we also have an ongoing study on how the growth profile of an oxygen obligate bacteria in our system will be to investigate how this system will expand for aerobic bacteria.

While bacterial colonies for rapidly dividing *E. coli* strains on solid agar media can be visualised in as little as 7 hours (Needs, Diep et al. 2019), these systems tend to be low-throughput and rarely is kinetic data collected due to the size of petri dishes. However, some studies have examined the kinetics of solid agar colony growth of organisms such as *S. aureus* (Bär, Boumasmoud et al. 2020), *Vibrio* spp (Huff, Aroonual et al. 2012), *E. coli*, *Klebsiella aerogenes*, and *Klebsiella pneumoniae* (Wang, Ceylan Koydemir et al. 2020) by time-lapse

imaging of petri dishes. The different imaging systems used are designed to examine petri dishes but can often only examine one petri dish at a time, the biggest limitation of this is the increase in test times and may need many the manual steps. Previously, we have reported that bacteria are segregated into the microcapillary test strips following a Poisson distribution (Needs, Osborn et al. 2021). In this method, resazurin, a bacterial metabolic reporter, was used to measure colour change in the entire capillary, resulting in fewer measurable ‘compartments’ per test strip (Wang, Ceylan Koydemir et al. 2020). Unlike other methods, our label free, light scattering sensor method can distinguish between multiple colonies per capillary.

6.1.3. Sensitivity of measurements are enhanced following sedimentation within capillaries

Sedimentation experiments demonstrated that bacteria and platelets settle within the capillaries over 30 minutes, increasing the intensity of the signal but reducing the line width. Although the concentration of samples did not change, bacteria and platelets that settled into the bottom base of the capillaries increased the intensity of light scattering. For the bacteria at starting time, the lowest bacterial concentration that can be measured at was OD 0.34, but even after 30 minutes it decreased to OD 0.1. Thus, the sensitivity of the system increased from $\sim 10^5$ cells/capillary to $\sim 10^4$ cells/capillary. This shows that bacteria can be observed and measured without the use of complex imaging system with cheaply available white LED light. With time, the system sensitivity is increasing. On the other hand, the growth curves of the bacteria determined using the spectrophotometer and MCF were measured and these showed similarity, showing that the measurements are comparable and label-free growth kinetics can be measured in microfluidics.

6.2. Future Perspectives

6.2.1. Phage-based products approved as biocontrol agents in food

Due to bacterial contamination, the food industry loses one-fourth of the food produced each year (Rai 2011). With the popularity of phage systems and applications, and the increase in AMR, many companies, especially in the food and agriculture field, are investing in phage-based products as biocontrol agents. Non-chemical antimicrobial preparation of phages is also used to overcome bacterial contamination both before and after harvest and during food production and storage. Thus, while ensuring the protection of harvests and foods in a cheaper, safer way, the number and range of FDA-approved phage-based products that are used directly on processed and packaged products have also increased (Table 6.1). Companies such as Intralytix, Omnilytics, Microcos FoodSafety, FINK TEC, Passport FoodSafetySolutions, APS BiocontrolLtd, Elanco, Phagelux have produced many lytic phage-based products for the main food pathogens such as *E. coli*, *Salmonella*, *Pseudomonas*, *L. monocytogenes*, *Shigella spp*, *Xanthomonas campestris* (Li, Zhao et al. 2022). In 2006, the first phage-based FDA-approved product was released, as phages were deemed safe for *Listeria* control. The increase in research institutes and companies participating in phage research significantly increases the future of phage-based products in the food industry (Li, Zhao et al. 2022). In the preparation of phage-based biocontrol products, strictly lytic phages have been used and shown to be effective. At the same time, phage cocktails were preferred in order to maximize the possible number of the target bacterial strains. Our system, which can detect lytic phage activity simply and quickly compared to traditional methods, has a high potential to be integrated into food biocontrol studies with its ability to work with many samples simultaneously.

Table 6.1. FDA-approved phage products for biological control

Product Name	Target	Used Phages	Application	Implementation	References
ECOShield PX™	<i>E. coli</i> O157:H7	3 <i>E. coli</i> O157:H7-specific lytic bacteriophages	contamination on surfaces and various foods	directly on food surfaces by spraying	(Carter, Parks et al. 2012)
ListShield™	<i>L. monocytogenes</i>	cocktail of 6 lytic bacteriophages	contamination on surfaces and various foods	directly on food surfaces by spraying	(Perera, Abuladze et al. 2015)
Listex P-100™	<i>L. monocytogenes</i>	<i>Listeria</i> phages	fish, meat and dairy	on line dipping / immersion / spray	(Chibeu, Agius et al. 2013)
SalmoFresh™	<i>Salmonella</i>	6 lytic phages	contamination on surfaces and various foods	directly on surfaces by spraying	(Zhang, Niu et al. 2019)
Salmonex™	<i>Salmonella</i>	2 lytic phages S16 and FO1a	contamination on surfaces and various foods	directly on surfaces by spraying	(Maciel, Campos et al. 2021)
PhageGuard S	<i>Salmonella</i>	2 lytic phages (Fo1a and S16)	food products	directly add or spray	(Sirdesai, Eraclio et al. 2018)
PhageGuard E	<i>E. coli</i> O157:H7	2 lytic phages (EP75 and EP335)	food products	directly add or spray	(Shebs, Lukov et al. 2020)
Agriphage™	<i>Xanthomonas campestris</i> pv. <i>Vesicatoria</i> , <i>Pseudomonas syringae</i> pv. <i>tomato</i>	lytic phage cocktail	tomato and Peppers	directly on crop surfaces by spraying	(Ingram and Lu 2009)
SalmoLyse®	<i>Salmonella enterica</i>	lytic phage cocktail	in pet food	directly on surfaces by spraying	(Soffer, Abuladze et al. 2016)
Ecolicide™	<i>E. coli</i> O157:H7	lytic phage cocktail	in pet food	directly on surfaces by spraying	(Moye, Woolston et al. 2018)
Finalyse SAL™	<i>Salmonella enterica</i>	lytic phage cocktail	poultry products	on line dipping	(Cristobal-Cueto, García-Quintanilla et al. 2021)
ShigaShield™ (ShigActive™)	<i>Shigella</i> spp.	5 lytic <i>Shigella</i> bacteriophages	ready-to-eat meat and poultry, fish, fresh and processed fruits and vegetables, and dairy products	directly on surfaces by spraying	(Soffer, Abuladze et al. 2016)

6.2.2. Phages as therapeutics

Bacterial resistance is not only limited to foods but is also a major problem with human infections. There are dozens of life-saving phage therapy studies for patients who cannot be treated with antibiotics in many parts of the world, but no FDA-approved product is available on the market yet, although FDA approved the use of phages for food in 2006 (Sarhan and Azzazy 2015, Furfaro, Payne et al. 2018). The most likely reasons for this may be that there are many factors that influence the success of clinical trials because phage therapy must be specific to each patient, for example, selection of suitable phages, formulations, dosing, and adequate characterization of target bacteria for patients. Another situation is the insufficiency of a single phage in infections caused by more than one pathogen. In this case, polymicrobial infections can be combated with phage cocktails or phage+antibiotic combinations (Suh, Lodise et al. 2022).

In one interesting study to prove that bacteriophages do not harm humans and can be used directly for treatment, *E. coli* T4 bacteriophage was given orally to 15 people for 30 days and no toxic effects were reported. However, there is not yet a long-term study of the potential detrimental effects of phages on human health (Bruttin and Brüssow 2005).

In addition, the FDA recently granted approval to Adaptive Phage Therapeutics for a personalized study of phage-based drugs for multi-drug resistance (MDR) infections. The study will focus on 165 patients with chronic urinary tract infections (UTI) and key UTI pathogens such as *E. coli* and *K. pneumoniae*. This clinical trial has started in 2021 and a first interim data analysis is expected in 2022 (Voelker 2019). Thus, the FDA has taken a major step forward in paving the way for phage therapy, and it is very likely that we might see possible phage-based drugs in the near future. Thus, we think that the system we designed has the potential to be used for many phage-based drug studies in the future, such as determining the host specificity, determining the phage dose, and enumeration of phage and bacteria.

6.2.3. Phage-based detection and future direction

Phage-based diagnostics can be adapted to a variety of applications. Along with the increase in phage-based studies such as biocontrol, phage-based diagnostic research studies are increasing. However, few commercial products are available that have made it into a clinical diagnostic tool (Table 6.2). At this point, the shortcomings of these methods can be grouped under three main areas. 1) cost 2) incubation time 3) sensitivity limit. The advantage of the MCF used in this thesis is that it is much cheaper than its competitors (10 microliter volume - 20p), while commercially available microfluidics are generally more expensive. As this directly increases the final test price. For this reason, although microfluidics are used in many research studies, they have found less use in practical application than expected. Secondly, there is still need an incubation time for the lysis effect. Although the process does not take days as in traditional methods, it is still difficult to diagnose for suitable phages in a very short time, requiring costly extra steps (modified phages, fluorescent dyes, etc.). Finally, and most importantly, the sensitivity limit of the tests plays a critical role. Especially in studies to be performed with clinical samples such as blood, urine, sputum, even if the patient shows symptoms, the bacterial load in the sample may be below the sensitivity limit of the test (Schofield, Sharp et al. 2012). This difficulty can be solved by increasing the MCF area in the darffield system, for example, if the total sample volume is increased from 4 μL to 10 μL , the detection sensitivity will increase from 2.5×10^2 to 10^2 CFU/mL. However, other microfluidic detection methods can increase their sensitivity by adding side processes or modifications such as luciferase, immunoassay amplification, GFP, β -galactosidase to overcome this difficulty. Darkfield scattering is just one of many bioassays that can be adapted for portable measurements using the latest digital imaging technology, and other opportunities are covered in more detail in Chapter 2.

Table 6.2. FDA-approved or commercially available phage-based pathogen detection products

Product Name	Target	Used Phages	Sample	Detection time	References
Microphage Keypath™	<i>S. aureus</i>	Phage cocktail	blood	5 h	(Bhowmick, Mirrett et al. 2013)
FastPlaqueT B	<i>M. tuberculosis</i>	bacteriophage D29	sputum	48 h	(Muzaffar, Batool et al. 2002)
PhageTek MB	<i>M. tuberculosis</i>	Mycobacteriophage	sputum specimens, bronchial or tracheal aspirate specimens, bronchoalveolar lavage specimens, transthoracic aspirate specimen	48 h	(Alcaide, Galí et al. 2003)
Bronx Box	<i>M. tuberculosis</i>	Luciferase Reporter Phage phAE85	25 <i>M. tuberculosis</i> reference and clinical strains	30 h	(Riska, Su et al. 1999)
Gamma phage assay	<i>B. anthracis</i>	γ phage	51 <i>B. anthracis</i> strains and 49 similar non- <i>B. anthracis</i> Bacillus species	6-8 h	(Abshire, Brown et al. 2005)
VIDAS® UP Salmonella	<i>Salmonella</i>	recombinant phage proteins	human food products and environmental samples	less than 24 h	(Bird, Fisher et al. 2013)
VIDAS® UP Listeria	<i>Listeria</i>	recombinant phage proteins	human food products and environmental samples	less than 24 h	(Crowley, Bird et al. 2019)
VIDAS® UP E. coli O157	<i>E. coli O157</i>	recombinant phage proteins	human food products and environmental samples	less than 24 h	(Incili, Koluman et al. 2019)

In general, the 1D liquid culture concept developed for colony and plaque enumeration demonstrates a new and efficient way of using miniaturization to speed up and simplify analytical microbiology compared to agar-based culture methods. Considering the advantages mentioned above, our system has the potential to be adapted to a variety of applications for phage-based detection and phage-based diagnostics.

Chapter 6 References

- Abshire, T. G., J. E. Brown and J. W. Ezzell (2005). "Production and Validation of the Use of Gamma Phage for Identification of *Bacillus anthracis*." Journal of Clinical Microbiology **43**(9): 4780-4788.
- Alcaide, F., N. Galí, J. Domínguez, P. Berlanga, S. Blanco, P. Orús and R. Martín (2003). "Usefulness of a new mycobacteriophage-based technique for rapid diagnosis of pulmonary tuberculosis." Journal of clinical microbiology **41**(7): 2867-2871.
- Bär, J., M. Boumasmoud, R. D. Kouyos, A. S. Zinkernagel and C. Vulin (2020). "Efficient microbial colony growth dynamics quantification with ColTapp, an automated image analysis application." Scientific Reports **10**(1): 16084.
- Bhowmick, T., S. Mirrett, L. B. Reller, C. Price, C. Qi, M. P. Weinstein and T. J. Kim (2013). "Controlled Multicenter Evaluation of a Bacteriophage-Based Method for Rapid Detection of *Staphylococcus aureus* in Positive Blood Cultures." Journal of Clinical Microbiology **51**(4): 1226-1230.
- Bird, P., K. Fisher, M. Boyle, T. Huffman, M. Juenger, M. J. Benzinger, Jr., P. Bedinghaus, J. Flannery, E. Crowley, J. Agin, D. Goins and R. L. Johnson (2013). "Evaluation of VIDAS UP Salmonella (SPT) assay for the detection of Salmonella in a variety of foods and environmental samples: collaborative study." J AOAC Int **96**(4): 808-821.
- Bruttin, A. and H. Brüssow (2005). "Human volunteers receiving *Escherichia coli* phage T4 orally: a safety test of phage therapy." Antimicrobial agents and chemotherapy **49**(7): 2874-2878.
- Carter, C. D., A. Parks, T. Abuladze, M. Li, J. Woolston, J. Magnone, A. Senecal, A. M. Kropinski and A. Sulakvelidze (2012). "Bacteriophage cocktail significantly reduces *Escherichia coli* O157." Bacteriophage **2**(3): 178-185.
- Chibeu, A., L. Agius, A. Gao, P. M. Sabour, A. M. Kropinski and S. Balamurugan (2013). "Efficacy of bacteriophage LISTEXTMP100 combined with chemical antimicrobials in reducing *Listeria monocytogenes* in cooked turkey and roast beef." Int J Food Microbiol **167**(2): 208-214.
- Cormier, J. and M. Janes (2014). "A double layer plaque assay using spread plate technique for enumeration of bacteriophage MS2." Journal of virological methods **196**: 86-92.
- Cristobal-Cueto, P., A. García-Quintanilla, J. Esteban and M. García-Quintanilla (2021). "Phages in Food Industry Biocontrol and Bioremediation." Antibiotics **10**(7): 786.
- Crowley, E., P. Bird, J. Flannery, J. Benzinger, M. Joseph, K. Fisher, M. Boyle, T. Huffman, B. Bastin, P. Bedinghaus, W. Judd, T. Hoang, J. Agin, D. Goins, R. L. Johnson and Collaborators: (2019). "Evaluation of VIDAS[®] UP *Listeria* Assay (LPT) for the Detection of *Listeria* in a Variety of Foods and Environmental Surfaces: First Action 2013.10." Journal of AOAC INTERNATIONAL **97**(2): 431-441.
- Furfaro, L. L., M. S. Payne and B. J. Chang (2018). "Bacteriophage Therapy: Clinical Trials and Regulatory Hurdles." Frontiers in Cellular and Infection Microbiology **8**.
- Gopal, A., L. Yan, S. Kashif, T. Munshi, V. A. L. Roy, N. H. Voelcker and X. Chen (2022). "Biosensors and Point-of-Care Devices for Bacterial Detection: Rapid Diagnostics Informing Antibiotic Therapy." Advanced Healthcare Materials **11**(3): 2101546.
- Huff, K., A. Aroonual, A. E. F. Littlejohn, B. Rajwa, E. Bae, P. P. Banada, V. Patsekina, E. D. Hirleman, J. P. Robinson, G. P. Richards and A. K. Bhunia (2012). "Light-scattering sensor for real-time identification of *Vibrio parahaemolyticus*, *Vibrio vulnificus* and *Vibrio cholerae* colonies on solid agar plate." Microbial Biotechnology **5**(5): 607-620.
- Incili, G. K., A. Koluman, A. Aktüre and A. Ataşalan (2019). "Validation and verification of LAMP, ISO, and VIDAS UP methods for detection of *Escherichia coli* O157:H7 in different food matrices." Journal of Microbiological Methods **165**: 105697.
- Ingram, D. M. and S.-E. Lu (2009). "Evaluation of Foliar Sprays of Bacteriophages for the Management of Bacterial Canker in Greenhouse Tomatoes." Plant Health Progress **10**(1): 19.
- Levin, P. A. and E. R. Angert (2015). "Small but Mighty: Cell Size and Bacteria." Cold Spring Harbor perspectives in biology **7**(7): a019216-a019216.
- Li, J., F. Zhao, W. Zhan, Z. Li, L. Zou and Q. Zhao (2022). "Challenges for the application of bacteriophages as effective antibacterial agents in the food industry." Journal of the Science of Food

and Agriculture **102**(2): 461-471.

Maciel, C., A. Campos, N. Komora, C. A. Pinto, R. Fernandes, J. A. Saraiva and P. Teixeira (2021). "Impact of high hydrostatic pressure on the stability of lytic bacteriophages cocktail Salmonex™ towards potential application on Salmonella inactivation." LWT **151**: 112108.

Moye, Z. D., J. Woolston and A. Sulakvelidze (2018). "Bacteriophage Applications for Food Production and Processing." Viruses **10**(4).

Muzaffar, R., S. Batool, F. Aziz, A. Naqvi and A. Rizvi (2002). "Evaluation of the FASTPlaqueTB assay for direct detection of Mycobacterium tuberculosis in sputum specimens." Int J Tuberc Lung Dis **6**(7): 635-640.

Needs, S. H., T. T. Diep, S. P. Bull, A. Lindley-Decaire, P. Ray and A. D. Edwards (2019). "Exploiting open source 3D printer architecture for laboratory robotics to automate high-throughput time-lapse imaging for analytical microbiology." PLoS one **14**(11): e0224878.

Needs, S. H., H. M. I. Osborn and A. D. Edwards (2021). "Counting bacteria in microfluidic devices: Smartphone compatible 'dip-and-test' viable cell quantitation using resazurin amplified detection in microliter capillary arrays." J Microbiol Methods **187**: 106199.

Perera, M. N., T. Abuladze, M. Li, J. Woolston and A. Sulakvelidze (2015). "Bacteriophage cocktail significantly reduces or eliminates Listeria monocytogenes contamination on lettuce, apples, cheese, smoked salmon and frozen foods." Food Microbiol **52**: 42-48.

Rai, M. C. M. C. A. B. I. O. T. I. (2011). "Natural antimicrobials in food safety and quality." Reinhart, K., R. Daniels, N. Kissoon, F. R. Machado, R. D. Schachter and S. Finfer (2017). "Recognizing sepsis as a global health priority—a WHO resolution." New England Journal of Medicine **377**(5): 414-417.

Riska, P. F., Y. Su, S. Bardarov, L. Freundlich, G. Sarkis, G. Hatfull, C. Carrière, V. Kumar, J. Chan and W. R. Jacobs (1999). "Rapid Film-Based Determination of Antibiotic Susceptibilities of Mycobacterium tuberculosis Strains by Using a Luciferase Reporter Phage and the Bronx Box." Journal of Clinical Microbiology **37**(4): 1144-1149.

Sarhan, W. A. and H. M. Azzazy (2015). "Phage approved in food, why not as a therapeutic?" Expert Rev Anti Infect Ther **13**(1): 91-101.

Schofield, D. A., N. J. Sharp and C. Westwater (2012). "Phage-based platforms for the clinical detection of human bacterial pathogens." Bacteriophage **2**(2): 105-283.

Shebs, E. L., M. J. Lukov, F. M. Giotto, E. S. Torres and A. S. de Mello (2020). "Efficacy of bacteriophage and organic acids in decreasing STEC O157:H7 populations in beef kept under vacuum and aerobic conditions: A simulated High Event Period scenario." Meat Science **162**: 108023.

Shin, Y.-H., M. T. Gutierrez-Wing and J.-W. Choi (2020). "Recent Progress in Portable Fluorescence Sensors." Journal of the Electrochemical Society.

Sirdesai, S., G. Eraclio, R. Peterson, J. van Mierlo and B. De Vegt (2018). "Efficiency of phage intervention on salmonella kill on lean pork, pork trim and bacon." Meat and Muscle Biology **2**(2).

Soffer, N., T. Abuladze, J. Woolston, M. Li, L. F. Hanna, S. Heyse, D. Charbonneau and A. Sulakvelidze (2016). "Bacteriophages safely reduce Salmonella contamination in pet food and raw pet food ingredients." Bacteriophage **6**(3): e1220347-e1220347.

Soffer, N., T. Abuladze, J. Woolston, M. Li, L. F. Hanna, S. Heyse, D. Charbonneau and A. Sulakvelidze (2016). "Bacteriophages safely reduce Salmonella contamination in pet food and raw pet food ingredients." Bacteriophage **6**(3): e1220347.

Suh, G. A., T. P. Lodise, P. D. Tamma, J. M. Knisely, J. Alexander, S. Aslam, K. D. Barton, E. Bizzell, K. M. C. Totten, J. L. Campbell, B. K. Chan, S. A. Cunningham, K. E. Goodman, K. E. Greenwood-Quaintance, A. D. Harris, S. Hesse, A. Maresso, V. Nussenblatt, D. Pride, M. J. Rybak, Z. Sund, D. v. Duin, D. V. Tyne and R. Patel (2022). "Considerations for the Use of Phage Therapy in Clinical Practice." Antimicrobial Agents and Chemotherapy **66**(3): e02071-02021.

Vaidya, A., S. Ravindranath and U. S. Annapure (2020). "Detection and differential identification of typhoidal Salmonella using bacteriophages and resazurin." 3 Biotech **10**(5): 196-196.

Voelker, R. (2019). "FDA Approves Bacteriophage Trial." JAMA **321**(7): 638-638.

Wang, H., H. Ceylan Koydemir, Y. Qiu, B. Bai, Y. Zhang, Y. Jin, S. Tok, E. C. Yilmaz, E. Gumustekin, Y. Rivenson and A. Ozcan (2020). "Early detection and classification of live bacteria using time-lapse coherent imaging and deep learning." Light: Science & Applications **9**(1): 118.

Wilson, B. K. and G. D. Vigil (2013). "Automated bacterial identification by angle resolved dark-field imaging." Biomedical optics express **4**(9): 1692-1701.

Yang, X., N. Wisuthiphaet, G. M. Young and N. Nitin (2020). "Rapid detection of Escherichia coli using bacteriophage-induced lysis and image analysis." PLOS ONE **15**(6): e0233853.

Zhang, X., Y. D. Niu, Y. Nan, K. Stanford, R. Holley, T. McAllister and C. Narváez-Bravo (2019). "SalmoFresh™ effectiveness in controlling Salmonella on romaine lettuce, mung bean sprouts and seeds." International Journal of Food Microbiology **305**: 108250.

APPENDIX

Publications not related to the thesis but made during the PhD period.



Challenges in Microfluidic and Point-of-Care Phenotypic Antimicrobial Resistance Tests

Sarah H. Needs¹, Sultan I. Donmez¹, Stephanie P. Bull¹, Conor McQuaid², Helen M. I. Osborn¹ and Alexander D. Edwards^{1*}

¹ Reading School of Pharmacy, University of Reading, Reading, United Kingdom, ² Department of Neuroscience, University of Rochester, Rochester, NY, United States

OPEN ACCESS

Edited by:

Xavier Munoz-Berbel,
Instituto de Microelectrónica de
Barcelona (IMB-CNM, CSIC), Spain

Reviewed by:

Michael Mauk,
University of Pennsylvania,
United States
Stefano Pagliara,
University of Exeter, United Kingdom

*Correspondence:

Alexander D. Edwards
a.d.edwards@reading.ac.uk

Specialty section:

This article was submitted to
Micro- and Nanoelectromechanical
Systems,
a section of the journal
Frontiers in Mechanical Engineering

Received: 05 May 2020

Accepted: 29 July 2020

Published: 15 September 2020

Citation:

Needs SH, Donmez SI, Bull SP,
McQuaid C, Osborn HMI and
Edwards AD (2020) Challenges in
Microfluidic and Point-of-Care
Phenotypic Antimicrobial Resistance
Tests. *Front. Mech. Eng.* 6:73.
doi: 10.3389/fmech.2020.00073

To combat the threat to public health of antimicrobial resistance, there is a need for faster, more portable diagnostic tools to aid in antibiotic selection. Current methods for determining antimicrobial resistance of pathogens in clinical samples take days to result and require high levels of user input. Microfluidics offers many potential benefits, reducing time to result, user input, and allowing point of care testing. This review focuses on the challenges of developing *functional* or *phenotypic* microfluidic antimicrobial susceptibility tests; such methods complement other vital tools such as nucleic acid detection. Some of the most important challenges identified here are not unique to microfluidics but apply to most antimicrobial susceptibility testing innovations and relate to the nature of the sample being tested. For many high priority samples, mixtures of bacteria, highly variable target cell density, and the sample matrix can all affect measurements, and miniaturization can create sensitivity problems if target bacteria are dilute. Recent advances including smartphone capability, new sensors, microscopy, and a resurgence in paper microfluidics offer important opportunities for microfluidic engineering to simplify functional and phenotypic antimicrobial susceptibility testing. But the complexity of most clinical samples remains one of the biggest barriers to rapid uptake of microfluidics for antimicrobial resistance testing.

Keywords: microfluidics, antimicrobial resistance, antimicrobial susceptibility tests, smartphone, microbiology

BACKGROUND: WHY ARE ANTIBIOTIC SUSCEPTIBILITY TESTS IMPORTANT AND WHAT ARE THE LIMITATIONS OF CURRENT METHODS?

Many infectious diseases are caused by microorganisms that can be effectively treated using antibiotics. However, antimicrobial resistance (AMR) remains a global threat as pathogens become drug resistant, with estimates of 10 million deaths caused by AMR annually by 2050 (Tagliabue and Rappuoli, 2018). One key priority identified by the World Health Organization (WHO) action plan to tackle AMR is increased testing and surveillance (Mendelson and Matsoso, 2015). Laboratory tests used to determine the antimicrobial sensitivity of these organisms are called antimicrobial susceptibility tests (AST). Traditional AST include broth microdilution, to determine minimum inhibitory concentration (MIC), and disc diffusion on agar. Both methods involve the initial isolation of a bacterial colony from a clinical sample after overnight incubation on solid medium. For broth microdilution, this monomicrobial cell suspension is grown in a microtitre plate in

2-fold dilutions of target antibiotics. The MIC is described as the lowest concentration of antibiotic for which bacterial growth is not seen, and growth is usually measured by light scattering or absorbance. For disc diffusion assays a lawn of the isolated bacteria is plated onto an agar plate and filter discs containing a fixed concentration of antibiotic are placed, allowing antibiotic to diffuse into the solid medium, and the size of the zone of inhibition is measured after overnight growth. These methods have been used for over 50 years and are used both for surveillance (to identify common resistance and inform empirical treatment guidelines) and diagnostics (to select effective treatments for bacterial infections) but are not without their challenges. For example, these methods require multiple rounds of culturing the sample, isolating colonies and growth before and during testing. Time to result is more than 48 h, delivering results after the start of treatment by empirical prescription of antibiotics. Evidence has suggested that up to one fifth of antibiotics prescribed in the UK from 2013–15 were inappropriate (Smieszek et al., 2018). One such way to reduce this figure is to have better diagnostic tools to identify AMR in infections prior to start of treatment, to reduce the inappropriate or ineffective use of antibiotics.

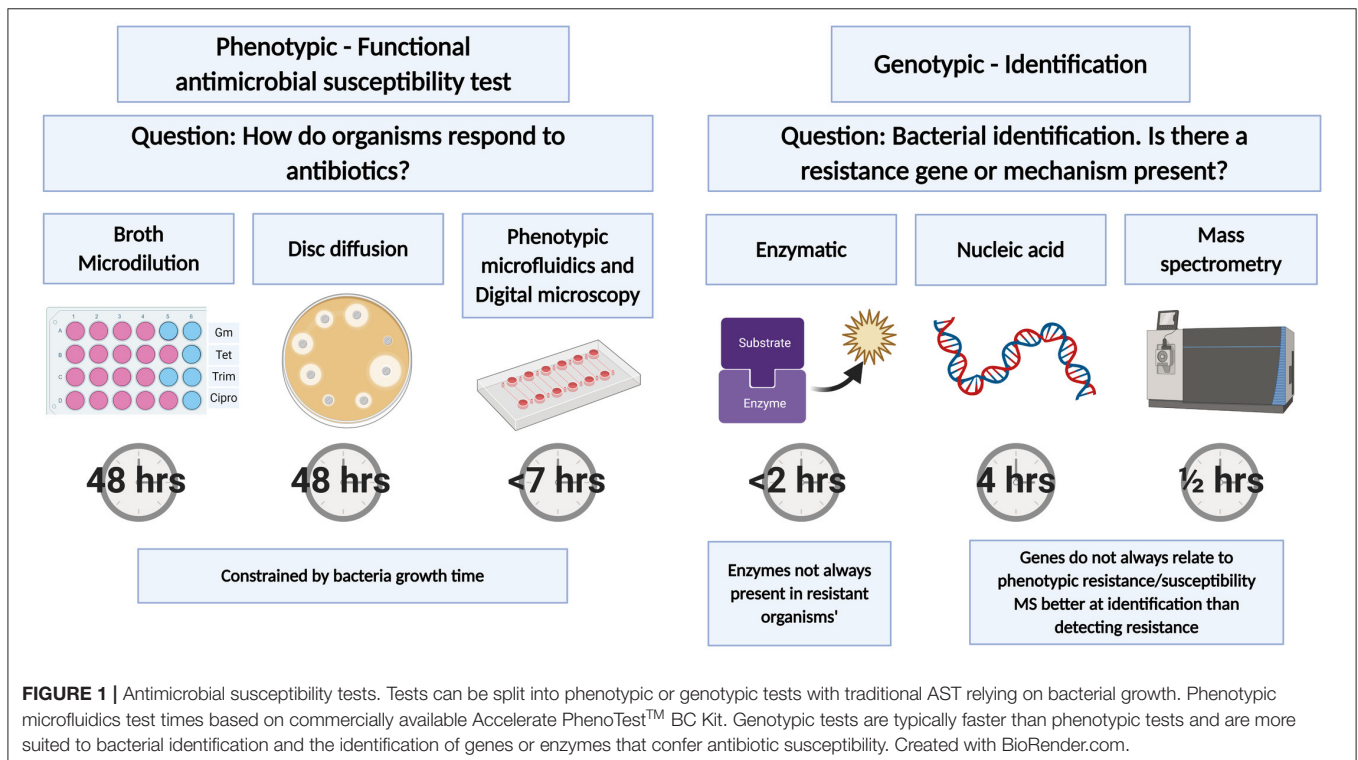
Microfluidic technologies have the potential to be faster and smaller than traditional microbiology phenotypic tests that identify bacteria and determine antimicrobial susceptibility. A number of preliminary microfluidic devices have demonstrated that time to result could be reduced to same day predictions. There are several strategies for the detection of bacteria and bacterial resistance profiles (Figure 1). This review focusses on

the challenges of implementing rapid, miniaturized *functional* or *phenotypic* measurements of antimicrobial susceptibility.

Current Conventional AST Measurements

Traditional AST measurements are dominated by broth microdilution and disc diffusion. While these are time consuming and labor intensive, they are built on decades of refining and standardizing the measurement of bacterial susceptibility, increasing reproducibility across labs. The European Committee on Antimicrobial Susceptibility testing (EUCAST) provides detailed guidance on correct media preparation to interpretation of results. For broth microdilution, results are only valid if there is clear growth in the positive control (i.e., no antibiotic), the sample is of a pure culture and is inoculated at or near to 5×10^5 CFU/mL. Variation from these exact conditions can significantly affect the MIC measured by these measures and despite standardized approaches, high variation between labs has been recorded (Conville et al., 2012; Espinel-Ingroff et al., 2013; Kavanagh et al., 2019).

Some innovations have accelerated the time to result for conventional methods. For example, the Clinical and Laboratory Standards Institute (CLSI) have identified that direct disc diffusion may be used for some clinical isolates such as blood. Positive blood culture samples are typically monomicrobial as blood is sterile apart from the pathogen (Chandrasekaran et al., 2018). The main variation from gold standard methodology is variation in the inoculum number. Categorical agreement for 20 isolates ranged from 87.8 to 92.2% depending on the media used. Earlier read times were also evaluated, however using both



traditional method and direct disc diffusion lead to > 20% of plates being too difficult to read due to light growth at 6 h. Direct testing was found to have the best readability at 7.6×10^7 – 5×10^8 CFU/mL, indicating that a wider range of bacterial inoculums may be able to be used for categorical identification, but not MIC. While this increases the time to result by around 24 h this method does not improve upon standard AST methodology but adapts it.

The Need for Faster Time to Result

The WHO has identified a lack of near-patient testing of bacterial identification and AST, such that antibiotics cannot be prescribed based on evidence, as a gap in existing diagnostics. This is a particular challenge within the context of sepsis, multidrug resistant gonorrhoeae, and distinguishing between bacterial and non-bacterial infections (World Health Organization, 2019). There is no “easy to use” platform for testing samples including blood, urine, stool or respiratory specimens without first culturing the organisms.

Depending on the type of infection, healthcare systems have different requirements for testing. There are a number of bacterial infections for which delaying treatment for 4–6 h does not impact patient outcome, (Naucler et al., 2020) but it would lead to increased workload by either withholding prescriptions or changing prescription based on results. For example, suspected urinary tract infections (UTI) are usually presented in a primary care setting. Because point of care (POC) testing to determine resistance profiles are not readily available, antibiotics are prescribed empirically. Studies using currently available POC tests have received mixed results depending on how they are used. One study considered the use of Flexicult[®] SSI urinary kits for bacterial identification and determining antimicrobial resistance in primary care settings in the UK. This test uses traditional agar techniques to grow bacteria directly from urine samples and can be used as a POC test without significant investment (37°C incubator). However, the test still requires overnight incubation. The agar contains chromogenic dyes allowing approximate bacterial identification. Portions of the plate contain antibiotics to determine resistant profiles. This study found no difference in patient recovery, UTI recurrence or hospitalization when managed with standard care or with a Flexicult[®] test (Butler et al., 2018). Comparing the gold standard and Flexicult[®] test identified a good agreement in resistance profiles, indicating the technique was technically accurate even if no direct patient benefit was found. Although these tests are unlikely to improve patient recovery or hospitalization of patients presenting at primary care with uncomplicated infections, they may still be useful in improving surveillance and reducing sample load for central microbiology labs. A similar study was conducted in Denmark using Flexicult[®] SSI urinary kit and Flexicult[®] ID in a general practice for women presenting with UTI symptoms. Similarly there was no improvement in prescription and patient outcome when using these tests however, resistance levels in this area were low and the biggest patient benefit would be expected where higher frequency of resistant bacteria are present, or where empirical selection guidelines are incomplete (Holm et al., 2017). Automated systems have been implemented in secondary care to decrease the hands-on user time. These allow higher throughput

but are not used as a point-of-care decision making tool. Many of these involve simple inoculation systems using 96 well plates preloaded with antibiotic solutions, or combined incubation with analysis systems to monitor growth. The Mast Uri[®] dot (Mast Group Ltd) is an automated inoculator that transfers multiple urine samples to plates containing pre-loaded media allowing for AST and bacterial identification. While the test still requires 18–24 h incubation it decreases user time as liquid handling and analysis are automated.

Beyond UTI, there are other infections such as sepsis where antibiotics cannot be withheld and time to treatment severely impacts patient outcome. These require sampling of different biological matrices with different challenges: for sepsis, a major problem is the very low bacterial concentration in blood (<50 CFU/mL) (Opota et al., 2015; Stranieri et al., 2018) making culture diagnosis difficult, necessitating high sample volume (recommended sample volume for sepsis diagnosis is between 10 and 30 mL Bouza et al., 2007) and long incubation times.

For phenotypic AST, there are alternative ways to measure bacterial growth. Instead of direct detection of bacteria by light scattering (e.g., absorbance in microplates), colorimetric or fluorogenic metabolic dyes can be used to detect growth at earlier timepoints before cell density is high enough detectable light scattering. Furthermore, microscopy can be used to examine cell growth directly, making it possible to measure cell growth even faster.

While growth-based detection tests require long incubation times, there are other important tools to detect AMR (Figure 1) many of which can be faster. Nucleic acid-based detection is fast but cannot directly detect *functional* resistance—instead, known resistance genes are detected. Likewise, some mass spectrometry microbiology methods have extended beyond bacterial species identification into detecting mass fingerprints of resistance. Finally, many resistance mechanisms are enzymatic (e.g., beta-lactamase) and can be detected with colorimetric or fluorogenic substrates. These methods share the same limitation, that not all resistance genes, enzymes or profiles for pathogens are known and the presence of a known resistant gene or enzyme does not always translate to resistant bacterial phenotype (let alone clinical treatment outcomes), and so functional phenotypic methods remain essential.

TECHNICAL CHALLENGES TO PHENOTYPIC AST INNOVATION RELATE TO SAMPLE COMPOSITION

There are many technical difficulties in miniaturizing or speeding up these universally accepted gold standard conventional tests: we focus on several specific technical challenges related to the sample in the following sections. Phenotypic AST methods are constrained fundamentally by the measurement of bacterial cell growth, with or without antibiotics. Different infections are associated with different bacteria with distinct growth rates and resistance profiles. This leads to a need for many distinct protocols. For a diagnostic test, either a flexible platform is required, or tests have to be designed for a very

specific and narrow use case. When considering UTI tests, it is unlikely that one single test could be developed that is suitable for UTI diagnosis and AMR identification in all clinical presentations (uncomplicated v complicated, primary v secondary v community care). The most common causative agent for UTI is uropathogenic *E. coli* (UPEC) with up to 90% of infections caused by Gram-negative bacteria (Kline and Lewis, 2016). But polymicrobial infections are more likely to occur in complicated UTI, such as immunocompromised individuals, those with catheterization, and the elderly (Kline and Lewis, 2016). Therefore, a novel AST for uncomplicated UTI may be much easier to develop than for complicated UTI; yet the latter may place a higher burden of morbidity and mortality than uncomplicated UTI that often resolves without treatment.

Alongside technical barriers, the field is also highly regulated and has clinical conventions that can be challenging and expensive to align with when developing new technology. Over many decades, overarching groups such as EUCAST have identified specific and reproducible methods for determining the AST conditions for many organisms that have known clinical implications. Any new device entering the market may need to demonstrate the same susceptibility profiles as current protocols approved by regulators. Aligning the results of novel microfluidic tests with the outputs of “gold standard” conventional methods such as disc diffusion that are widely familiar to clinicians and public health systems may require expensive wide-scale clinical trials. Innovative devices can use diverse measurements that can be difficult to align with inhibition zone diameters. The most directly comparable results should be the more quantitative MIC that are typically measured by broth microdilution, as these are designed to be directly linked to growth in clinically significant concentrations of antibiotic related to therapeutic levels achieved in patients. However, many devices use single concentration breakpoints to identify susceptibility profiles of multiple antibiotics; it becomes critical to ensure these breakpoint concentrations are aligned to clinically accepted values.

Influence of Sample Matrix on Assays

The first step in using gold standard methods of AST is the overnight culture and isolation of bacteria from the sample. Using a sample directly for AST tests without plating and colony isolation immediately reduces the time to result by 18–24 h, cuts labor in picking colonies, and simplifies sample preparation. Together, direct sample testing is an attractive target and represents a “holy grail” for AST innovation. However, biological samples are a complex mixture of molecules many of which can significantly affect most biological analysis methods. This is even more problematic as samples can vary significantly between individuals. Samples can vary widely in pH, nutrient composition, inoculum number, the number of bacterial species (polymicrobial populations). They can also contain varying levels of components that directly affect bacterial growth, not only antimicrobial agents but also components that can bind and inactivate the test antibiotic. Different patient groups (catheterized, elderly, pregnant) and clinical history (diet, medication, liquid intake before sampling, complicated

or uncomplicated infection etc.) can dramatically alter sample matrix composition, making the composition of clinical samples from patients often very different from healthy controls. Studies looking at the growth of *E. coli* in different canine urine composition found that increased urine concentration (higher urine specific gravity) and higher pH levels showed decreased levels of *E. coli* growth after 4 h (Thornton et al., 2018).

Urine components such as high levels of ascorbic acid can lead to false negative results in dipstick tests (Mambatta et al., 2015). Resazurin dye reduction is commonly used to detect metabolism changing from blue to a pink color and from non-fluorescent to a strong red fluorescence in the presence of metabolically active bacteria. Resazurin has been incorporated in a number of AMR microfluidic devices as well as traditional broth microdilution methods (Boedicker et al., 2008; Elavarasan et al., 2013; Elshikh et al., 2016; Hsieh et al., 2018; Kao et al., 2020). However, the fluorescence of resorufin (the product of resazurin) is susceptible to changes in pH. Furthermore, high ascorbic acid levels can directly reduce resazurin in the absence of bacteria (Natto et al., 2012). Urine pH also causes complications for many diagnostic tests. Other chromogenic dyes used to detect bacterial growth are pH dependent. Urine pH can range from pH 4–9 with more alkaline pH associated with *P. mirabilis* in contrast to *E. coli* that is associated with more acidic pH (Lai et al., 2019). Devices using pH dependent dyes to monitor bacterial growth such as phenol red (Cira et al., 2012; Reis et al., 2016; Lee et al., 2019) may risk false positive results when using direct urine samples. The application of the microfluidic test is an important factor when choosing which indicator to use.

Agar based methods are good for direct sampling as this dilutes the biological sample such as urine or blood with the solid agar medium and can provide semi-quantitative measurement of bacteria number. Flexicult® Vet is used in veterinary surgeries to determine UTI and AST on direct urine samples from cats and dogs (Guardabassi et al., 2015). The sample is applied to the plate and excess sample is removed. The plates do not provide an MIC or zone of inhibition but can functionally identify which bacteria grow or are inhibited by certain antibiotics which can aid in prescription practices. Similar products using agar methods for adaptable point of care testing include Diaslide, Uricult Trio, and Dipstreak. But the benefits of solid media are offset by the need for 18–24 h incubation, likely to be too slow in a primary care setting to change current prescription practices. The ease of use and availability does make it attractive for decentralized surveillance schemes or in areas with high prevalence of resistant bacteria or limited data to inform empirical antibiotic selection.

Polymicrobial Populations in Samples

Measuring bacterial growth directly in samples also raises the challenge of potential polymicrobial populations. This can be a pathogen plus harmless commensal organisms, or multiple pathogens. Many tests do not distinguish between different bacterial species because they are designed for single colony isolates. Isolation of bacteria from a sample using agar plates provides partial identification, either using chromogenic agar to identify enzyme activity of different bacteria (Chaux et al., 2002) or selective agar plus identification of colony morphology.

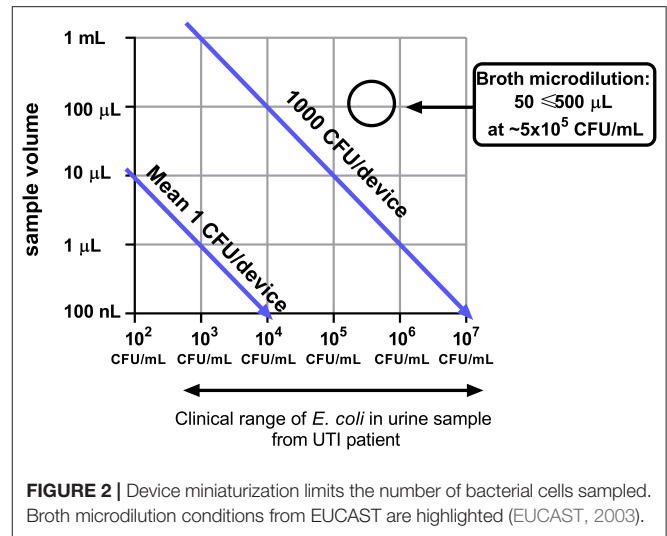
Antibiotic treatment of polymicrobial infections is not fully understood and treatment is made to target the most likely organism (Lasa and Solano, 2018; Hebert et al., 2020). UTI infections that involve two or more pathogens are much rarer and analysis of mixed cultures is unclear. Public Health England (PHE) determines a polymicrobial infection if each isolate is 10^5 CFU/mL but for analytical technology polymicrobial culture should be considered to also include a single pathogen mixed with commensal contaminants (Lough et al., 2019). There is a lack of consensus as to the definition and role of polymicrobial infections (Garg and Garg, 2017). This can make the need for bacterial identification more or less important depending on the infection. For UTIs polymicrobial infections are more common in complicated infections making identification more important than uncomplicated infections. It may be possible and advantageous for infections with a high risk to be paired with a rapid genotypic method to positively identify certain specific target pathogenic bacteria that are associated with the most patient harm.

Inoculum Effect

The initial inoculum cell density significantly affects MIC determination as higher cell densities of susceptible organisms may still show measurable growth in the presence of an inhibitory concentration of antibiotic (Postek et al., 2018; Smith and Kirby, 2018). This poses a significant challenge for direct testing measurements as the initial concentration of bacteria in patient samples is unknown. The inoculum effect (IE) refers to decreased antibiotic efficacy on increasing bacterial numbers, and this effect is more pronounced for measuring β -lactam susceptibility in β -lactamase positive bacteria (Smith and Kirby, 2018). The Clinical and Laboratory Standards Institute (CLSI) define the accepted range of inoculum number between 2×10^5 – 8×10^5 CFU/mL. Within this accepted inoculum range, when *Enterobacteriaceae* were tested against meropenem, an 8-fold-difference in MIC was observed (Smith and Kirby, 2018). Many potential diagnostic tools for AMR use a single breakpoint concentration based on EUCAST guidelines. EUCAST breakpoints are calculated from MIC results and categorizes bacteria as susceptible, resistant or intermediate for different antibiotics (Turnidge and Paterson, 2007). However, using an unknown inoculum concentration with a fixed breakpoint antibiotic concentration may lead to errors in susceptibility classification.

To control for this effect, some microfluidic devices include an initial inoculum normalization step such as sample filtering and dilutions. One example uses a pre-filtering step using syringe filters to trap bacteria followed by resuspension, manual counting and final dilution to EUCAST guidelines in growth media. While this still requires a lot of user time, it reduces the overnight culture step from 18 to 24 h to under 1 h and eliminates the matrix effect. The bacteria are then grown in nanoliter volumes using resazurin to detect bacterial growth in the presence of antibiotics (Avesar et al., 2017). Using time-lapse fluorescence microscopy, a difference in growth curves is evident within 5.5 h.

This effect can also be overcome using microfluidic bacterial counting techniques. Due to the miniaturized nature of microfluidics, hundreds of conditions in microlitre-picolitre



volumes can be run simultaneously in a single device. The multi-RAPiD method takes serial dilutions of a sample loaded into picochambers on chip in the presence of resazurin. Chambers with bacteria present become fluorescent and using Poisson distribution of the positive and negative chambers the initial inoculum number can be determined. This method identified good match between expected and counted positive chambers for both *E. coli* and *S. aureus* (Hsieh et al., 2018). The same outcome can be achieved using time-lapse imaging to build growth curves with dilutions of starting inoculum number. The time taken to reach a certain density or fluorescence intensity if using a dye such as resazurin can be used to calculate the starting inoculum (Travnickova et al., 2019). These counting methods can be incorporated with devices containing antibiotics to generate AST or MIC results.

Analytical Sensitivity Following Miniaturization

Miniaturization can reduce detection times and allow detection of single cells. However, the cell concentration in some samples may not be directly compatible with some microdevices because the smaller the sample volume tested, the fewer cells will be present and for example 10^3 CFU/mL is equivalent to only 1 CFU per 1 microlitre of sample (Figure 2). The clinical range for UTI diagnosis can range from $\geq 10^3$ CFU/mL (Wilson and Gaido, 2004). A device that has an average of 1 CFU/device with a sample volume of 1 μ L can potentially detect 10^3 CFU/mL. Therefore, it is important when engineering microdevices that the sample volume tested will have sufficient bacterial cells at the clinically relevant pathogen concentration for that infection. Within this range, speed of detection can be increased by increasing sample volume because for cell-growth based analysis the more bacteria per device the faster the detection will be (Elshikh et al., 2016).

Microfluidics uses different approaches for miniaturization of reactions including microdroplet formation (Idelevich et al., 2018) and microchambers in fabricated devices (Avesar et al., 2017; Azizi et al., 2018). The high surface to volume ratios

TABLE 1 | Summary of phenotypic antimicrobial susceptibility tests.

Organisms	Time to result	Equipment used	Approach	References
GFP expressing <i>E. coli</i> DH5 α	<90 min	Fluorescence time-lapse microscopy	Immobilized single cell microscopy	Busche et al., 2019
GFP expressing <i>E. coli</i> , <i>E. coli</i> (25922), <i>S. aureus</i> (29213)	1–3 h	Fluorescence time-lapse microscopy	Microscopy of single cells in chambers	Sun et al., 2019
Methicillin resistant <i>S. aureus</i>	16–24 h	Visual color change	Phenol red color change in microchambers	Lee et al., 2019
<i>E. coli</i> 25922, <i>K. pneumoniae</i> 700603, <i>S. aureus</i> 29213, <i>E. faecalis</i> 29212	0.25–0.5 h	Bright-field time-lapse microscopy	Growth in microdroplets	Kang et al., 2019
YFP expressing <i>E. coli</i>	16 h	Fluorescence microscopy	Fluorescence intensity in microdroplets	Postek et al., 2018
<i>K. pneumoniae</i> , <i>E. coli</i>	< 5.5 h	Fluorescence time-lapse microscopy	Fluorescence intensity of resazurin in microchambers	Avesar et al., 2017
<i>E. coli</i> , <i>K. pneumoniae</i> , <i>E. faecalis</i>	1–3 h	Fluorescence microscopy	Fluorescence intensity of resazurin in nanochambers	Azizi et al., 2018
<i>E. coli</i>	< 4 h	Phase contrast microscopy	Motility of single cells	Pitruzzello et al., 2019
<i>E. coli</i> 25922, <i>S. aureus</i> 29213, <i>P. aeruginosa</i> 27853	3–4 h	Time-lapse microscopy	Single cell growth immobilized in agar	Choi et al., 2013
<i>E. coli</i> , <i>K. pneumoniae</i> , <i>E. cloacae</i> , <i>P. aeruginosa</i>	2 h	Fluorescence time-lapse microscopy	Live/dead staining in single cells trapped in microchannels	Kalashnikov et al., 2017
<i>E. coli</i> , <i>K. pneumoniae</i> , <i>S. saprophyticus</i>	0.5 h	Time-lapse phase contrast microscopy	Single cell growth in microchannels	Baltekin et al., 2017

of microdevices have shown increased bacterial growth rates compared to larger volume containers (10 μ L v 13 mL) such as conical flasks (Chen et al., 2010). Studying the single cell dynamics in these high surface area to volume devices allow faster bacterial growth detection and therefore divergence of growth curves in the presence of antibiotics will be able to determine AST faster than bulk analysis relying on color change or OD measurements. However, using smaller sample volumes also reduces the number of bacteria in the devices. Some microfluidic devices enhance bacterial detection by flowing larger sample volumes through the device, capturing or trapping bacteria. This can be achieved by immunocapture (Olanrewaju et al., 2017; Pereiro et al., 2017; Alves and Reis, 2019) or by physical boundaries (Pitruzzello et al., 2019).

The majority of these challenges are innate to the sample tested rather than the methodology. The power of conventional AST methods becomes clearer as they overcome these challenges by apparently simple steps. For example, plating on agar plates simultaneously removes the sample matrix, normalizes cell number, and provides a monomicrobial culture, before subsequent AST measurements. Rapid AST devices must either bypass some of these steps or optimize the speed for each step.

NEW OPPORTUNITIES FOR MICROFLUIDIC ANTIBIOTIC SUSCEPTIBILITY TESTING

In spite of these challenges, recent developments around microfluidic devices still offer massive potential for rapid portable AST. Although some microfluidic devices still require laboratory

equipment to record results (e.g., fluorescence microscopy), the increased availability of low-cost yet high performance hardware—such as imaging devices and other optoelectronics—makes developing microfluidic reader systems more affordable (Needs et al., 2019). For instance, smartphone cameras combined with imaging systems built from microscopy components make POC fluorescence microscopy affordable (Chen et al., 2019). A summary of recent phenotypic AST microfluidic devices is shown in **Table 1**.

Digital Microscopy

Digital microscopy is used to monitor changes in microfluidic devices allowing imaging of single cells and monitoring color or fluorescence changes in microchambers. Visually monitoring motile bacteria such as *E. coli* using microscopy can be a fast, but a user intensive method to identify urine bacteraemia. After an incubation with different antibiotics, changes in cell motility can be observed by eye. However, to increase throughput and reproducibility automated analysis systems are required. The majority of imaging-based detection methods of AST use time-lapse imaging to identify the earliest divergence in bacterial growth in reaction to different antibiotic exposure. The Accelerate PhenoTest BC system received FDA approval in 2017 for determining susceptibility in direct, positive blood cultures within 7 h. This approved method uses time-lapse imaging to follow bacterial growth in the presence of antibiotics. For life threatening infections like blood infections this advance is needed (Charnot-Katsikas et al., 2018). This automated microscopic AST system illustrates the opportunities for cell imaging.

Microfluidics and digital microscopy can be combined with computation to examine cell behavior in the presence of antibiotics and to automate the analysis of antibiotic susceptibility. One such device uses cup-shaped traps to monitor the motility of single bacteria in the presence of different antibiotics to identify susceptible strains within 2 h of exposure. Phase contrast microscopy is used to monitor the individual traps, and simple pixel intensity of the trap over time monitors the motility of the bacteria (Pitruzzello et al., 2019). Other devices use physical traps in conjunction with time lapse imaging of single cells to monitor growth rather than motility. These methods both accumulate bacteria from a sample and can potentially replace the biological sample matrix (i.e., blood/urine) with growth media. GFP expressing *E. coli* were trapped in a channel-based device using hydrodynamic pressure. Parallel channels linked by a nanogap allowed media exchange while retaining cells along the edge of a single channel. The cells were monitored every 30 s for 90 min and cell chain length was calculated for bacterial growth. Within 90 min it was possible to determine decreased growth in samples with media containing 200 µg/mL kanamycin (Busche et al., 2019). Other trap designs have used narrow channels ($1.25 \times 1.25 \times 50 \mu\text{m}$) with a block at one end that captures bacteria but maintains media flow. Using phase contrast microscopy, the length of the channel occupied with bacterial cells is calculated over time with either growth media or in the presence of the antibiotic of choice. Using this method, differences in growth time are detected within 30 min (Baltekin et al., 2017). Alternatives to physical traps include non-specific binding to epoxide modified microchannels. Antibiotic containing media can then be flowed through the channels and live/dead cells were monitored by time-lapse microscopy using phase contrast and SYTOX orange fluorescence marker (Kalashnikov et al., 2017). This method was able to detect susceptibility of Gram-negative bacteria within 60 min.

Additional approaches for bacterial immobilization in microfluidic devices use agar based techniques. The microfluidic agarose channel device flows liquid agarose and bacteria mix into the device which solidifies. Antibiotic containing media flows over the agarose layer and diffuses into the agarose/bacteria mix. Bacterial growth is monitored using time-lapse imaging and simple image analysis generating binary images the area of bacteria growth in different channels can be calculated. MIC and AST measurements can be detected within 4 h (Choi et al., 2013).

Other single cell microscopy methods have combined antibiotic gradient generators with bacteria cell culture microchambers (Li et al., 2014b; Kim et al., 2015; Malmberg et al., 2016). GFP-expressing *E. coli* were monitored by fluorescence microscopy in cultivation chambers linked to an antibiotic gradient device (Sun et al., 2019). The challenge of using this method is to create a gradient of significant range for clinical relevance as many gradient generators have a small range. Broth microdilution methods use a 2-fold dilution series over multiple dilutions (between 8 and 11 dilutions). This has been demonstrated by using a gradient generator that provides 2-fold dilutions over 7 channels (Kim et al., 2015).

Trap-based assays are less likely to be affected by sample matrix or inoculum effect. The biological sample is flowed through the device, the bacterial cells are captured/immobilized, and the biological sample is replaced with nutrient media or a constant flow of nutrient media. These techniques reduce the effects of sample matrix on results and can rapidly detect differentials in growth curves. They are also beneficial for samples containing low levels of bacteria, such as blood infections as higher volumes of sample can be passed through the devices. Other methods, such as the agarose immobilization, do not allow this and the bacteria measured are limited to the concentration in the sample (Figure 2). The use of high-resolution fluorescence microscopy and liquid handling machinery makes the usage of these devices in a clinical setting unlikely since they require high investment, user training and are unlikely to provide high throughput testing capacity.

Smartphone Imaging

Smartphone use is being explored to enhance the usability or analysis of POC testing. Many microfluidic and POC tests are based on color changes which can be read by the eye while with devices using micro- or picochambers this can be challenging. Adding an imaging technique, can allow devices to use automatic image analysis techniques or provide quantitative or semi-quantitative data based on the level of color or fluorescence intensity relating to the level of biomarkers/growth. Recent advances in smartphone camera systems and the combination of microscopy accessories can be added to provide low-cost, portable microscopy systems for bright-field, dark-field or fluorescence imaging (Hernández-Neuta et al., 2019; Kheireddine et al., 2019). Smartphones have also been used for complex analysis, increased usability through patient interface for home testing or as a controller to drive mechanical parts of microfluidic devices (Li et al., 2014a; Arango et al., 2018; Temiz and Delamarche, 2018). As many microfluidics devices are targeting POC tests, the readability of the results is an important aspect of the overall system. When used as a companion to microfluidic tests, smartphones are a prospective low-cost clinical device. The images obtained can be analyzed either by a custom app or processed manually.

One example of quantitative smartphone detection uses immunocapture of *E. coli* in synthetic urine in microcapillaries. This sandwich-based ELISA device uses fluorescent substrate to detect captured bacteria. Using a simple LED and emission filter setup, the fluorescent intensity of the microcapillaries were detected using a smartphone camera with magnification lens (Alves and Reis, 2019). This technique can determine quantitative levels of bacteria in samples based on the fluorescence production. Similarly, smartphone imaging has been used for the immuno-detection of norovirus on a paper microfluidic device. An external objective lens was added with low-cost filters to detect fluorescent color changes (Chung et al., 2019). The virus particles are captured by antibodies and particle aggregation allows detection of single viral particles enabling an extremely low limit of detection (LOD).

One challenge when using smartphone camera detection is that software embedded in the camera often automatically adjusts the settings to deliver the “best” image for a consumer user. Different images may be recorded with different exposure settings. The camera settings may be fixed (Chung et al., 2019) which can be challenging for different models and requires the same model phone to be used with the specific test, limiting potential users of the device, and making the use of personal phones unlikely. Others include a color chart (Shen et al., 2012) or reference sample of known fluorescence intensity so images can be normalized during image analysis (Alves and Reis, 2019).

Bacteriophage Based Sensors

While antibiotic susceptibility tests dominate the diagnostic need, developments are being made for the exploration of bacteriophage treatments (Kutateladze and Adamia, 2010). Bacteriophages have a different mechanism of action to antibiotics. To fully take advantage of this method as a therapy, complimentary systems for the rapid, low-cost, and reliable detection of bacteria and determination of phage specificity of an infectious organism are needed (Farooq et al., 2018). Bacteriophage can also be engineered and used as tools for bacterial detection. Bacteriophage can bind to bacteria with high specificity potentially determining bacterial identification and AST. This is already being put into practice in the Smarticles (Roche) system. Bacteriophage reporters containing luciferase genes are used to measure viable bacterial growth measuring luminescence instead of turbidity. This method was also used in conjunction with a model of blood infections. Bacteria were separated from red blood cells using an acoustophoretic microfluidic chip comprised of a single channel with side and center inlets and outlets. The acoustophoresis causes the red blood cells but not the bacteria to move to the center channel and these are discarded via the center outlet, while the bacterial cells are collected via the side outlets. After bacteria collection a plate based luminescent bacteriophage assay was performed (Dow et al., 2018), indicating microfluidic devices can be used for the rapid purification of bacteria from samples which can be adapted into an AST workflow.

Paper Microfluidics

Microfluidic paper-based analytical devices (μ PADs) are another alternative for AMR detection. These are especially robust for transport and storage and are typically made of low-cost fabrication materials. They can be produced in a wide variety of sizes, shapes and layers, and desired molecules can be easily immobilized onto the paper, so the area of use and the target cell can be diverse. Hydrophilic regions provide a spontaneous microfluidic platform on μ PADs reducing the need for complex laboratory equipment such as pumps for liquid handling and are therefore easy to use (one-step procedure). Colourimetric methods are generally preferred for μ PADs so the results can be visualized by eye and do not require a dedicated reader (Martinez et al., 2010; Hu et al., 2014).

A panel of four common antibiotics was tested against *E. coli* using a laser-patterned paper based device. This device used

chromogenic agar as a nutrient source and to visualize the bacteria when incubated at 37°C overnight (He et al., 2020). A filter paper layer then wicks the sample via capillary action and distributes throughout the device without the need for additional equipment. The final layer contains laser-patterned wells containing different antibiotics. Another paper-based device was used to measure β -lactam resistance in bacterial samples taken from wastewater. This study used enzyme based β -lactamase detection using the substrate nitrocefin for color change which was captured by camera phone and was able to quantify the color change in nitrocefin which was found to deliver the same LOD as measured in a microtitre plate and plate reader. In another paper-based system, antibiotic susceptibilities of *E. coli* and *S. typhimurium* were examined using resazurin-based detection. The system uses standard culture media in a reservoir and requires 18 h incubation (Deiss et al., 2014). Paper microfluidics may not provide a faster detection method, although researchers are exploring direct sampling methods such as urine and environmental samples for bacterial detection and AST. The strength of these methods relies on portability, stability and reduced need for laboratory equipment. Paper microfluidics offer a cheap alternative at a cost of \$ 0.20 (Boehle et al., 2017). They are also more likely to be useful in samples that have a higher density of bacteria and where a high volume of sample is available, such as UTI.

CONCLUSION

Microfluidic techniques have many benefits for developing portable, point-of-care diagnostics but there are significant hurdles to overcome to develop rapid AST methods. Sample matrix, inoculum effect and polymicrobial populations are still challenges for conventional AST measurements. Whilst aPOC phenotypic AST is a long way off, significant improvements in the use of digital microscopy and smartphone imaging and novel sensors are likely to increase the use of single cell detection for rapid AST. An important factor in deciding which microfluidic strategy to use is the type of infection being targeted, and the clinical pathway it is expected to add to or disrupt. For instance, devices which accumulate bacteria may be useful for low concentration threshold infections such as blood stream infections and would be expected to join a secondary care setting whereas POC tests for uncomplicated UTI would need minimal sample preparation and equipment. The use of paper microfluidic in this area can provide stable point of care testing. Not only are these devices needed for the effective treatment of life-threatening infections and effective treatment of disease, surveillance of antibiotic resistance in health, agriculture, and environmental samples are also needed to monitor and better tackle the emergence of antimicrobial resistance.

AUTHOR CONTRIBUTIONS

SN, SB, SD, and AE were involved in writing—original draft preparation. SN, SB, SD, HO, CM, and AE were involved in

writing—review and editing. SN, CM, and AE were involved in visualization. AE was responsible for funding acquisition. All authors contributed to the article and approved the submitted version.

REFERENCES

- Alves, I. P., and Reis, N. M. (2019). Microfluidic smartphone quantitation of *Escherichia coli* in synthetic urine. *Biosens. Bioelectron.* 145:111624. doi: 10.1016/j.bios.2019.111624
- Arango, Y., Temiz, Y., Gökçe, O., and Delamarche, E. (2018). Electrogates for stop-and-go control of liquid flow in microfluidics. *Appl. Phys. Lett.* 112:153701. doi: 10.1063/1.5019469
- Avesar, J., Rosenfeld, D., Truman-Rosentsvit, M., Ben-Arye, T., Geffen, Y., Bercovici, M., et al. (2017). Rapid phenotypic antimicrobial susceptibility testing using nanoliter arrays. *Proc. Natl. Acad. Sci. U.S.A.* 114:E5787. doi: 10.1073/pnas.1703736114
- Azizi, M., Zaferani, M., Dogan, B., Zhang, S., Simpson, K. W., and Abbaspourrad, A. (2018). Nanoliter-sized microchamber/microarray microfluidic platform for antibiotic susceptibility testing. *Anal. Chem.* 90, 14137–14144. doi: 10.1021/acs.analchem.8b03817
- Baltekin, Ö., Boucharin, A., Tano, E., Andersson, D. I., and Elf, J. (2017). Antibiotic susceptibility testing in less than 30 min using direct single-cell imaging. *Proc. Natl. Acad. Sci. U.S.A.* 114:201708558. doi: 10.1073/pnas.1708558114
- Boedicker, J. Q., Li, L., Kline, T. R., and Ismagilov, R. F. (2008). Detecting bacteria and determining their susceptibility to antibiotics by stochastic confinement in nanoliter droplets using plug-based microfluidics. *Lab Chip* 8, 1265–1272. doi: 10.1039/b804911d
- Boehle, K. E., Gilliland, J., Wheeldon, C. R., Holder, A., Adkins, J. A., Geiss, B. J., et al. (2017). Utilizing paper-based devices for antimicrobial-resistant bacteria detection. *Angew. Chem. Int. Ed. Engl.* 56, 6886–6890. doi: 10.1002/anie.201702776
- Bouza, E., Sousa, D., Rodríguez-Créixems, M., Lechuz, J. G., and Muñoz, P. (2007). Is the volume of blood cultured still a significant factor in the diagnosis of bloodstream infections? *J. Clin. Microbiol.* 45, 2765–2769. doi: 10.1128/JCM.00140-07
- Busche, J. F., Moller, S., Stehr, M., and Dietzel, A. (2019). Cross-flow filtration of *Escherichia coli* at a nanofluidic gap for fast immobilization and antibiotic susceptibility testing. *Micromachines* 10:691. doi: 10.3390/mi10100691
- Butler, C. C., Francis, N. A., Thomas-Jones, E., Longo, M., Wootton, M., Llor, C., et al. (2018). Point-of-care urine culture for managing urinary tract infection in primary care: a randomised controlled trial of clinical and cost-effectiveness. *Br. J. Gen. Pract.* 68, e268–78. doi: 10.3399/bjgp18X695285
- Chandrasekaran, S., Abbott, A., Campeau, S., Zimmer, B. L., Weinstein, M., Thrupp, L., et al. (2018). Direct-from-blood-culture disk diffusion to determine antimicrobial susceptibility of gram-negative bacteria: preliminary report from the clinical and laboratory standards institute methods development and standardization working group. *J. Clin. Microbiol.* 56, e01678–17. doi: 10.1128/JCM.01678-17
- Charnot-Katsikas, A., Tesic, V., Love, N., Hill, B., Bethel, C., Boonlayangoor, S., et al. (2018). Use of the accelerate pheno system for identification and antimicrobial susceptibility testing of pathogens in positive blood cultures and impact on time to results and workflow. *J. Clin. Microbiol.* 56, e01166–17. doi: 10.1128/JCM.01166-17
- Chaux, C., Crepy, M., Xueref, S., Roure, C., Gille, Y., and Freydiere, A. M. (2002). Comparison of three chromogenic agar plates for isolation and identification of urinary tract pathogens. *Clin. Microbiol. Infect.* 8, 641–645. doi: 10.1046/j.1469-0691.2002.00433.x
- Chen, C. H., Lu, Y., Sin, M. L. Y., Mach, K. E., Zhang, D. D., Gau, V., et al. (2010). Antimicrobial susceptibility testing using high surface-to-volume ratio microchannels. *Anal. Chem.* 82, 1012–1019. doi: 10.1021/ac9022764
- Chen, K. L., Ven, T. N., Crane, M. M., Chen, D. E., Feng, Y. C., Suzuki, N., et al. (2019). An inexpensive microscopy system for microfluidic studies in budding yeast. *Transl. Med. Aging* 3, 52–56. doi: 10.1016/j.tma.2019.05.001

FUNDING

This work was funded by grants from the EPSRC reference number EP/R022410/1 and EP/S010807/1.

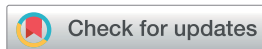
- Choi, J., Jung, Y. G., Kim, J., Kim, S., Jung, Y., Na, H., et al. (2013). Rapid antibiotic susceptibility testing by tracking single cell growth in a microfluidic agarose channel system. *Lab Chip* 13, 280–287. doi: 10.1039/C2LC41055A
- Chung, S., Breshears, L. E., Perea, S., Morrison, C. M., Betancourt, W. Q., Reynolds, K. A., et al. (2019). Smartphone-based paper microfluidic particulometry of norovirus from environmental water samples at the single copy level. *ACS Omega* 4, 11180–11188. doi: 10.1021/acsomega.9b00772
- Cira, N. J., Ho, J. Y., Dueck, M. E., and Weibel, D. B. (2012). A self-loading microfluidic device for determining the minimum inhibitory concentration of antibiotics. *Lab Chip* 12, 1052–1059. doi: 10.1039/C2LC20887C
- Conville, P. S., Brown-Elliott, B. A., Wallace, R. J. Jr., Witebsky, F. G., Koziol, D., Hall G. S., et al. (2012). Multisite reproducibility of the broth microdilution method for susceptibility testing of *Nocardia* species. *J. Clin. Microbiol.* 50, 1270–1280. doi: 10.1128/JCM.00994-11
- Deiss, F., Funes-Huacca, M. E., Bal, J., Tjhung, K. F., and Derda, R. (2014). Antimicrobial susceptibility assays in paper-based portable culture devices. *Lab Chip* 14, 167–171. doi: 10.1039/C3LC50887K
- Dow, P., Kotz, K., Gruszka, S., Holder, J., and Fiering, J. (2018). Acoustic separation in plastic microfluidics for rapid detection of bacteria in blood using engineered bacteriophage. *Lab Chip* 18, 923–932. doi: 10.1039/C7LC01180F
- Elavarasan, T., Chhina, S. K., Parameswaran, M., and Sankaran, K. (2013). Resazurin reduction based colorimetric antibiogram in microfluidic plastic chip. *Sens. Actuators B Chem.* 176, 174–180. doi: 10.1016/j.snb.2012.10.011
- Elshikh, M., Ahmed, S., Funston, S., Dunlop, P., MCGaw, M., Marchant, R., et al. (2016). Resazurin-based 96-well plate microdilution method for the determination of minimum inhibitory concentration of biosurfactants. *Biotechnol. Lett.* 38, 1015–1019. doi: 10.1007/s10529-016-2079-2
- Espinel-Ingroff, A., Arendrup, M. C., Pfaller, M. A., Bonfietti, L. X., Bustamante, B., Canton, E., et al. (2013). Interlaboratory variability of Caspofungin MICs for *Candida* spp. Using CLSI and EUCAST methods: should the clinical laboratory be testing this agent? *Antimicrob. Agents Chemother.* 57, 5836–5842. doi: 10.1128/AAC.01519-13
- EUCAST (2003). Determination of minimum inhibitory concentrations (MICs) of antibacterial agents by broth dilution. *Clin. Microbiol. Infect.* 9, ix–xv. doi: 10.1046/j.1469-0691.2003.00790.x
- Farooq, U., Yanga, Q., Ullah, M. W. and Wang, S. (2018). Bacterial biosensing: recent advances in phage-based bioassays and biosensors. *Biosens. Bioelectron.* 118, 204–216. doi: 10.1016/j.bios.2018.07.058
- Garg, S. K., and Garg, P. (2017). Polymicrobial blood stream infection: consensus definition is required. *Indian J. Crit. Care Med.* 21, 712–713. doi: 10.4103/ijccm.IJCCM_129_16
- Guardabassi, L., Hedberg, S., Jessen, L. R., and Damborg, P. (2015). Optimization and evaluation of Flexicult(R) Vet for detection, identification and antimicrobial susceptibility testing of bacterial uropathogens in small animal veterinary practice. *Acta Vet. Scand.* 57:72. doi: 10.1186/s13028-015-0165-4
- He, P. J. W., Katis, I. N., Kumar, A. J. U., Bryant, C. A., Keevil, C. W., Somani, B. K., et al. (2020). Laser-patterned paper-based sensors for rapid point-of-care detection and antibiotic-resistance testing of bacterial infections. *Biosens. Bioelectron.* 152:112008. doi: 10.1016/j.bios.2020.112008
- Hebert, C., Gao, Y., Rahman, P., Dewart, C., Lustberg, M., Pancholi, P., et al. (2020). Prediction of antibiotic susceptibility for urinary tract infection in a hospital setting. *Antimicrob. Agents Chemother.* 64:e02236-19. doi: 10.1128/AAC.02236-19
- Hernández-Neuta, I., Neumann, F., Brightmeyer, J., Ba Tis, T., Madaboosi, N., Wei, Q., et al. (2019). Smartphone-based clinical diagnostics: towards democratization of evidence-based health care. *J. Intern. Med.* 285, 19–39. doi: 10.1111/joim.12820
- Holm, A., Cordoba, G., Møllersørens, T., Rem Jessen, L., Frimodt-Møller, N., Siersma, V., et al. (2017). Effect of point-of-care susceptibility testing in general practice on appropriate prescription of antibiotics for patients with

- uncomplicated urinary tract infection: a diagnostic randomised controlled trial. *BMJ Open*. 7:e018028. doi: 10.1136/bmjopen-2017-018028
- Hsieh, K., Zec, H. C., Chen, L., Kaushik, A. M., Mach, K. E., Liao, J. C., et al. (2018). Simple and precise counting of viable bacteria by resazurin-amplified picoarray detection. *Anal. Chem.* 90, 9449–9456. doi: 10.1021/acs.analchem.8b02096
- Hu, J., Wang, S., Wang, L., Li, F., Pingguan-Murphy, B., Lu, T. J., et al. (2014). Advances in paper-based point-of-care diagnostics. *Biosens. Bioelectron.* 54, 585–597. doi: 10.1016/j.bios.2013.10.075
- Idelevich, E. A., Storck, L. M., Sparbier, K., Drews, O., Kostrzewa, M., and Becker, K. (2018). Rapid direct susceptibility testing from positive blood cultures by the matrix-assisted laser desorption ionization-time of flight mass spectrometry-based direct-on-target microdroplet growth assay. *J. Clin. Microbiol.* 56, e00913–18. doi: 10.1128/JCM.00913-18
- Kalashnikov, M., Mueller, M., Mcbeth, C., Lee, J. C., Campbell, J., Sharon, A., et al. (2017). Rapid phenotypic stress-based microfluidic antibiotic susceptibility testing of Gram-negative clinical isolates. *Sci. Rep.* 7:8031. doi: 10.1038/s41598-017-07584-z
- Kang, W., Sarkar, S., Lin, Z. S., Mckenney, S., and Konry, T. (2019). Ultrafast parallelized microfluidic platform for antimicrobial susceptibility testing of gram positive and negative bacteria. *Anal. Chem.* 91, 6242–6249. doi: 10.1021/acs.analchem.9b00939
- Kao, Y. T., Kaminski, T. S., Postek, W., Guzowski, J., Makuch, K., Ruszczak, A., et al. (2020). Gravity-driven microfluidic assay for digital enumeration of bacteria and for antibiotic susceptibility testing. *Lab Chip* 20, 54–63. doi: 10.1039/C9LC00684B
- Kavanagh, A., Ramu, S., Gong, Y., Cooper, M. A., and Blaskovich, M. A. T. (2019). Effects of microplate type and broth additives on microdilution mic susceptibility assays. *Antimicrob. Agents Chemother.* 63, e01760–18. doi: 10.1128/AAC.01760-18
- Kheireddine, S., Sudalaiyadum Perumal, A., Smith, Z. J., Nicolau, D. V., and Wachsmann-Hogiu, S. (2019). Dual-phone illumination-imaging system for high resolution and large field of view multi-modal microscopy. *Lab Chip* 19, 825–836. doi: 10.1039/C8LC00995C
- Kim, S. C., Cestellos-Blanco, S., Inoue, K., and Zare, R. N. (2015). Miniaturized antimicrobial susceptibility test by combining concentration gradient generation and rapid cell culturing. *Antibiotics* 4, 455–466. doi: 10.3390/antibiotics4040455
- Kline, K. A., and Lewis, A. L. (2016). Gram-positive uropathogens, polymicrobial urinary tract infection, and the emerging microbiota of the urinary tract. *Microbiol. Spectr.* 4. doi: 10.1128/microbiolspec.UTI-0012-2012
- Kutateladze, M., and Adamia, R. (2010). Bacteriophages as potential new therapeutics to replace or supplement antibiotics. *Trends Biotechnol.* 28, 591–596. doi: 10.1016/j.tibtech.2010.08.001
- Lai, H. C., Chang, S. N., Lin, H. C., Hsu, Y. L., Wei, H. M., Kuo, C. C., et al. (2019). Association between urine pH and common uropathogens in children with urinary tract infections. *J. Microbiol. Immunol. Infect.* doi: 10.1016/j.jmii.2019.08.002. [Epub ahead of print].
- Lasa, I. A. O., and Solano, C. (2018). Polymicrobial infections: do bacteria behave differently depending on their neighbours? *Virulence* 9, 895–897. doi: 10.1080/21505594.2018.1426520
- Lee, W. B., Chien, C. C., You, H. L., Kuo, F. C., Lee, M. S., and Lee, G. B. (2019). An integrated microfluidic system for antimicrobial susceptibility testing with antibiotic combination. *Lab Chip* 19, 2699–2708. doi: 10.1039/C9LC00585D
- Li, B., Li, L., Guan, A., Dong, Q., Ruan, K., Hu, R., et al. (2014a). A smartphone controlled handheld microfluidic liquid handling system. *Lab Chip* 14, 4085–4092. doi: 10.1039/C4LC00227J
- Li, B., Qiu, Y., Glidle, A., Mcilvenna, D., Luo, Q., Cooper, J., et al. (2014b). Gradient microfluidics enables rapid bacterial growth inhibition testing. *Anal. Chem.* 86, 3131–3137. doi: 10.1021/ac5001306
- Lough, M. E., Shradar, E., Hsieh, C., and Hedlin, H. (2019). Contamination in adult midstream clean-catch urine cultures in the emergency department: a randomized controlled trial. *J. Emerg. Nurs.* 45, 488–501. doi: 10.1016/j.jen.2019.06.001
- Malmberg, C., Yuen, P., Spaak, J., Cars, O., Tängdén, T., and Lagerbäck, P. (2016). A novel microfluidic assay for rapid phenotypic antibiotic susceptibility testing of bacteria detected in clinical blood cultures. *PLoS ONE* 11:e0167356. doi: 10.1371/journal.pone.0167356
- Mambatta, A. K., Jayarajan, J., Rashme, V. L., Harini, S., Menon, S., and Kuppusamy, J. (2015). Reliability of dipstick assay in predicting urinary tract infection. *J. Family Med. Prim. Care* 4, 265–268. doi: 10.4103/2249-4863.154672
- Martinez, A. W., Phillips, S. T., Whitesides, G. M., and Carrilho, E. (2010). Diagnostics for the developing world: microfluidic paper-based analytical devices. *Anal. Chem.* 82, 3–10. doi: 10.1021/ac9013989
- Mendelson, M., and Matsoso, M. P. (2015). The world health organization global action plan for antimicrobial resistance. *S Afr. Med. J.* 105, 325–325. doi: 10.7196/SAMJ.9644
- Natto, M. J., Savioli, F., Quashie, N. B., Dardonville, C., Rodenko, B., and De Koning, H. P. (2012). Validation of novel fluorescence assays for the routine screening of drug susceptibilities of *Trichomonas vaginalis*. *J. Antimicrob. Chemother.* 67, 933–943. doi: 10.1093/jac/dkr572
- Naucler, P., Huttner, A., Van Werkhoven, C. H., Singer, M., Tattevin, P., Einav, S., et al. (2020). Impact of time to antibiotic therapy on clinical outcome in patients with bacterial infections in the emergency department: implications for antimicrobial stewardship. *Clin. Microbiol. Infect.* doi: 10.1016/j.cmi.2020.02.032. [Epub ahead of print].
- Needs, S. H., Diep, T. T., Bull, S. P., Lindley-Decaire, A., Ray, P., and Edwards, A. D. (2019). Exploiting open source 3D printer architecture for laboratory robotics to automate high-throughput time-lapse imaging for analytical microbiology. *PLoS ONE* 14:e0224878. doi: 10.1371/journal.pone.0224878
- Olanrewaju, A. O., Ng, A., Decorwin-Martin, P., Robillard, A., and Juncker, D. (2017). Microfluidic capillary circuit for rapid and facile bacteria detection. *Anal. Chem.* 89, 6846–6853. doi: 10.1021/acs.analchem.7b01315
- Opota, O., Jatou, K., and Greub, G. (2015). Microbial diagnosis of bloodstream infection: towards molecular diagnosis directly from blood. *Clin. Microbiol. Infect.* 21, 323–331. doi: 10.1016/j.cmi.2015.02.005
- Pereiro, I., Bendali, A., Tabnaoui, S., Alexandre, L., Srbova, J., Bilkova, Z., et al. (2017). A new microfluidic approach for the one-step capture, amplification and label-free quantification of bacteria from raw samples. *Chem. Sci.* 8, 1329–1336. doi: 10.1039/C6SC03880H
- Pitruzzello, G., Thorpe, S., Johnson, S., Evans, A., Gadêlha, H., and Krauss, T. F. (2019). Multiparameter antibiotic resistance detection based on hydrodynamic trapping of individual *E. coli*. *Lab Chip* 19, 1417–1426. doi: 10.1039/C8LC01397G
- Postek, W., Gargulinski, P., Scheler, O., Kaminski, T. S., and Garstecki, P. (2018). Microfluidic screening of antibiotic susceptibility at a single-cell level shows the inoculum effect of cefotaxime on *E. coli*. *Lab Chip* 18, 3668–3677. doi: 10.1039/C8LC00916C
- Reis, N. M., Pivetal, J., Loo-Zazueta, A. L., Barros, J. M. S., and Edwards, A. D. (2016). Lab on a stick: multi-analyte cellular assays in a microfluidic dipstick. *Lab Chip* 16, 2891–2899. doi: 10.1039/C6LC00332J
- Shen, L., Hagen, J. A., and Papautsky, I. (2012). Point-of-care colorimetric detection with a smartphone. *Lab Chip* 12, 4240–4243. doi: 10.1039/c2lc40741h
- Smieszek, T., Pouwels, K. B., Dolk, F. C. K., Smith, D. R. M., Hopkins, S., Sharland, M., et al. (2018). Potential for reducing inappropriate antibiotic prescribing in English primary care. *J. Antimicrob. Chemother.* 73, ii36–ii43. doi: 10.1093/jac/dkx500
- Smith, K. P., and Kirby, J. E. (2018). The inoculum effect in the era of multidrug resistance: minor differences in inoculum have dramatic effect on MIC determination. *Antimicrob. Agents Chemother.* 62, e00433–18. doi: 10.1128/AAC.00433-18
- Stranieri, I., Kanunfre, K. A., Rodrigues, J. C., Yamamoto, L., Nadaf, M. I. V., Palmeira, P., et al. (2018). Assessment and comparison of bacterial load levels determined by quantitative amplifications in blood culture-positive and negative neonatal sepsis. *Rev. Inst. Med. Trop. São Paulo* 60, e61–e61. doi: 10.1590/s1678-9946201860061
- Sun, H., Chan, C. W., Wang, Y., Yao, X., Mu, X., Lu, X., et al. (2019). Reliable and reusable whole polypropylene plastic microfluidic devices for a rapid, low-cost antimicrobial susceptibility test. *Lab Chip* 19, 2915–2924. doi: 10.1039/C9LC00502A
- Tagliabue, A., and Rappuoli, R. (2018). Changing priorities in vaccinology: antibiotic resistance moving to the top. *Front. Immunol.* 9, 1068–1068. doi: 10.3389/fimmu.2018.01068
- Temiz, Y., and Delamarque, E. (2018). Sub-nanoliter, real-time flow monitoring in microfluidic chips using a portable device and smartphone. *Sci. Rep.* 8:10603. doi: 10.1038/s41598-018-28983-w

- Thornton, L. A., Burchell, R. K., Burton, S. E., Lopez-Villalobos, N., Pereira, D., Macewan, I., et al. (2018). The effect of urine concentration and pH on the growth of *Escherichia coli* in canine urine *in vitro*. *J. Vet. Intern. Med.* 32, 752–756. doi: 10.1111/jvim.15045
- Travnickova, E., Mikula, P., Oprsal, J., Bohacova, M., Kubac, L., Kimmer, D., et al. (2019). Resazurin assay for assessment of antimicrobial properties of electrospun nanofiber filtration membranes. *AMB Expr.* 9:183. doi: 10.1186/s13568-019-0909-z
- Turnidge, J., and Paterson, D. L. (2007). Setting and revising antibacterial susceptibility breakpoints. *Clin. Microbiol. Rev.* 20, 391–408. doi: 10.1128/CMR.00047-06
- Wilson, M. L., and Gaido, L. (2004). Laboratory diagnosis of urinary tract infections in adult patients. *Clin. Infect. Dis.* 38, 1150–1158. doi: 10.1086/383029
- World Health Organization. (2019). *Technical Consultation on in vitro Diagnostics for AMR, 27–28 March 2019, WHO Headquarters, Geneva: Meeting Report*. Geneva: World Health Organization.

Conflict of Interest: The authors declare that the research was conducted in the absence of any commercial or financial relationships that could be construed as a potential conflict of interest.

Copyright © 2020 Needs, Donmez, Bull, McQuaid, Osborn and Edwards. This is an open-access article distributed under the terms of the Creative Commons Attribution License (CC BY). The use, distribution or reproduction in other forums is permitted, provided the original author(s) and the copyright owner(s) are credited and that the original publication in this journal is cited, in accordance with accepted academic practice. No use, distribution or reproduction is permitted which does not comply with these terms.


 Cite this: *RSC Adv.*, 2021, 11, 38258

Direct microfluidic antibiotic resistance testing in urine with smartphone capture: significant variation in sample matrix interference between individual human urine samples†

Sarah Helen Needs, * Sultan İlayda Dönmez and Alexander Daniel Edwards *

Rapid and portable direct tests for antibiotic resistance in human clinical samples such as urine could reduce misuse of precious antimicrobials, by allowing treatment decisions to be informed by microfluidic diagnostic tests. We demonstrate that the variable composition of human urine can significantly affect the antibiotic minimum inhibitory concentration (MIC) measured using microfluidic devices. The urine sample matrix interference was not observed in pooled normal urine, emphasising the critical importance of assessing matrix interference with a wide range of individual urine samples, rather than a few standardised or pooled controls. Both dilution into assay medium and inclusion of buffer could reduce the matrix interference, but dilution may affect analytical sensitivity by increasing the minimum bacterial cell density needed in a sample for growth to be detected, especially for miniaturised devices that test small sample volumes. We conclude it is vital to fully assess and optimise novel analytical microbiology tools using multiple individual urine samples, otherwise the high variation in matrix interference will compromise the clinical performance of these rapid diagnostics that are urgently needed to tackle the global threat of antimicrobial resistance.

 Received 13th September 2021
 Accepted 11th November 2021

DOI: 10.1039/d1ra06867a

rsc.li/rsc-advances

Introduction

Improved diagnostics and rapid testing is vital to minimise mis- and overuse of antibiotics to reduce the global threat of antimicrobial resistance (AMR),^{1,2} and miniaturised analytical technology is emerging to achieve this.³ Urinary tract infection (UTI) is a widespread clinical need where initial antibiotic selection is not routinely guided by antibiotic susceptibility tests (AST), and instead surveillance information is used to develop empirical guidelines to minimise risk of resistance.⁴ Microfluidics offer portability, speed, and ease of use compared to traditional laboratory microbiology methods, including broth microdilution and disc diffusion, which take at least 48 h from sample collection. Whilst molecular methods and other emerging analytical microbiology tools are increasingly able to rapidly detect certain pathogens or resistance genes, phenotypic AST remains vital to measure pathogen response to antibiotic functionally, and for this reason remains the clinical reference standard.

Significant time could be saved if clinical samples can be tested directly, avoiding overnight plating and colony isolation.

Many of the emerging novel and microfluidic devices for rapid phenotypic AST determination use urine as the clinical sample. UTI represent a sample with a high clinical need and a high bacterial load, allowing direct testing without bacteria enrichment. However, although urine matrix components are known to be able to affect analytical performance of established functional microbiology tests,⁵ this has not been extensively studied in the emerging microfluidic microbiology tools.

Some recently described methods remove the sample matrix effect by using bacteria traps or filters to exchange the urine with growth media.^{6–8} However, these methods add further liquid handling steps. Other systems dilute the sample by at least 1 : 2 (ref. 9) but usually more, by 1 : 10.^{10,11} While many novel microfluidic microbiology devices have been recently published that deliver AST results, few of these have been validated with large numbers of normal human urine or clinical samples from patients and antibiotic combinations (Table S1†).

Here we present data examining the impact of variation in urine matrix composition on MIC measured in a low-cost microcapillary device, based on simple disposable microcapillary arrays. The test strips are a miniaturised version of the clinical reference standard microplate broth microdilution (BMD) method. Each test strip has 10 parallel capillaries, each of which is analogous to one well of a microplate, simplifying operation and increasing throughput compared to microplates. The microcapillary strips are mass-produced by melt-extrusion,

School of Pharmacy, University of Reading, UK. E-mail: a.d.edwards@reading.ac.uk; s.h.needs@reading.ac.uk

† Electronic supplementary information (ESI) available. See DOI: 10.1039/d1ra06867a



allowing high volume of the AST strips to be made in comparison to other experimental microfluidic systems (Fig. S1†). The results of the AST are readable by both smartphone and robotic timelapse imaging, ideal for systematic analysis of matrix interference in microfluidic microbiology assays. Having previously established proof-of-concept of microbial identification, viable cell counting, and monitoring bacteriophage lysis^{12–15} in this system, we have not previously used the system to interrogate the impact of urine sample matrix on microfluidic antibiotic resistance assays. Here we assessed in detail the impact of urine matrix on microfluidic AST, by systematically quantifying minimum inhibitory concentration (MIC) in the presence or absence of a wide range of human urine samples. For direct testing of clinical urine samples to be successful with microfluidic versions of current clinical reference standard (e.g. microplate broth microdilution), a full understanding of urine matrix interference is essential. Of particular note, we evaluated the impact of urine on performance using a panel of individual urines vs. pooled controls. The mass-produced nature of the tests allowed greater than >2000 urine/isolate/antibiotic combinations to be analysed, with full growth kinetics monitored in every condition. Our findings are applicable to many other microfluidic researchers developing direct AST systems for urinary tract infections.

Results and discussion

One of the simplest ways to eliminate matrix interference in any analytical technique is dilution, which both reduces the concentration of interfering agents, and provides an opportunity to mitigate interference for example by buffering. However, dilution decreases analyte concentration, potentially compromising clinical measurements if the limit of detection no longer matches the clinical threshold. For AST, the ‘analyte’ is pathogenic bacteria, and in UTI the clinical threshold is 10^5 colony forming units (CFU) per mL.¹⁶ This allows us to calculate an absolute threshold for measuring antibiotic susceptibility such that ≥ 1 CFU is present per test, for different urine dilutions, in small sample volumes. Microfluidic device design varies considerably, so test volumes vary from picolitres to mL.^{7,11,17} However, for microdevices having test volumes below $1 \mu\text{L}$, high dilution is likely to compromise utility for clinical UTI samples. The distribution of bacteria in microfluidic devices is often dictated by Poisson statistics.^{12,18} Even if one single CFU can be detected, the limit of pathogen detection, where 99% of the time a $1 \mu\text{L}$ device will contain at least 1 bacterium, is 5×10^3 CFU mL⁻¹; a 1 : 10 sample dilution raises this to 5×10^4 CFU mL⁻¹ (Fig. 1a). Fewer cells can also make detection slower.¹² We conclude that urine matrix interference becomes an especially important consideration for microfluidic microbiology, given this connection between sample volume and limit of detection, compared to established microplates or agar Petri dishes assays where sample and assay volumes are larger.

Antibiotic sensitivity can be quantified by measurement of MIC; the MIC can be compared to standards, reference strains and internationally agreed breakpoint antibiotic concentration to score resistance vs. sensitivity. We therefore explored how

urine matrix affects the measured MIC in microfluidics, compared to controls without adding urine. The MIC was determined for one quality control strain (*E. coli* ATCC 25922) and two uropathogenic *E. coli* isolates, spiked into human urine: firstly with pooled control urine; and secondly with a panel of individual urine samples. Even when diluted by only 1 : 2 in growth detection media, the observed MIC in the presence of pooled urine was within the reference range, differing by a maximum of 1 doubling dilution of antibiotic, for three important UTI antibiotics (Fig. 1b and S2†).

However, a very different picture emerged with individual urine samples. Whilst observed MIC for QC strain 25922 for nitrofurantoin were within the reference range for all urines, significant variation in observed MIC appeared for cefoxitin, and 1 out of 8 urine samples diluted at 1 : 2 gave an observed MIC 1 doubling dilution outside the reference range. The urine matrix interference was greatest with ciprofloxacin, with the observed MIC ranging over 6 doubling dilutions. This high variation in observed MIC was consistent in all strains tested. The breakpoint for ciprofloxacin is 0.25 mg L^{-1} , indicating that if tested in a range of normal human urines, 12.5% (1/8) of the urine samples containing *E. coli* 25922 would be miscategorised as resistant. The MIC of the UPEC isolates was too close to the breakpoint to categorise (resistant or susceptible), but this high variation in observed MIC suggests that individual urines contain matrix components that can significantly interfere with microfluidic AST.

Urine is a complex mixture of different components and can vary significantly between and within patient samples depending on diet and hydration, time of collection, and age, among other factors. We investigated the different elements of urine matrix that might interfere with microfluidic AST using our panel of human urine samples spiked with bacteria. We found that urine pH accounted for a significant portion, but not all of the variation of observed MIC. The urine samples that changed MIC the most were the most acidic, all having pH lower than 7 (Fig. 1c, d and Table S2†).

The activity of several antibiotics can be influenced by pH, possibly explaining the impact of urine pH variation on *in vitro* tests. For example ciprofloxacin, meropenem, trimethoprim, fosfomicin, amikacin, colistin and ertapenem have higher observed MIC values in acidic media.^{19–21} An acid environment lowered the MIC of nitrofurantoin indicating an acid environment increases efficacy.²²

To establish how much of the interference by urine matrix could be attributed to pH variation, we added 10 mM HEPES to urine samples by inclusion in growth indicator medium. Buffering decreased the variation in observed MIC between individual urines, such that with HEPES 83% (20/24 urine sample/isolate combinations) were within the reference range in contrast to only 46% without buffer (11/24) (Fig. 1c). This demonstrates that pH is a major source of urine matrix interference on microfluidic AST, but does not account for all the variation.

To achieve the fastest AST results, minimising time to detection is an important target. As well as influencing antibiotic activity, urine matrix can interfere with growth kinetics.



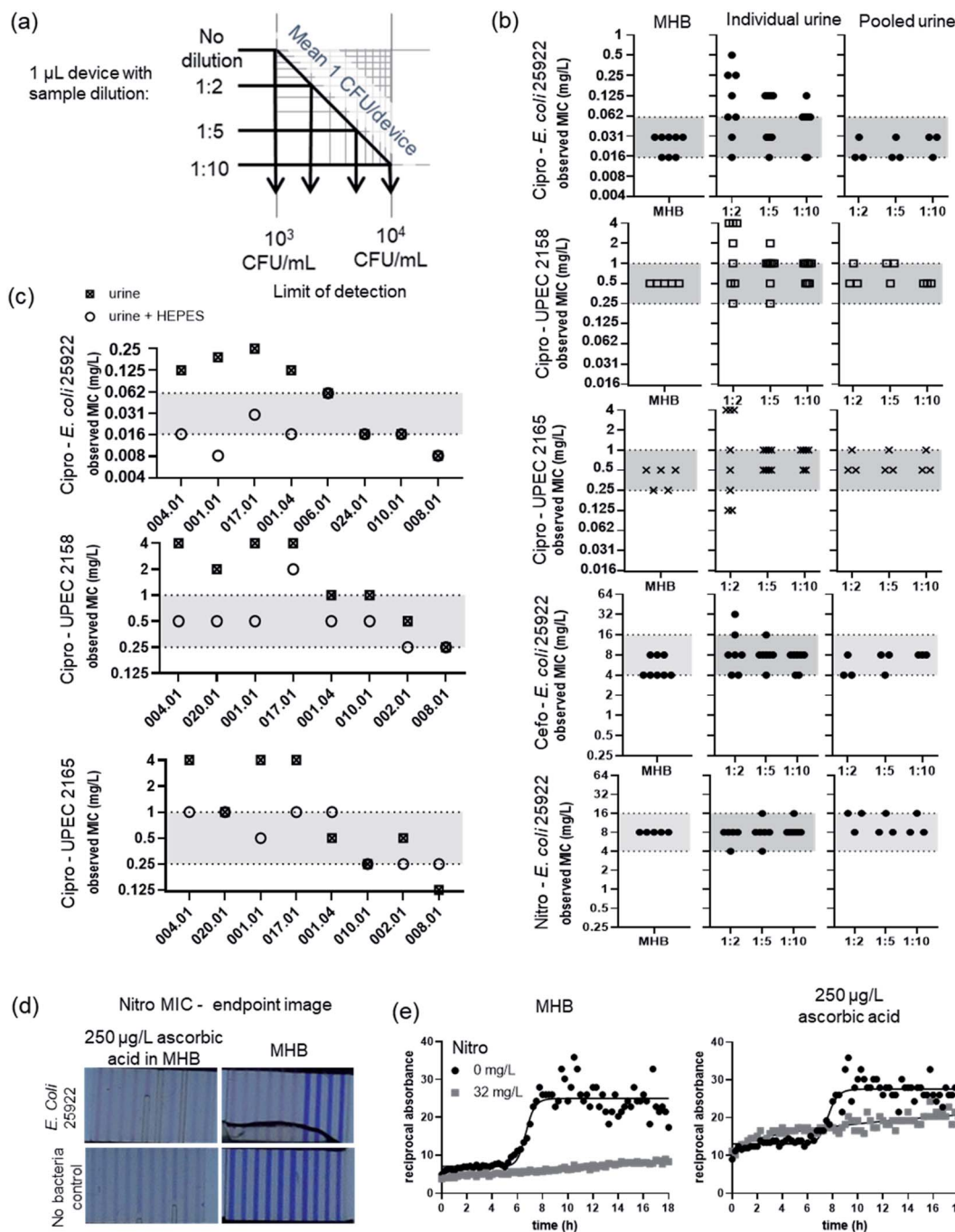


Fig. 1 Variation in AST measurements in individual urine samples. (a) Dilution of sample can reduce inter sample variation but decreases limit of detection. (b) Variation in MIC for ciprofloxacin for *E. coli* 25922 QC strain and 2 uropathogenic *E. coli* strains 2158 and 2165. MIC performed for *E. coli* 25922 for cefoxitin and nitrofurantoin. MIC performed in Mueller–Hinton broth, 7 individual healthy urine samples or 3 pooled urine samples. Horizontal grey area indicates the highest MIC determined in MHB ± 1 log₂ antibiotic dilution (c) MIC for ciprofloxacin performed in individual urine samples diluted 1 : 2 for isolates 25922, 2158 and 2165 with and without 10 mM HEPES. Urine samples are sorted from left to right with lowest pH to highest. pH ranges from 6.44–8.42 (d) images of nitrofurantoin MIC microcapillary BMD tests after 18 h incubation. (e) Timelapse resazurin colour change of *E. coli* 25922 grown in the absence and presence of 32 mg L⁻¹ nitrofurantoin in MHB or MHB supplemented with 250 µg L⁻¹ ascorbic acid. Solid line indicates 4 parameter logistic curve.

High levels of urine can increase the time for bacterial detection, with pH being a significant factor.²³ Analysis of growth kinetics can deliver faster results than endpoint measurements: for fast growing *E. coli* this can cut time from overnight

(endpoint) to just a few hours.¹² Kinetic analysis revealed that the addition of HEPES to growth media into which urine sample 001.01 was diluted, achieved the same MIC result as that of the MHB control, and with the same rapid time to detection.



Bacteria were detected at 4.2 h for MHB, 4.3 h for urine with HEPES and 4.8 h for urine without buffer (Fig. S3†). This indicates that the variation in pH of urine samples can delay microfluidic bacterial growth detection, as well as measurement of antibiotic MIC.

Ascorbic acid is found at variable concentration in urine. There is already significant evidence of ascorbic acid interference with POC urine dipstick tests.^{24,25} Ascorbic acid can also interfere with phenotypic tests that use resazurin as growth indicator, as it can reduce the dye even in the absence of bacteria.²⁶ Here, we found concentrations above $125 \mu\text{g L}^{-1}$ ascorbic acid in MHB lead to a significant decrease in the colour of resazurin in microdevices, levels that were exceeded in ascorbic acid tests on the panel of individual urine samples (Table S2†). This steady decrease in resazurin associated with high ascorbic acid levels could be mistaken for bacterial growth if a simple endpoint readout is used (Fig. 1d). A loss of blue colour is seen at $250 \mu\text{g L}^{-1}$ ascorbic acid even in the absence of bacteria and MIC cannot be determined. Timelapse imaging has been used in a number of novel rapid AST systems including microfluidic devices, as it allows the earliest time point for bacterial growth detection to be used for fastest results. Here, we show that kinetic analysis has a further benefit, allowing discrimination between characteristic exponential changes following bacterial growth, from linear changes associated with interfering factors such as high levels of ascorbic acid in urine sample matrix. If using a single measurement timepoint, it is difficult to distinguish growth in samples with ascorbic acid levels, because the starting colour of resazurin can be reduced in the absence of bacteria, with control sample colour being similar to that seen after bacterial growth. Kinetic growth analysis of a nitrofurantoin microcapillary BMD revealed clear evidence of bacterial growth (s-curve) in contrast to the steady linear change indicating no growth at a concentration of nitrofurantoin that inhibits bacterial growth, even in the presence of $250 \mu\text{g L}^{-1}$ ascorbic acid – higher than found in any individual urine sample (Fig. 1e). At concentrations of ascorbic acid that affected the colour change of resazurin there was still no significant difference in MIC for nitrofurantoin or ciprofloxacin (Fig. S4†).

Urea is the most abundant chemical in urine; when we included up to 20 mg mL^{-1} urea in artificial urine no effect was found on resazurin indicator. Increasing urea concentration only started to affect MIC measurement for nitrofurantoin at 60 mg mL^{-1} , and the MIC for ciprofloxacin remained within the expected range up to 60 mg mL^{-1} urea (Fig. S4†). This suggests that urea is unlikely to interfere in microfluidic AST.

Conclusion

We conclude that microfluidic microbiology systems developed to test urine should be optimised using multiple individual urine samples, as pooling urine to make controls removes the high level of variation in composition. For resazurin-based growth measurements in microsystems, variation in pH appears to have the biggest impact on accuracy of antibiotic susceptibility testing, with higher levels of ascorbic acid found

in some urine samples being particularly problematic for colorimetric endpoint assays. Kinetic growth analysis can partly overcome this interference, and offers improvement over endpoint growth estimation. Adding buffer to the growth medium reduces but does not completely eliminate variation. Higher dilutions of urine can reduce or eliminate matrix interference, at the cost of slower growth detection and with implications for microfluidic device design, especially the lower limit of sample volume able to detect microbes in clinical samples with lower pathogen cell concentrations.¹² Furthermore, for isolates with a large difference between MIC and breakpoint, using only a single antibiotic concentration to determine susceptibility/resistance can miss this variation, minimum inhibitory concentration for some samples should be evaluated.

The potential for microfluidics to address the global challenge of AMR can only be realised if careful attention is paid to the analytical challenge of clinical samples. The panel of individual urine samples assessed in this article was taken from healthy volunteers, and clinical samples from patients presenting with urinary tract infection are likely to be more complex and with higher variation in matrix composition. Further pathological changes such as patient cells present in the sample (red blood cells and leukocytes) may also cause further interference in novel AST devices. However, the factors described here will certainly vary in clinical samples and this key insight into individual variation in urine matrix interference on microfluidic microbial measurement will also relate to other direct AST systems. Validating and optimising novel assays in pooled or synthetic urine is likely to lead to analytical problems arising in real samples where higher variation in composition can be expected.

Experimental section

Urine samples and isolates

Ethical consent for the collection of urine from healthy donors was received from the University of Reading, reference code 19/59. Informed written consent was obtained from all participants. Urine samples were collected in Brand Urine beakers under instruction to collect a midstream urine sample. Samples were collected and tested within 4 h using Uritest 10V Urinalysis strips and Quantofix Ascorbic Acid test (Sigma Aldrich, UK). pH was determined by pH electrode. Following this urine samples were filtered using a $5 \mu\text{m}$ syringe filter and stored at $-20 \text{ }^\circ\text{C}$ until use. *E. coli* 25922 was purchased from ATCC. Uropathogenic *E. coli* (UPEC) isolates 2158 and 2165 were collected at a tertiary care hospital of Pakistan from community acquired UTI patients.^{27,28} Ethical approval was obtained from the ethical review board of the Pakistan Institute of Medical Sciences.

Microcapillary broth microdilution

Microfluidic MIC test strips were prepared as described.¹³ Briefly, microcapillary film with 10 parallel capillaries of $270 \mu\text{m}$ capillary diameter were hydrophilic coated by incubating 5 mg mL^{-1} polyvinyl alcohol (PVOH) (M_w 146, 000–186, 000, >99%



hydrolysed, Sigma Aldrich, UK) for 2 h at room temperature. The PVOH was removed by washing the capillaries with sterile Ultrapure Milli-Q water. Antibiotics at the concentration indicated were injected into individual capillaries, frozen at $-80\text{ }^{\circ}\text{C}$ for $>1\text{ h}$ and freeze-dried for $>4\text{ h}$ on an Edwards Modulyo freezer-drier. Test strips were vacuum sealed and stored at $-20\text{ }^{\circ}\text{C}$ until use for no longer than 1 week.

E. coli were grown in MHB and diluted to $5 \times 10^5\text{ CFU mL}^{-1}$ in urine and MHB with resazurin indicator medium to a final concentration of 0.25 mg mL^{-1} . Samples were loaded into the microfluidic test strips by adding $200\text{ }\mu\text{L}$ to a well of a 96 well plate and dipping the test strip into the well. The sample is taken up into the capillaries by capillary action. Each end of the test were sealed with silicone grease and incubated overnight at $37\text{ }^{\circ}\text{C}$. MIC was recorded using iPhone 6s or Canon Powershot S120 and scored by eye based on colour change of resazurin from blue to pink or recorded on an imaging robot.²⁹

Microplate broth microdilution

E. coli were grown in MHB and diluted to 0.5 McFarland standard equivalent. Bacteria isolates were then diluted 1 : 100 in MHB and $50\text{ }\mu\text{L}$ were added to microplate wells. Microplate wells already contained $50\text{ }\mu\text{L}$ of antibiotic solutions and resazurin. The final concentration of the wells contained doubling dilutions of antibiotics, resazurin dye at 0.25 mg mL^{-1} and bacteria at $5 \times 10^5\text{ CFU mL}^{-1}$. Plates were incubated overnight at $37\text{ }^{\circ}\text{C}$. MIC was determined by the lowest concentration of antibiotic in which the resazurin remained blue.

Funding

This research was supported by the EPSRC (EP/R022410/1).

Ethical approval

The collection of urinary pathogenic *E. coli* from a tertiary care hospital of Pakistan from community acquired UTI patients and was approved by Ethical Review Board (ERB) of Pakistan Institute of Medical Sciences. Ethical consent for the collection of urine from healthy donors was received from the University of Reading, reference code 19/59. Informed written consent was obtained from all participants.

Conflicts of interest

ADE is one the inventors of patent application protecting aspects of the novel microfluidic devices tested in this study and is a director and shareholder in Capillary Film Technology Ltd, a company holding a commercial license to this patent application: WO2016012778 "Capillary assay device with internal hydrophilic coating" AD Edwards, NM Reis.

Acknowledgements

We thank Simon Andrews, Wajiha Imtiaz and Zara Rafaque for the UPEC isolates which was supported by Higher Education Commission, Pakistan (Pin Number: 2BM2-093) and

Commonwealth Scholarship Commission (CSC Ref # PKCN-2017-215).

References

- 1 WHO, *Technical Consultation on In Vitro Diagnostics for AMR*, 27–28, World Health Organization, Geneva, 2019.
- 2 DHSC, in *Contained and controlled: the UK's 20-year vision for antimicrobial resistance*, Department of Health and Social Care, 2019, <https://www.gov.uk/government/publications/uk-20-year-vision-for-antimicrobial-resistance>.
- 3 N. Qin, P. Zhao, E. A. Ho, G. Xin and C. L. Ren, Microfluidic Technology for Antibacterial Resistance Study and Antibiotic Susceptibility Testing: Review and Perspective, *ACS Sens.*, 2021, **6**(1), 3–21.
- 4 V. Watts, B. Brown, M. Ahmed, A. Charlett, C. Chew-Graham, P. Cleary, *et al.*, Routine laboratory surveillance of antimicrobial resistance in community-acquired urinary tract infections adequately informs prescribing policy in England, *JAC Antimicrob. Resist.*, 2020, **2**(2), dlaa022.
- 5 L. Yang, K. Wang, H. Li, J. D. Denstedt and P. A. Cadieux, The Influence of Urinary pH on Antibiotic Efficacy Against Bacterial Uropathogens, *Urology*, 2014, **84**(3), 731.e1–731.e7.
- 6 B. A. Baltekin Ö, E. Tano, D. I. Andersson and J. Elf, Antibiotic susceptibility testing in less than 30 min using direct single-cell imaging, *Proc. Natl. Acad. Sci. U. S. A.*, 2017, **114**(34), 9170.
- 7 J. Avesar, D. Rosenfeld, M. Truman-Rosentsvit, T. Ben-Arye, Y. Geffen, M. Bercovici, *et al.*, Rapid phenotypic antimicrobial susceptibility testing using nanoliter arrays, *Proc. Natl. Acad. Sci. U. S. A.*, 2017, **114**(29), E5787.
- 8 P. Zhang, A. M. Kaushik, K. E. Mach, K. Hsieh, J. C. Liao and T.-H. Wang, Facile syringe filter-enabled bacteria separation, enrichment, and buffer exchange for clinical isolation-free digital detection and characterization of bacterial pathogens in urine, *Analyst*, 2021, **146**(8), 2475–2483.
- 9 M. Mo, Y. Yang, F. Zhang, W. Jing, R. Iriya, J. Popovich, *et al.*, Rapid Antimicrobial Susceptibility Testing of Patient Urine Samples Using Large Volume Free-Solution Light Scattering Microscopy, *Anal. Chem.*, 2019, **91**(15), 10164–10171.
- 10 W.-B. Lee, C.-C. Chien, H.-L. You, F.-C. Kuo, M. S. Lee and G.-B. Lee, An integrated microfluidic system for antimicrobial susceptibility testing with antibiotic combination, *Lab-on-a-Chip*, 2019, **19**(16), 2699–2708.
- 11 F. Zhang, J. Jiang, M. McBride, Y. Yang, M. Mo, R. Iriya, *et al.*, Direct Antimicrobial Susceptibility Testing on Clinical Urine Samples by Optical Tracking of Single Cell Division Events, *Small*, 2020, **16**(52), 2004148.
- 12 S. H. Needs, H. M. I. Osborn and A. D. Edwards, Counting bacteria in microfluidic devices: Smartphone compatible 'dip-and-test' viable cell quantitation using resazurin amplified detection in microliter capillary arrays, *J. Microbiol. Methods*, 2021, 106199.
- 13 S. H. Needs, Z. Rafaque, W. Imtiaz, P. Ray, S. Andrews and A. D. Edwards, High-throughput, multiplex microfluidic test strip for the determination of antibiotic susceptibility



- in uropathogenic *E. coli* with smartphone detection, *bioRxiv*, 2021, DOI: 10.1101/2021.05.28.446184.
- 14 D. SÍ, S. H. Needs, H. M. I. Osborn and A. D. Edwards, Label-free smartphone quantitation of bacteria by darkfield imaging of light scattering in fluoropolymer micro capillary film allows portable detection of bacteriophage lysis, *Sens. Actuators, B*, 2020, **323**, 128645.
 - 15 N. M. Reis, J. Pivetal, A. L. Loo-Zazueta, J. M. S. Barros and A. D. Edwards, Lab on a stick: multi-analyte cellular assays in a microfluidic dipstick, *Lab-on-a-Chip*, 2016, **16**(15), 2891–2899.
 - 16 M. G. Coulthard, M. Kalra, H. J. Lambert, A. Nelson, T. Smith and J. D. Perry, Redefining Urinary Tract Infections by Bacterial Colony Counts, *Pediatrics*, 2010, **125**(2), 335.
 - 17 F.-E. Chen, A. Kaushik, K. Hsieh, E. Chang, L. Chen, P. Zhang, *et al.*, Toward Decentralizing Antibiotic Susceptibility Testing via Ready-to-Use Microwell Array and Resazurin-Aided Colorimetric Readout, *Anal. Chem.*, 2021, **93**(3), 1260–1265.
 - 18 D. J. Collins, A. Neild, A. deMello, A.-Q. Liu and Y. Ai, The Poisson distribution and beyond: methods for microfluidic droplet production and single cell encapsulation, *Lab-on-a-Chip*, 2015, **15**(17), 3439–3459.
 - 19 M. Kamberi, K. Tsutsumi, T. Kotegawa, K. Kawano, K. Nakamura, Y. Niki, *et al.*, Influences of urinary pH on ciprofloxacin pharmacokinetics in humans and antimicrobial activity *in vitro* versus those of sparfloxacin, *Antimicrob. Agents Chemother.*, 1999, **43**(3), 525–529.
 - 20 A. K. Nussbaumer-Pröll, S. Eberl, B. Reiter, T. Stimpfl, C. Dorn and M. Zeitlinger, Low pH reduces the activity of ceftolozane/tazobactam in human urine, but confirms current breakpoints for urinary tract infections, *J. Antimicrob. Chemother.*, 2020, **75**(3), 593–599.
 - 21 A. Burian, Z. Erdogan, C. Jandrisits and M. Zeitlinger, Impact of pH on activity of trimethoprim, fosfomicin, amikacin, colistin and ertapenem in human urine, *Pharmacology*, 2012, **90**(5–6), 281–287.
 - 22 F. Fransen, M. J. B. Melchers, C. M. C. Lagarde, J. Meletiadis and J. W. Mouton, Pharmacodynamics of nitrofurantoin at different pH levels against pathogens involved in urinary tract infections, *J. Antimicrob. Chemother.*, 2017, **72**(12), 3366–3373.
 - 23 S. Carlsson, N. P. Wiklund, L. Engstrand, E. Weitzberg and J. O. N. Lundberg, Effects of pH, Nitrite, and Ascorbic Acid on Nonenzymatic Nitric Oxide Generation and Bacterial Growth in Urine, *Nitric Oxide*, 2001, **5**(6), 580–586.
 - 24 A. Unic, N. Nikolac Gabaj, M. Miler, J. Culej, A. Lisac, A. Horvat, *et al.*, Ascorbic acid—A black hole of urine chemistry screening, *J. Clin. Lab. Anal.*, 2018, **32**(5), e22390.
 - 25 N. Nikolac Gabaj, M. Miler, A. Unic, L. Milevoj Kopicinovic, A. Vrtaric and J. Culej, Ascorbic acid in urine still compromises urinalysis results, *Ann. Clin. Biochem.*, 2019, **57**(1), 64–68.
 - 26 F. Wang, Y. Li, W. Li, Q. Zhang, J. Chen, H. Zhou, *et al.*, A facile method for detection of alkaline phosphatase activity based on the turn-on fluorescence of resorufin, *Anal. Methods*, 2014, **6**(15), 6105–6109.
 - 27 Z. Rafaque, J. I. Dasti and S. C. Andrews, Draft genome sequence of a multidrug-resistant CTX-M-15 β -lactamase-producing uropathogenic *Escherichia coli* isolate (ST131-O25b-H30) from Pakistan exhibiting high potential virulence, *J. Glob. Antimicrob. Resist.*, 2018, **15**, 164–165.
 - 28 Z. Rafaque, J. I. Dasti and S. C. Andrews, Draft genome sequence of a uropathogenic *Escherichia coli* isolate (ST38 O1:H15) from Pakistan, an emerging multidrug-resistant sequence type with a high virulence profile, *New Microbes New Infect.*, 2019, **27**, 1–2.
 - 29 S. H. Needs, T. T. Diep, S. P. Bull, A. Lindley-Decaire, P. Ray and A. D. Edwards, Exploiting open source 3D printer architecture for laboratory robotics to automate high-throughput time-lapse imaging for analytical microbiology, *PLoS One*, 2019, **14**(11), e0224878.

